Meteorological and Hydrological Data and Analysis Report for Foothills/Umiat Corridor and Bullen Projects: 2006–2011

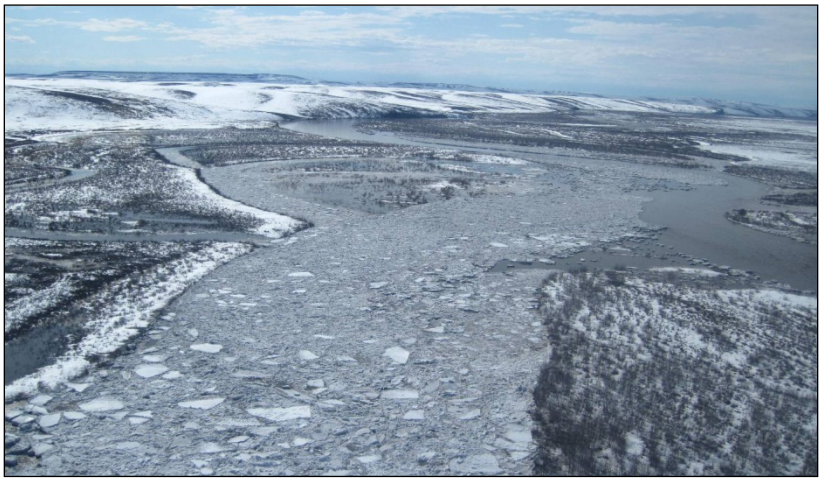

Ice Jam on the Chandler River May 23, 2011

by

Douglas L. Kane, Emily K. Youcha, Sveta Stuefer, Horacio Toniolo, William Schnabel, Robert Gieck, Greta Myerchin-Tape, Joel Homan, Erica Lamb, and Ken Tape

January 2012

Umiat Corridor/Bullen Hydrology Projects

Report No. INE/WERC 12.01

Water and Environmental Research Center

UAF INE WERC

Meteorological and Hydrological Data and Analysis Report for Foothills/Umiat Corridor and Bullen Projects: 2006–2011

by

Douglas L. Kane, Emily K. Youcha, Sveta Stuefer, Horacio Toniolo, William Schnabel, Robert Gieck, Greta Myerchin-Tape, Joel Homan, Erica Lamb, and Ken Tape

A report on research sponsored by the

Alaska Department of Transportation and Public Facilities

Alaska Department of Natural Resources

January 2012

Umiat Corridor and Bullen Hydrology Projects

Report Number INE/WERC 12.01

Recommended Citation:

Kane, D.L., Youcha, E.K., Stuefer, S., Toniolo, H., Schnabel, W., Gieck, R., Myerchin-Tape, G., Homan, J., Lamb, E., and K. Tape, K. 2012. Meteorological and Hydrological Data and Analysis Report for Foothills/Umiat Corridor and Bullen Projects: 2006–2011. University of Alaska Fairbanks, Water and Environmental Research Center, Report INE/WERC 12.01, Fairbanks, Alaska, 260 pp.

Fairbanks, Alaska
January 2012

For additional information write to:

Publications
Water and Environmental Research Center
University of Alaska Fairbanks
Fairbanks, Alaska 99775
http://ine.uaf.edu/werc/

TABLE OF CONTENTS

DISCLAIMER

The contents of this report reflect the views of the authors, who are responsible for the accuracy of the data presented herein. This research was funded by the Alaska Department of Transportation and Public Facilities (ADOT&PF) and earlier by the Alaska Department of Natural Resources (ADNR). The contents of the report do not necessarily reflect the views or policies of the ADOT&PF, ADNR, or any other project sponsor. This work does not constitute a standard, specification, or regulation.

The use of trade and firm names in this document is for the purpose of identification only and does not imply endorsement by the University of Alaska Fairbanks, Alaska Department of Transportation and Public Facilities, Alaska Department of Natural Resources, or any other sponsors.

CONVERSION FACTORS, UNITS, WATER QUALITY UNITS, VERTICAL AND HORIZONTAL DATUM, ABBREVIATIONS AND SYMBOLS

Conversion Factors

Multiply	By	To obtain
	Length	
inch (in.)	25.4	millimeter (mm)
inch (in.)	2.54	centimeter (cm)
foot (ft)	0.3048	meter (m)
mile (mi)	1.609	kilometer (km)
	Area	
acre	43560.0	square feet (ft^2)
acre	0.405	hectare (ha)
square foot (ft^2)	3.587e-8	square mile (mi^2)
square mile (mi^2)	2.590	square kilometer (km^2)
	Volume	
gallon (gal)	3.785	liter (L)
gallon (gal)	3785.412	milliliter (mL)
cubic foot (ft^3)	28.317	liter (L)
acre-ft	1233.482	cubic meter (m^3)
acre-ft	325851.43	gallon(gal)
gallon(gal)	0.1337	cubic feet (ft^3)
	Velocity and Discharge	
foot per day (ft/d)	0.3048	meter per day (m/d)
square foot per day (ft^2/d)	0.0929	square meter per day (m^2/d)
cubic foot per second (ft^3/s)	0.02832	cubic meter per second (m^3/sec)

Units

In this report, both metric (SI) and English units were employed. The choice of "primary" units employed depended on common reporting standards for a particular property or parameter measured. The approximate value in the "secondary" units may also be provided in parentheses. Thus, for instance, runoff was reported in cubic meters per second (m^3/s) followed by the cubic feet per second (ft^3/s) value in parentheses.

Physical and Chemical Water-Quality Units:

Temperature:

Water and air temperatures are given in degrees Celsius (°C) and in degrees Fahrenheit (°F). Degrees Celsius can be converted to degrees Fahrenheit by use of the following equation:

$$°F = 1.8(°C) + 32$$

Milligrams per liter (mg/L) or micrograms per liter (µg/L):

Milligrams per liter is a unit of measurement indicating the concentration of chemical constituents in solution as weight (milligrams) of solute per unit volume (liter) of water. One thousand micrograms per liter is equivalent to one milligram per liter. For concentrations less than 7000 mg/L, the numerical value is the same as for concentrations in parts per million (ppm).

Horizontal Datum:

The horizontal datum for all locations in this report is the World Geodetic System of 1984 (WGS84).

Vertical Datum:

"Sea level" in the following report refers to either the WGS84 datum (for approximate elevations of station locations) or the GEOID09AK datum for water level elevations.

Abbreviations, Acronyms, and Symbols

ADCP	acoustic doppler current profiler
ADOT&PF	Alaska Department of Transportation and Public Facilities
ADNR	Alaska Department of Natural Resources
AUTC	Alaska University Transportation Center
bgs	below ground surface
C	Celsius (°C)
cm	centimeter
d	day
DO	dissolved oxygen
ET	evapotranspiration
F	Fahrenheit (°F)
ft	feet
GWS	Geo-Watersheds Scientific
GPS	Global Positioning System
HDPE	high-density polyethylene
in.	inch
INE	Institute of Northern Engineering
km	kilometers
m	meter
mg/L	milligrams per liter, equivalent to ppm
mi	mile
mm	millimeter
NGVD	National Geodetic Vertical Datum
NRCS	Natural Resources Conservation Service
NSF	National Science Foundation
NTU	nephelometric turbidity units
P-T	Priestley-Taylor
QA	quality assurance
QC	quality control
s	second
SBAS	satellite based augmentation system
SWE	snow water equivalent
RTK	real-time kinematic
TSS	total suspended solids
TT	threshold temperature
UAF	University of Alaska Fairbanks
USGS	U.S. Geological Survey
W	watt
WB	water balance
WAAS	Wide Area Augmentation System
WERC	Water and Environmental Research Center
WGS	World Geodetic System
WWW	World Wide Web

ACKNOWLEDGMENTS

Much of the data presented in this project was funded by grants from the Alaska Department of Natural Resources (ADNR) and the Alaska Department of Transportation and Public Facilities (ADOT&PF). Data collected on other research projects, such as National Science Foundation (NSF) Office of Polar Programs Grant OPP-0335941, and by other governmental agencies, such as the stream-gauging data of the U.S. Geological Survey, are included or used in this report for comparison/analyses purposes. We thank Michael Lilly and Geo-Watershed (GW) Scientific staff who earlier in the project provided significant contributions to data-collection efforts, project reporting, and data analysis. We also thank Ken Irving, Robert Busey, Nathan Stephan, Peter Prokein, Joel Bailey, Erica Betts, and Fabien Rigault at UAF/WERC who provided technical assistance and/or field support.

ABSTRACT

The North Slope of Alaska is a large, mainly undeveloped area with considerable natural resources. Environmental monitoring in this area of Alaska is quite limited. The first significant hydrologic effort occurred shortly after the discovery of oil on the North Slope at Prudhoe Bay in November 1968, when the U.S. Geological Survey established three stream-gauging sites nearby. Unfortunately, no other complementary hydrometeorological data were collected at that time. In the mid-1980s, several hydrometeorological stations were installed on the North Slope in conjunction with funded research; there was little or no coordination between projects at that time. The North Slope extends from the divide of the Brooks Range in the south to the Arctic Ocean in the north with Canada to the east and the Chukchi Sea to the west; it is essentially treeless, underlain by continuous permafrost, and exposed to an Arctic climate. We installed a number of meteorological stations in what we refer to as the Bullen/Sagavanirktok area (east of the Dalton Highway to Canning River) and the Umiat Corridor/Kuparuk Foothills area (west of the Dalton Highway to the Umiat area). A summary of the data collected during 2006 to 2008 is presented in Kane et al. (2009). This report covers additional data collected through 2011. We made meteorological observations of wind speed and direction, net radiation, snow water equivalent on the ground at the end of winter, continuous snow depth throughout the winter, summer precipitation, relative humidity, air temperature, soil temperature, and soil moisture. In 2009, we began collecting runoff data on the Kadleroshilik, Shaviovik, No Name, and Anaktuvuk Rivers. In the summer of 2010, we began measuring runoff on the Chandler and Itkillik Rivers. Because we have made observations for only two or three years, it is not possible to look at the variability from year to year; we have utilized long-term data sets from other sources. These short-term data are better utilized for looking at the spatial variability of each variable over a large area in the central Alaska Arctic that ranges from the flat Coastal Plain to the mountains. For example, summer precipitation varies significantly over the study area, with much greater summer precipitation in the Mountain and Foothills regions that also produces considerable runoff from watersheds in these two regions. In contrast, cold-season precipitation is fairly uniform over the central Alaska Arctic.

1 INTRODUCTION

In general, hydrological and meteorological understanding in the Alaska Arctic is poor at best (Kane et al., 1992; Hinzman et al., 2005; Woo et al., 2008). Two main reasons for this are the sparseness of field data (limited operational data collection agenda by state and federal agencies) and the lack of complementary data when some data are collected. For example, where past stream-gauging data were collected on the North Slope of Alaska, no supporting meteorological data (like rainfall or end-of-winter snow water equivalent) were collected. Ideally, state and federal water-related agencies would undertake this data-collection effort in an integrated fashion. There are a few federally operated meteorological stations in northern Alaska, but in almost all cases, they are located close to sea level along the coast (therefore, poorly distributed and not representative of the unpopulated and remote foothills and mountains). An additional problem is that often the quality of the measurements is poor. For instance, the undercatch of annual precipitation (both solid and liquid) by the gauges used has been shown to be low by a factor of two to three (Benson, 1982) at the windy coastal village of Barrow, Alaska.

Hydrologically, precipitation conditions range from a few weeks to a season or more of drought to prolonged periods of significant precipitation. Unfortunately, the length of record for many data sets is too short to determine with confidence the likelihood of many of these events at low probabilities or long return periods. There is also the issue of climatic warming and how it may affect water resources on the North Slope in the near term and long term. It is predicted through global climate models that annual precipitation (snow and rain) will increase, although this has not been verified by any data sets for any part of the Arctic.

The purpose of this study is to improve our understanding of the spatial variability of hydrology and meteorology in the central region of the Alaska Arctic including the Dalton Highway corridor. Researchers in the Water and Environmental Research Center (WERC), Institute of Northern Engineering (INE) at the University of Alaska Fairbanks (UAF) submitted complementary proposals to the Alaska Department of Natural Resources (ADNR) for areas east of the Dalton Highway (2006–2010) and to the Alaska Department of Transportation and Public Facilities (ADOT&PF) for areas west of the Dalton Highway (2006–present), to collect and

analyze hydrometeorological data north of the Brooks Range Divide. From past measurement programs by various groups, it is clear that the hydrology and meteorology on the Alaska North Slope vary considerably, both spatially and temporally. Since this study is expected to last just a few years, we are trying to capture spatial variability. By using the minimal amount of long-term data available, we can compare our new data against the long-term data to get additional insight into the hydrology of this region.

2 STUDY AREA

To improve our understanding of the hydrological and meteorological spatial variability of the central Alaska Arctic, in 2006 we installed twelve meteorological stations in the Kuparuk, Sagavanirktok, Kadleroshilik, Shaviovik, and Kavik River basins as part of an Alaska Department of Transportation and Public Facilities (ADOT&PF) and Alaska Department of Natural Resources (ADNR) joint study (Figure 1). Three of the stations were located east of the Dalton Highway in the Brooks Range, which is part of the Arctic National Wildlife Refuge (ANWR); the remaining stations are in the northern foothills of the Brooks Range and the Coastal Plain. A concerted effort was made to blend these stations with existing research sites that have been installed in and adjacent to the Kuparuk and Putuligayuk River basins by researchers at WERC through funding from the National Science Foundation. Of these original twelve stations installed in 2006, seven in the Sagavanirktok, Kadleroshilik, Shaviovik, and Kavik River basins were decommissioned in August 2010, after funding for the Bullen/Sagavanirktok study for ADNR ended. In June 2009, five new meteorologic and one hydrologic observation stations were installed throughout the Anaktuvuk River basin, along with a hydrologic station at both the Itkillik and Chandler Rivers (Figure 1) as part of the Umiat Corridor hydrologic study (funded by ADOT&PF). In 2010, five additional meteorological stations were installed throughout the Chandler River basin (Figure 1), also funded by ADOT&PF for the Umiat Corridor study.

All the rivers in the study area drain north and eventually empty into the Arctic Ocean. The Putuligayuk lies entirely within the Coastal Plain region. The Kuparuk and Kadleroshilik Rivers emanate from the foothills; the Sagavanirktok, Shaviovik, Kavik, Itkillik, Anaktuvuk, and Chandler Rivers originate in the Brooks Range. The Sagavanirktok basin has the largest percentage of area in the Brooks Range (>50%). The entire area is underlain by continuous permafrost (250 to 300 m in the Brooks Range and up to 600 m along the coast), with numerous permafrost-related characteristics visible, such as high- and low-centered polygons, thaw lakes, drained lakes, strangmoor ridges, and reticulate-patterned ground. All of these features play a role in the runoff response from Arctic watersheds. Kane et al. (2003) discuss the effect that permafrost landforms have on the surface hydrologic response. Generally, flows are attenuated

by permafrost landforms, particularly in low-gradient watersheds where these landforms are more prevalent. Surficial soils in the region are mainly organic, covering deeper mineral soils. The thickness of the surficial organic layer varies considerably, but typically is around 25 cm (Hinzman et al., 1991). The active layer (the layer that freezes and thaws each year at the ground surface) is typically around 50 cm deep at summer's end; however, it can vary considerably (25 to 100 cm) depending upon, slope, aspect, soil type and thickness, vegetation, etc. (Hinzman et al., 1998). Dry sites, where latent heat is minimized during freezing/thawing processes, have a deeper active layer. Particularly in the mountainous regions of the study area (but frequently in the foothills and occasionally on the Coastal Plain), fractured or weathered bedrock may be exposed at the surface.

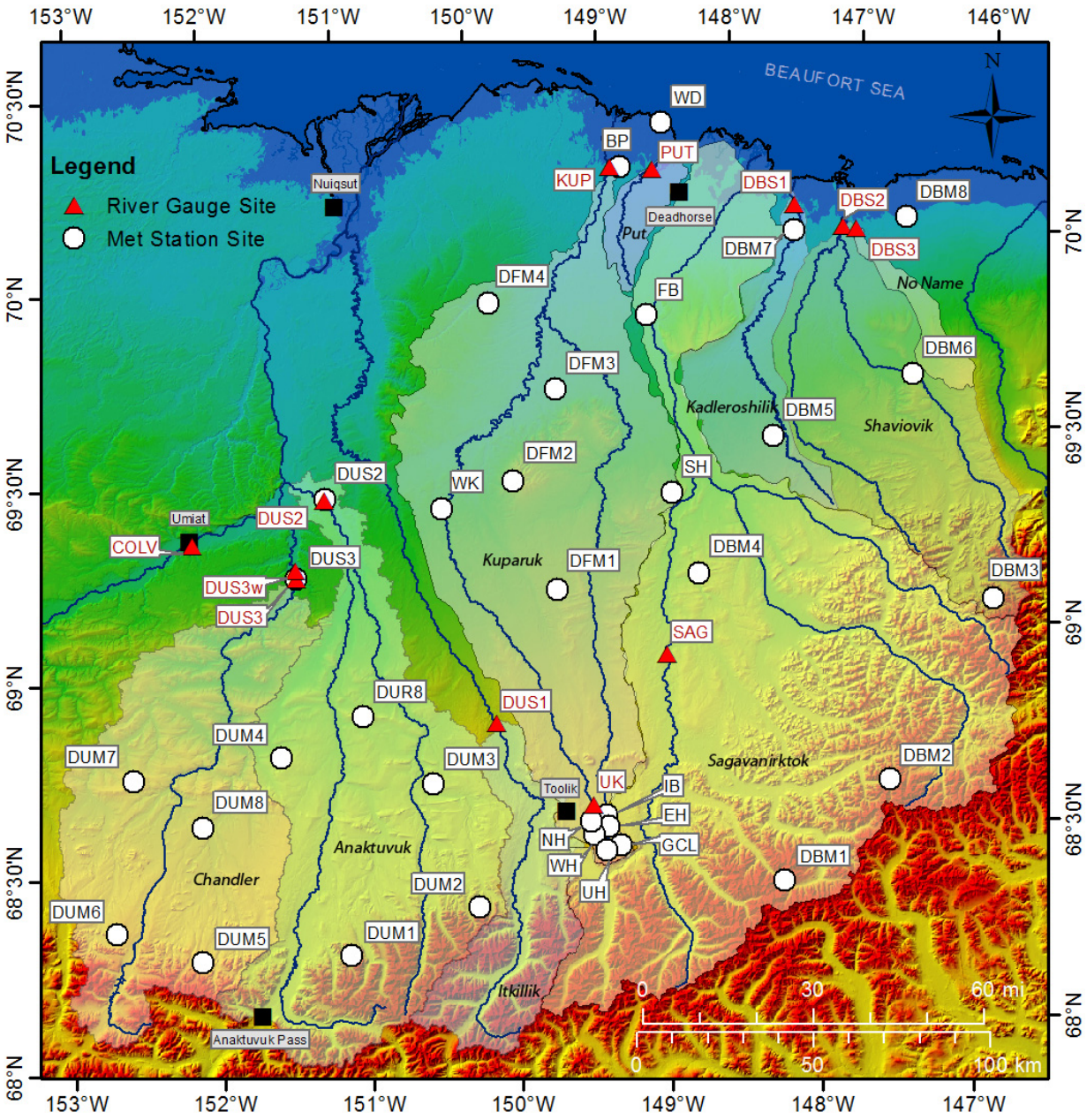

Figure 1. Hydrometeorological study area and location map of field stations for the Kuparuk Foothills/Umiat Corridor and Sagavanirktok River/Bullen study areas, North Slope, Alaska. The duration of observations at each site varies, plus some sites have been removed.

The study area is mostly a treeless region (some patches of trees in riparian areas in the foothills). Vegetation consists of alpine communities in the mountainous region, tussock tundra in the foothills, and sedge tundra on the Coastal Plain. Willow and birch shrubs are common in riparian areas and shrub height is variable, from approximately 30 cm to over 1 m in height.

Shrubs up to 10 m in height have been identified along major river valleys in the foothills and Coastal Plain; these areas are heavily browsed by moose.

In addition to extensive permafrost, aufeis is present in all of the watersheds (Sloan et al., 1975; Yoshikawa et al., 2007). Most of the accumulation of aufeis occurs in early winter (October through December), and the source of the water is either subsurface flow below the stream or from springs. In the Kuparuk and Toolik (a tributary of the Kuparuk) Rivers, the source of the water is from recent precipitation, usually from the last year. Aufeis formations to the east of the Kuparuk basin result from springs originating from ancient groundwater (~3000 years, Yoshikawa et al., 2007). Aufeis formations result in decreased winter base flow and increased summer flow downstream from the formations. The largest aufeis fields observed on the west side of the Dalton Highway (within our study area) include the Kuparuk and Nanushuk aufeis fields.

We do not yet have a good understanding of several components of the hydrologic cycle in the Arctic. Most of the past hydrologic studies have been on small catchments over a short period of time. Spatial variability (on multiple scales) of all hydrologic processes is also a limiting factor in describing the hydrologic processes in Arctic basins. Distribution of snow water equivalent over a basin varies spatially and is still a critical input variable in water balance computations and runoff modeling. Convective summer storms over relatively small areas cause some areas of a basin to receive significant amounts of precipitation, while other areas receive very little. Often we see in the hydrometeorological data a stream runoff response without the measurement of any significant precipitation. This likely can be explained by the sparse precipitation network not capturing convective events in this large study area of the North Slope. Additional research and measurement of evapotranspiration are needed; this data are important in runoff modeling, as well. Currently, only one site (Imnavait) measures pan evaporation within the Bullen and Kuparuk Foothills regions. Estimates of evapotranspiration are usually made using the Priestley-Taylor method because of the limited data required. Often there are large differences in Priestley-Taylor calculations of evapotranspiration, evapotranspiration determined from measured pan evaporation, and water balance-calculated evapotranspiration. Priestly-Taylor

estimates may be problematic due to the spatial and temporal variability of the empirical alpha (α) coefficient used in this equation.

A long-term record is necessary to better quantify and understand the hydrologic processes during extreme flood and drought events. Little is known about sediment transport in most Arctic basins. The process of sediment transport during break-up on rivers of various sizes is not totally understood (McNamara et al., 2008a). Stream-gauging measurement programs are limited on the North Slope of Alaska (as elsewhere in the Arctic). Only the Kuparuk River (drainage area of 8140 km^2) near Deadhorse on the North Slope has a continuous record of runoff estimates, beginning in the early 1970s. Over the years, several consulting firms have conducted individual runoff measurements on the Sagavanirktok River (near Deadhorse) and the Colville River (near Nuiqsut) for the oil industry, but much of this data are not published. PND Engineers, Inc. (2006, 2009a, 2009b, 2009c) conducted stream-gauging activities in 2005 and 2006 on the Kadleroshilik River, Shaviovik River, and No Name River (east of the Shaviovik River) as part of a study on river crossings for ADOT&PF. Based on what we know about extreme events after 10–20 years of data collection at a few sites, collecting precipitation and runoff data for only a short period is inadequate for understanding extreme events. It is more challenging to quantify hydrologic processes in the larger basins, but by both continuing and expanding existing stream gauging and meteorological monitoring measurements and using more technology like remote sensing, we are beginning to better understand the relationship between precipitation and runoff in the Arctic.

3 DATA COLLECTION METHODS

Remote meteorological stations were established at the Bullen and Kuparuk Foothills/Umiat Corridor study areas to collect meteorological data for use in understanding important hydrologically related processes (Table 1). Figure 2 is a picture of a typical meteorological station in the Bullen and Kuparuk Foothills network. The station measures air temperature, relative humidity, wind speed and direction, summer precipitation, soil temperature and soil moisture, net radiation, and winter snow depth on an hourly basis. This station is enclosed by an electric fence to deter wildlife from damaging the equipment. The hydrologic stations also record continuous water levels and water temperatures; we use the former to estimate river discharge. Most of the newest stations are equipped with cameras to record images of the river and weather conditions on an hourly basis. The data are transmitted via radio telemetry to a base station where data are downloaded to the project websites in "near real time":

http://ine.uaf.edu/werc/projects/bullen/stations.html

http://ine.uaf.edu/werc/projects/umiat_corridor/stations.html

Additionally, individual measurements of discharge, along with sediment samples (suspended and bed) are collected at the hydrologic observation stations (Chandler, Anaktuvuk, and Itkillik Rivers) during the spring runoff event and periodically during summer visits. We attempt to make discharge measurements daily during break-up, but only occasionally during the ice-free season.

Other UAF/WERC-operated stations existed throughout the Kuparuk basin including Imnavait, Upper Kuparuk, Sagwon Hills, West Kuparuk, Franklin Bluffs, Betty Pingo, and West Dock. Table 1 is a summary of meteorological stations installed for the Bullen and Kuparuk Foothills/Umiat Corridor projects, including previously existing UAF/WERC-operated stations.

Table 1. Summary of meteorological stations in the UAF/WERC network.

Station Name	Station ID	Region	Project	Basin Name	Elevation (m)	Coordinates	Period of Record
Accomplishment Creek	DBM1	Mountain	Bullen	Sagavanirktok	1474	68° 24' 41" N 148° 8' 11" W	Jul/2006 – present
Ribdon	DBM2	Mountain	Bullen	Sagavanirktok	1478	68° 38' 32" N 147° 21' 6" W	Jul/2006 - Aug/2010
Juniper Creek	DBM3	Mountain	Bullen	Shaviovik	1319	69° 4' 34" N 146° 30' 17" W	Jul/2006 - Aug/2010
Sag-Ivishak	DBM4	Foothills	Bullen	Sagavanirktok	431	69° 12' 55" N 148° 33' 06" W	Jul/2006 - Aug/2010

Station Name	Station ID	Region	Project	Basin Name	Elevation (m)	Coordinates	Period of Record
Upper Kadleroshilik	DBM5	Foothills	Bullen	Kadleroshilik	209	69° 32' 58" N 147° 56' 30" W	Jul/2006 - Aug/2010
Kavik	DBM6	Foothills	Bullen	Shaviovik	198	69° 40' 24" N 146° 54' 02" W	Jul/2006 - Aug/2010
Lower Kadleroshilik	DBM7	Coastal Plain	Bullen	Kadleroshilik	24	70° 04' 24" N 147° 39' 00" W	Jul/2006 - Aug/2010
Bullen	DBM8	Coastal Plain	Bullen	Near No Name	26	70° 04' 47" N 146° 49' 09" W	Jul/2006 - Sept/2011
Kadleroshilik River	DBS1	Coastal Plain	Bullen	Kadleroshilik	12	70° 8'25.80"N 147°38'38.76"W	May/2009 - Aug/2010
Shaviovik River	DBS2	Coastal Plain	Bullen	Shaviovik	14	70° 4'17.40"N 147°17'30.84"W	May/2009 - Aug/2010
No Name River (U1)	DBS3	Coastal Plain	Bullen	No Name	17	70° 3'45.00"N 147°11'46.68"W	May/2009 - Aug/2010
South White Hills	DFM1	Foothills	Kuparuk Foothills	Kuparuk	293	69° 12' 2" N 149° 33' 30" W	Jul/2006 – present
White Hills	DFM2	Foothills	Kuparuk Foothills	Kuparuk	337	69° 29' 11" N 149° 49' 17" W	Jul/2006 – present
North White Hills	DFM3	Coastal Plain	Kuparuk Foothills	Kuparuk	84	69° 42' 53" N 149° 28' 13" W	Jul/2006 – present
Northwest Kuparuk	DFM4	Coastal Plain	Kuparuk Foothills	Kuparuk	124	69° 56' 51" N 149° 55' 0" W	Jul/2006 – present
Itikmalakpak	DUM1	Mountains	Umiat Corridor	Anaktuvuk	1168	68°17'24" N 151° 6'54.00"W	Jun/2009- present
Upper May Creek	DUM2	Mountains	Umiat Corridor	Anaktuvuk	1378	68°23'54.60"N 150°13'39.84"W	Jun/2009- present
Nanushuk	DUM3	Foothills	Umiat Corridor	Anaktuvuk	540	68°43'14.52"N 150°30'10.80"W	Jun/2009- present
Tuluga	DUM4	Foothills	Umiat Corridor	Anaktuvuk	497	68°48'14.76"N 151°32'45.60"W	Jun/2009- present
Encampment Creek	DUM5	Mountains	Umiat Corridor	Chandler	1224	68°17'11.34"N 152° 7'54.36"W	Sept/2010- present
White Lake	DUM6	Mountains	Umiat Corridor	Chandler	1081	68°21'46.56"N 152°42'24.36"W	Sept/2010- present
Hatbox Mesa	DUM7	Foothills	Umiat Corridor	Chandler	624	68°45'15.48"N 152°34'22.80"W	Sept/2010- present
Siksikpuk River	DUM8	Foothills	Umiat Corridor	Chandler	463	68°37'48.36"N 152° 6'7.92"W	Sept/2010- present
Rooftop Ridge	DUR9	Foothills	Umiat Corridor	Anaktuvuk	745	68°54'1.38"N 150°57'50.76"W	Jun/2009- present
Itkillik River	DBS1	Foothills	Umiat Corridor	Itkillik	420	68°51'59.46"N 150° 2'24.00"W	May/2009- present
Anaktuvuk River	DBS2	Foothills	Umiat Corridor	Anaktuvuk	81	69°27'51" N 151°10'07"W	May/2009- present
Chandler River Bluff	DBS3	Foothills	Umiat Corridor	Chandler	86	69°15'42.60"N 151°23'45.60"W	May/2009- present
Chandler River Water	DBS3w	Foothills	Umiat Corridor	Chandler	62	69°17'0.30"N 151°24'16.14"W	May/2011- present
Imnavait	IB	Foothills	NSF	Kuparuk	897	68° 36' 48" N 149° 19' 3" W	Aug/1986 - present
Upper Kuparuk	UK	Foothills	NSF	Kuparuk	778	68° 38' 24.5" N 149° 24' 23.4" W	Aug/1993 - present
Upper Headwaters	UH	Foothills	NSF	Kuparuk	968	68° 31' 19.8" N 149° 20' 18.0" W	May/1996- Aug/2010
North Headwaters	NH	Foothills	NSF	Kuparuk	904	68° 36' 04.8" N 149° 25' 52.8" W	May/1996- Aug/2010
East Headwaters	EH	Foothills	NSF	Kuparuk	919	68° 35' 04.7" N 149° 18' 21.6" W	May/1996- Aug/2010
West Headwaters	WH	Foothills	NSF	Kuparuk	1027	68° 33' 48.0" N 149° 24' 30.0" W	May/1996- Aug/2010
Green Cabin Lake	GCL	Foothills	NSF	Kuparuk	908	68° 32' 01.0" N 149° 13' 47.4" W	May/1996- present
West Kuparuk	WK	Foothills	NSF	Kuparuk	159	69° 25' 34.3" N 150° 20' 25.3" W	Jul/1995 - Jul/2008
Sagwon Hill	SH	Foothills	NSF	Sagavanirktok	275	69° 25' 27.5" N 148° 41' 45.1" W	Aug/1986 - present
Franklin Bluffs	FB	Coastal Plain	NSF	Sagavanirktok	71	69° 53' 31.8" N 148° 46' 4.8" W	Aug/1986 - Present

Station Name	Station ID	Region	Project	Basin Name	Elevation (m)	Coordinates	Period of Record
Betty Pingo	BM	Coastal Plain	NSF	Kuparuk	15	70° 16' 46.3" N 148° 53' 44.5" W	Jun/1994 - present
West Dock	WD	Coastal Plain	NSF	Near Kuparuk	5	70° 22' 50" N 148° 33' 39" W	Jul/1995 - Oct/2009
Putuligayuk	Put	Coastal Plain	NSF	Putuligayuk	9	70°16'3.03"N 148°37'48.48"W	Jun/1999 - present

Figure 2. The Anaktuvuk station (DUS2) is an example of a hydrometeorological station.

3.1 Air Temperature and Relative Humidity

Air temperature and relative humidity are measured with a Campbell Scientific HMP45C Temperature Relative Humidity Sensor. These probes are housed in a 12-gill self-aspirating radiation shield and mounted at a height of 2 m. The reported temperature operating range is -40°C to +60°C, with accuracy typically ±0.3°C and a worst-case accuracy of ±0.5°C. The relative humidity operating range is 0–100%, with accuracy at 20°C of ±2% from 0–90% and ±3% from 90–100%. Rime ice accumulations can affect the air temperature and especially the relative humidity reading. Accumulating rime insulates the sensors within the radiation shield, isolating them from ambient conditions. Should this occur, air temperature readings would be slightly affected in the time required to respond to changes in the ambient air temperature, and relative humidity would be greatly affected by being isolated from ambient conditions. Recorded humidity is related to the vapor pressure of the surface of the rime ice adhering to the radiation

shield and the wire mesh inner enclosure surrounding the relative humidity sensor, and is not indicative of actual ambient conditions.

Since the HMP45C sensor is not designed to give readings below -40°C/F and it is necessary to have backup sensors as well as multiple sensors for QA/QC, three YSI series 44033 thermistors were installed in a 6-gill radiation shield at a height of 2 m. The operating range of the three sensors is -80°C to +75°C (-112° to 167°F). These sensors are used if the temperature drops below -40°C/F or when the primary air temperature sensor (HMP45C) is malfunctioning.

3.2 Wind Speed and Direction

Wind speed is measured using an RM Young 05103 anemometer, mounted at a height of 3 m. The starting threshold of the wind measurement is 1.0 m/s (2.2 mph), accuracy ±0.3 m/s (0.6 mph), and operating range of 0–60 m/s (0–134 mph). The wind-direction vane range is 0–360° with ±3° accuracy and a starting threshold at 10° displacement of 1.1 m/s (2.2 mph). Field calibration tests of the wind speed sensors are difficult to obtain. Suspect sensors are replaced and sent to the manufacturer for calibration and replacement of bearings. Additionally, the heading of the wind-direction sensors are checked periodically each year by pointing the vane at aiming points for four compass points. There are problems of note at these remote sites pertaining to wind speed and direction measurements. The most significant of these problems are rime ice and freezing precipitation that can alter the aerodynamics of the sensors and possibly stop them completely. Prolonged periods of calm and/or constant wind direction are rare at the stations and should not be considered in the data as indicators of these conditions. However, since the stations are unmanned, it is possible that a calm period could occur. Rime ice and freezing precipitation can occur during any season, but they occur most commonly during late fall, winter, and spring. Sensors are cleaned at each site visit, but due to the remoteness of the stations, visits are 6-12 months apart. Another problem, specific to the wind sensors, is perching birds. Since these sites are located in treeless tundra, large birds including ravens, rough-legged hawks, eagles, and snowy owls can damage vanes and anemometers by repeatedly perching on them. Perching rarely causes data loss but may slightly affect the accuracy of the wind vanes if they are bent.

3.3 Net Radiation

Net radiation is measured with a Kipp and Zonen NR-Lite Net Radiometer at all Bullen and Umiat Corridor/Foothills stations. The operating range of the Kipp and Zonen instrument is ±2000 W m^{-2}. The sensitivity is reported as 10 uV $W^{-1}m^2$. The spectral response range is reported by the manufacturer as 0 to 100 uM. Temperature range for the instrument is -30° to 70°C (-22° to 158°F). The calibrated accuracy of this instrument, which was not reported by the manufacturer, varies with temperature, wind, and sensor symmetry. Sensor readings are corrected for errors caused at high wind speeds. The instrument is installed at a height of approximately 2 m and oriented to the south to minimize shadow effect from the mounting pole. Keeping the sensor level is a challenge, especially at summer's end when the active layer thaw is at a maximum.

3.4 Summer Precipitation

Summer precipitation is recorded at each meteorological station with a Texas Electronics (TE) 525WS or 525MM tipping-bucket gauge surrounded by an Alter (wind) shield. The gauge catches precipitation in an 8-inch-diameter collector, and the water is funneled into the tipping bucket. Once the bucket is full of water, it tips and empties, and each tip is recorded by the datalogger. The gauge is typically installed at a height off the ground of 0.7–1.0 m (2.3–3.3 ft). The resolution of the TE525WS tipping bucket gauge is 0.254 mm (0.01 in.), and the accuracy is 1% up to 25.4 mm/hr (1 in./hr), +0 to -3.0% for 25.4–50.8 mm/hr (1 to 2 in./hr) and +0 to -5% for 50.8–76.2 mm/hr (2 to 3 in./hr) rainfall rates. The TE525MM resolution is 0.1 mm per tip, and the accuracy is 1% up to 25.4 mm/hr, +0 to -2.5% for 25.4–50.8 mm/hr, and +0 to-3.5% (50.8–76.2 mm/hr), with greater undercatch as intensity increases; this does not include the impact of wind or other environmental factors. A known problem with most precipitation gauges is the undercatch of precipitation. Undercatch may occur during low-intensity or trace rainfalls (not enough precipitation to tip the bucket, and evaporation occurs) or high-wind events during which the gauge alters the path of rain particles. Undercatch may also occur due to evaporative wetting losses from the gauge. We recognize that this is a potential source of error, particularly for hydrological analysis and modeling of runoff, but we have not yet examined this problem in

detail for the Bullen and Kuparuk Foothills stations. An additional potential error is due to the installation of the gauge. During site visits, we observed that the gauge is not level because it is attached to a single pole in the ground and guy wires often become loose as the active layer thaws. Improvements to the installation are required to decrease potential measurement errors.

3.5 Snow Depth

The study domain includes (from east to west) the Bullen Point region, Shaviovik River, Kadleroshilik River, Sagavanirktok River, Kuparuk River, Itkillik River, Anaktuvuk River, and Chandler River basins. The snow-monitoring network includes of twenty-two meteorological stations (funded through the Bullen/Foothills/Umiat studies), each equipped with a sonic snow depth sensor (Figure 1, Table 2). Twelve stations in the Sagavanirktok and Kuparuk River basin were established in August 2006. Five stations were established in the Anaktuvuk River basin in June 2009, and five stations were installed in the Chandler River basin in September 2010. The snow depth sensor type is a Campbell Scientific Sonic Ranger SR50 or SR50(A). The only difference between the SR50 and the SR50(A) is the housing that encases the ultrasonic sensor. The sensor emits a 50 kHz sound pulse and measures the time the pulse takes to return to the sensor. Ultrasonic sensors can measure the distance to any reflective surface, like the ground or water, but sensitivity of the SR50(A) is designed for measuring distance to a snow surface.

Table 2. Meteorological stations with an SR50 snow depth sensor included in this report.

	Site Name	General Location
1	Accomplishment Creek (DBM1)	Sagavanirktok River, Brooks Range
2	Ribdon (DBM2)	Sagavanirktok River, Brooks Range
3	Juniper Creek (DBM3)	Shaviovik/Kavik River, Brooks Range
4	Sag-Ivishak (DBM4)	Sagavanirktok River, Foothills
5	Upper Kadleroshilik (DBM5)	Kadleroshilik River, Foothills
6	Kavik (DBM6)	Shaviovik/Kavik River, Foothills
7	Lower Kadleroshilik (DBM7)	Kadleroshilik River, Coastal Plain
8	Bullen (DBM8)	Bullen Point, Coastal Plain
9	South White Hills (DFM1)	Kuparuk River, Foothills
10	White Hills (DFM2)	Kuparuk River, Foothills
11	North White Hills (DFM3)	Kuparuk River, Foothills
12	Northwest Kuparuk (DFM4)	Kuparuk River, Foothills
13	Itikmalakpak (DUM1)	Anaktuvuk River, Brooks Range
14	Upper May Creek (DUM2)	Anaktuvuk River, Brooks Range
15	Nanushuk (DUM3)	Anaktuvuk River, Foothills
16	Tuluga (DUM4)	Anaktuvuk River, Foothills
17	Anaktuvuk (DUS2)	Anaktuvuk River, Foothills
18	Encampment Creek (DUM5)	Chandler River, Brooks Range
19	White Lake (DUM6)	Chandler River, Brooks Range
20	Hatbox Mesa (DUM7)	Chandler River, Foothills
21	Siksikpuk (DUM8)	Chandler River, Foothills
22	Chandler River Bluff (DUS3)	Chandler River, Foothills

The method for measuring snow depth with the SR50 is simple subtraction. When there is no snow on the ground, the distance measured is the sensor's height above the ground. When snow has accumulated under the sensor, the distance measured is to the snow surface. The difference between distance-to-ground and distance-to-snow is used to calculate snow depth. For example, if the sensor height above the ground is 100 cm and the new distance to surface is 90 cm, then subtracting 90 cm from 100 cm gives a snow depth of 10 cm under the sensor.

It is important to understand the problems of measuring and processing any observational data. Particular to ultrasonic snow-depth sensors is high-frequency small-amplitude noise, which is inherent in this technology and can be an impediment to accurate snow-accumulation measurements in real time (Brazenec, 2005). For example, since the speed of sound in air is affected by the air temperature it is traveling in, an air temperature measurement is required to correct distance readings. Additionally, sensor-mounting height can influence data quality, with higher mounting heights resulting in noisier data. Inaccuracies also can be caused by poor calibration and/or environmental weathering of the sensor. Physically related errors include high wind, falling snow, low-density snow, blowing snow, difficulty in establishing a zero point due to tussocks, low shrubs, grass, etc., and changes in sensor height due to ground heave and

wildlife curiosity. Diligent field practices are essential for accurate measurements and for post-processing data correction and QA/QC purposes.

Field procedures include:

- Measuring the distance from the bottom of the sensor to the ground
- Measuring snow depth under the sensor
- Measuring the sensor to snow surface
- Conducting snow surveys near the station (50 snow depths and 5 densities/snow water equivalent)
- Inspecting the sensor and supporting structure for proper leveling and structural soundness
- Inspecting the sensor for corrosion and ice accumulation

3.6 Field Snow Survey

Our snow surveys include gravimetric snow water equivalent (SWE) sampling and snow depth measurements collected over an area of 25 m by 25 m; this technique is often referred to as *double sampling*. The snowpack in Alaska is extremely heterogeneous, with snow depth more variable than density (Benson and Sturm, 1993). Usually, double sampling yields an areal SWE estimate with a lower variance than is possible using collected snow cores only. Rovansek et al. (1993) showed that double sampling provides improved SWE estimates; they recommended sampling 12 to 15 snow depths for each snow core. This optimal ratio of snow depths to water equivalent, however, appears to vary greatly (from 1 to 23), depending on site, weather, and snow conditions. Currently, we use an optimal ratio of 10; that is, 50 depths accompany 5 snow cores.

Snow cores are sampled using a fiberglass tube ("Adirondack") with an inside area of 35.7 cm^2, equipped with metal teeth on the lower end to cut through dense layers of snow. The advantage of the Adirondack for shallow snowpack is that its diameter is larger than many other types of snow tubes (like the Mt. Rose); thus, it provides a larger sample of the shallow Arctic snowpack. To obtain a complete snow core, the Adirondack tube is pushed vertically through the snow while turning, until soil is encountered. At this point, snow depth is recorded. The tube is then

driven further into the organic layer and tipped sideways, retaining a vegetation plug; this method ensures that the complete snow column was sampled. The vegetation plug is removed and the snow is either collected for weighing later in the laboratory or weighed in the field.

We use constant 50 m lengths for the snow depth course, with a 1 m sampling interval along an L-shaped transect. Twenty-five depth measurements are made on each leg of the L; this strategy is used to account for the presence of snowdrifts in the area of measurement. The directions of measurement are chosen randomly. Snow depth measurements are made using a T-shaped graduated rod (T-probe). The probe is simply pushed through the snow to the snow-ground interface.

Snow water equivalent is defined as:

$$SWE = SD * (\rho_s / \rho_w) \quad (1)$$

where ρ_s is average snow density from the 5 snow core samples, ρ_w is water density, and *SD* is an average of 50 snow depths.

3.7 Soil Temperature and Moisture

Soil temperature and unfrozen soil-moisture content data are monitored at 10 stations in the Bullen and Umiat Corridor/Foothills monitoring network. Several sites in the mountainous region are not instrumented for soil temperature and moisture because they are too rocky for installation. Soil-water content is monitored at each station with Campbell Scientific, Inc. CS616 TDR-type sensors at depths of 10, 20, 30, and/or 40 cm. The installation depths at some sites vary slightly due to soil conditions during sensor installation. The soil-water content sensors are installed horizontally with minimal soil disturbance. Factory calibration is used to convert raw readings to volume-fraction water content. TDR-type sensors respond to the soil dielectric constant, and since ice has a dielectric constant similar to dry soil, the sensor effectively responds to changes in unfrozen soil-water content. For greatest accuracy, soil-water content

sensors should be calibrated specifically to each soil, especially under conditions that depart from normal (Campbell Scientific, Inc., 2006). Although the absolute soil-water content may differ from that given by the factory calibration, the relative water content and the behavior of phase change in relation to temperature should be accurate. Hourly readings of unfrozen soil-water content are recorded.

Soil temperature is monitored at each station with YSI thermistors, mounted in a string at intervals to provide temperatures at 0, 5, 10, 15, 20, 40, 60, 80, 100, 120, 135, and 150 cm below the soil surface. The soil temperature string is placed into a hole drilled into the soil, and the evacuated soil is used to backfill the hole. Hourly readings of soil temperature are recorded.

3.8 Water Levels

Water level stations for the Bullen project are at the Kadleroshilik (DBS1), Shaviovik (DBS2), and No Name (DBS3, also known as Unnamed 1) Rivers. These three stations were previously monitored by PND during the 2005 and 2006 spring break-up for ADOT&PF. UAF observed water levels and discharge at the stations from spring 2009 through August 2010. Water level stations for the Umiat Corridor project were installed at the Itkillik (DUS1), Anaktuvuk (DUS2), and Chandler (DUS3) Rivers in spring 2009 before the road river crossings were established by ADOT&PF, and may be up to 16 km (10 mi) from the present proposed river crossing. In spring 2011, the water level station at the Chandler River was relocated downstream approximately 1.7 km (1.0 mi). Station locations are selected based on whether discharge can be safely and accurately measured during flood events. Water level (also known as river stage) is measured continuously with pressure transducers, and discharge measurements are individual point measurements in time. Point measurements of water levels are also collected with traditional surveying equipment and staff gauges. A rating curve is developed to establish a relationship between the stage and the discharge in order to predict the discharge at a particular river stage site. In addition to quantitative measurements, hourly photographs from cameras at the stations help us to evaluate the water levels in the rivers, observe ice conditions during break-up, and monitor the weather for field logistics.

Water levels are measured with two Instrumentation Northwest, Inc., Aquistar PT12 (SDI12) pressure transducers at each station, with one or two HOBO U20 water level logger pressure transducers for backup, located at or near the station. Measurements are made every 15 minutes, and an average water depth or pressure is reported. Water depth above the pressure transducer is reported by the datalogger and is converted into water level elevations (above the reference datum GEOID09AK) during post-processing.

Manual water level measurements consist of staff gauge readings or "tape downs," which are measurements from the top of a reference point such as rebar to the water surface. The staff gauge and rebar are surveyed to the datum as well. These discrete measurements of water level are used to adjust the continuous pressure transducer data to the datum and for verification purposes.

Cameras located at the surface water station take an image every hour (or more frequently as needed) to capture the river stage and weather conditions. A Campbell Scientific CC640 camera is used, and images are transmitted to the base station and uploaded to the project website each hour. The photos are used during the field season to observe river stage and ice conditions, and to corroborate the pressure transducer data. If the pressure transducer is not working properly, we can review the photographs to qualitatively confirm the river stage.

The vertical datum for water level elevations is GEOID09AK. Long-term static differential GPS surveys are conducted to determine the elevations of temporary benchmarks, reference points, and staff gauges at each station. A Trimble R8 and Trimble 5700 are used to conduct the survey. Continuously Operating Reference Station (CORS) base stations at Deadhorse, Barrow, and Sag River DOT are used during post-processing. Traditional level loop surveys are conducted on each trip to tie the water surface and staff gauges to the temporary benchmarks (with a known elevation).

Table 3 shows the accuracy specifications for the Aquistar and HOBO pressure transducers. Errors associated with the pressure transducer itself are generally less than 1 cm under ideal

conditions. Additional errors associated with the pressure transducer unit may occur if the sensor does not have a secure installation and is moving in the water.

Table 3. Specifications for the pressure transducers used during the study.

Sensor	*Full Scale Range*	*Accuracy (typical)*	*Accuracy (typical)*	*Water Level Range*
Aquistar	0-15 PSI Gauge	0.06% Full Scale	0.009 PSIG, 0.6 cm	0-10 m
Aquistar	0-5 PSI Gauge	0.06% Full Scale	0.003 PSIG, 0.2 cm	0-3.5 m
HOBO	0-21 PSI Absolute	0.075% Full Scale	0.016 PSIA, 0.3 cm	0-4 m

The two largest errors with manually measuring water levels are generally (1) surveying and vertical datum issues and (2) mistakes during manual measurements (i.e., reading staff gauges). Staff gauges may be read incorrectly, but it also may be difficult to read the staff gauge because of wave action that may yield an error in the water level of up to plus or minus several centimeters. We recognize that movement of the temporary benchmarks and staff gauges may occur from frost heave, ice damage, etc. Multiple level loop surveys and the use of static differential GPS survey to compare the temporary benchmark elevations from year to year help pinpoint movement.

All water level measurements are affected by ice or snow in the channel, which displaces water. This is important to be aware of during spring break-up and the winter months, because during this time, the rating curve is not valid since the channel geometry can be altered significantly due to the presence of ice or snow. During spring break-up, we take discharge measurements as frequently as possible and do not rely solely on the rating curve to calculate continuous discharge. The shift in the control during ice-affected measurements is visible in the rating curve; when the stage and discharge are plotted, the points will fall consistently above the rating curve (stage is higher for the same discharge when affected by ice).

3.9 Discharge Measurements

3.9.1 Acoustic Doppler Current Profiler

Discharge measurements are conducted at or near the station on each river using the acoustic doppler current profiler (ADCP) technique. Measurements are made by driving or paddling a boat slowly across the river along a transect. Typically at least four transects are made, and an

average discharge is calculated from the multiple transects. At times of high flow, the transects may be in an oblique angle (diagonal and downstream direction) across the river. Whenever possible, two transects from the left to right bank and two transects from the right to left bank are made to calculate river discharge and determine any directional bias. When the coefficient of variation (standard deviation / mean) of the four measurements is less than 5%, an average is calculated. If the coefficient of variation is greater than 5%, additional transects/measurements are made.

Both ADCP bottom tracking and GPS options are used to measure river velocity. If bottom tracking is used, a moving bed test is generally conducted in order to correct for a moving bed. However, if a moving bed may be an issue, the GPS reference is used. The GPS used is a Novatel Smart V1-2US-L1. Typically, a base station is set up and a real-time kinematic (RTK) GPS is used, but satellite-based augmentation system (SBAS or WAAS) differential correction is also used and is considered acceptable (Wagner and Mueller, 2011). The horizontal position accuracy of the RTK is 0.2 m and 1.2 m when using SBAS/WAAS.

The ADCPs used in 2009, 2010, and 2011 are the RDI Streampro, RDI Rio Grande, Sontek River Surveyor, and Sontek Flowtracker units. The Streampro is most useful in shallow water (less than 5 m), and the Rio Grande is used if the water depth is greater than 5 m.

Once enough discharge measurements are collected at a station, a stage-discharge relationship (rating curve) is developed to calculate the discharge for a range of stages. The stage is plotted against the discharge and a best-fit curve is fitted through the points (and represented by an equation) on both normal and logarithmic scales. We attempt to collect discharge measurements at many different river stages in order to have a good relationship at all river stages. Extrapolation for low and high flows is necessary due to the lack of measurements in these ranges of the curve. Caution is used in extrapolating the discharges at high stages due to changes in the control at high stage. Once the stage increases above the banks (over bankfull conditions) onto the floodplain, the channel geometry changes, and the stage-discharge relationship developed for the channel is no longer valid. Also, since the geometry of the channel controls the relationship we try to make the measurements in the same location each time. However, due to a

dynamic river channel during break-up, it is not always possible to measure the same river location each time. Changes in water flow paths at low versus high stage, multiple channels during high stage, and ice in the channel make it problematic to measure discharge at exactly the same location each day. It is common to have a shifting control, and therefore many measurements need to be made, along with adjustments (shifts) to the rating curve. At this time, our rating curves and continuous discharge estimates are preliminary because we only have a limited number of measurements to use on the rating curve.

The biggest challenge associated with making a good quality ADCP discharge measurement is locating a single straight parabolic cross section of the river with steady and uniform flow. A bad measurement section usually results in poor data quality. This is primarily a problem during the spring flood when ice is present in the channels, when flows may be high and unsteady, and when the river consists of multiple channels.

Technical problems and limitations of the ADCP and associated equipment are other factors that degrade the quality of the measurement. Technical problems may include GPS problems, radio communication failures, and incorrect baud rates. Typical ADCP limitations include turbulent water, too much or too little sediment in the water column, or insufficient water depth for use of a particular ADCP. However, we believe that ADCP measurements are far superior to traditional current meter measurements because the number of ADCP velocity measurements through the cross section is so much greater than could be measured with a conventional current meter.

The following field procedures occur before the ADCP discharge measurement:

- ADCP diagnostic and quality tests
- Moving bed test
- Compass calibration for GPS
- Assessment/description of the river reach characteristics for suitability of ADCP measurement

The following are reviewed during both quality assurance and control of the data:

- Measurement reach characteristics

- ADCP configuration
- Review of each transect and set of velocity contours for bad/lost velocity data
- Determine percentage of flow that is measured vs. estimated
- Review moving bed test and adjust discharge as needed
- Assess GPS quality if GPS is used
- Check each transect for consistency (discharge, area, width, boat speed, water speed, flow direction, measurement duration, etc.)
- Check that the transect coefficient of variation for discharge is within 5%

After the measurement at a site is reviewed, a quality rating that is both qualitative and quantitative is assigned to that measurement. The quality rating is based on both the transect coefficient of variation (i.e., measurement repeatability) and the overall general quality of the measurement (such as the river reach characteristics, ADCP limitations, transect consistency, etc.). The quality rating given to each measurement is either excellent (2%), good (5%), fair (8%), or poor (10% or more). These quality ratings are carried over to the rating curve.

Errors in water level and discharge measurements propagate to the rating curve. We assign quality indicators to each measurement and use these during the rating curve development. The complex and dynamic nature of these river channels adds additional uncertainty to the rating curve. Changes in the discharge measurement location may occur due to changes in stage that result in river access problems (i.e., too shallow to drive a boat), braiding of the river channel, and even safety issues. The change in the measurement cross section is not ideal and results in more uncertainty (and shifts) in the rating curve; however, there is probably little measurable change in flow between the measurement sites (typically they are all within a kilometer of the station).

Shifts can be applied to the rating curve when there is a change in channel shape or a change in the control. Channel shape can change during spring break-up when the river is affected by ice or during periods of sediment aggradation and degradation. However, at this time we have not applied shifts to the rating curve because additional measurements are still needed to better define the curve.

Additional errors may occur during the extrapolation of the rating curve beyond the highest or lowest measured discharge. It is typical that none or few measurements occur at the highest flows (for either safety reasons or we are not present during the high flows), so we extend the rating curve to these higher stage discharges. However, the rating curve may not be extended too high without consideration of the river cross section and changing controls. As we collect additional measurements and a better understanding of the river geometry and behavior, our rating curve will likely improve.

3.9.2 Dye Trace

The measurement of river flow during spring break-up is one of the primary goals of this project. However, due to the relatively high water velocities and presence of moving ice in the channels during the period leading up to peak flow, the collection of velocity and discharge data via boat-mounted ADCPs can at times be hazardous. As a result, we are employing and refining a dye tracer technique to allow us to measure flows without entering the water. The objective of this activity is to supplement ADCP measurements at times when river conditions will not allow us to safely enter the water. When feasible, we perform both the dye tracer and ADCP measurements in parallel to allow for a comparison of results.

The dye tracer technique has been used to measure streamflow for over a century, and studies are well described in a USGS summary publication by Kilpatrick and Cobb (1985), which was the primary reference from which our methods were developed. In short, through the addition of a known mass of dye at an upstream location, followed by an intensive sampling effort at a downstream location, the amount of water into which the dye is diluted (i.e., the flow) can be calculated. In this study, we injected the dye as an instantaneous slug and measured the downstream concentration at discrete time intervals. Other variations of the technique call for a continuous upstream dye injection followed by only a single downstream measurement of the plateau concentration. In both methods, the distance between injection and sampling locations must be sufficient for the dye to be considered well-mixed from bank to bank.

While previous researchers have employed dyes, salts, and even radionuclides as tracers, we used the fluorescent dye Rhodamine WT for our study. Rhodamine WT is ecologically inert, formulated and certified for use in surface waters, and detectable at extremely low concentrations (approximately 0.1 ppb) as compared with salts. Indeed, while the dye formed a vivid magenta plume at the point of injection in our studies, it was invisible to the naked eye by the time it reached the sampling point.

Due to the need for dye in excessive amounts, dye tracer measurements are not often attempted on flows as large as the break-up flows observed in this study's three rivers. Consequently, the dye measurements are considered a developmental component of the overall study. Accordingly, all dye measurements are limited to the Itkillik River in order to evaluate the method prior to broader applications. Due to its lower discharge, the Itkillik is more amenable to tracer studies than the Anaktuvuk and Chandler. Additionally, the Itkillik was observed to be more turbulent and potentially more hazardous than the other two rivers during the springtime flood.

3.9.2.1 Injection Methods

As discussed, all dye application events in this study utilize the slug injection method rather than the continuous injection method. However, we modified the manner in which the slug was injected over the course of the study in order to evaluate the impacts of the various injection methods upon test results. The dye has been injected as a mixed liquid in all cases thus far. During the first application event, a commercial liquid dye containing 20% Rhodamine WT was injected directly into the flow. In all remaining trials, powdered Rhodamine WT was premixed in an aliquot of river water prior to injection. During three application events, the dye was injected at a single point (point injection) in the flow from either the right bank (one event) or a gravel bar in the middle of the channel (two events). In the remaining three application events, an attempt was made to distribute the dye laterally across the stream at the time of injection. In the first distributed injection event, dye was poured from a manned watercraft while ferrying across the river. In the second two distributed injections events, a fire pump was employed to spray and distribute the slug into the main channel from the right bank. Illustrations of the injection methods are presented in Figure 3 through Figure 5.

Figure 3. Researchers utilized the point slug injection method from a midstream gravel bar on May 25, 2011.

Figure 4. A cataraft was employed to distribute dye during the first application event on September 4, 2010.

Figure 5. In two trials, a fire pump was utilized to distribute dye from the bank (May 20, 2011).

3.9.2.2 Sampling Methods

The methods used to collect downstream water samples remained relatively consistent over the course of the study. During the first application event (low flow), a sampling container was attached to a length of rope and tossed into the main channel from the left bank. Samples were retrieved at approximately 1-minute intervals and stored in 50 mL glass vials for same-day analysis.

The sampling protocol used for all remaining application events employed a modified 250 mL high-density polyethylene (HDPE) sampling bottle, casted and retrieved from the river using standard fish angling apparatus (Figure 6). The sampling device was designed to sink below the water surface upon insertion into the flow. A corking mechanism was installed to minimize inflow after tension was applied to the line, thus ensuring that water samples were collected only at the point of sampler insertion. This allowed water samples to be collected at discrete intervals across the river.

As discussed, a single set of samples was collected from midstream during the first application event. For all remaining application events, multiple samples were collected throughout the sampling period from discrete spatial intervals across the river. This replication was necessary in order to evaluate whether sufficient mixing had occurred at the downstream sampling location. In order to accomplish this evaluation, a lateral transect across the river was divided into sections (right bank, midstream, and left bank), and each sample was labeled according to the section of the river from which it was collected.

The right bank sample was collected at approximately one-quarter of the distance from the right to left bank; the midstream sample was collected in the approximate middle of the channel; and the left bank sample was collected at approximately three-quarters of the distance from the right to left bank. During the second application event, samples were collected from all three spatial intervals. After evaluation of the data revealed that lateral mixing was likely sufficient, samples for all remaining application events were collected from the right bank and midstream intervals only.

Figure 6. Sampling apparatus used to collect water samples at discrete intervals across the river.

3.9.2.3 Experimental Trials

Six dye tracer applications were performed on the Itkillik River during the study (Table 4). The first trial (T0) was conducted under low flow conditions in autumn 2010 in order to evaluate whether the method produced results similar to a simultaneous ADCP discharge measurement. The remaining trials were performed during the period surrounding the spring melt event in 2011. In all trials, dye was injected into the river near the Itkillik hydrometeorological station. Specific injection locations were modified from trial to trial based upon flow conditions and river access. During all springtime application events, samples were collected at the proposed road crossing location, approximately 6.6 km downstream from the hydrometeorological station, near temporary benchmarks labeled ITKIL1 and ITKIL2 (LS 11297, 2010, DOT/PF). During the low flow event, samples were collected approximately midway between the meteorological station and the proposed crossing location. The reach length term in Table 4 describes the approximate distance traveled by the flow between the injection and sampling points.

Table 4. Experimental trials used for dye tracer measurements.

Trial #	Date of Injection	Time of Injection	Quantity of Dye Added (g)	Slug Injection Method	Reach Length (km)	Flow Description
T0	9/4/2010	15:53	238	Distributed (cataraft)	3.73	Low flow (autumn)
T1	5/20/2011	17:05	1,338	Distributed (fire pump)	6.60	Spring flood rising limb
T2	5/22/2011	15:05	3,819	Point (midstream)	7.56	Spring flood rising limb
T3	5/25/2011	16:15	3,120	Point (midstream)	7.76	Spring flood near peak
T4	5/29/2011	15:40	2,662	Distributed (fire pump)	6.38	Spring flood falling limb
T5	5/31/2011	10:52	2,029	Point (right bank)	6.38	Spring flood falling limb

3.10 River Sediment

In a small, highly complementary study (funded by the Alaska University Transportation Center (AUTC) at the University of Alaska, we proposed to investigate the feasibility of monitoring the sediment dynamics of three major rivers (same three rivers that are gauged in this study) crossed by the proposed road to Umiat. Basically, we are looking at quantifying both the suspended and bed sediment fluxes at three sites in remote Arctic Alaska. Limited sediment studies have been performed in this part of the world.

3.10.1 Suspended Sediments

Suspended sediment samples were taken with an Isco 3700 Portable Autosampler on the Anaktuvuk, Chandler, and Itkillik Rivers; grab samples were also taken on all rivers when staff were on-site stream gauging, with the majority of these taken during break-up when autosamplers could not be deployed because of ice conditions. During the spring break-up, Isco samples were taken every six hours; from early June to September, a sample was taken with the autosampler once daily at 15:00 ADT. The samplers were moved multiple times throughout the spring break-up, but were installed in permanent locations from June through September. During this time, the intake hose was clamped to rebar and located roughly six inches above the riverbed.

Several problems occurred with the autosamplers in this unpredictable environment that is the North Slope. It is unfeasible to suspend the intake at a constant height above the bed during break-up due to the debris and ice carried by the river, the frozen nature of the bed, and the high water levels. Large gaps occur in the data set in the early summer. The Chandler River Isco was disconnected from its battery, presumably by an animal, while the Itkillik Isco tipped over during high flow when it was inundated. The fact that the Iscos can take only a maximum of twenty-four samples created periods without data, as the sites were not visited every twenty-four days. To address the breaks in data between visits, two Iscos will be deployed at each river in the summer of 2012, with each Isco taking a sample every forty-eight hours, staggered to have one sample per day. With this method, there can be 48 days of continuous data without a site visit, and if one sampler is disrupted, the density of sampling will be reduced, but a broad picture of sediment load can still be achieved with samples collected every other day.

Integrated suspended sediment samples were also taken on the Anaktuvuk and Chandler Rivers using a Rickly Hydrological depth-integrating sampler (Model DH76), with a one-quarter inch nozzle. By taking an average of two samples per day during break-up with the integrated sampler, a representation of sediment load throughout the water column can be achieved. This method also addresses the problem of the Isco hose being on the riverbed during break-up,

allowing for a comparison between the Isco and integrated samples in order to ensure that the Isco samples accurately represent the sediment load in the rivers.

Samples taken by the Iscos and the integrated sampler are analyzed in the lab to determine total suspended solids (TSS). Following ASTM Standard 3977-97, the samples are vacuum filtered through Whatman GF/C glass microfiber filters, with a particle retention of 1.2 μm. The percentage of organic matter in each sample is then determined using ASTM Standard 2974 (Test Method C), in which samples are placed in a muffle furnace at 440°C for twelve hours. For this study, only the inorganic solids, referred to as TSS, were considered.

3.10.2 Turbidity

Campbell Scientific OBS-3+ turbidity sensors were also installed at the Anaktuvuk, Chandler, and Itkillik stream gauging sites on July 10, 2011. These sensors have optics on the side of the body, which emit a near-infrared light to detect turbidity levels in the water. Operating at wavelengths of 850 nanometers (±5 nm), these sensors are capable of measuring turbidity levels from 0 to 4000 NTUs (nephelometric turbidity units). Turbidity readings have an accuracy of 2% of the reading or 0.5 NTU, whichever is greater. Installation involved mounting the sensor on rebar driven into the streambed, with the optics facing the middle of the channel and 180° away from the rebar. The sensor was installed roughly 15 cm above the channel bed on all three rivers, and in close proximity to the intake of the Isco sampler. Each turbidity sensor was electrically connected into the surface-water observation station datalogger at each river to record readings at 15-minute intervals; data were then transmitted via radio telemetry back to UAF/WERC. In the fall, the turbidity sensors were removed from each river, with reinstallation planned for the spring of 2012.

We did not know how well these sensors would work in the arctic environment. One additional and costly component of the sensor is a wiper to occasionally clean off the optical window. We did not equip the sensors with wipers, because we felt that growth on the window would not be a problem in this nutrient-poor environment. However, it was clear from the data that just after 7 to

10 days the turbidity reading was in error (turbidity reading increasing while the flow was decreasing). For the summer of 2012, we will install wipers on all of the turbidity sensors.

3.10.3 Bed Sediment Distribution

The bed sediment distribution is calculated for each river using a taped grid of 1 m by 1 m on exposed gravel bars near the end of the spring fieldwork. Photographs of each grid are taken, with the sediments later measured and separated into size intervals. In the photographs, only those sediment particles large enough to be seen without magnification and not obscured by other particles are measured. Nine rocks were brought back from each grid in order to precisely weigh and measure them in a lab.

3.10.4 Longitudinal Bed Profiles and Roughness Coefficients

One of the key parameters involved in river hydraulics is the friction coefficient or roughness coefficient. Commonly, the factor used by design engineers is the Manning's *n* coefficient (ASCE, 2008; Yang, 2003; Julien, 2002; among many others). This coefficient provides an integrated value for the entire river cross section; in general, it is used in conjunction with other data to estimate average cross-sectional velocities and discharge.

The total roughness of an alluvial channel is composed of two parts: (a) grain or skin roughness due to sediment particle size, and (b) form roughness due to the presence of bedforms (Yang, 2003). Thus, data on longitudinal riverbed profiles can provide insights on the importance of form roughness on the total friction coefficient. While the existing literature on skin and form friction in temperate regions is vast, the available literature on extreme cold regions is, to the best of our knowledge, essentially nonexistent. Furthermore, the available data on sediment transport and total friction factor in Alaska rivers are very limited (see, for instance, Oatley, 2002; McNamara et al., 2008b).

To estimate the importance of bedform, several longitudinal riverbed profiles were determined during spring fieldwork in the Chandler River. The three instruments used in the field were a

water vehicle, an ADCP, and a GPS. Typically, a longitudinal profile was recorded after discharge measurements were completed.

Bedforms were identified in the profiles, and steepness ratios, which are defined as the bedform height/bedform wavelength, were calculated later. Due to the natural variability of bedforms in rivers, minimum, average, and maximum steepness ratios were computed.

The steepness ratio provides information on the river's hydraulic adjustment to different discharge. As mentioned before, bedforms are the main contributors to form resistance.

4 RESULTS

This section details the results of all data collected during the study period of summer 2006 through fall 2011 for the Umiat Corridor/Kuparuk Foothills and Bullen projects. The results presented here are given so the reader can form an idea of the magnitude of the variables measured that are displayed in either graphs or tables. The original digital data can be found on one of the websites or, in some cases, in the appendices at the end of this report.

4.1 Air Temperature and Relative Humidity

Appendix A contains a detailed table of mean, maximum, and minimum monthly air temperatures for each station within the Bullen, Kuparuk Foothills, and Umiat Corridor study areas. Also in Appendix A are time series graphs of the hourly air temperature and relative humidity at each station for the period of record. Monthly air temperatures (collectively averaged for each physiographic region) from 2006 through 2011 demonstrated a pronounced seasonal cycle typical of high latitudes (Figure 7).

Within the Bullen, Kuparuk Foothills and Umiat Corridor study region, monthly mean air temperatures at the stations range from 7.5°C to 12.6°C (45.5°F to 54.7°F) during July, the average warmest month. The coldest month at the stations within the study area occurs in March with the average monthly temperature ranging from -29.3°C to -10.8°C (-20.7°F to 12.6°F). However, the air temperature in the Mountain region is slightly colder in December and January (Figure 7). The temperature extremes recorded during the reporting period were -49.8°C (-57.6°F) at Anaktuvuk (DUS2) station in January 2010, and 30.9°C (87.7°F) at Chandler (DUS3) station in June 2011. Stations typically recorded air temperatures below freezing at least once during each month of the period of record.

During the cold season (November through May), stations in the Mountain region were, on average, warmer than those in the Foothills and Coastal Plain regions. During the summer season, the Foothills had the warmest air temperatures. Temperatures at the Coastal Plain and Mountain stations were similar June through September. Interestingly, during the summer

months, all stations experienced similar minimum temperatures; however, Mountain stations exhibited lower maximum temperatures than the Foothills and Coastal Plain stations. Moreover, summer daily air temperatures exhibited more pronounced diurnal fluctuations than winter daily air temperatures at all stations. These results suggest that there is a strong relationship between latitudinally dependent solar radiation, elevation, and air temperatures along the North Slope of Alaska.

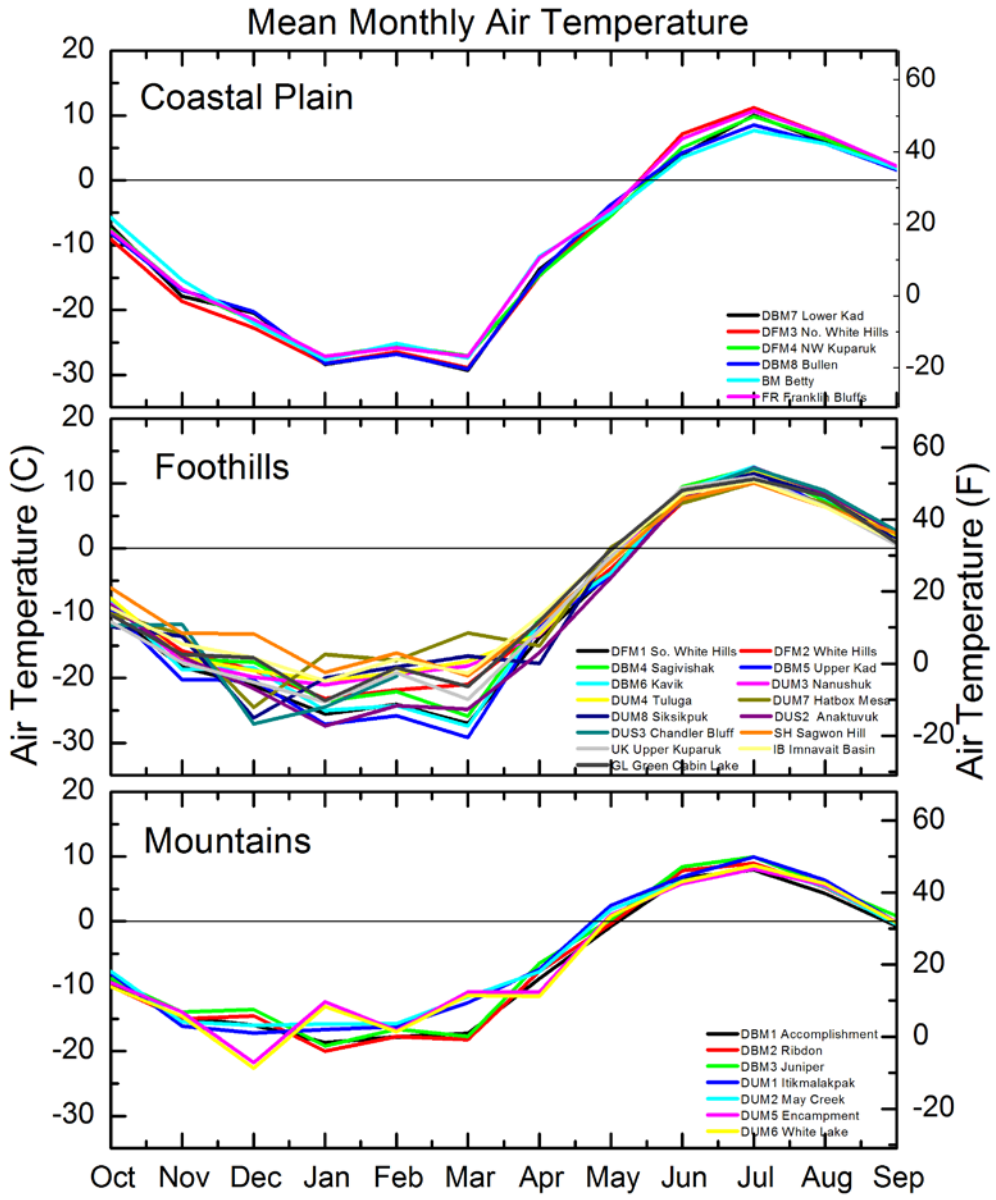

Figure 7. Monthly mean air temperature for meteorological stations in the Mountain, Foothills, and Coastal Plain regions of the Bullen/Foothills project area. Note that stations in the Chandler basin only have one year of record.

Mean monthly relative humidity values for all stations are presented in Table 5 through Table 8. The monthly average relative humidity at typical stations representing Mountain (DFM4 Northwest Kuparuk), Foothills (DUM4 Tuluga), and Coastal Plain (DUM5 Encampment) regions are presented in Figure 8. Monthly mean relative humidity is consistently lowest in the Mountain region (49–86%), followed by the Foothills (58–92%) and Coastal Plain (73–93%) regions. Data show a pronounced annual cycle with relative humidity correlating closely to temperature, except during the summer months. The most humid conditions occurred during October and May, whereas the driest conditions occurred during February in the Mountain region and during March in the Foothills and Coastal Plain regions. Relative humidity tended to surge in the spring (March through May) as air temperatures and incoming radiation increase and the snowpack ablates. In the summer, relative humidity displayed a strong diurnal cycle, with highest humidity in the morning and lowest humidity in the evening (corresponding to the air temperature pattern). During the winter months, no diurnal patterns exist, with relative dry or wet conditions occurring anytime. It should be noted that high relative humidity in winter months can be misleading, because at very cold temperatures, below -35°C (-31°F), little moisture is contained in the air at saturation (100%).

Table 5. Mean monthly relative humidity at Bullen stations, 2006–2010.

Month	Mean Monthly Relative Humidity (%)							
	DBM1 Accomplish-ment	DBM2 Ribdon	DBM3 Juniper	DBM4 Sag-Ivishak	DBM5 Upper Kad	DBM6 Kavik	DBM7 Lower Kad	DBM8 Bullen
Oct	75	77	72	84	87	84	86	91
Nov	70	69	65	77	82	79	82	86
Dec	64	65	62	74	78	76	80	83
Jan	64	68	64	71	73	71	76	75
Feb	63	65	63	71	74	73	79	77
Mar	58	61	57	69	72	69	85	75
Apr	64	66	59	77	83	78	85	85
May	68	70	64	85	88	85	89	91
Jun	73	70	63	72	75	73	86	86
Jul	76	74	71	74	76	75	81	83
Aug	77	77	77	83	81	83	87	88
Sep	77	75	69	81	82	83	89	92

Table 6. Mean monthly relative humidity at Kuparuk Foothills stations, 2006–2011.

Month	Mean Monthly Relative Humidity (%)								
	DFM1 S White Hills	DFM2 White Hills	DFM3 N White Hills	DFM4 NW Kuparuk	Betty Pingo	Franklin Bluffs	Sagwon	Imnavait Basin	Upper Kuparuk
Oct	86	90	89	93	93	92	88	79	92
Nov	81	84	84	87	89	87	83	73	87
Dec	76	77	78	84	83	81	76	68	81
Jan	73	73	73	77	78	77	74	68	77
Feb	75	75	75	78	80	77	74	67	77
Mar	70	73	72	76	77	75	71	61	75
Apr	78	80	80	87	88	83	80	71	83
May	83	85	86	90	91	91	85	73	91
Jun	74	77	76	83	88	88	77	71	88
Jul	75	75	77	79	87	81	75	72	81
Aug	82	84	84	86	91	88	83	78	88
Sep	84	85	87	90	93	91	86	78	91

Table 7. Mean monthly relative humidity at Umiat Corridor stations (Anaktuvuk Basin), 2009–2011.

Month	Mean Monthly Relative Humidity (%)				
	DUM1 Itikmalakpak	DUM2 Upper May Creek	DUM3 Nanushuk	DUM4 Tuluga	DUS2 Anaktuvuk
Oct	78	78	85	88	88
Nov	76	77	82	86	83
Dec	67	69	72	74	74
Jan	64	63	70	71	77
Feb	67	65	73	77	77
Mar	52	49	66	67	75
Apr	62	61	75	77	80
May	64	62	87	80	87
Jun	80	75	78	78	79
Jul	73	76	73	74	74
Aug	74	79	78	79	80
Sep	80	78	81	86	87

Table 8. Mean monthly relative humidity at Umiat Corridor stations (Chandler basin), 2010–2011.

Month	Mean Monthly Relative Humidity (%)				
	DUM5 Encampment	DUM6 White Lake	DUM7 Hat Box Mesa	DUM8 Siksikpuk	DUS3 Chandler
Oct	79	82	89	90	91
Nov	85	86	91	90	88
Dec	73	74	82	77	75
Jan	61	63	72	78	78
Feb	69	70	76	77	76
Mar	51	55	65	73	75
Apr	68	68	75	77	na
May	67	68	73	76	81
Jun	77	76	78	73	72
Jul	77	76	79	75	76
Aug	77	77	82	79	80
Sep	83	85	90	88	88

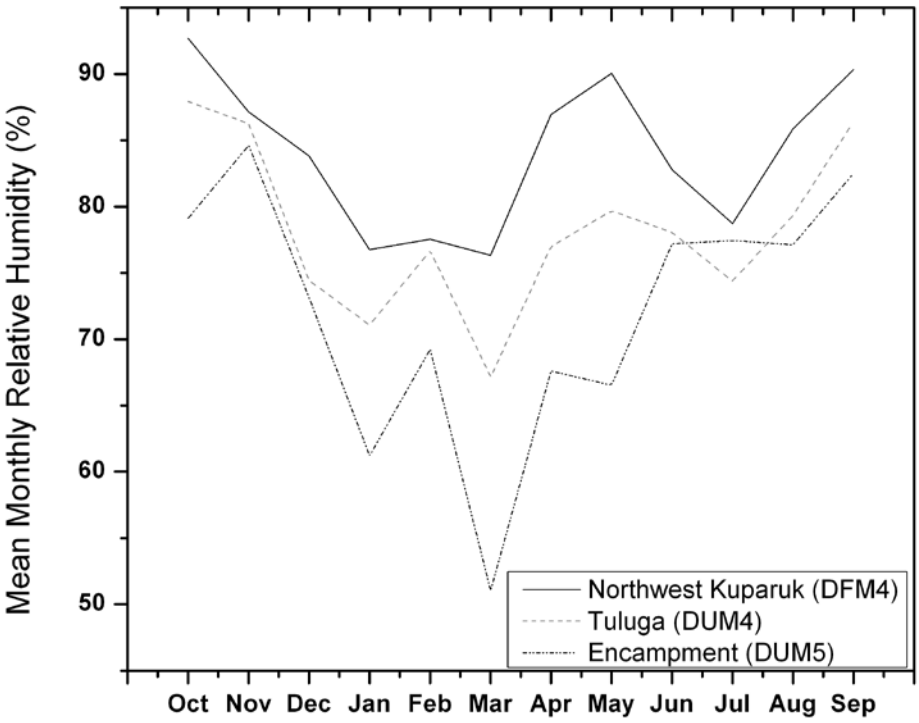

Figure 8. Mean monthly relative humidity at three select stations. Northwest Kuparuk is representative of Coastal Plain region, Tuluga is representative of Foothills region, and Encampment is representative of Mountain region.

4.2 Wind Speed and Direction

The majority of wind events along the North Slope of Alaska are produced by one of two predominant weather regimes. The most common regime is typified by high pressure over the Beaufort Sea and low pressure over northern Alaska, producing easterly winds. Westerly wind events are typically produced when low-pressure systems over the Chukchi or Beaufort Seas set up alongside high-pressure systems to the south and east. Strong storm systems to the west can produce Chinook conditions with especially strong winds through mountain passes.

Mean monthly 3-meter wind speeds for all stations are presented in Table 9 through Table 12. Wind roses showing the prominent wind directions and magnitude were constructed using WRPLOT software for the period of record for each station in the Bullen, Kuparuk Foothills, and Umiat Corridor monitoring network (see Appendix B). Table 13 presents the annual mean wind speed, along with the summer (May 15 to September 15) and winter (September 16 to May 14) mean wind speed. Wind speeds recorded near the Beaufort Sea coast were significantly higher than those recorded at stations in the Foothills and Mountain region, and Mountain region stations generally had the lowest average wind speeds. December through May winds were higher than winds during the months of June through November.

Table 9. Monthly mean wind speed for meteorological stations in the Bullen Project study area, 2006–2011.

	Mean Monthly Wind Speed (m/s)							
Month	DBM1 Accomplish-ment	DBM2 Ribdon	DBM3 Juniper	DBM4 Sag-Ivishak	DBM5 Upper Kad	DBM6 Kavik	DBM7 Lower Kad	DBM8 Bullen
Oct	2.7	2.0	1.3	2.6	2.7	3.0	4.4	4.7
Nov	3.3	2.4	1.4	2.6	2.3	3.2	4.2	5.4
Dec	3.5	2.7	1.9	3.2	3.4	3.4	4.1	4.2
Jan	3.3	2.6	1.7	3.3	3.8	4.0	4.7	6.2
Feb	3.8	2.9	1.9	3.0	3.4	4.2	5.5	4.5
Mar	3.2	2.7	1.3	2.4	3.2	4.0	4.3	5.1
Apr	3.1	3.1	1.5	2.8	3.0	3.4	3.8	4.3
May	2.5	2.8	1.7	2.6	3.3	3.6	4.6	5.0
Jun	2.7	2.9	2.0	3.1	3.5	3.8	5.7	5.4
Jul	2.6	2.9	2.0	2.8	3.1	3.0	4.4	4.5
Aug	2.6	2.6	1.7	2.7	2.7	2.7	4.1	3.6
Sep	2.4	2.7	1.6	2.4	2.5	2.6	4.3	3.9

Table 10. Monthly mean wind speed for meteorological stations in the Kuparuk Foothills Project study area, 2006–2011.

Month	Mean Monthly Wind Speed (m/s)									
	DFM1 S White Hills	DFM2 White Hills	DFM3 N White Hills	DFM4 NW Kuparuk	Betty Pingo	Franklin Bluffs	Sagwon	Imnavait Basin	Upper Kuparuk	Green Cabin Lake
Oct	2.4	4.9	3.0	3.9	5.8	4.4	3.0	2.3	4.4	1.5
Nov	2.7	4.4	2.9	3.3	5.5	3.9	2.8	2.5	3.9	1.8
Dec	3.3	5.2	3.1	3.6	3.9	4.2	3.8	2.7	4.2	1.8
Jan	3.1	4.7	3.8	4.5	4.1	3.7	3.5	2.7	3.7	1.9
Feb	3.6	5.0	4.0	4.8	5.7	4.2	5.0	4.0	4.2	2.4
Mar	2.7	4.7	3.4	4.9	4.5	4.0	3.2	2.3	4.0	1.5
Apr	2.9	4.7	3.4	4.0	5.0	4.7	3.9	2.6	4.7	1.9
May	2.7	4.9	3.8	4.5	5.1	4.8	3.5	2.7	4.8	2.1
Jun	3.1	5.5	3.9	4.7	6.1	5.1	4.5	3.1	5.1	2.8
Jul	2.7	4.5	3.0	3.5	5.2	4.1	4.2	2.9	4.1	2.6
Aug	2.6	4.4	2.9	3.4	4.6	3.8	3.9	2.8	3.8	4.0
Sep	2.4	4.3	2.8	3.4	5.1	3.9	3.6	2.3	3.9	2.1

Table 11. Monthly mean wind speed for meteorological stations in the Umiat Project study area, Anaktuvuk River basin, 2009–2011.

Month	Mean Monthly Wind Speed (m/s)				
	DUM1 Itikmalakpak	DUM2. May Creek	DUM3 Nanushuk	DUM4 Tuluga	DUS2 Anaktuvuk
Oct	0.8	1.5	1.7	2.4	4.4
Nov	1.0	2.4	2.6	3.1	4.2
Dec	1.1	2.7	2.6	2.8	4.1
Jan	0.9	2.7	2.2	2.6	4.7
Feb	1.6	3.5	3.2	3.9	5.5
Mar	0.8	2.0	2.0	2.0	4.3
Apr	1.1	2.4	2.0	2.6	3.8
May	1.1	2.0	1.8	2.0	4.6
Jun	1.8	2.5	3.1	3.0	5.7
Jul	1.8	2.5	2.7	2.8	4.4
Aug	1.7	2.7	2.7	3.1	4.1
Sep	1.1	2.3	2.4	2.5	4.3

Table 12. Monthly mean wind speed for meteorological stations in the Umiat Project study area, Chandler River basin, 2010–2011. Note that the period of record for these data is only one year.

Month	Mean Monthly Wind Speed (m/s)				
	DUM5 Encampment	DUM6 White Lake	DUM7 Hat Box Mesa	DUM8 Siksikpuk	DUS3 Chandler
Oct	2.6	2.8	1.9	1.1	1.2
Nov	2.9	3.7	3.4	2.4	2.3
Dec	2.9	2.9	N/A	1.9	2.5
Jan	3.3	3.2	2.8	1.7	1.6
Feb	7.7	6.0	5.2	4.4	3.7
Mar	2.9	2.6	2.3	1.5	1.9
Apr	2.3	2.2	2.7	1.3	N/A
May	2.9	2.6	2.3	1.6	1.6
Jun	3.1	3.1	3.3	2.8	2.2
Jul	3.6	3.0	2.7	2.3	1.6
Aug	3.7	3.2	2.8	2.3	1.7
Sep	3.0	2.7	2.5	1.9	1.7

Table 13. Summary of WRPLOT wind rose analysis for the period of record from July 2006 through September 2011. Summer period is May 15 through September 15 and winter period is September 16 through May 14. See Appendix B for wind roses.

Station	Overall Average Hourly Wind Speed (m/s)	Summer Average Hourly Wind Speed (m/s)	Winter Average Hourly Wind Speed (m/s)	Overall Calm Winds (%)	Summer Calm Winds (%)	Winter Calm Winds (%)	Total Data Count (hr)	Missing Data (hr)
Accomplishment (DBM1)	2.9	2.5	3.1	3.1	1.9	3.3	45671	4362
Ribdon Creek (DBM2)	2.7	2.8	2.6	10.8	4.2	13.8	34004	382
Juniper Creek (DBM3)	1.6	1.9	1.5	18.1	8.1	22.9	35809	1600
Sag-Ivishak (DBM4)	2.8	2.8	2.8	2.9	0.7	4.0	35760	2434
Upper Kadleroshilik (DBM5)	3.1	3.0	3.2	2.9	0.8	3.8	35989	3147
Kavik (DBM6)	3.3	3.0	3.5	2.5	1.0	3.2	35733	4166
Kadleroshilik (DBM7)	4.6	4.5	4.6	2.0	0.6	2.7	34151	1073
Bullen (DBM8)	4.6	4.2	4.9	1.2	0.3	1.4	31601	7529
South White Hills (DFM1)	2.8	2.7	2.9	2.9	0.8	3.9	45879	2276
White Hills (DFM2)	4.8	4.7	4.9	1.9	0.2	2.7	45501	13489
North White Hills (DFM3)	3.3	3.2	3.4	3.3	0.9	4.5	44906	2934
Northwest Kuparuk (DFM4)	4.0	3.8	4.2	2.3	0.4	3.2	45012	6528
Itikmalakpak (DUM1)	1.2	1.7	0.9	26.3	10.4	35.9	20357	1280
Upper May Creek (DUM2)	2.4	2.6	2.3	9.5	3.8	13.2	19773	778
Nanushuk (DUM3)	2.4	2.7	2.2	5.7	1.2	8.6	20291	1293
Tuluga (DUM4)	2.7	2.9	2.6	4.5	0.9	6.7	20436	2343
Anaktuvuk River (DUS2)	2.9	2.9	2.8	1.9	0.5	2.6	20466	5591
Encampment Creek (DUM5)	3.3	3.5	3.3	4.9	0.8	6.7	10209	1205
White Lake (DUM6)	3.1	3.0	3.1	4.9	1.6	6.3	9650	1231
Hatbox Mesa (DUM7)	2.9	2.7	3.0	4.2	1.4	5.1	9684	2308
Siksikpuk (DUM8)	2.1	2.3	1.9	8.3	1.7	11.3	9597	1443
Chandler River Bluff (DUS3)	1.9	1.7	2.1	5.9	2.6	6.8	9597	1875

Average annual wind speed and direction data over the period of record for each site are presented in the wind roses in Figure 9 through Figure 12. Wind direction was variable in the project area; different wind patterns appeared for the Coastal Plain, Foothills, and Mountain regions. In addition to a prevailing southwest wind, stations closer to the Coastal Plain experience winds from an easterly direction, as indicated at the Northwest Kuparuk station (Figure 9). In the Foothills region, wind directions from the northeast and south–southwest are observed, as indicated in the wind roses for North White Hills stations (Figure 10).

Additionally, the analysis was divided into a summer period (May 15 through September 15) and a winter period (September 16 through May 14) to examine seasonal differences in wind direction and speed (see wind roses in Appendix B). A seasonal trend was observed at most stations, and in general, most of the stations in the Coastal Plain and northern Foothills regions had strong south/southwest winds during the winter period and strong northeast winds during the summer period. However, in the Chandler basin to the west, no clear trends were observed, possibly because we only have one year of data.

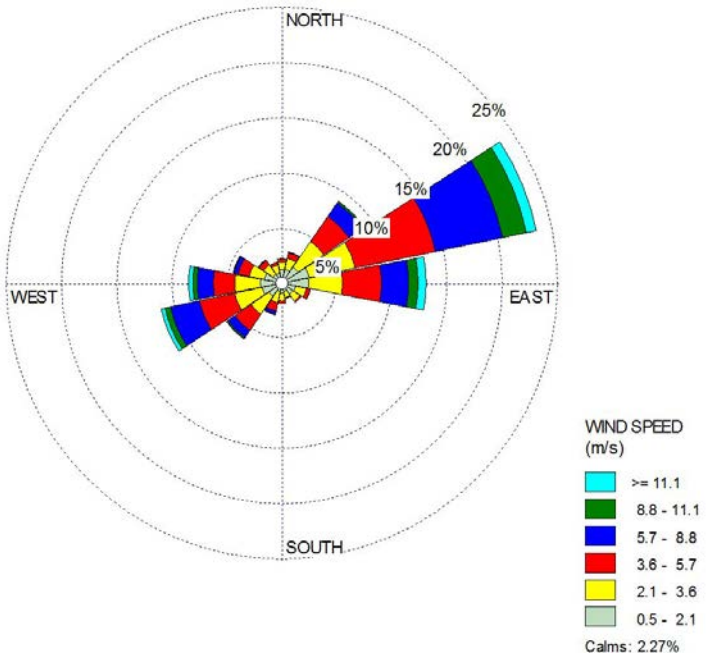

Figure 9. Northwest Kuparuk (DFM4) station is located in the northern part of the Kuparuk drainage near the Coastal Plain. The terrain is flat. Winds are mostly from the east-northeast in the summer and both the east-northeast and west-southwest in the winter.

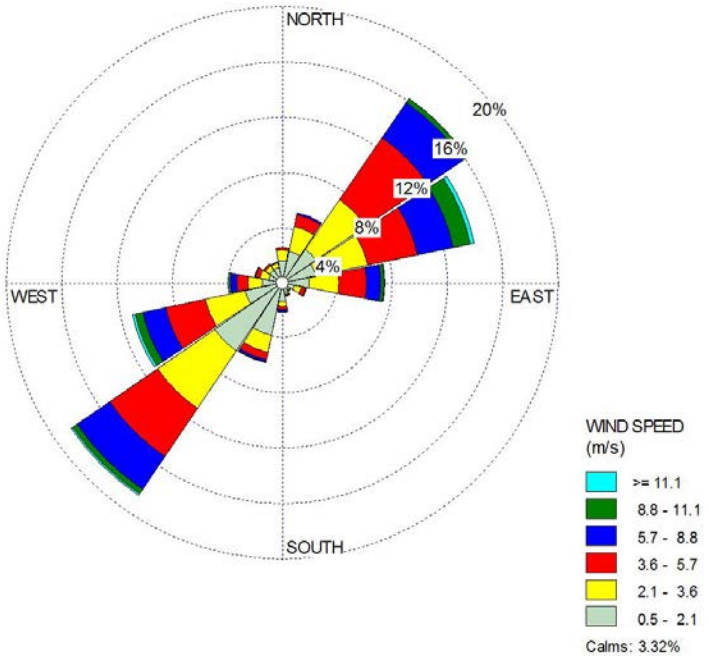

Figure 10. North White Hills station (DFM3) is located in the foothills of the Kuparuk River drainage. Winds at this station are from the northeast in the summer and southwest in the winter.

Wind direction at all stations in the Mountain region tends to be more variable and/or dominated by orographic influences. Orographic influence on wind can be substantial, and is observed in the three stations located in the Mountain region. The predominantly southeasterly winds reported at Accomplishment Creek station (Figure 11) are likely due to the northwest–southeast orientation of the valley in which the station is located. Additionally, the hilltop location of the White Hills station (Figure 12) likely contributes to the relatively high average wind speed (4.8 m/s) observed there.

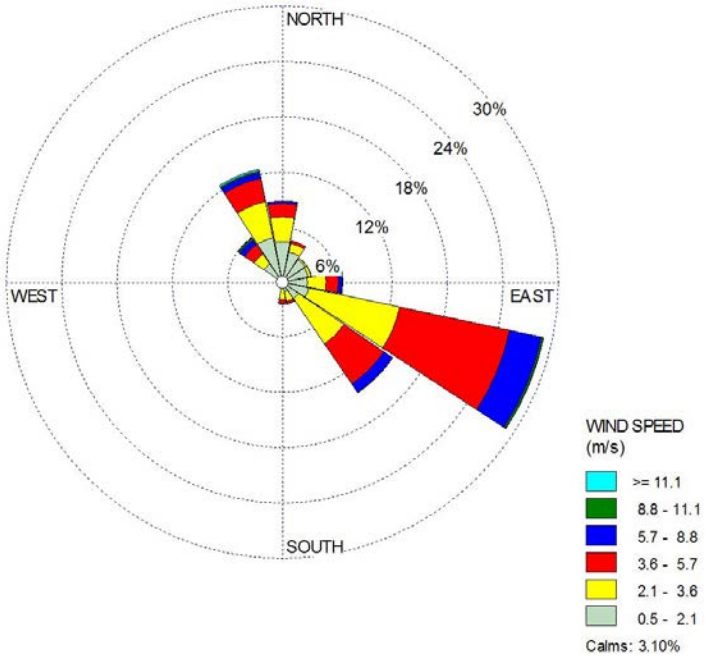

Figure 11. Winds are primarily from the southeast at Accomplishment Creek station (DBM1). During the summer months, winds also come from the northwest. The station is located in a SE–NW-oriented mountain valley that may channel winds from the SE up the valley. Winds are rarely calm at this station.

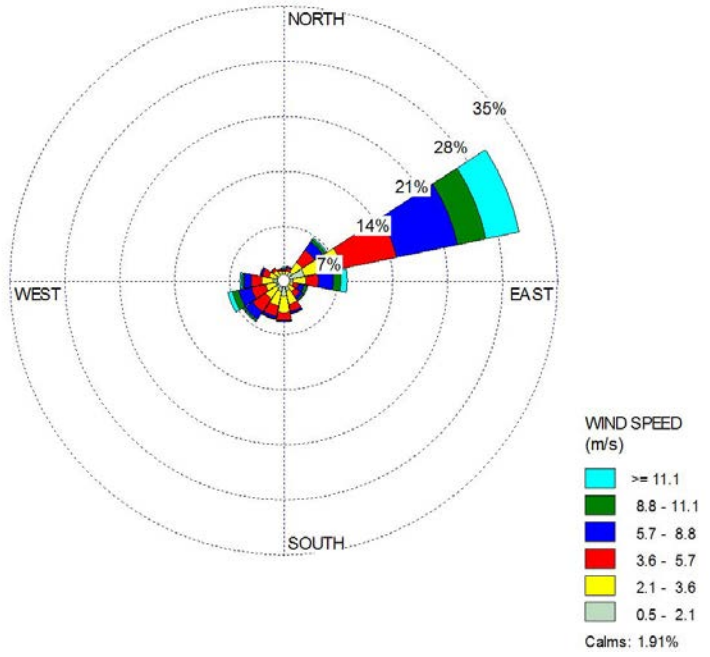

Figure 12. White Hills station (DFM2) is located in the hills of the Kuparuk River foothills area. This station is located on top of one of the hills, and the highest winds are from the northeast. The average wind speed (4.8 m/s) at this station is one of the highest speeds in the network.

High wind events exhibit regional tendencies, with highest wind speeds at the Coastal Plain stations (Figure 13), though extreme events can occur in mountainous areas during Chinook conditions. Using the Northwest Kuparuk station as an example that typifies the Coastal Plain region, high wind events (greater than 8.0 m/s) occurred much more frequently than typical stations representing the Foothills region (Tuluga) and Mountain region (May Creek). The wind roses for most stations in Appendix B show high wind events are primarily from the northeast and occasionally from the southwest. The high wind events in Foothills and Mountain stations occurred less than the Coastal Plain station and ranged evenly from southwest to northeast. The Mountain region stations reported slightly more high wind events than the Foothills region stations, with variable wind directions ranging from the southeast to southwest. The Foothills and Mountain stations report few high wind events during summer months, while the Coastal Plain station still reports high winds albeit of lesser magnitude than winter.

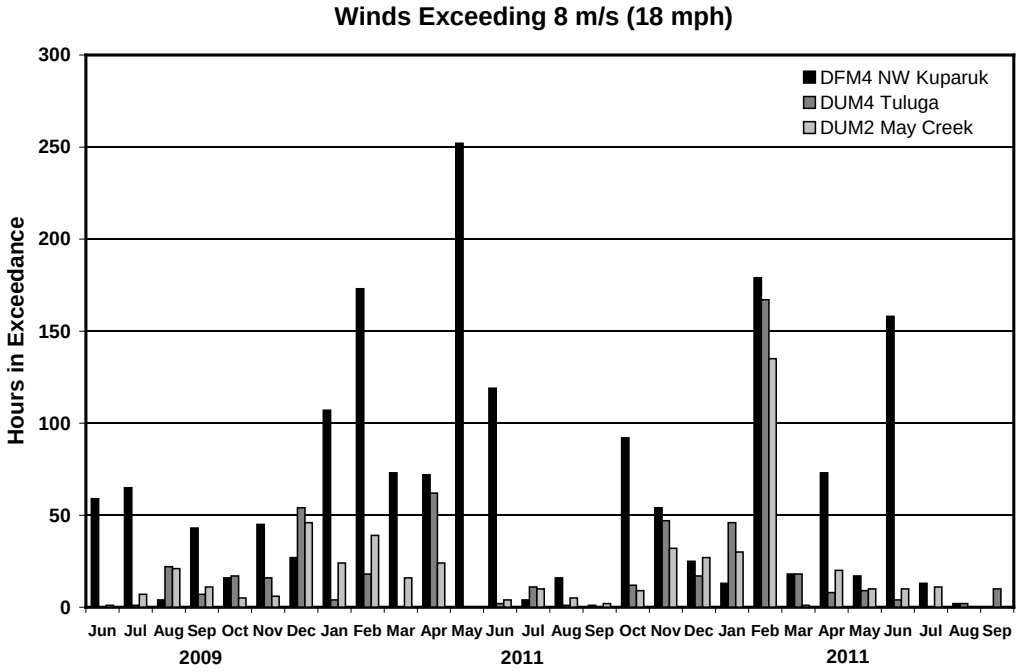

Figure 13. Hours of wind speed exceeding 8.0 m/s by month for Northwest Kuparuk (DFM4, Coastal Plain), Tuluga (DUM4, Foothills), and May Creek (DUM2, Mountain) from June 2009 through September 2011.

4.3 Net Radiation

Mean monthly net radiation is presented for each station in Table 14 through Table 17. Net radiation is affected by many factors such as latitude, albedo, soil moisture, soil temperature, incident solar radiation, and atmospheric radiation. Large areas are affected by cloudiness and incoming radiation. However, soil temperature, soil moisture, and albedo can vary significantly over small areas. In Table 15, a comparison of net radiation at the Betty Pingo station, over light-colored, well-drained tussock tundra (Betty Upland, BU) and a poorly drained, dark, wet area (Betty Wetland, BW), shows that even though these sites are only 25 m apart, net radiation is very different. With the upland's much higher albedo and warmer surface, the outgoing radiation signal is much higher, which lowers the net radiation. In contrast, the wetland area loses much of its radiation to evapotranspiration and conduction, resulting in higher net radiation. The net radiation is often reduced in the Mountain and Foothills regions over uneven terrain by the development of convective clouds as each day progresses.

Table 14. Monthly mean net radiation (W/m^2) during the warm season for meteorological stations in the Bullen project area, 2006–2010.

Month	Mean Monthly Net Radiation (W/m²)							
	DBM1 Accomplish-ment	DBM2 Ribdon	DBM3 Juniper	DBM4 Sag-Ivishak	DBM5 Upper Kad	DBM6 Kavik	DBM7 Lower Kad	DBM8 Bullen
May	21.2	13.7	33.9	32.7	21.6	62.3	62.8	20.9
Jun	88.9	94.1	91.6	142.0	137.5	139.3	140.3	142.1
Jul	70.8	62.1	71.8	103.4	102.4	100.5	113.5	115.9
Aug	37.4	29.0	40.2	60.9	54.0	55.4	64.7	58.2
Sep	-2.9	-11.0	-1.0	15.5	17.9	15.8	25.4	16.9

Table 15. Monthly mean net radiation (W/m^2) during the warm season for meteorological stations in the Kuparuk Foothills project area, 2006–2011.

Month	Mean Monthly Net Radiation (W/m²)									
	DFM1 S White Hills	DFM2 White Hills	DFM3 N White Hills	DFM4 NW Kuparuk	Betty Pingo Wetland	Betty Pingo Upland	Franklin Bluffs	Sag-won	Imnavait Basin	Upper Kuparuk
May	36.3	70.9	57.4	12.6	na	na	na	na	na	na
Jun	128.4	121.0	131.5	127.0	223.1	144.9	189.2	146.8	129.2	122.4
Jul	98.9	94.7	96.5	99.1	183.5	115.9	107.1	130.4	115.1	104.7
Aug	57.6	49.2	54.4	41.8	102.7	65.3	78.8	74.7	72.0	74.1
Sep	15.5	8.0	15.8	15.8	na	na	na	na	na	na

Table 16. Monthly mean net radiation (W/m^2) during the warm season for meteorological stations in the Umiat Corridor project area 2009–2011 (Anaktuvuk River basin).

Month	Mean Monthly Net Radiation (W/m^2)				
	DUM1 Itikmalakpak	DUM2 Upper May Creek	DUM3 Nanushuk	DUM4 Tuluga	DUS2 Anaktuvuk
May	40.2	44.9	39.4	44.7	25.2
Jun	88.4	80.9	113.5	123.0	113.7
Jul	69.4	66.9	88.9	94.7	84.0
Aug	44.7	44.1	54.7	62.1	53.5
Sep	1.7	5.6	11.8	11.4	12.7

Table 17. Monthly mean net radiation (W/m^2) during the warm season for meteorological stations in the Umiat Corridor project area 2010–2011 (Chandler River basin).

Month	Mean Monthly Net Radiation (W/m^2)				
	DUM5 Encampment	DUM6 White Lake	DUM7 Hat Box Mesa	DUM8 Siksikpuk	DUS3 Chandler
May	53.0	44.7	-2.3	39.5	104.0
Jun	101.0	106.5	na	121.3	137.9
Jul	81.4	87.0	na	92.6	101.4
Aug	54.3	56.9	na	62.8	66.6
Sep	1.3	0.8	na	12.0	16.2

Table 18 shows mean monthly net radiation for May through September and seasonal averages for the three topographic regions. Figure 14 shows the monthly average net radiation (May through September) for the period of record at three selected stations within each region. The Coastal Plain region receives the highest net radiation, followed by the Foothills region and the Mountain region. Net radiation peaks in June in all regions. The Foothills and Coastal Plain regions typically have similar values, while the Mountain region has, on average, 39% less net radiation than the Coastal Plain region. This difference is due, primarily, to the cloudier conditions in the Mountain region.

Table 18. Mean monthly net radiation for the Coastal Plain, Foothills, and Mountain region stations.

	Mean Monthly Net Radiation (W/m^2)		
Month	**Coastal Plain**	**Foothills**	**Mountain**
May	38.4	43.1	35.9
Jun	156.9	128.9	93.1
Jul	118.8	100.9	72.8
Aug	66.6	61.3	43.8
Sep	18.5	12.4	-0.8
Seasonal Mean	79.8	69.3	49.0

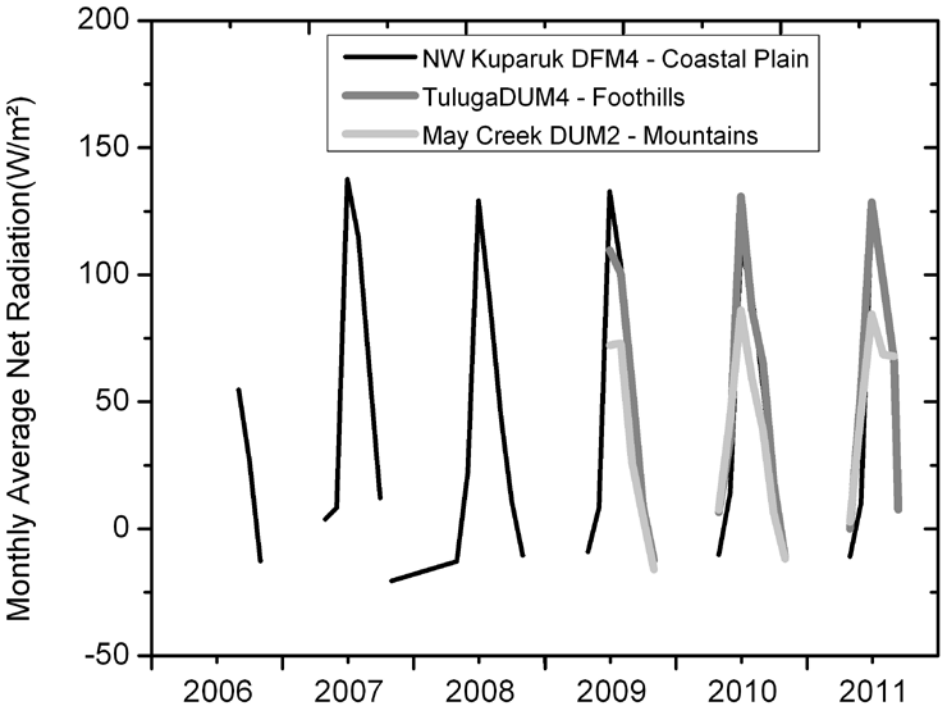

Figure 14. Mean monthly average net radiation for three meteorological stations representing the Coastal Plain, Foothills, and Mountain regions. The stations transect the North Slope north to south. The period of record for Northwest Kuparuk station is longer than the period of record for Tuluga and May Creek.

4.4 Summer Precipitation

Summer precipitation is obviously an important component of the water balance in the study area. Summer (liquid) precipitation was measured with Texas Electronics 525WS and 525MM tipping-bucket gauges. Tipping buckets have been recording summer precipitation at other WERC-operated stations, such as Imnavait since 1985, Sagwon Hill since 1987, and Betty Pingo since 1996. Tipping-bucket gauges were installed at all the Bullen (DBM1–DBM8) and Kuparuk Foothills (DFM1–DFM4) stations in summer 2006. The cumulative precipitation for 2006 is not reported due to a partial period of record during that summer season. Tipping buckets were installed at the Umiat Corridor Anaktuvuk basin stations (DUM1–DUM4, DUS2) in mid-June 2009. Several widespread rain events occurred in early June prior to the installation of the Anaktuvuk basin tipping buckets; these data are not included in the total precipitation for summer 2009. In the fall of 2010, tipping buckets were installed in the Chandler basin stations (DUM5–DUM8, DUS3). Additionally, in late August 2010, the Bullen stations (DBM2–DBM8) and several Upper Kuparuk stations (NH, UH, EH, WK) were decommissioned, and tipping buckets were removed. Any rain events occurring after approximately August 20, 2010, are not included in the total summer precipitation at those stations for 2010.

Summer period begins when temperatures are consistently above freezing and liquid precipitation can be measured in the tipping-bucket gauges, around mid-May in the southern reaches of the watersheds and late May in the northern reaches. Missing data were estimated for periods up to 15 days with the inverse-distance method, using data from adjacent stations (with the exception of the Anaktuvuk stations in early June 2009 and the Upper Kuparuk basin stations in August/September 2010, where missing data were not estimated due to lack of nearby stations). At Imnavait station, missing data can be replaced with a secondary gauge located in the Upper Imnavait basin. Cumulative summer precipitation for each station is shown in Table 19.

Table 19. Station cumulative summer precipitation 2007–2011 for stations in the central Arctic of Alaska. Note that some stations are not in operation certain years.

Station ID	Station Name	2007 Cumulative Precipitation	2008 Cumulative Precipitation	2009 Cumulative Precipitation	2010 Cumulative Precipitation	2011 Cumulative Precipitation	Terrain
		mm	mm	mm	mm	mm	
DBM1	Accomplishment	179	228	275	160	n/a	Mountains
DBM2	Ribdon	247	261	334	331**	-	Mountains
DBM3	Juniper	144	259	252	258**	-	Mountains
DBM4	Sag-Ivishak	50	213	157	125**	-	Foothills
DBM5	Upper Kadleroshilik	n/a	180	135	84**	-	Foothills
DBM6	Kavik	37	133	156	91**	-	Foothills
DBM7	Lower Kadleroshilik	16	100	94	35**	-	Coastal Plain
DBM8	Bullen	18	97	104	n/a	-	Coastal Plain
DFM1	S. White Hills	47	134	198	124	114	Foothills
DFM2	White Hills	34	179	178	83	n/a	Foothills
DFM3	N. White Hills	18	102	108	45	75	Coastal Plain
DFM4	Northwest Kuparuk	21	93	97	93	62	Coastal Plain
IB	Imnavait	72	231	272	221	128	Foothills
BP	Betty Pingo	15	61	87	53	55	Coastal Plain
FB	Franklin Bluffs	9	73	n/a	n/a	55	Coastal Plain
SH	Sagwon Hill	27	122	128	65	98	Foothills
WD	West Dock	22	59	86		n/a	Coastal Plain
UK	Upper Kuparuk	111	257	286	247	116	Foothills
WK	West Kuparuk	66	n/a	n/a	n/a	n/a	Foothills
NH	North Headwaters	73	146	162	125**	n/a	Foothills
UH	Upper Headwaters	158	233	266	n/a	n/a	Foothills
GCL	Green Cabin Lake	130	187	213	200**	120	Foothills
EH	East Headwaters	150	206	240	178**	n/a	Foothills
WH	West Headwaters	70?	87?	206	213**	n/a	Foothills
DUM1	Itikmalakpak	-	-	154*	134	117	Mountains
DUM2	Upper May Creek	-	-	234*	362	246	Mountains
DUM3	Nanushuk	-	-	78*	162	127	Foothills
DUM4	Tuluga	-	-	163*	158	211	Foothills
DUM5	Encampment	-	-	-	-	270	Mountains
DUM6	White Lake	-	-	-	-	262	Mountains
DUM7	Hatbox Mesa	-	-	-	-	189	Foothills
DUM8	Siksikpuk	-	-	-	-	134	Foothills
DUS2	Anaktuvuk River	-	-	55*	86	107	Foothills
DUS3	Chandler River	-	-	-	-	66	Foothills
DUR8	Rooftop Ridge	-	-	246*	102		Foothills

*station installed mid-June, early June rainfall events missing from record, **station removed before end of rainy season; therefore, late August and September rainfall events missing from record.

A strong orographic effect is present each year, with the highest precipitation in the Mountain region to the south and the lowest in the Coastal Plain region to the north, as shown for 2008 in Figure 15. Summer precipitation ranged from an average of 60 mm in the Coastal Plain region to an average of 225 mm in the Mountain region (based on the 2007–2011 period of record). Very

low streamflow conditions occurred across the study area for summer of 2007 in response to the record-low summer precipitation across the North Slope. Although the summer of 2007 was a period of drought, the rainfall (Table 19) was still relatively high at Ribdon station (DBM2) in the mountains.

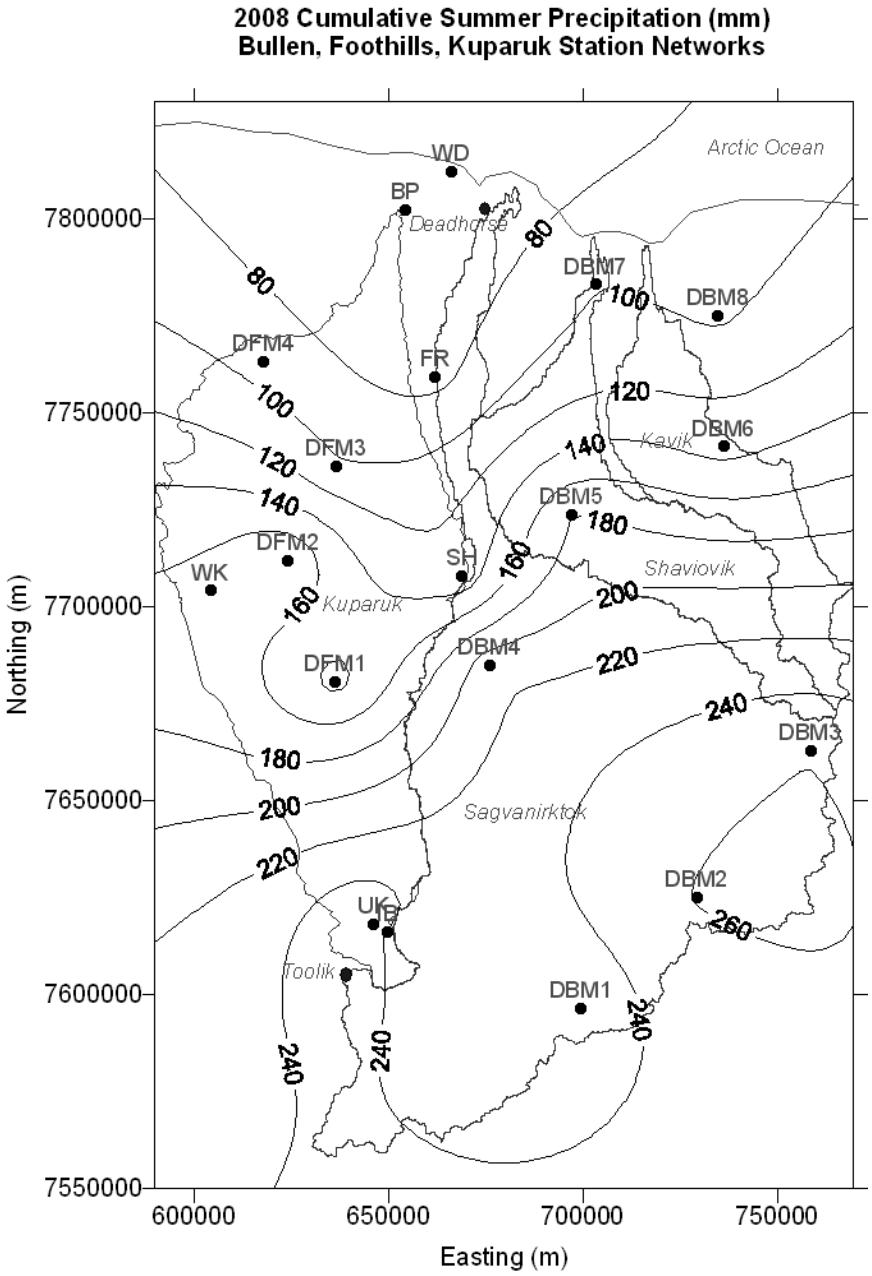

Figure 15. Interpolated (kriged) summer precipitation in 2008 for the central Arctic of Alaska, showing a strong orographic effect with greater precipitation at higher elevations. This relationship holds true each summer; only the absolute amount changes.

Figure 16 through Figure 20 show the time periods when the majority of precipitation occurs for each region. Figure 16 and Figure 17 show cumulative rainfall in the Kuparuk region, which is approximately 44% Coastal Plain and 56% Foothills regions. No stations are located specifically in the Mountain region of the Kuparuk basin, but a few stations located in the upper basin of the Upper Kuparuk River record nearly as much rainfall as the Mountain stations in the upper part of the Sagavanirktok basin. Figure 18 and Figure 19 show cumulative rainfall at all stations in the Bullen and Sagavanirktok project, which encompasses all three regions (Coastal Plain, Foothills, and Mountain) and includes three higher elevation stations that receive the most rain. Figure 20 includes stations from the Umiat Corridor region, which is located to the west of the Kuparuk basin and encompasses mostly the Mountain and Foothills regions. For most years, the Mountain stations had a relatively steady increase in cumulative precipitation through the entire summer period. In 2007, the Foothills and Coastal Plain stations had few precipitation events overall. In 2008, most of the rainfall fell in June and July, with little in August at nearly all the stations. In 2009, early June and July rainfall events caused flows to quickly increase in many rivers in the Umiat/Foothills region (Figure 20). Additionally, a three-week period from mid to late July (2009) was dry, but August and September were wetter months. In 2010, June was dry at many stations, but mid-July to mid-August was wet. In 2011, August was dry at most of the Kuparuk and northern Umiat area stations, but rainfall in early September caused increased flows in the Kuparuk, Anaktuvuk, and Chandler Rivers. These figures also demonstrate the wide variability in cumulative summer precipitation throughout the study area and the importance of understanding this spatial variability for rainfall-runoff predictions.

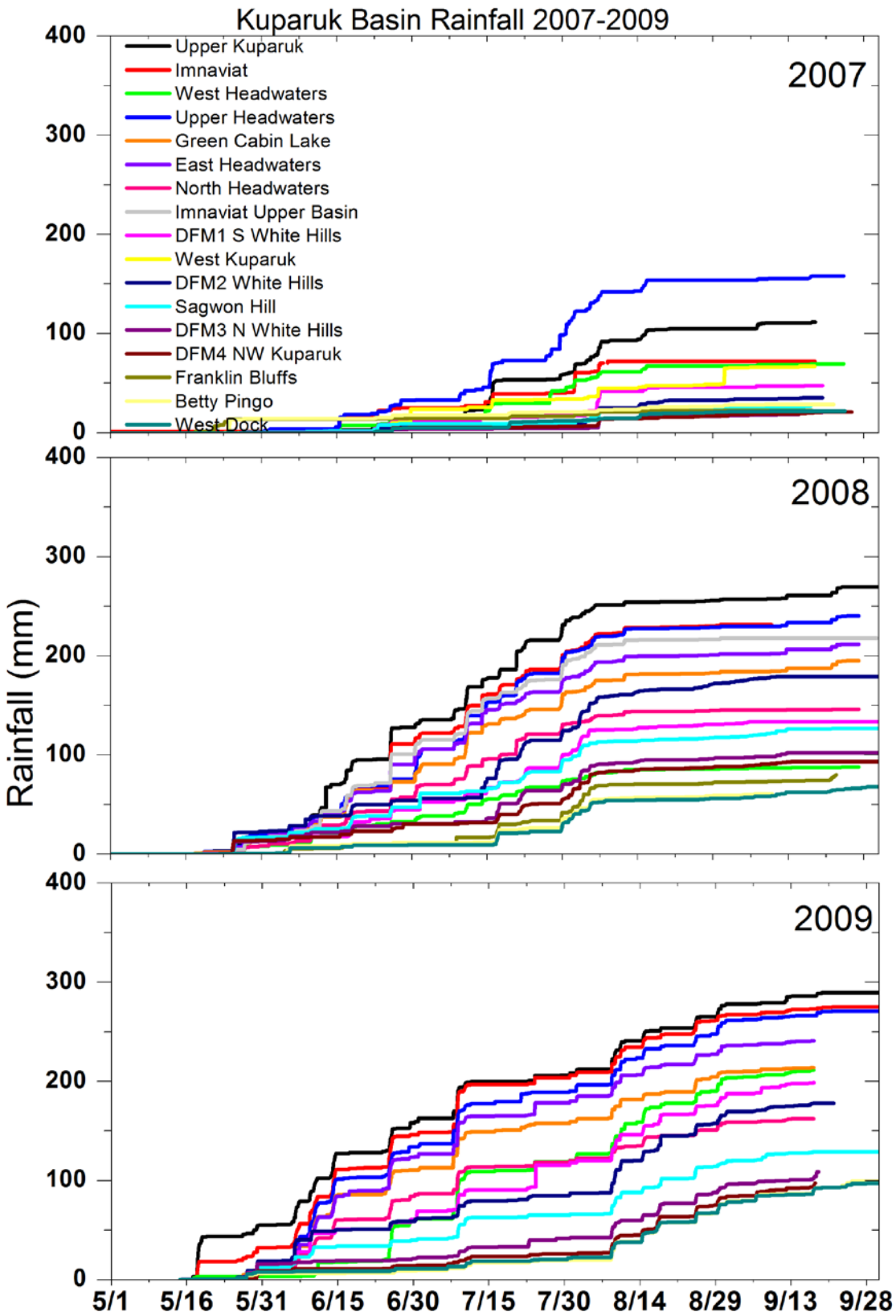

Figure 16. Cumulative summer precipitation for the Kuparuk Basin 2007–2009.

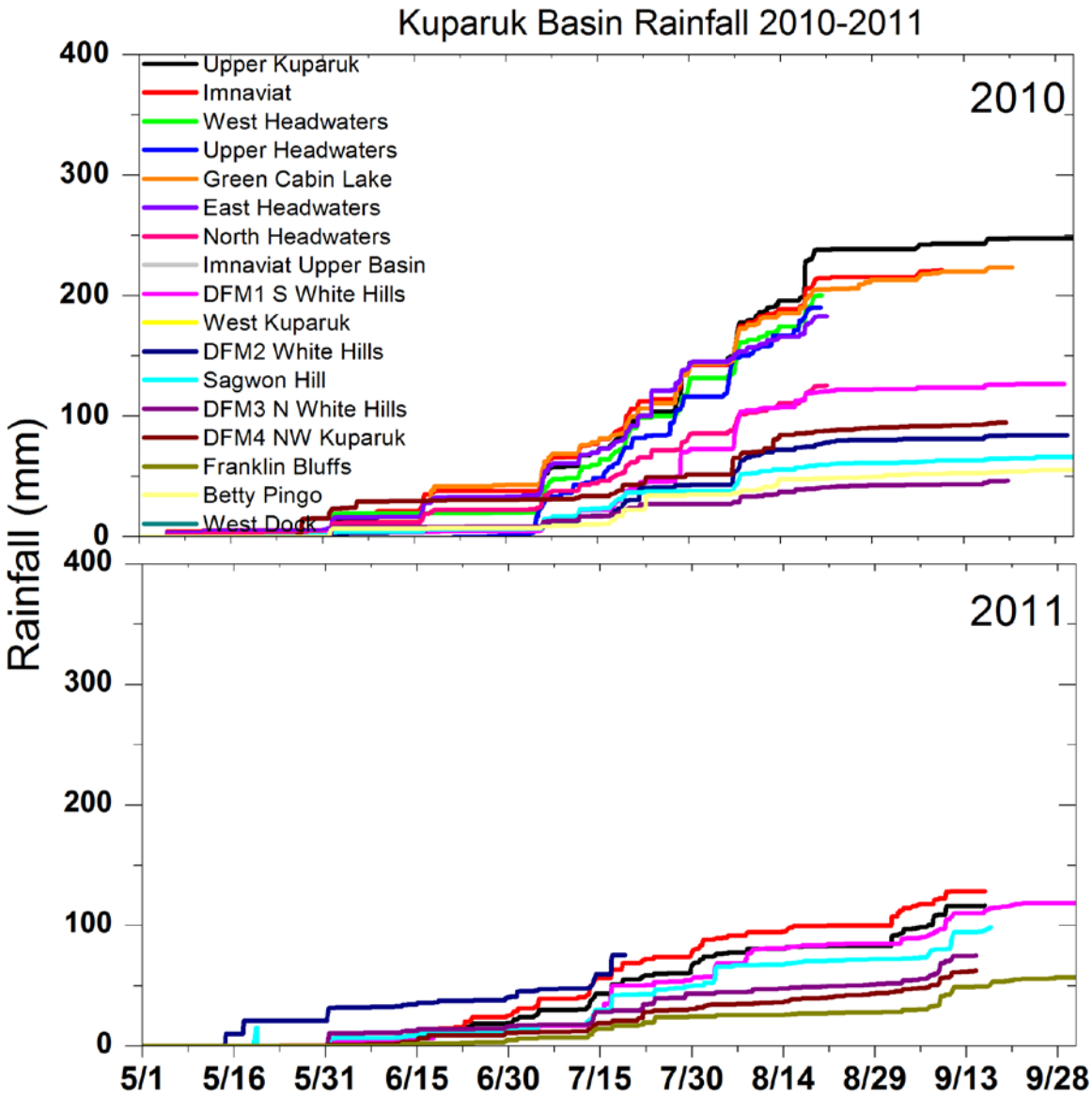

Figure 17. Cumulative summer precipitation for the Kuparuk Basin 2010–2011.

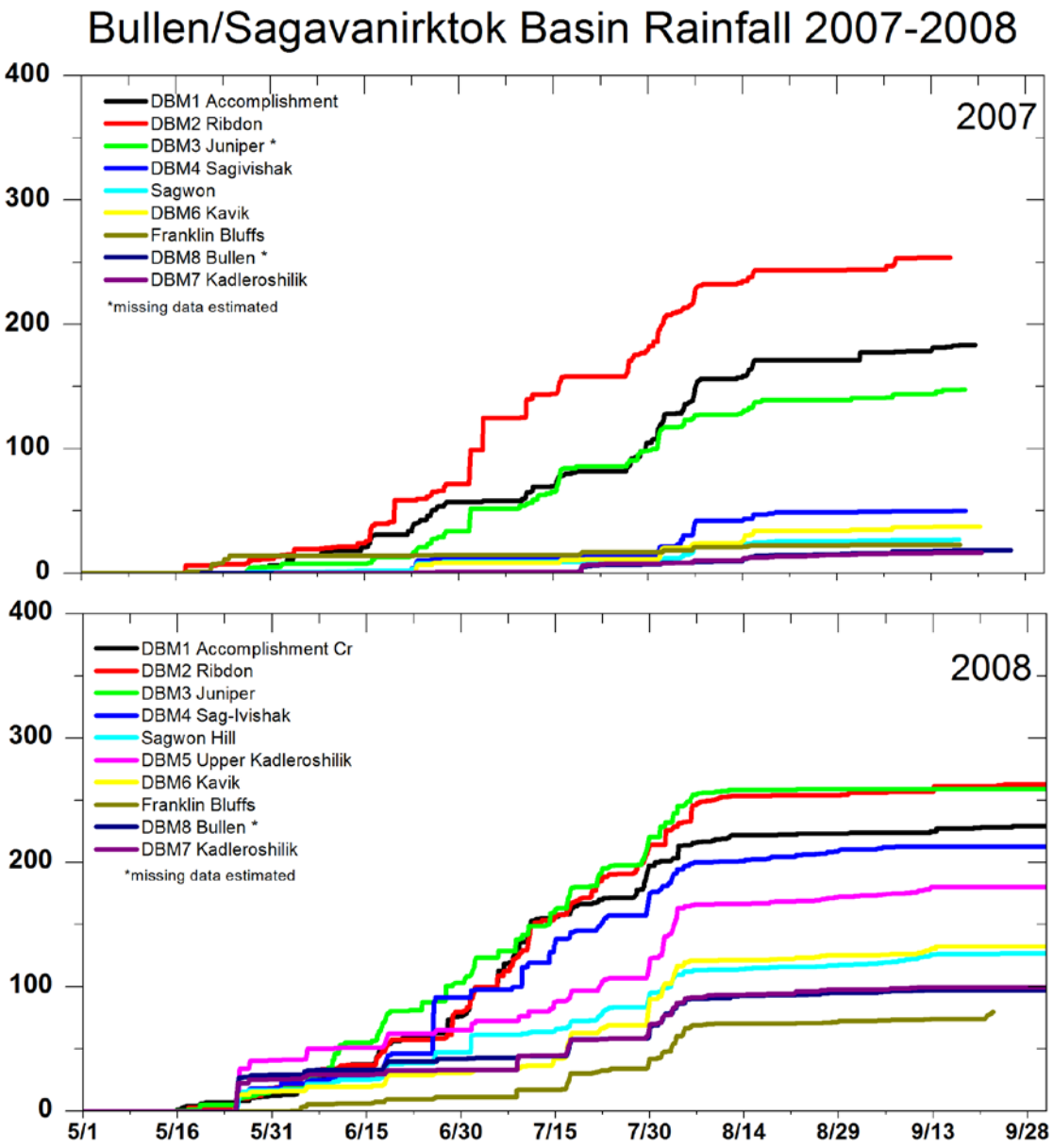

Figure 18. Cumulative summer precipitation for the Bullen/Sagavanirktok Basin region for 2007–2008.

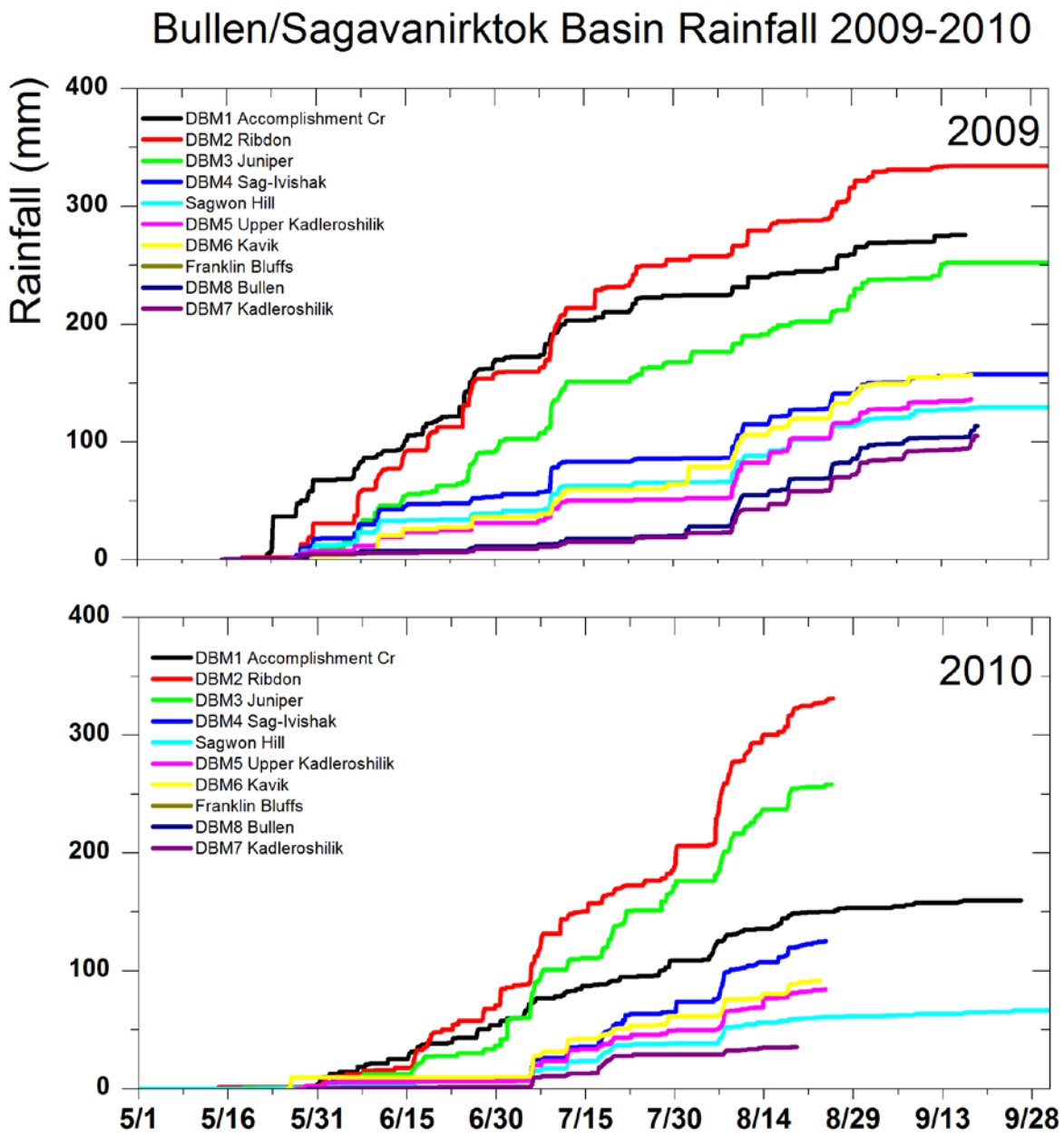

Figure 19. Cumulative summer precipitation for the Bullen/Sagavanirktok Basin region for 2009–2010.

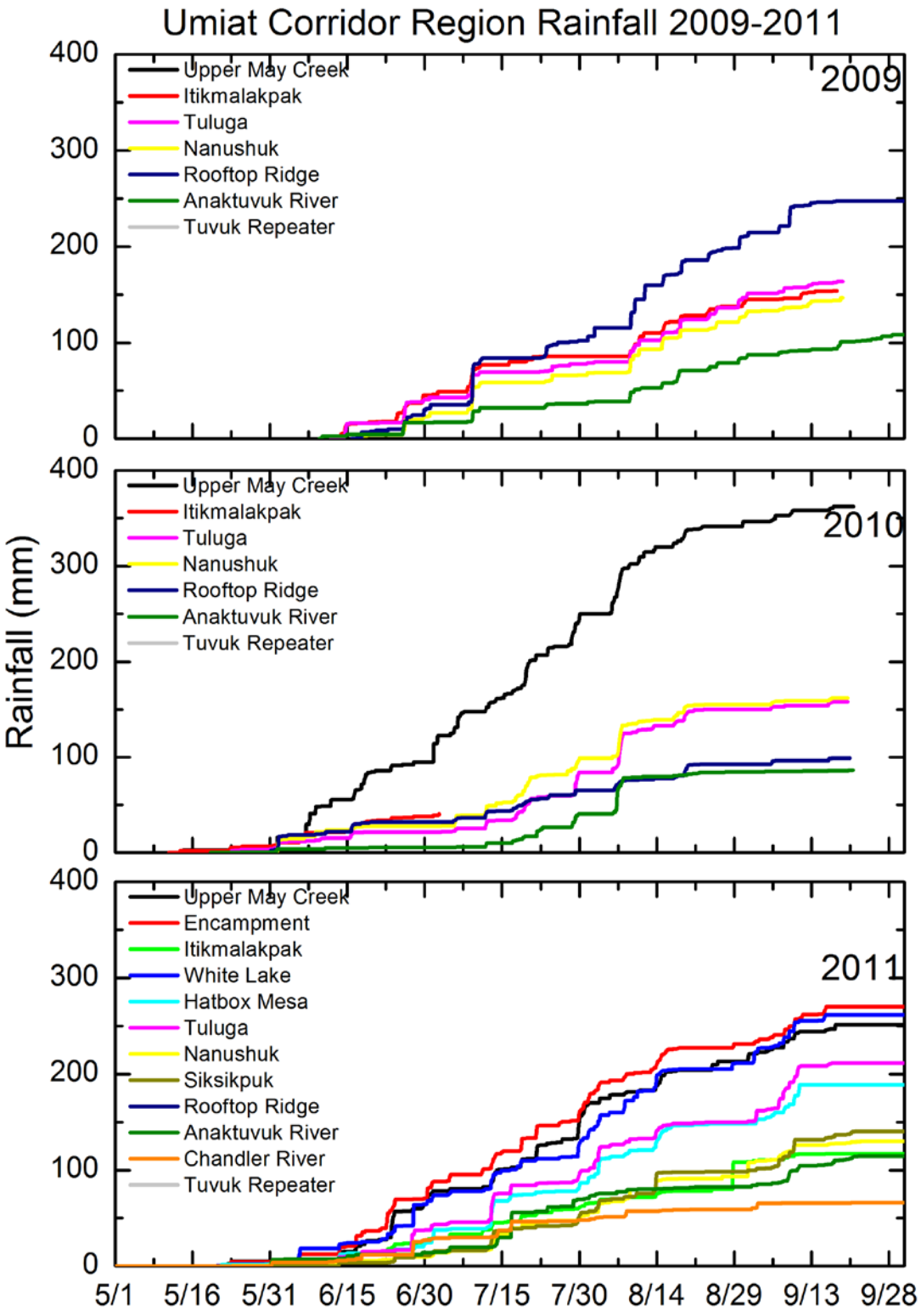

Figure 20. Cumulative summer precipitation for the Umiat Corridor region (Chandler, Anaktuvuk, Itkillik basins) for 2009–2011.

4.5 Snow Depth

Snow hydrology is obviously a very important component of the Arctic hydrologic cycle. Spring break-up, from the melt of approximately nine months of snow accumulation, is usually the biggest hydrologic event of the year. Because of the disparity in the watershed areas that contribute to runoff (potentially the entire basin for snowmelt and only part of the basin for rainfall), the snowmelt flood is usually the largest flood of the year, especially for large north-draining rivers.

Snow depth recorded by sonic sensors at the weather station is used in conjunction with snow survey data to expand the information gained from both sampling methods. Since an ultrasonic sensor (see Stuefer et al. [2011] for details) records snow depth at a single point, the additional fifty snow depth measurements near each station are taken to represent local-scale variability (Table 20). There is considerable variability in terms of how well snow sensors represent local snow course depths from year to year, which in large part is dependent on the location of the snow depth sensor. For example, the SR50 sensor at North White Hills (DFM3) station consistently records a lower snow depth than the fifty observed depths near the station (Stuefer et al. 2011).

Table 20. Snow depth information from meteorological stations and co-located snow surveys in 2011.

Meteorological Station	Snow Survey Depth Range (cm)	Snow Survey Depth Average (cm)	Observed Depth Under SR50 (cm)	SR50 Reported Depth at Time of Observed Depth (cm)	Difference Between Observed and SR50 Reported Depth (cm)
Accomplishment Creek (DBM1)	28-141	102.4	79	82.3	-3.3
South White Hills (DFM1)	41-76	55.2	NA	50.1	NA
White Hills (DFM2)	0-21	12	16	16	0
North White Hills (DFM3)	15-52	30.6	22	26	-4
Northwest Kuparuk (DFM4)	28-79	51.5	61	61.4	-0.4
Itikmalakpak (DUM1)	16-51	26.5	18	16	2
Upper May Creek (DUM2)	1-15	6.4	5	4.3	0.7
Nanushuk (DUM3)	5-66	32.9	17	15.2	1.8
Tuluga (DUM4)	11-87	53.5	54	53.6	0.4
Encampment Creek (DUM5)	0-37	12.2	1	NA	NA
White Lake (DUM6)	10-45	23.1	27	24.9	2.1
Hatbox Mesa (DUM7)	38-64	53.4	85	84	1
Siksikpuk (DUM8)	31-87	60.6	77	76.7	0.3
Anaktuvuk (DUS2)	21-51	37.4	37	39.9	-2.9
Chandler (DUS3)	35-70	55.6	48	NA	NA

The SR50 sensor at Northwest Kuparuk (DFM4) station recorded a lower snow depth in winter 2006-2007, a higher snow depth in winter 2007-2008, and close to average snow depths for the winters of 2008-2009, 2009-2010, and 2010-2011 (Stuefer et al., 2011). This is an example of the challenges associated with siting the sensor and using SR50 snow depth data for quantitative analysis.

During the last winter (2010-2011), SR50 measurements were recorded at fifteen meteorological stations. The number of weather stations has changed over the years, depending on funding sources. Of those stations, seven (DBM2–DBM8) were removed from the Sagavanirktok, Kadleroshilik, and Shaviovik basins in fall 2010, due to the ending of the Bullen project (funded by Alaska Department of Natural Resources). One station from the Bullen project (DBM1, Accomplishment Creek) remains in the Sagavanirktok basin. Four stations (DFM1-4) are still collecting data in the Kuparuk basin as part of the former Kuparuk Foothills (ADOT&PF study). As part of the Umiat Corridor project (ADOT&PF), five new stations (DUM5–DUM8 and DUS3) were installed in the Chandler basin during the fall of 2010 and five stations (DUM1-4, DUS2) were installed in the Anaktuvuk basin in June 2009, bringing the 2010-2011 SR50 sensor count to fifteen for the 2010-2011 winter.

The advantage of snow sensor information is its high temporal resolution, which captures the timing and magnitude (depth) of solid precipitation and wind blowing events. On February 23, 2011, a major wind event occurred that is visible in most of the continuous snow depth measurements. An increase in air temperature from -20°C to 0°C was also observed. The strong winds significantly redistributed the snow and completely removed the snowpack from some locations (e.g., Encampment Creek and Itikmalakpak). Figure 21 and Figure 22 show the web camera, wind speed, and snow depth at the high-elevation Itikmalakpak (DUM1) station in the Anaktuvuk basin. There was a decrease of 40 cm in snow depth in two days according to the SR50 snow depth sensor and camera images. At the Encampment Creek (DUM5) station in the upper Chandler basin, the average hourly wind speed was measured up to 35 m/s (78 mph), with a maximum wind speed of 49 m/s (109 mph). Evidence of this wind event was also visible at the Imnavait Creek snow fence, where snow depth at the snow fence increased 1.8 m within a few hours. Although most of the stations located in the Mountain region had decreases in snow depth

during the wind event, local redistribution was observed at Accomplishment Creek (DBM1), where the snow depth increased by 30 cm. This difference means that the Accomplishment Creek site is located in an area where snow is deposited during snow redistribution by wind (i.e., snowdrift), whereas other sites with decreased snow depth (e.g., Encampment Creek) are located in snow-erosion areas.

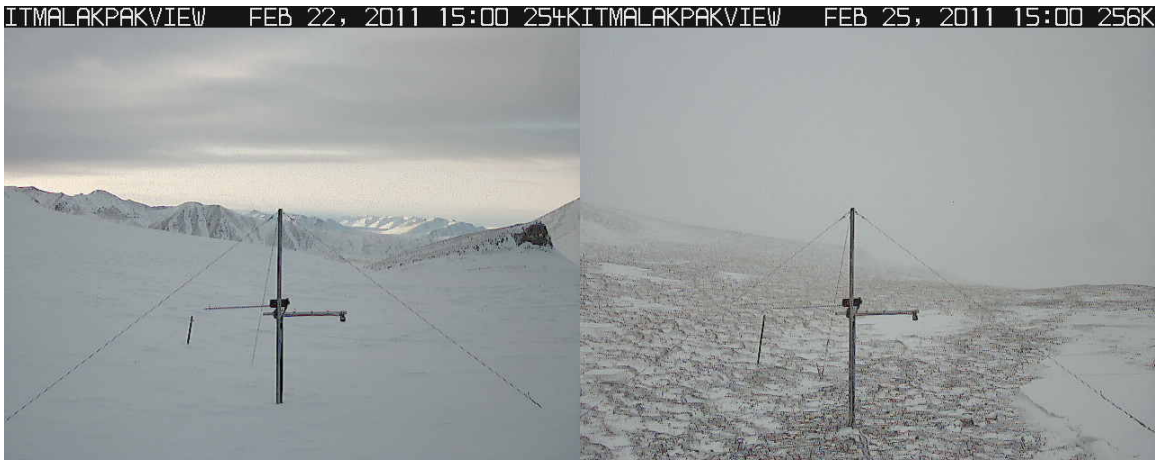

Figure 21. Webcam images at Itikmalakpak station show a decrease in snow depth during the February 23 wind event.

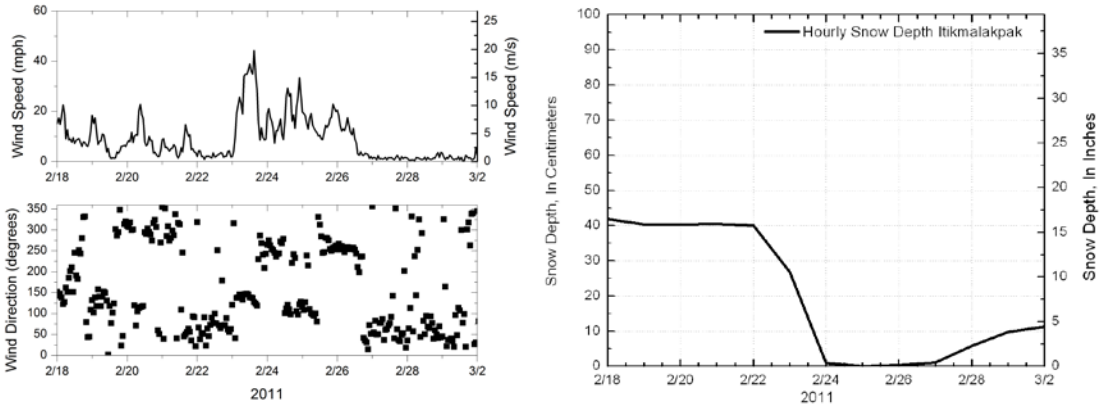

Figure 22. Wind speed, direction, and snow depth recorded at Itikmalakpak before and after the February 23, 2011, storm event.

4.6 Field Snow Surveys

Snow survey sites are generally chosen to represent snow characteristics over a wide range of vegetation and terrain conditions (Figure 23). Snow water equivalent (SWE) is measured at elevations from 5 to 1478 m (16.4 to 4849 ft). To determine regional average SWE, snow sites are classified as Coastal Plain, Foothills, and Mountain, based on elevation and surrounding topography. Coastal sites are generally located below an elevation contour of 152 m (500 ft). Foothills sites are located above 152 m (500 ft) and below an elevation contour of 1000 m (3300 ft). Elevation alone is not always representative for the classification of Mountain sites; because many of them are located in lower elevation valley bottoms where a helicopter can safely access the site. We selected Mountain sites either based on elevation (above an elevation of 1000 m (~3300 ft) or based on surrounding topography. If the mountain ridges around the snow survey site are above 1000 m (3300 ft), we classified this site as Mountain, even if the site itself is located at the lower elevation.

Observations from year to year suggest that regional end-of-winter SWEs and snow depth of the Foothills and Coastal Plain regions are generally higher than those of the Mountain region. The average Coastal Plain snow density is generally higher than the Foothills and Mountain snow density. As an example, averaged snow depth and SWE at each snow survey site visited in 2011 are shown in Figure 24 and Figure 25 (from Stuefer et al., 2011).

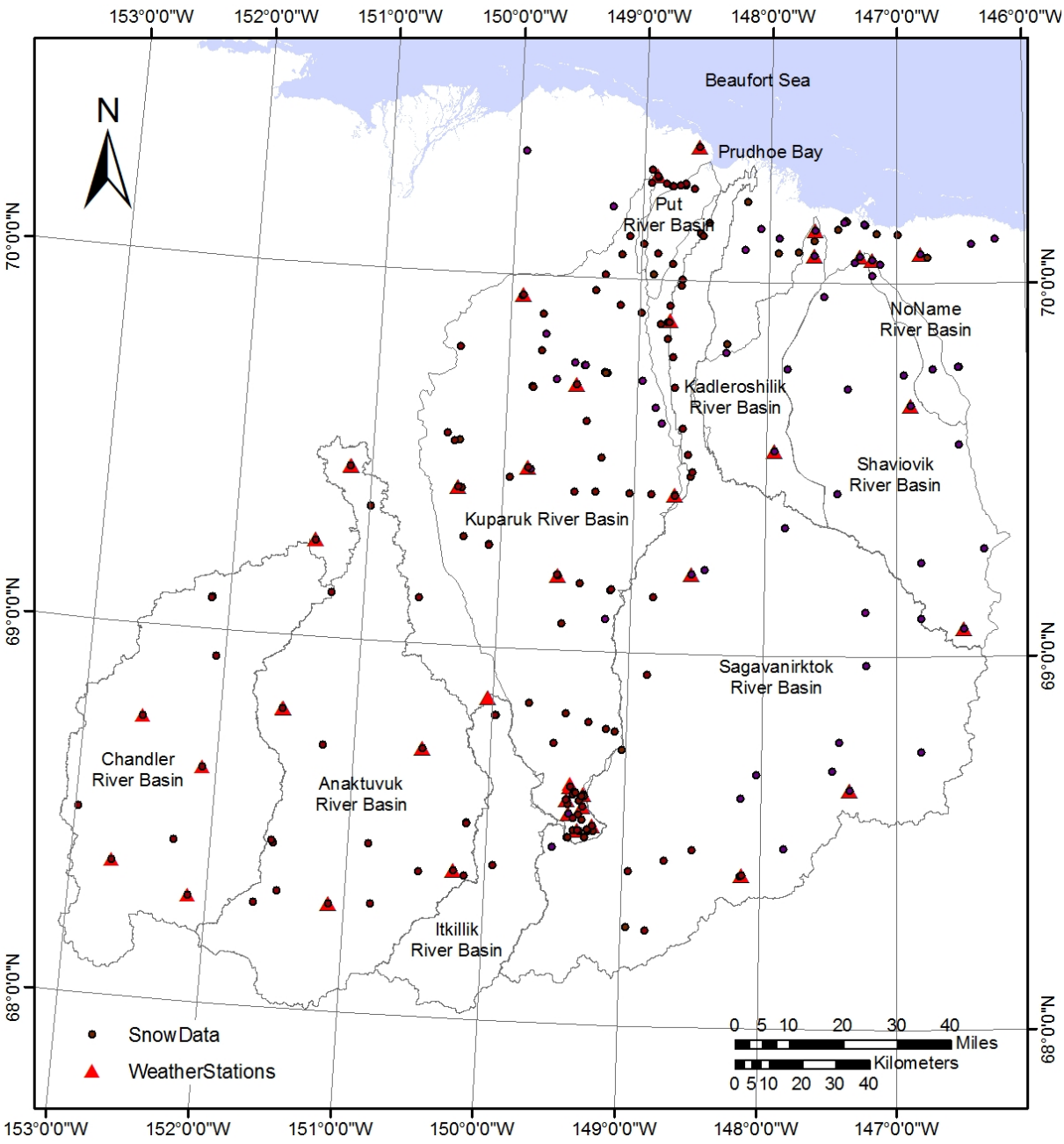

Figure 23. Geographical map of study area shows location of all snow survey sites visited from 2007 to 2011. Some of the sites were visited every year, but not all of them. All weather stations from 2007 to 2011 (they also double as snow survey sites) are shown in red triangles. Plotted watershed boundaries above hydrologic observation stations were derived from the digital elevation model by WERC researchers.

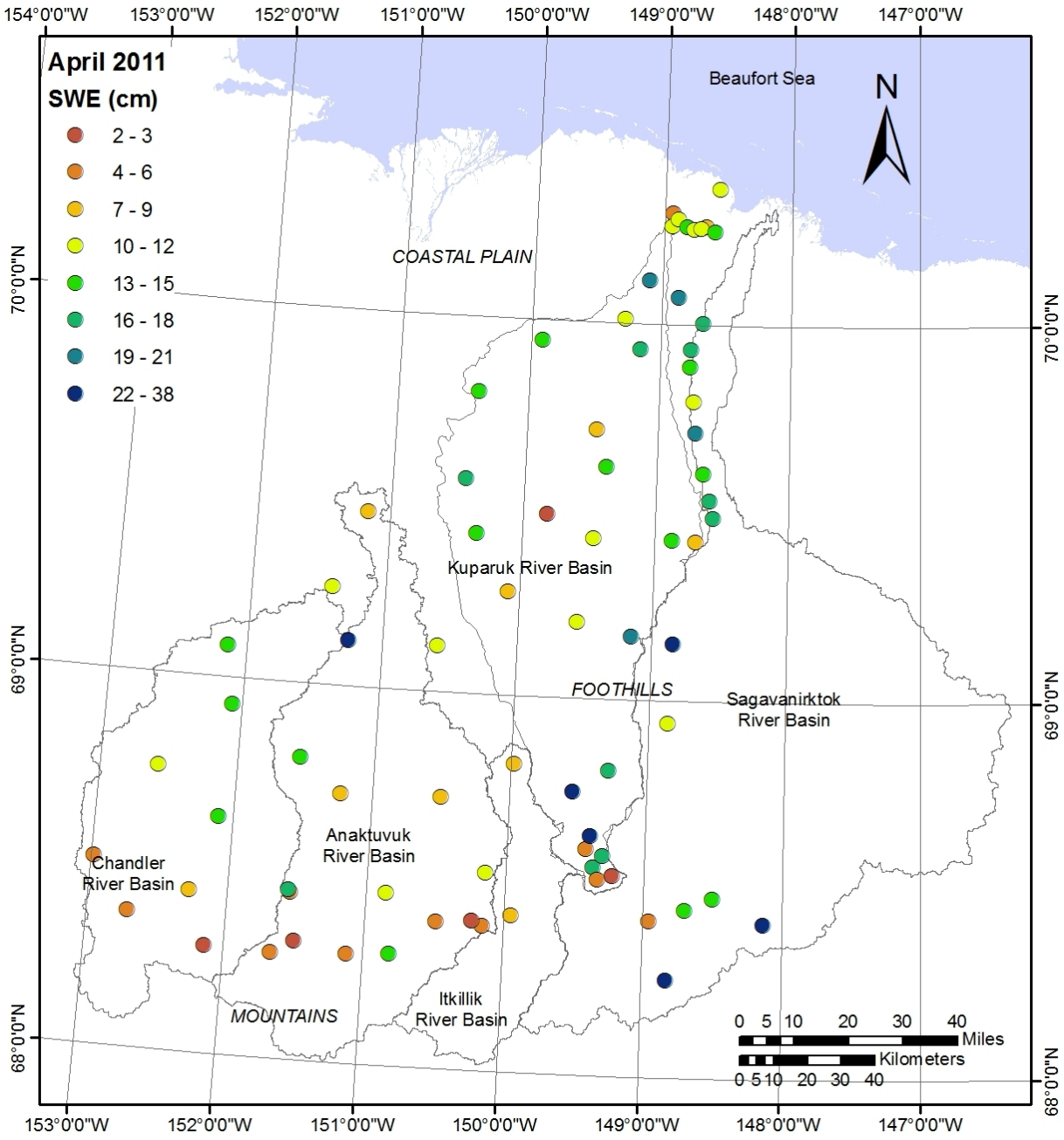

Figure 24. End-of-winter snow water equivalent (cm) in the central North Slope of Alaska in spring 2011. Each point represents the average from 50 snow depths.

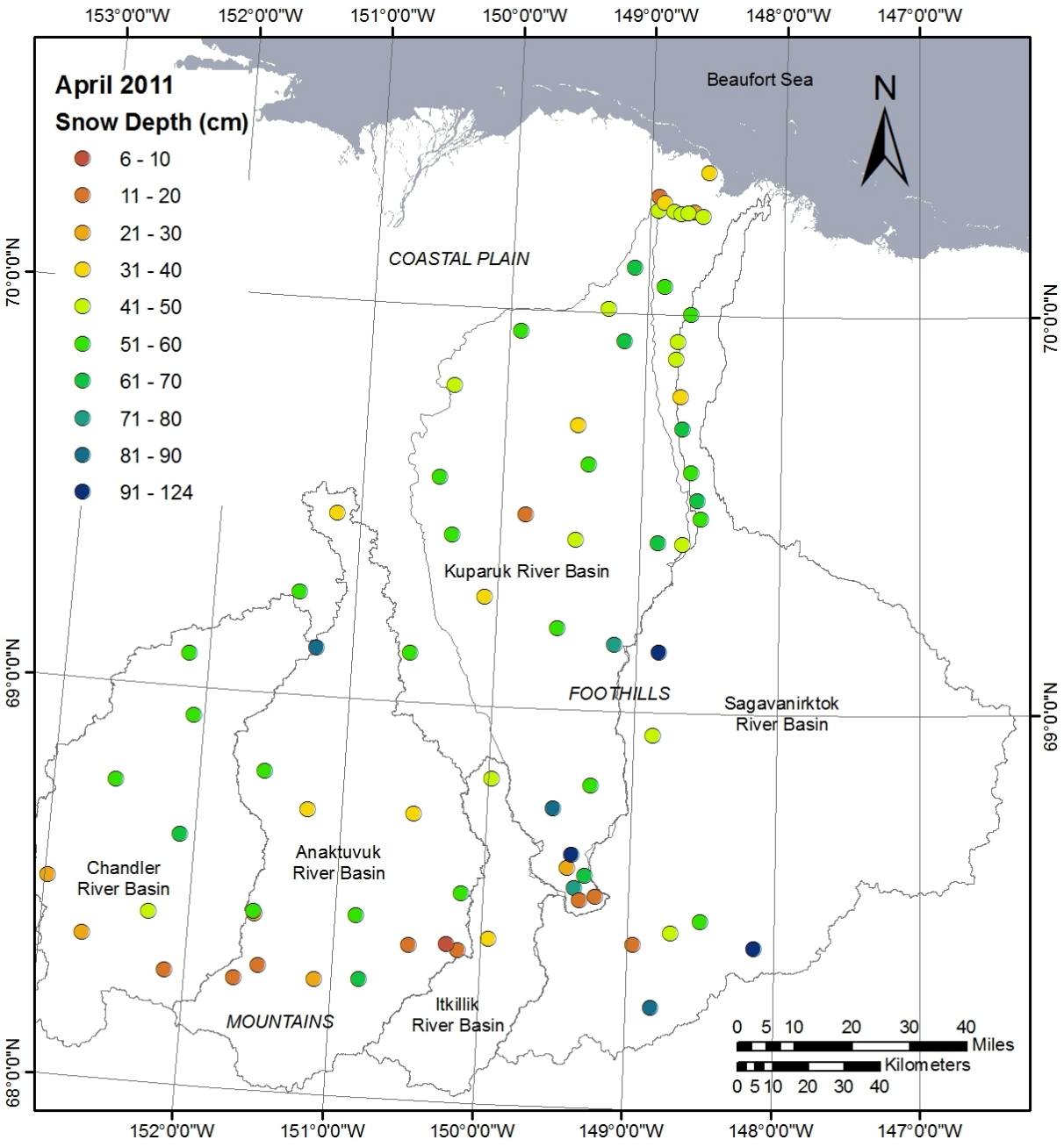

Figure 25. End-of-winter snow depth (cm) in the central North Slope of Alaska in spring 2011.

The number of visited snow survey sites at each basin varies from year to year because weather conditions do not always allow access to all the stations by helicopter and because research funding varies from year to year. Average SWE and number of stations within each watershed are summarized in Table 21 for the period 2006 to 2011. The average SWE, presented in Table 21, should be interpreted with caution, as a slightly different number of stations are visited each

year. Note that observations in the Anaktuvuk River watershed began in 2009. Data collection for the Itkillik and Chandler basins began in 2010. Since we have a limited number of sites in the Itkillik basin, nearby sites are included in the basin average. As of 2010, we no longer measure SWE at most of the former Sagavanirktok sites and those further east. The Kuparuk River watershed has the most complete snow record over the last 6 years; however, the number of sites visited each year varies from 25 (in 2011) to 89 (in 2007), which is more than a factor of three. This varying number of snow survey sites affects basin-averaged SWE in Table 21.

Table 21. Snow water equivalent (cm) from 2006 to 2011, averaged across the different watersheds on the central North Slope of Alaska. Note that the varying number of sites visited each year affects the representativeness of the averaged SWE in the watersheds.

Basin	2006		2007		2008		2009		2010		2011	
	n	SWE (cm)	n	SWE (cm)	n	SWE (cm)	n	SWE (cm)	n	SWE (cm)	n	SWE (cm)
Kuparuk	63	8.4	89	10.3	73	8.6	63	19.3	25	10.3	25	12.6
Upper Kuparuk	20	7.9	21	9	21	5.8	21	11.4	6	7.2	6	12.4
Sagavanirktok	19	7.8	25	7.4	23	6.5	26	13.1	24	9.2	13	17.3
Putuligayuk	5	9.9	5	6.9	5	8.3	5	14.1	4	10	4	12.7
Kadleroshilik	1	9.4	1	14.3	0	-	3	12.2	3	8.7	0	-
Shaviovik	8	7.5	9	6.9	7	6.6	10	11.5	11	10.3	0	-
No Name	1	6.6	2	12.3	0	-	1	8.8	2	9.8	0	-
Anaktuvuk	0	-	0	-	0	-	14	9.3	14	8	15	7.6
Itkillik	0	-	0	-	0	-	9	11.4	8	10.1	8	8.7
Chandler	0	-	0	-	0	-	0	-	7	10.6	9	10.4

n=number of sites in basin

For the period of record from 2006 to 2011, the highest SWEs were measured in 2009 and 2011, while 2006 and 2008 were relatively low snow years. This observation is true for the Kuparuk, Sagavanirktok, and Putuligayuk River watersheds. This is hydrologically important as the magnitude of the snowmelt runoff event is closely linked to the snow water equivalent. The basin average SWE for the Anaktuvuk, Chandler, and Itkillik basins for 2011 is lower than expected due to a decrease in snowpack after the February 2011 wind event (many of these sites are located at high elevations in the Mountains and Foothills).

4.7 Solid Precipitation

Our weather stations are equipped with rainfall gauges that measure precipitation in liquid phase. Measurements of solid precipitation at a specific location are taken with USDA Natural

Resources Conservation Service (NRCS) snow telemetry SNOTEL gauges that have been installed in the area since the 1980s. Winter precipitation is measured with the Wyoming wind-shielded gauge. This gauge is composed of a reservoir with a 12 in. orifice, filled with antifreeze and surrounded by the Wyoming-type wind shield. The gauges are located within several meters of WERC-operated 10 m meteorological towers at Imnavait, Sagwon, and Betty Pingo. The gauge records daily precipitation. A field check of the manometer usually occurs in April (at the time of WERC snow surveys) and later in summer by NRCS specialists. Cumulative solid precipitation through the winter starts around September 15 and ends usually around May 15. The snowy season is usually longer at high elevations and farther north. Figure 26 through Figure 28 shows accumulated precipitation plotted for five winters, 2006-2007, 2007-2008, 2008-2009, 2009-2010, and 2010-2011, for the three Wyoming gauge sites. While these gauges do a fair job of measuring solid precipitation at a gauge at the time of precipitation, they may not represent the conditions locally at the end of winter because of wind and sublimation. In general, there is poor comparison between cumulative gauge measurements and end-of-winter snow surveys of SWE. The Wyoming gauge catch ratio for the Imnavait gauge was reported to vary from 70% to 83% for 6 years from 1985 to 1991 (Yang et al., 2000). Typically, Wyoming gauges undercatch the snowfall in windy environments, with the undercatch increasing with wind speed. The end-of-year gauge data for three winters (2006-2007, 2007-2008, and 2009-2010) show a decreasing north-to-south trend in cumulative precipitation. For the other two winters (2008-2009 and 2010-2011), precipitation gauge data show an increasing north-to-south trend in cumulative precipitation. Both cumulative snowfall and average snow survey data suggest that spring 2009 and spring 2011 had higher than average end-of-winter snow water equivalent.

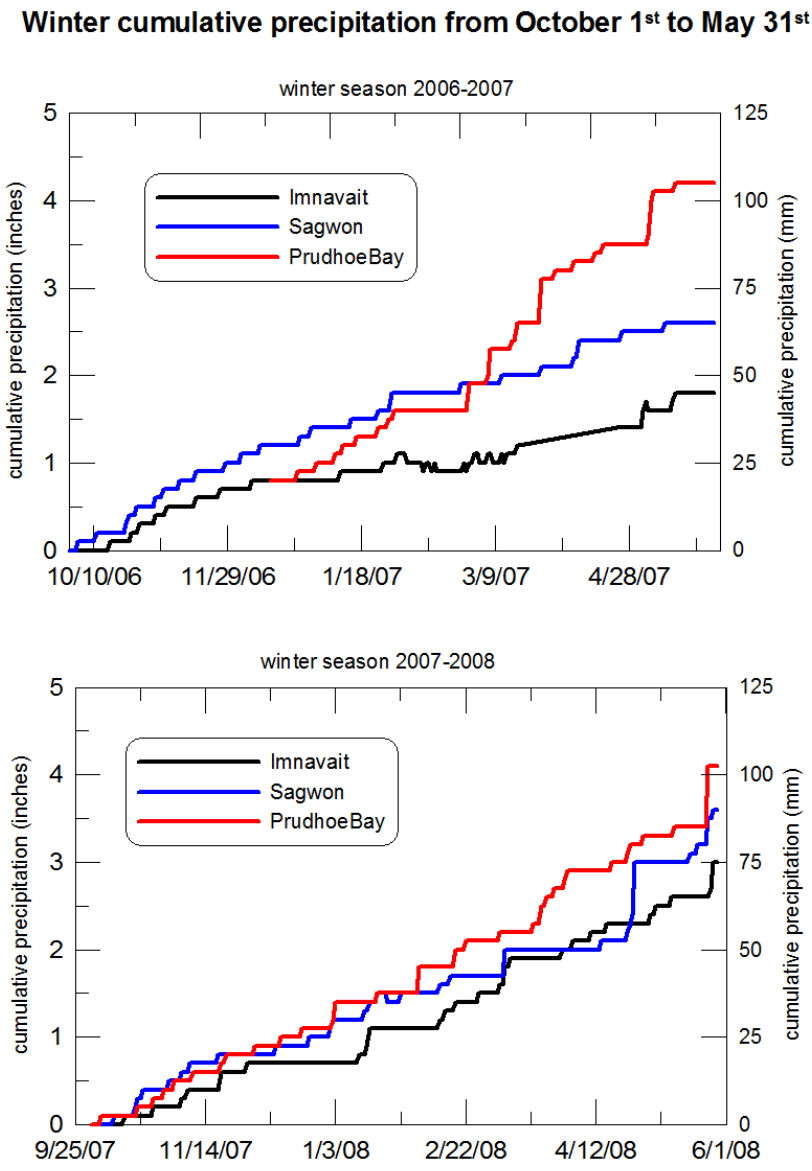

Figure 26. Winter cumulative daily precipitation for Wyoming gauge system from October 1 to May 31 for the following winter seasons: 2006-2007 and 2007-2008.

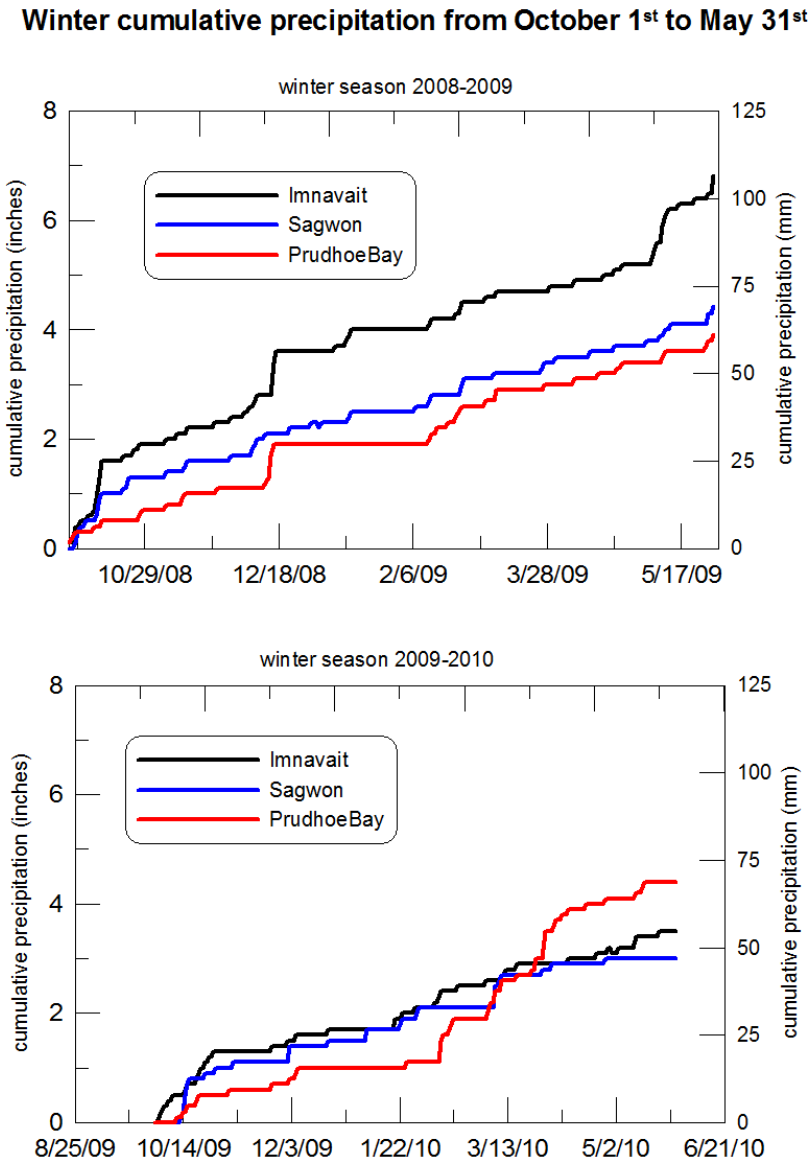

Figure 27. Winter cumulative daily precipitation for Wyoming gauge system from October 1 to May 31 for the following winter seasons: 2008-2009 and 2009-2010.

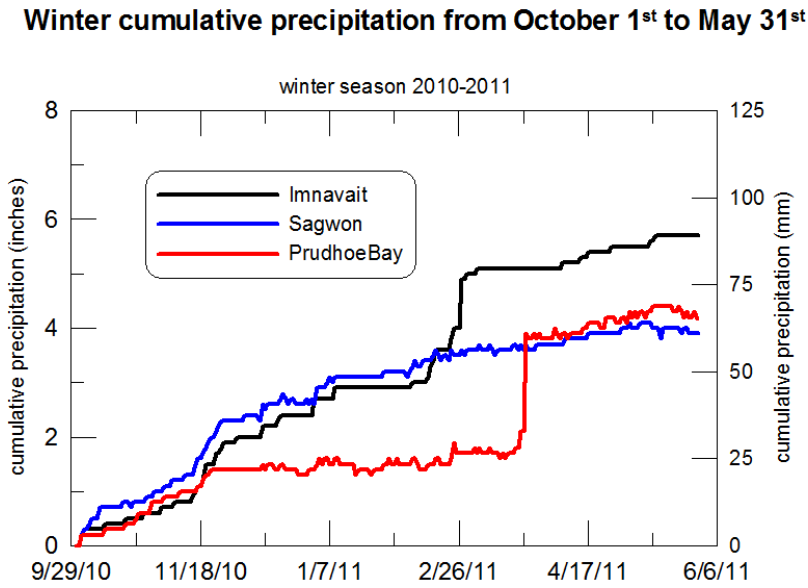

Figure 28. Winter cumulative daily precipitation for Wyoming gauge system from October 1 to May 31 for the 2010-2011 winter season.

4.8 Ablation

The ablation of the snowpack, defined as the net volumetric decrease in SWE, usually starts in the southern Foothills (areas equivalent in latitude to Imnavait basin, Upper Kuparuk sites); a week or two later snow starts melting on the Coastal Plain (Franklin Bluffs, Betty Pingo, and West Dock). We monitor ablation at seven locations distributed between the Mountain region in the south and the Coastal Plain in the north, maintaining long-term snowmelt records from previously funded National Science Foundation, Office of Polar Programs projects (Table 22). We also take ablation measurements at remote stream-gauging sites, as we visit these sites frequently during snowmelt.

Table 22. Summary of snow ablation sites.

Site Name	Period of Record	Comments
Betty Pingo	1993 to 2011	Surveyed near NRCS precipitation gauge.
West Dock	1999 to 2009	150 m east of West Dock–GC1 Road, approximately 1 mi south of West Dock Meteorological Site.
Franklin Bluffs	1988 to 2011	Surveyed near Met site 1988 to 1998 (with some missing years), snow site moved west 700 m along access road from 1999 to 2010.
Anaktuvuk	2011	10 m north (upstream) of Anaktuvuk hydro-meteorologic station
Sagwon Hill	1988 to 2011	Adjacent to the Sagwon Meteorological Site
Chandler	2011	Helicopter landing area near Chandler River meteorological station on bluff above the river
Happy Valley	1999 to 2011	Survey site 150 m west of Dalton Highway from Happy Valley Airfield.
Oil Spill Hill	2010	Surveyed 250 m west of pullout on top of Oil Spill Hill along the Dalton Highway.
Itkillik	2011	Right bank on lower terrace, 200 m north of Itkillik River surface-water observation station
Upper Kuparuk	1999 to 2011	Adjacent to the Upper Kuparuk Meteorological Site.
Imnavait basin	1985 to 2009	Snow ablation measured at 4 sites on west-facing slope at mid-basin 1985 to 1988, at a 6-site mid-basin transect 1989 to 1997 and at a 6-site transect along UTM 612800 northing from 1999 to 2010.
Galbraith	2010	West of Galbraith Airport, adjacent to gravel pit access road.
Atigun Pass	2010	30 m north of NRCS precipitation gauge.

Measurement methods have changed over time as techniques have been modified to improve sampling accuracy and as the study area has expanded. From 1985 to 1992, SWE was estimated from 10 randomly collected snow cores. These cores were sampled using Adirondack tubes and weighed using mechanical scales, calibrated in inches of water. To overcome the difficulty of weighing samples in frequent high wind conditions, cores were placed in bags in the field and weighed later indoors, using the Adirondack mechanical scale and, after 1999, digital scales. Following Rovansek et al. (1993), the double sampling technique, which was adopted in 1996, is still used (Section 3.1). During the transition period (1993–1995), 5 to 20 snow cores were taken, along with 50 snow depths. Snow depths have been measured using a variety of devices, such as the Adirondack snow tube, avalanche probes, T-handled graduated probes, MagnaProbe, and ski poles and rods with added graduated scales.

A number of observational sites have changed over time (Table 22). In 1985, SWE and ablation were observed only in the Imnavait Creek basin. Sagwon Hill (SH) and Franklin Bluffs (FR) sites were added in 1986 (although measurements were often lacking). Snow surveys at the Sagwon site were usually made just east of the meteorological site. From 1986 through 1998, the Franklin Bluffs sampling site was located adjacent to the meteorological site 1 km east of the Dalton Highway. In 1999, the snow survey and ablation site were moved west approximately 300 m from the highway. The Betty Pingo site on the Prudhoe Bay Oilfield was established in 1992. This snow survey site is located near the NRCS Wyoming snow gauge about 200 m north of the Kuparuk Pipeline Road between P-Pad and Gathering Center 2. Upper Kuparuk, Happy Valley, and West Dock snow survey and ablation sites were added in 1999. Three snow ablation sites at Oil Spill Hill, Galbraith, and Atigun Pass were monitored only one year, in 2010.

Imnavait Creek basin (IB) differs from others in that it has the longest period of record and more detailed observations. Several sites were sampled across the basin to capture basin average SWE. From 1985 through 1997, the Imnavait basin SWE was determined from a transect made across the basin, perpendicular to the stream channel. At that time, snow ablation was tracked only at the west-facing slope adjacent to 4 runoff plots (Hinzman, 1990). In 1989, two additional sites were added: one in the valley bottom and one on the low east-facing slope of the basin. To provide consistent identification of sites, the transect has been aligned with the 7612800 northing (NAD27, UTM6) since 1999.

Snow ablation measurements were supported initially by the U.S. Department of Energy and then the National Science Foundation (NSF). Support from NSF was no longer available after spring 2009, which resulted in the reduction of snow survey and ablation sites. Ablation observations were discontinued at the West Dock (WD) and at 6 sites across the Imnavait basin (IB1–IB6). Instead, three more sites (Itkillik, Anaktuvuk, and Chandler surface-water observation stations) were added in 2011. These sites are visited daily or every other day during ablation to capture the net volumetric decrease in SWE. We continue to take 5 snow density and 50 snow depth measurements at each site. The snow depth course during snowmelt has an assigned location because of numerous repeated measurements (usually 7 to 12 visits during ablation).

The ablation window varies greatly from year to year, depending on meteorological conditions, such as radiation and air temperature, and on snowpack depth (Figure 29 through Figure 35). Meteorological conditions conducive to snowmelt are southerly winds over the Brooks Range; northerly winds off the Arctic Ocean typically result in zero or reduced snowmelt rates. Most of the sites report the onset of ablation between May 15 and May 31. The entire snowpack melts usually between June 1 and June 10. The snow at the Happy Valley site (located along Dalton Highway between Upper Kuparuk and Sagwon) is often the last location to melt, because it has very deep snowpack (38 cm of SWE, 124 cm of snow depth in 2011). This area generally has high snow accumulation due to the local topography and vegetation.

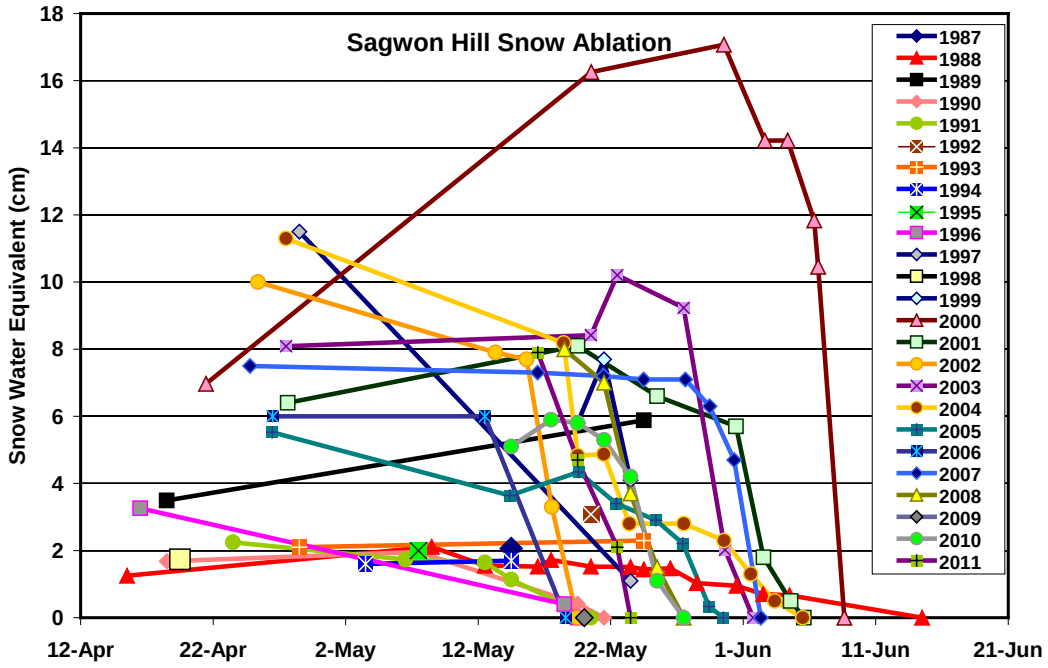

Figure 29. Historical ablation at Sagwon Hill station, 1987–2011. Spring 2000 was a big snow year in the Kuparuk River basin.

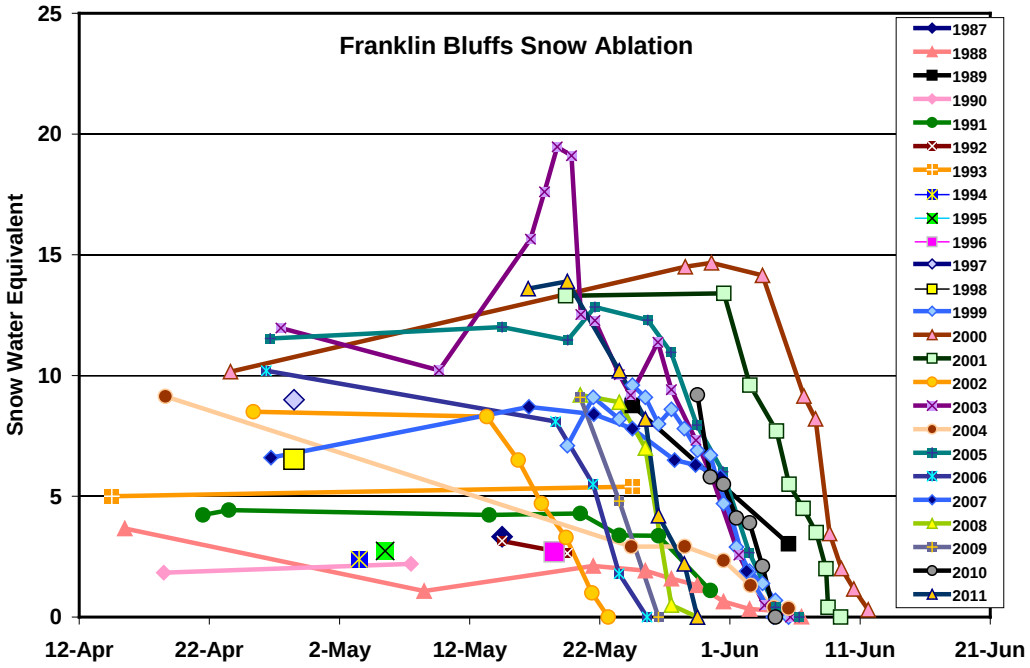

Figure 30. Historical ablation at Franklin Bluffs station, 1987–2011. The snowpack in 2003 almost doubled at this site due to a spring snowstorm.

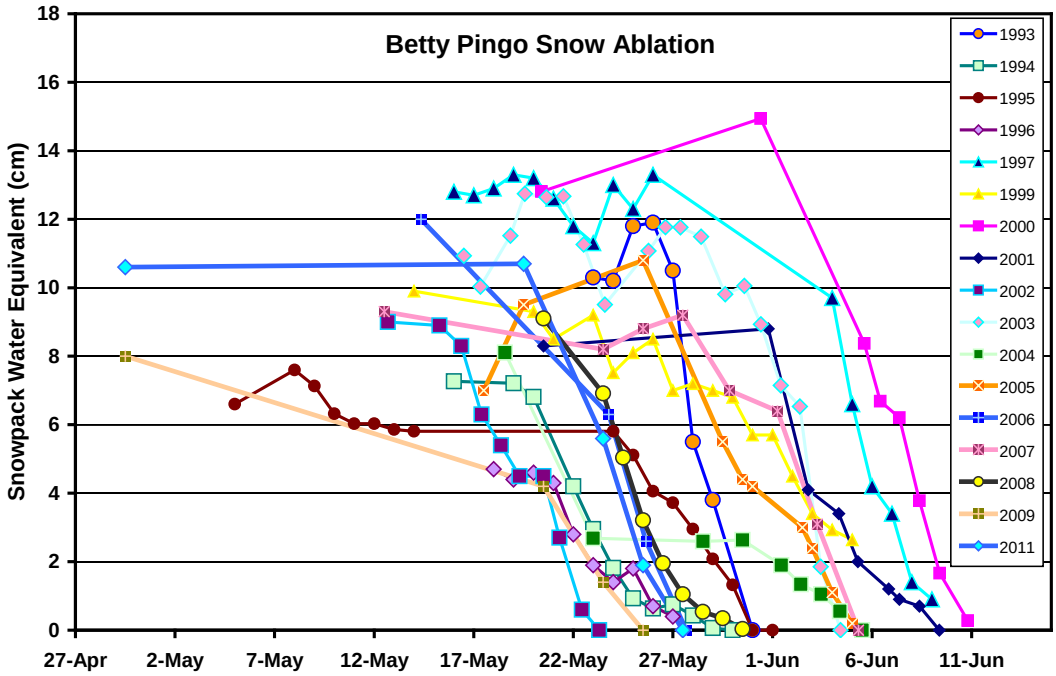

Figure 31. Historical ablation at Betty Pingo station, 1993–2011.

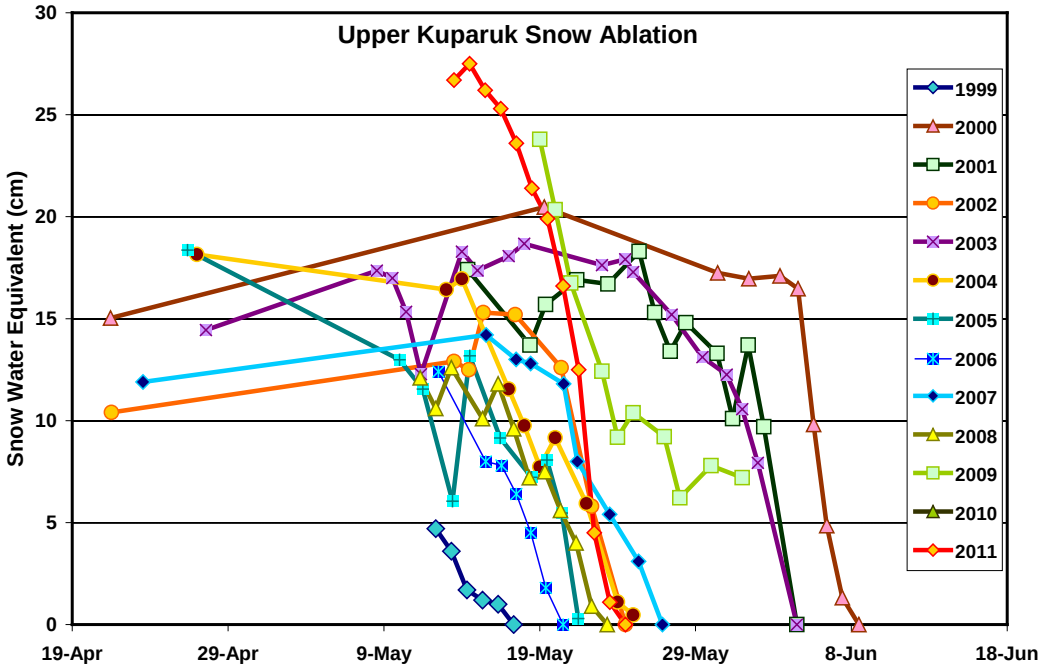

Figure 32. Historical ablation at Upper Kuparuk station, 1999–2011. This station generally experiences locally higher SWEs.

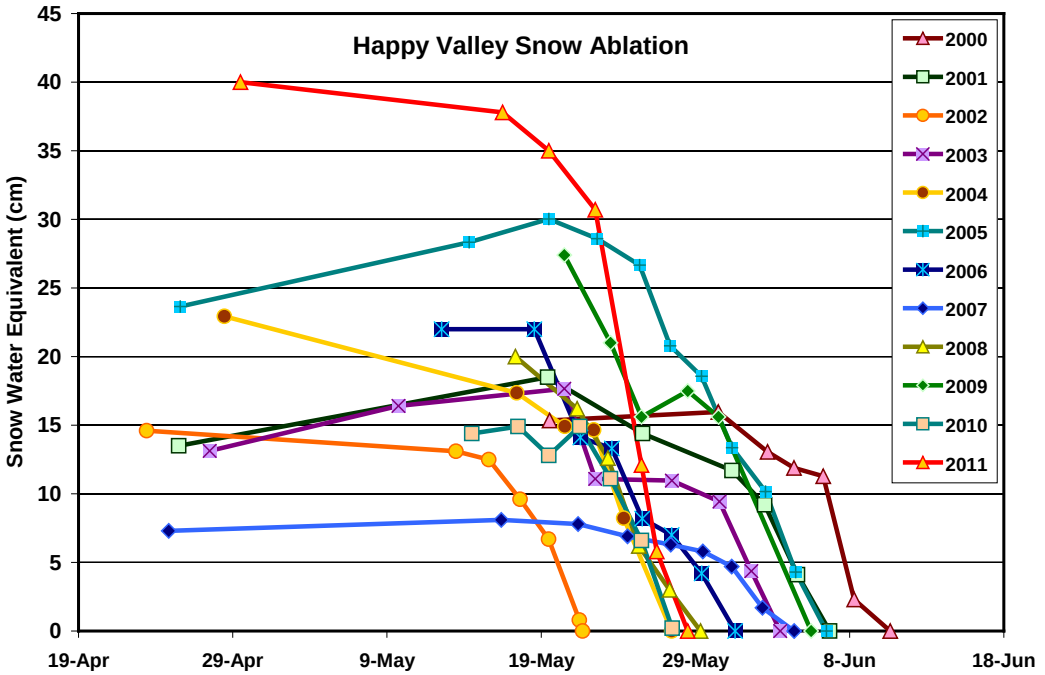

Figure 33. Historical ablation at Happy Valley station, 2000–2011. Happy Valley typically has one of the highest SWEs of the ablation sites due to drifting.

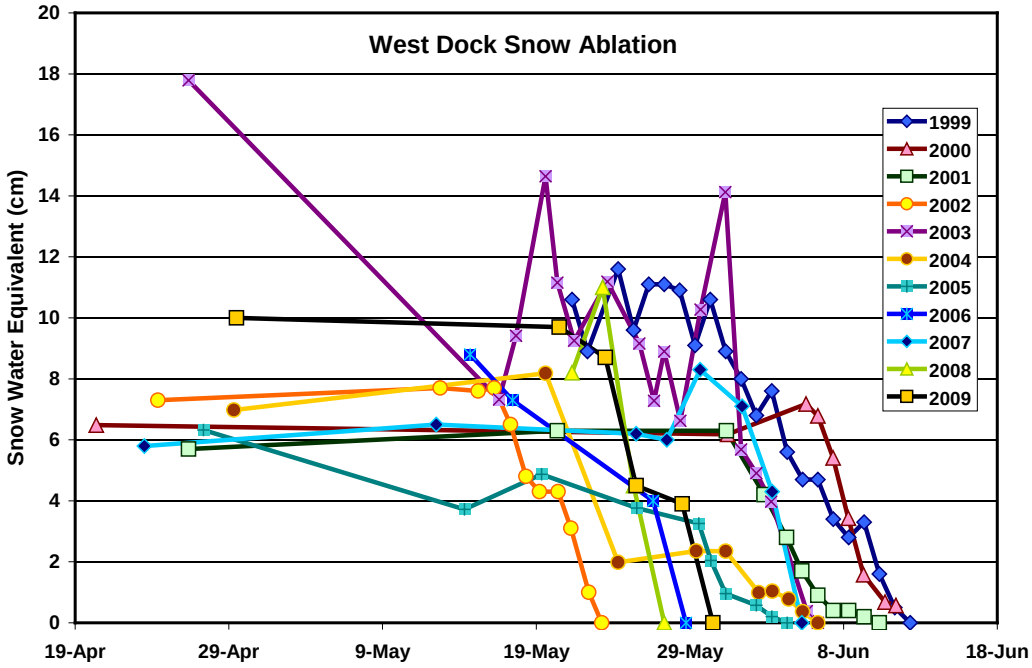

Figure 34. Historical ablation at West Dock station, 1999–2009.

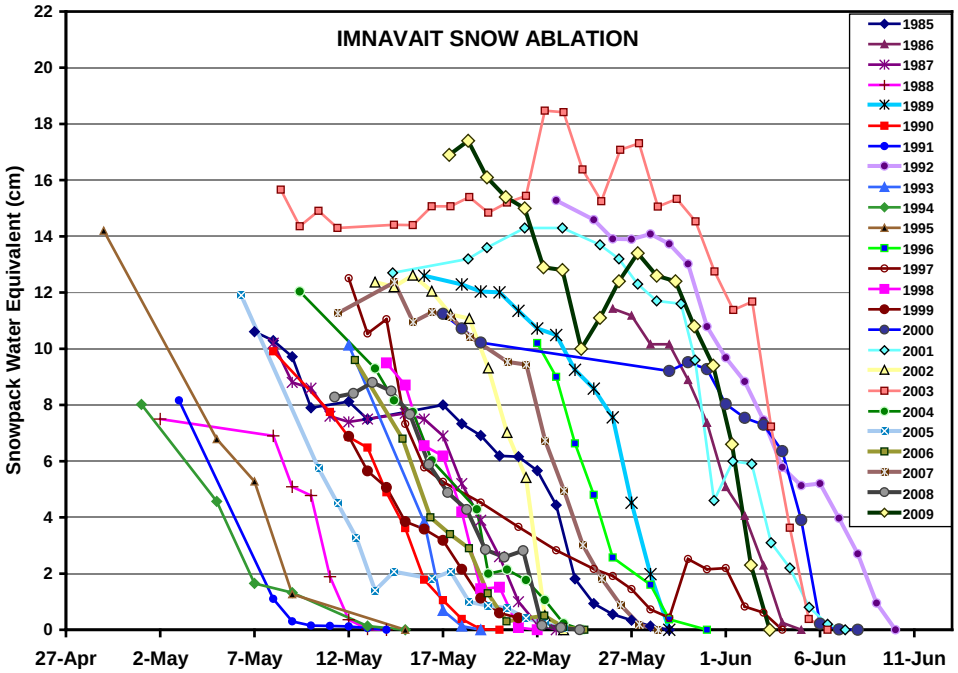

Figure 35. Historical ablation at Imnavait basin, 1985–2009. Note the six-week window of melt and the generally later snowmelt for higher SWEs. The maximum slopes of the ablation curves each year are quite similar and indicate an upper limit to the rate of snowmelt.

4.8.1 Snow Disappearance Date

In light of climate change discussion, great attention was paid to the duration of the snow cover season and dates of snow cover disappearance. We have heard, for example, that the length of the Arctic snow cover season has decreased by more than 10 days (Groisman and Davies, 2002; Stone et al., 2002). Remote sensing products are consistent in detecting the decreasing trend in snow cover duration over the Pan-Arctic from 1967 to 2010 (Derksen et al., 2010). Brown et al. (2011) highlight a close relationship between the air temperature in June, sea ice extent, and shortened snow cover season. We have collected snow ablation measurements for the last couple of decades at seven sites (see Section 3.6 for details). In this section, we summarize the dates of snow disappearance at each site to examine whether we can observe any trends or patterns in the timing of snow cover duration in the spring.

Ablation observations from seven sites (Figure 36) show that the date of snow disappearance varies greatly depending on meteorological conditions and snowpack depth at a particular site. Complete melt of snowpack can occur any time from May 14 until June 11 in the Foothills and from May 24 to June 12 on the Coastal Plain. Often snow first disappears in the southern part of the Kuparuk basin (1999, 2004, 2005, 2010), but in some years the Foothills and Coastal Plain have been snow-covered for the same duration (2000, 2001, 2003, 2011).

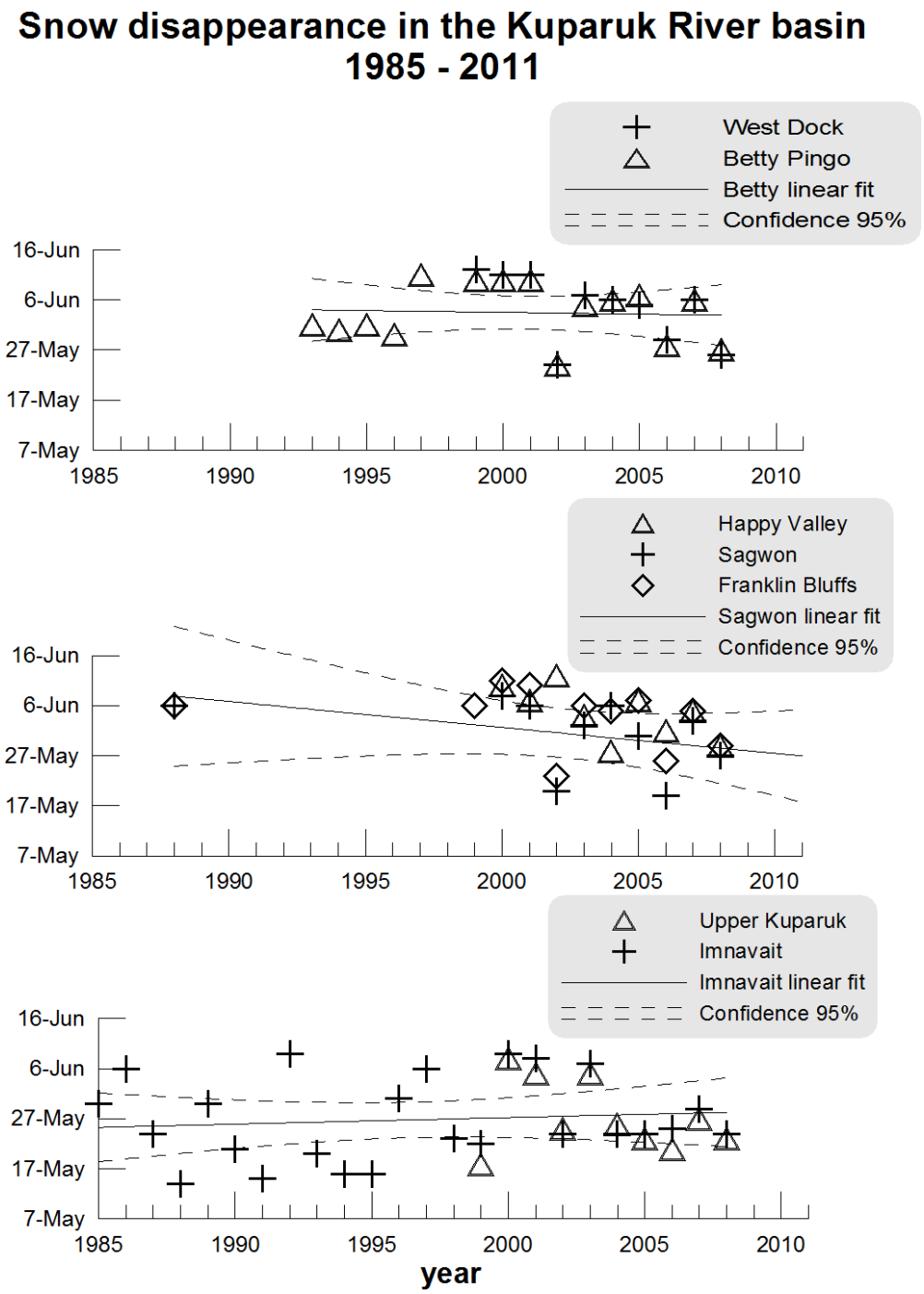

Figure 36. Date of snow disappearance in the Kuparuk River basin. Linear trend and 95% confidence intervals are shown for the selected sites (Betty Pingo, Sagwon, and Imnavait Creek).

The longest time series from the Imnavait site exhibits change in variance and almost no change in mean. Note that for this site, non-homogeneity of variance before and after 1999 is associated

with changes in observational methods and sampling locations. Coastal Plain sites (West Dock and Betty Pingo) exhibit weak negative trends. From our observations, records at the Sagwon site show the most pronounced tendency towards earlier snow cover disappearance. Snow conditions at this site would be representative of the ridgetop (or hilltop) areas exposed to wind, with relatively shallow snow accumulation in the winter. This trend is heavily influenced by one data point in 1988. Other sites, including Happy Valley at the deep snowdrift, Betty Pingo, and Franklin Bluffs at the wide-open area on the Coastal Plain, show little negative trend in the date of snow disappearance. Continuing observations will allow us to identify long-term trends in the data and determine whether they are associated with climate change or inter-annual variability caused by local weather and terrain conditions.

4.9 Soil

Improving our understanding of soil conditions throughout the year is necessary to interpret the hydrologic response of arctic watersheds. Soil temperature is needed for certain hydrologic or energy-balance models, geotechnical applications, winter tundra-travel requirements, and climate studies. Soil moisture content, further discussed in the section on water balance (Section 5.1), is an important part of the hydrologic cycle. The surplus or deficit of soil moisture in the active layer is often a major component of the storage term in the water balance computation. In addition, the amount of soil moisture during late summer and fall greatly influences the next spring snowmelt-runoff response on most arctic rivers. By understanding soil moisture conditions throughout the summer, we can better understand the relationship between precipitation and runoff in hydrologic modeling (Section 5.3).

As part of the Bullen Point and Kuparuk Foothills/Umiat Corridor projects, soil pits are dug at nearly all meteorological stations in order to describe the soil conditions at the station and install soil moisture and temperature sensors. The study area covers a large area, from the Shaviovik River basin in the east to the Chandler River basin in the west. Pictures, samples, and written observations are collected in order to document the soil characteristics of each site. In addition to soil moisture sensors, soil temperature profiles are installed in nearby pits to a depth of up to 1.5 m when possible. A brief summary of the soil properties of each station are included in Table 23.

Table 23. Soil description for each station.

Station Name	Max Depth of Soil Temp. Sensor	Site Description	Soil Description
DBM1 - Accomplishment Creek	N/A	Mountainous	Large rocks and weathered bedrock at surface.
DBM2 - Ribdon	120	Mountainous	Weathered bedrock. Soil pit was dry and consisted of gravelly mineral soil.
DBM3 - Juniper	N/A	Mountainous	Large rocks and weathered bedrock at surface.
DBM4 - Sag/Ivishak	150	Upland with rolling hills	Shallow, thin organic layer (0-5 cm) underlain by mixed mineral organic soil. Mineral layer contains some gravel. Substantial water pooled at bottom of pit at time of installation.
DBM5 - Upper Kadleroshilik	100	Upland with small rolling hills	Organic layer (0-15 cm) underlain by mineral soil. Both organic and mineral layers appear moist with water collecting at pit bottom. Little to no gravel.
DBM6 - Kavik	120	Foothills, Kavik River floodplain	Organic layer (0-25 cm) underlain by mineral soil. Bottom of pit at ~75 cm.
DBM7 - Lower Kadleroshilik	40	Coastal Plain, adjacent (10 m) to Kadleroshilik River above bank	Organic layer (0-15 cm) underlain by mineral soil
DBM8 - Bullen Point	120	Coastal Plain	Organic layer (0-15 cm) underlain by possibly mixed mineral soil. Mineral soil may contain gravel/ boulders.
DFM1 - South White Hills	150	Upland with small rolling hills	Thin organic layer (0-5 cm) underlain by dense, homogenous grey mineral soil. One vein of organic soil within pit. Bottom of soil pit at 50 cm is dry.
DFM2 - White Hills	150	Foothills, located at the flat ridgetop of a large hill	Weathered bedrock at surface.Poorly consolidated mineral soil with pebbles. No organic layer.
DFM3 - North White Hills	120	Boundary of Foothills/Coastal Plain with small rolling hills. Poorly drained, fairly flat, tussock tundra with small shrubs.	Organic layer (0-20 cm) underlain by mineral soil. Gradual transition to mineral with some mixing.
DFM4 - Northwest Kuparuk	150	Coastal Plain, flat, tussock tundra.	Organic layer (0-10 cm) underlain by mineral soil. Water accumulation at bottom of pit at ~75 cm bgs.
DUM1 - Itikmalakpak	80	Rocky mountain site with tundra at surface in vicinity of station. Pass saddle.	Coarse-loamy, mixed, pergelic Ruptic Histoturbel. Organic layer (0-15 cm), and mineral soil at 15-50+ cm bgs.
DUM2 - Upper May Creek	N/A	Mountainous region, flat rocky ridgetop	Fragmental, mixed pergelic Lithic Eutrogelepts. Weathered bedrock at surface. Mineral and rocky soil from 0-35 cm bgs. Large gravel and cobbles up to 25 cm width.
DUM3 - Nanushuk	100	Foothills region, tundra. Moraine, upper part of ridge.	Fragmental, mixed, pergelic Lithic Eutrogelepts; Rocky for first 1-15cm; Organic layer (0-20 cm) underlain by mineral soil 20-100+ cm bgs.
DUM4 - Tuluga	100	Foothills region, site on a rocky ledge, sparse tundra in area. Moraine. Upper shoulder/ridge of hill.	Organic layer 0-20 cm bgs, Mineral soil ~20-120 cm bgs.
DUM5 - Encampment Creek	N/A	Mountainous ridge up against high mountains	Large rocks and boulders at surface.

Station Name	Max Depth of Soil Temp. Sensor	Site Description	Soil Description
DUM6 - White Lake	60	Upland mountainous site with sedges, mosses, lichen and many boulders. 100 m from crest of ridge.	Thin organic layer above weathered bedrock.
DUM7 - Hatbox Mesa	60	Foothills region, at the edge of wide water track. Very broad area of grass/sedge. Wet between tussocks. Slightly sloping to the south.	~10 cm of organic layer at surface.
DUM8 - Siksikpuk	60	Foothills region, Upland tundra, sedge, mosses, lichens.	N/A
DUS2 - Anaktuvuk River	80	On boundary between foothills and Coastal Plain. Thaw-lake basin within Anaktuvuk River floodplain, sedge, tussocks, mosses. Polygons 6 m diameter	Coarse-silty, euic, pergelic Terric Sapristel. Organic layer (0-20 cm) and mineral soil to 85 cm bgs. Frozen rocky mineral soil below 85 cm.
DUS3 - Chandler River	N/A	Adjacent to river on bluff above floodplain. Frost/mud boils with nearby thermokarst feature causing erosion. At depth bedrock is present (based on observations of river cutbank)	N/A

4.9.1 Soil Temperature

As an example to aid in the general understanding of soil temperatures within the study area, the soil temperature profile (0 to up to 150 cm below ground surface depending upon local conditions) over the period of record for the South White Hills station (DFM1) is shown in Figure 37. Soil temperatures at each depth below ground surface rise rapidly in the spring. Fall freezing is a slower process, and the temperature remains near 0°C during the period of water-to-ice phase change (known as the zero curtain). The deeper soils (~> 50 cm) warm significantly during the spring, but soil temperatures never rise above 0°C. The deeper soil is warmer in the winter and cooler in the summer (also shown in Figure 37). Soil temperature variability decreases with increasing depth from the ground surface. Annual differences in soil temperature are apparent; especially in this case where the summer maximum and winter minimum have a positive trend over the five-year period.

Phase changes during freezing and thawing are evident in Figure 37. It can be seen that the freezing phase change during the fall takes longer than the thawing phase change during the spring; the time record for this phase-change cycle to occur is directly related to the soil type and soil moisture content. These soils generally have a shallow layer of organic material at the

surface (15–20 cm). Generally, the soil moisture content of this layer is quite low except following snowmelt and significant rain events. The mineral soils are generally near saturation. When frozen, these soils have a low hydraulic conductivity. Deeper mineral soils do not show rapid warming in spring, which implies that water does not migrate into the soils during ablation.

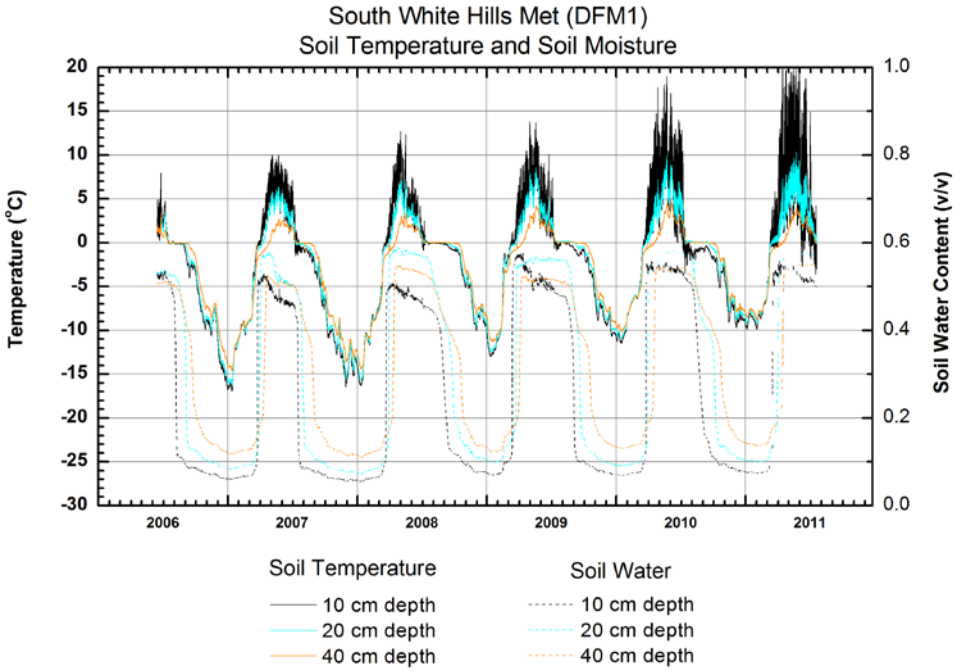

Figure 37. Soil temperatures and moisture at the South White Hills (DFM1) station as a function of depth for the period of record.

4.9.1.1 Results

Surface soil-temperature (temperature at the ground surface) statistics (averages, maximum, and minimum) for each station by month are included in Appendix C. Soil surface temperature and soil temperature at depth as time series plots are also available for all stations for the period of record in Appendix C. Maximum periods of record length span from October 1, 2006, to September 31, 2011. Period of records for each station are indicated on the table in Appendix E.

We present here the results of three stations for use as reference stations to aid in the discussion of results. The Ribdon (DBM2) station, which is located in the Mountain region of the Sagavanirktok basin, is located furthest south of the three reference stations (note that data are

missing for some intermediate depths in Figures 57 to 60). Table 23 describes soil conditions as lacking in organics—mostly well-drained, rocky mineral soil. The South White Hills (DFM1) station is classified as a Foothills station; it is located in the Kuparuk River basin, just north of the Slope Mountain area. The station's soil characteristics are described as a shallow surface layer of organics, underlain by well-drained mineral soil (Table 23). The Northwest Kuparuk (DFM4) station, located within the coastal plain of the Kuparuk River basin, is the furthest north station of the three reference stations. The soil consists of a shallow layer of organics underlain by mineral soil, and appears to be poorly drained because it was observed to be very wet with ponded water at the bottom of the soil pit (late summer).

Average monthly soil temperature through the soil profile at the three reference stations for selected months are shown in Figure 38 through Figure 41. March (Figure 38) represents the coldest soil conditions, and average soil temperatures range from -15 to -6°C, with the coldest temperatures near the surface. As expected, the Northwest Kuparuk (DFM4) station in the Coastal Plain region has the coldest temperatures. Figure 39 shows the soil temperature at depth during the month of June, when soil temperatures begin to warm. Surface temperatures are the warmest, and temperatures drop below freezing at about 25–30 cm bgs (below ground surface) for all three stations. Late August and early September is when the active layer thickness reaches its maximum. Figure 40 shows September soil temperatures. In September, the soil temperatures for the Foothills and Coastal Plain stations are unfrozen above 65 cm bgs; the Mountain region station is unfrozen until a depth of ~100 cm bgs. December (Figure 41) represents a period when freezing conditions occur throughout the entire soil profile for all three reference stations.

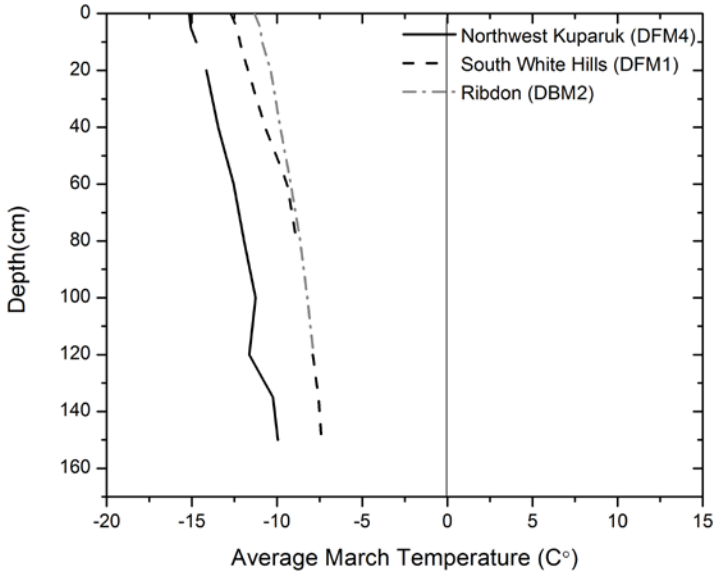

Figure 38. Average March soil temperature vs. depth at three selected stations.

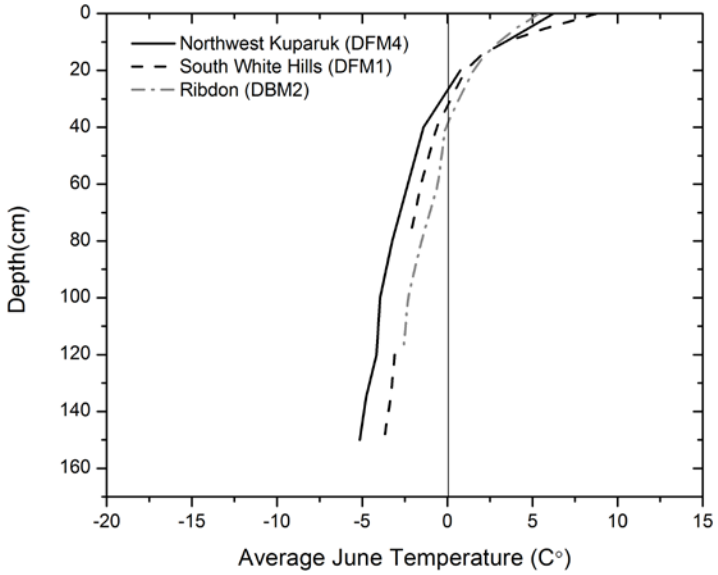

Figure 39. Average June soil temperature vs. depth at three selected stations.

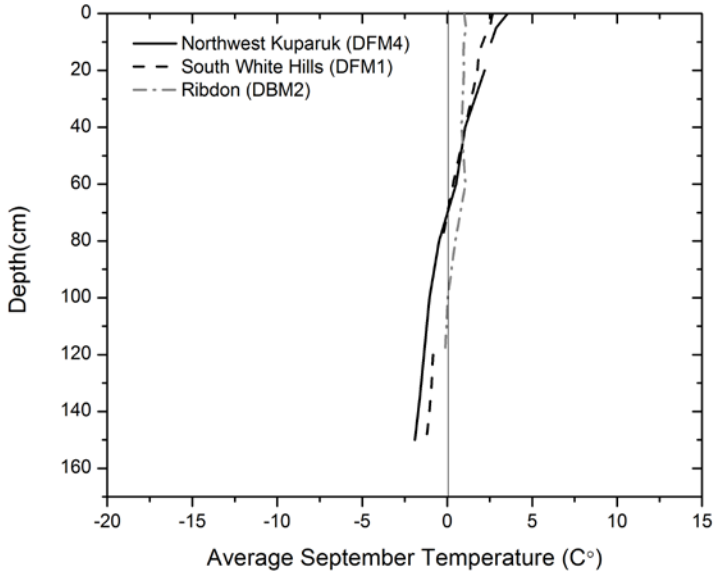

Figure 40. Average September soil temperature vs. depth at three selected stations.

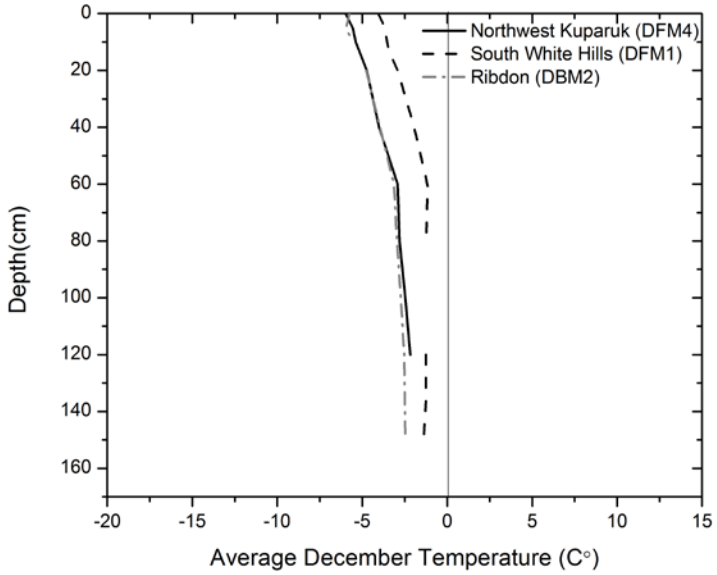

Figure 41. Average December soil temperature vs. depth at three selected stations.

We can also compare average soil temperatures by year and by region by examining the average soil temperature at each station. Table 24 shows the average soil temperatures for 2007 through 2011 water years (October 1 through September 30) at depths of 60 cm and 100 cm bgs. Temperature sensor depths vary for each station and range from 0 to 150 cm bgs. The two depths are selected based on availability of data. The measurement duration of each site varies due to funding for ongoing research and lack of data due to faulty equipment (environment, animal damage, etc.). Averages are not presented in Table 22 for stations with incomplete or absent data sets for the 60 cm or 100 cm depths below ground surface.

Table 24. Average annual soil temperature at 60 and 100 cm bgs (generally listed from south to north in latitude).

Station	Average Soil Temperature (°C) by water year (Oct 1 – Sept 30)									
	2007		2008		2009		2010		2011	
	60 cm bgs	100 cm bgs	60 cm bgs	100 cm bgs	60 cm bgs	100 cm bgs	60 cm bgs	100 cm bgs	60 cm bgs	100 cm bgs
Ribdon (DBM2)[m]	-2.97	-3.55	-3.62	-3.91	-2.39	-2.89				
Itikmalakpak (DUM1)[m]							-1.21		-0.61	
Nanushuk (DUM3)[f]							-0.86	-1.03	-1.11	-1.20
Tuluga (DUM4)[f]							-0.67	-0.86	-0.56	-0.08
Sag-Ivishak (DBM4)[f]	-4.23	-4.35	-4.62	-4.85	-3.19	-3.40				
S. White Hills (DFM1)[f]	-4.22		-4.52		-2.41		-0.13		-2.11	
White Hills (DFM2)[f]	-5.80	-5.89				-2.89				
Upper Kadleroshilik (DBM5)[f]			-5.78	-5.87	-3.84	-4.19				
Kavik (DBM6)[f]	-5.13	-5.06	-4.42	-4.45	-4.86	-4.71				
Anaktuvuk River (DUS2)[f]							-5.92		-4.27	
N. White Hills (DFM3)[f]			-7.23		-6.34		-2.20		-5.03	
Northwest Kuparuk (DFM4)[c]	-6.12	-6.16	-6.22	-6.36	-4.13	-4.53	-1.08	-1.05	-2.43	-3.15
Bullen (DBM8)[c]			-7.03	-7.02	-6.48	-6.42				

m=Mountain, f=Foothills, c=Coastal Plain, bgs=below ground surface

The Coastal Plain region has the coldest regional soil temperatures, and the Mountain (or the most southern Foothills stations) region has the warmest regional soil temperatures. The average soil temperature in the profiles ranges from about -0.1°C at Tuluga (DUM4, 2011) to -7.0°C at Bullen (DBM8, 2008). Average annual soil temperatures at two southern Foothills region stations in the Anaktuvuk basin, Nanushuk (DUM3), and Tuluga (DUM4) are only slightly below freezing. In general, we observe the warmest annual average soil temperature in the south and the coolest soil temperature in the north. Based on the limited available data, water year

2010 (October 1, 2009, through September 30, 2010) appears to be the warmest year during the study period of 2007 through 2011.

4.9.1.2 Active Layer Delineation

The depth at which maximum annual soil temperature is always less than 0°C is a good indication of the maximum thaw depth for that year, or the active layer thickness. The active layer thickness varies from year to year and depends on many factors, including seasonal air temperature, snow cover, date of the onset of snow in fall and spring snowmelt, winds, soil moisture, and cloudiness. Maximum soil temperatures are generally reached during late August or early September. The September maximum soil temperature at the three reference stations are presented in Figure 42. The active layer thickness at Northwest Kuparuk (DFM4) and South White Hills (DFM1) stations is similar at about 75 cm bgs on average. At the Ribdon (DBM2) station, which has a different soil type and is located in the Brooks Range, the soil below a depth of about 110 cm is continuously frozen.

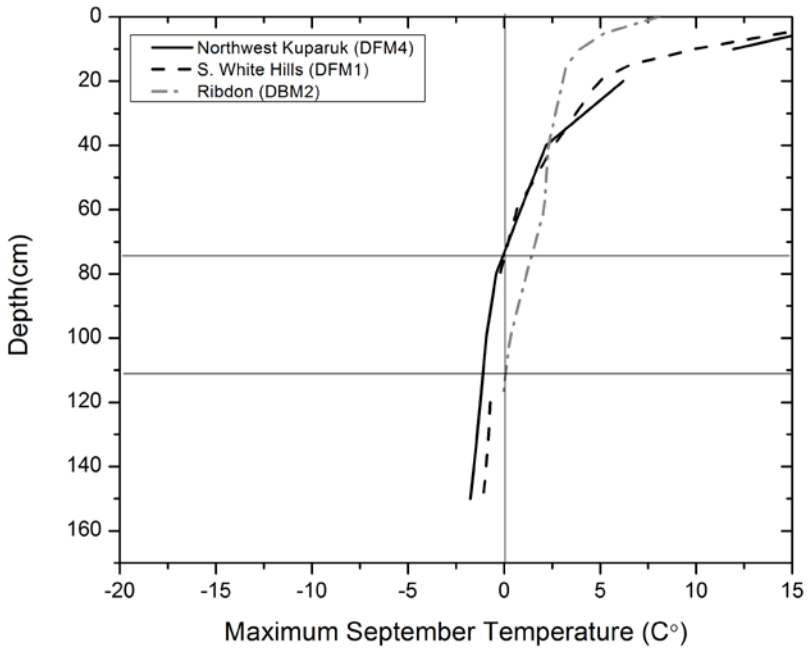

Figure 42. Maximum soil temperatures (September) at Northwest Kuparuk (DFM4), South White Hills (DFM1), and Ribdon (DBM2) stations as a function of depth.

4.9.2 Soil Moisture

The sensors used to measure soil moisture just measure the unfrozen (liquid) water content of the soil; therefore, in the winter months (when ice is in the soils) the unfrozen soil moisture levels are quite low. During the summer months, the Foothills stations usually have the highest soil-water content, although quite similar to the Coastal Plain. Because there are few stations and considerable heterogeneity over short distances, these conclusions should only be accepted generally. The Mountain region has the lowest soil-water content in the summer, which is attributed to better drainage, coarser soils, and lower organic content. Fine-grained mineral soils with considerable surface area generally tend to have the highest unfrozen water content. During the winter, the Foothills stations have the highest unfrozen soil-water content and the Mountain stations have the lowest. Note that only Ribdon (DBM2) and Itikmalakpak (DUM1) stations in the Mountain region have soil moisture sensors installed due to the challenges of installing the sensors in rocky, mountainous soils.

Soil moisture sensors are only sensitive to unfrozen soil-water content; thus, soils appear quite dry during the winter months, as much of the water is in the ice phase. Soils on the Alaska North Slope typically thaw from the top down during spring, but freeze from both the top and bottom in the fall. The rate of freezing depends upon the air temperature and the timing and amount of snowfall. These phenomena have been noted by others (Osterkamp and Romanovsky, 1997; Romanovsky and Osterkamp, 1997).

As soil water freezes in the fall, the temperature remains near 0°C during the period of water-to-ice phase change. This phenomenon is often referred to as zero curtain and is the result of the release of latent energy during the phase change from water to ice. The unfrozen-water content curve remains nearly constant during the initial period of zero curtain. At the point when most of the liquid water is frozen and minimal latent heat is released, rapid freezing occurs, as shown by the steep slopes of the soil moisture curves in Figure 37 and Section 4.9.2.1. The unfrozen soil-water content curves then transition to a constant level where very little further freezing occurs over the winter, even as the temperature markedly decreases. Sometimes this transition is rather abrupt; sometimes it is gradual.

The surface soils in the study area thawed from the top down following snowmelt. In the spring as the days grow longer, the surface energy balance delivers more energy to the surface, first initiating snowmelt and then active layer thawing. Snowmelt water moves downward in response to gravitational and thermal gradients, warming the soil below to the freezing point if it is colder than 0°C (a small amount of water freezes and releases latent heat, similar to the process that occurred earlier in the snowpack).

In the spring, during thawing conditions, the soil temperature changes rapidly in response to liquid water moving into and through the seasonally frozen active layer. The temperature curve shows a slower rate of increase during the melting of water at a particular depth below ground surface. This slower rate of increase is attributed to the latent heat required to thaw the soil water. After the soil water is thawed, the active layer resumes a more-rapid warming.

During winter months, soils can desiccate and form thermal contraction cracks, which increase the effective hydraulic conductivity of the soils, allowing more infiltration of water during snowmelt (Kane et al., 2001).

Soils in Arctic Alaska are wettest in the spring and early summer after snowmelt, and drier in mid-summer. The fall conditions depend upon how much precipitation fell during the summer (August is the wettest month usually). During the summer, down-gradient drainage and evapotranspiration dry the soil. The soil-water content at saturation in this soil is around 60% by volume. Normal mineral soils have a saturated water content of 40 to 45% by volume. The high level of water saturation in the soils studied is attributed to the large amount of organic matter in the soil and the physical impact of repeated freezing and thawing.

4.9.2.1 Results

Soil moisture statistics (averages, maximum, and minimum) for each station by month, as well as soil moisture time series plots for all stations for the period of record are included in Appendix C. Maximum periods of record length span from October 1, 2006, to September 31, 2011. Individual period of records for each station are indicated on the table in Appendix C.

Soil moisture data for the entire period of record at the three reference stations are presented in Figure 43 to Figure 49. The unfrozen soil moisture content at the Brooks Range station (Ribdon, DBM2) for the period of record is shown in Figure 43. Though this region receives the greatest amount of rainfall, the overall soil moisture content is low at Ribdon station due to its well-drained rocky subsurface. As previously mentioned, the active layer at this station is thicker than the other two reference stations. The unfrozen soil moisture content at both depths (10 and 20 cm) within the profile is the same due to similar properties throughout the soil column. The trend for each year is also similar, with highest unfrozen soil moisture after snowmelt runoff, followed by a general decline in soil moisture through the summer/fall, with only small increases due to rain events. The winter period shows practically no unfrozen soil moisture.

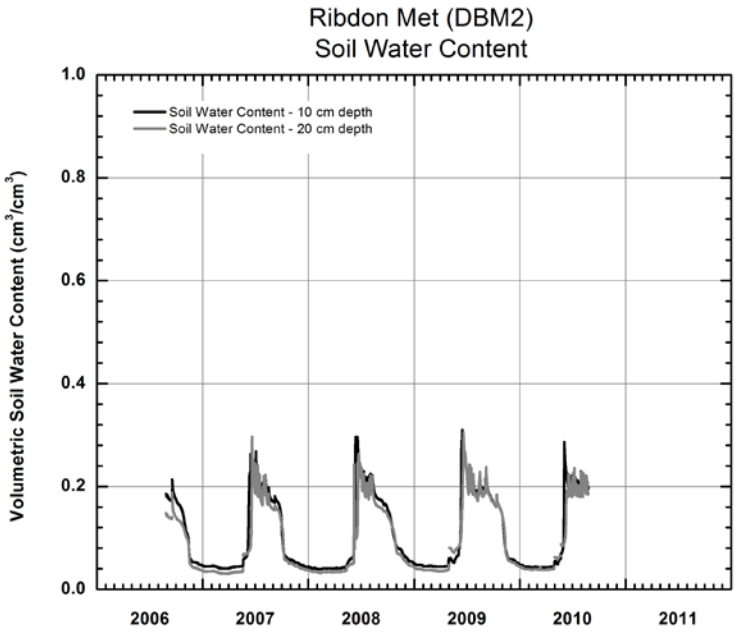

Figure 43. Soil moisture at the Ribdon (DBM2) station, 2006–2010.

Besides looking at the entire period of record in a single graph, we have examined the summer period for the Ribdon station and compared the soil moisture during two clearly different summers. The year 2007 has been examined because it was the driest summer on record. The year 2009 is unique because of an unusually early warm-up in late-April, which resulted in several larger rivers flowing in late April/early May. Additionally in 2009, several widespread

rainfall events occurred in early June and July, with a very dry three-week period from mid to late July, followed by a rainy August and September.

At the Ribdon station (Figure 44 and Figure 45), both in 2007 and 2009, soil moisture was detected by the sensors beginning in early June at the 10 cm depth, and in mid-June at the 20 cm depth. Soil moisture declined throughout the summer as evapotranspiration increased. Small increases in soil moisture occurred both years in response to rainfall events in July and August at both the 10 and 20 cm depth. Despite the decrease in evapotranspiration rates in late summer and early fall (late August [2007] and September [2009]), unfrozen soil moisture further declined, first due to the lack of additional rainfall and then to freezing of the soil (conversion of liquid water to ice). During 2007, soil moisture at the 20 cm depth was slightly lower than the 10 cm depth for the entire period, but in 2009, soil moisture at the two depths was the same. The biggest difference between the two years is the length of time that unfrozen soil moisture was detected by the sensors going into winter. By early October 2007, the soil moisture content quickly decreased as compared with 2009, when the soil moisture remained relatively high until early November. According to the soil temperature data, the ground from 0–40 cm bgs rapidly fell below freezing from mid-September to early November. In 2009, the ground temperature hovered just below freezing from the end of September to the end of October, but did not start dropping significantly below freezing until around November 1.

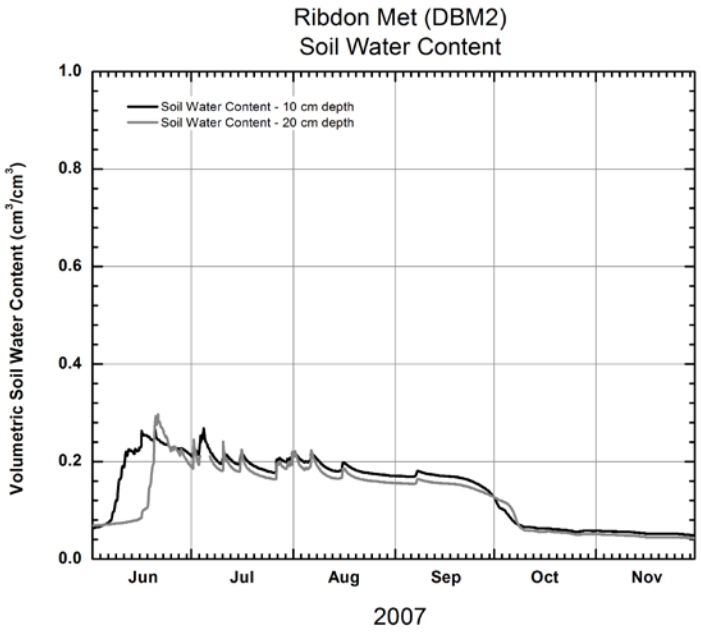

Figure 44. Ribdon (DBM2) station soil moisture record for summer/fall 2007.

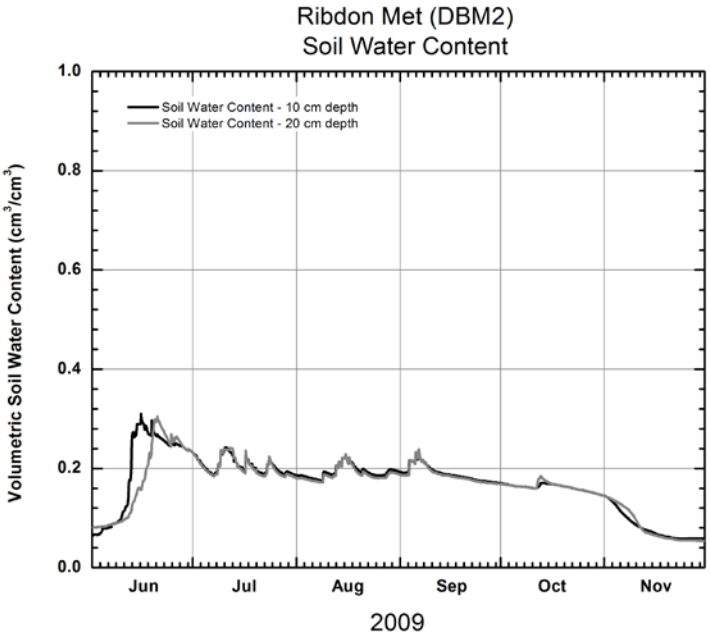

Figure 45. Ribdon (DBM2) soil moisture record for summer/fall 2009.

The unfrozen soil moisture content at South White Hills (DFM1) station, located in the Kuparuk Foothills region, for the period of record is shown in Figure 46. The soil moisture content is

higher at this station than at the mountain station due to its differing soil characteristics. At South White Hills, the soil consists of an organic layer underlain by a loamy mineral soil as compared with weathered bedrock at the mountainous station. After the snowmelt period, soil moisture was highest at the 20 cm depth and lowest at the 10 cm depth. In Figure 46, we can see the year-to-year variability in soil moisture. The soil moisture for 2007 (the driest year on record) decreased quickly after snowmelt because of the lack of summer rainfall throughout the soil column. In 2008, there was a more gradual decline in soil moisture throughout the summer at all depths. In 2009, soil moisture declined throughout the summer at the 10 cm depth, but at the deeper parts of the soil column (20 and 40 cm), the soil moisture remained relatively stable all summer. Due to a deficit of summer rainfall in the early part of 2010, there was a late summer increase in soil moisture at the 20 cm depth (in response to late summer rain) that is not observed in other years.

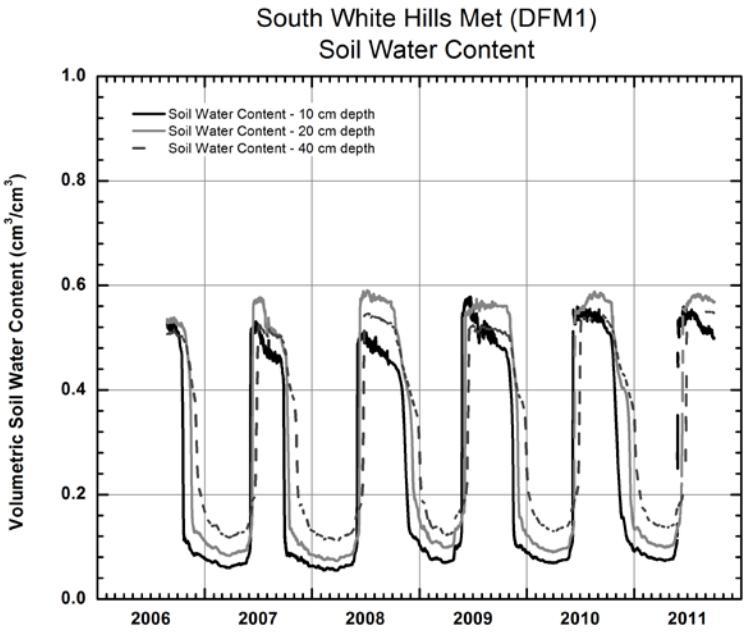

Figure 46. Soil moisture at South White Hills (DFM1) station, 2006–2011.

Soil moisture records for individual seasons at the South White Hills station are presented in Figure 47 (2007, a dry year) and Figure 48 (2009, which had an unusually early warm-up in late April and a widespread early June rain event, along with several other rain events throughout the summer). In 2007, the unfrozen soil moisture content increased in early June at the shallowest depth (10 cm), but in late June/early July, at the 40 cm depth, well after the end of spring runoff.

In 2009, the increase in unfrozen soil moisture content occurred much earlier than in 2007 (in mid-May at the 10 cm depth), due to the unusual warm-up in late April and despite the freezeback in May. The unfrozen soil moisture content is lowest in late summer/early fall. During the 2009 observational period, the soil moisture content was stable throughout the entire summer at the 20 and 40 cm depth. In early June 2009, the soil moisture at 20 cm depth was higher than usual due to a very wet early June, causing high runoff in many nearby high-gradient rivers. However, this increased soil moisture at the 20 cm depth was not observed at 40 cm depth, indicating the ground was still frozen and much of the early June runoff occurred at shallower depths. As observed at the Ribdon station, the unfrozen soil moisture content during the fall months in 2007 decreased much earlier than in 2009. In 2009, unfrozen soil moisture was still detected in December at the 40 cm depth.

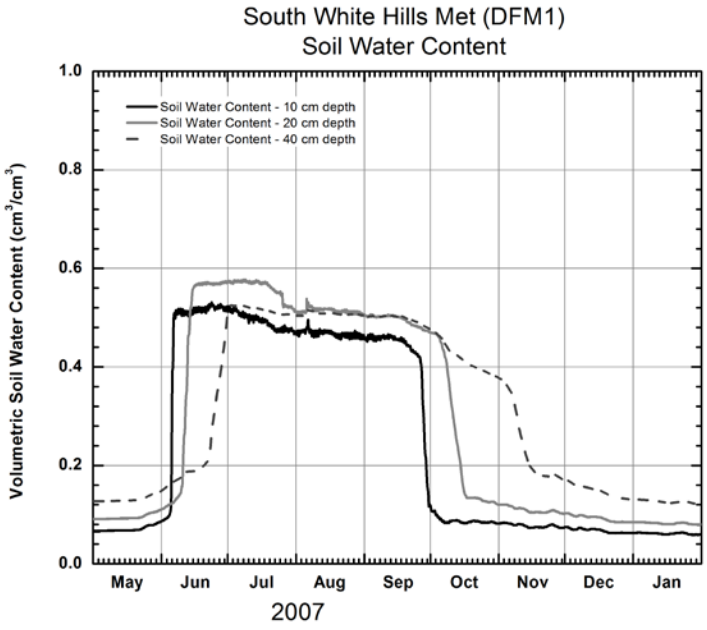

Figure 47. South White Hills (DFM1) soil moisture record for summer/fall 2007.

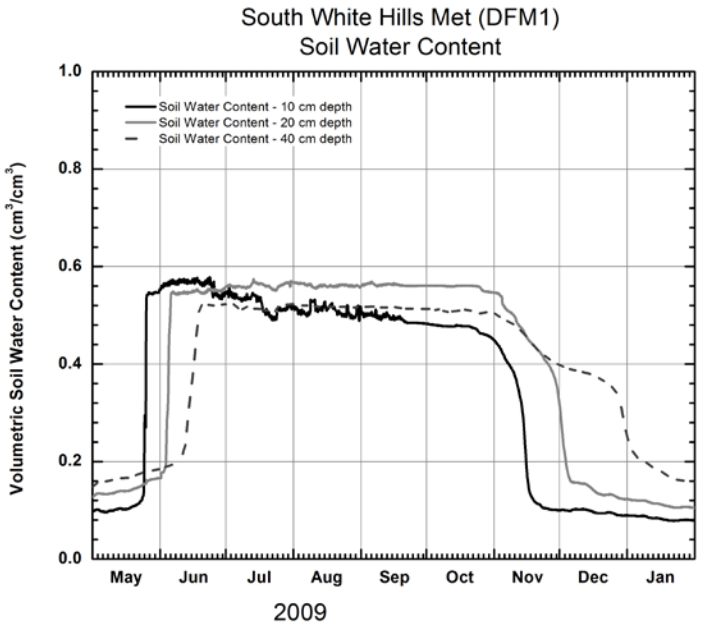

Figure 48. South White Hills (DFM1) soil moisture record for summer/fall 2009

The unfrozen soil moisture content at the Coastal Plain station Northwest Kuparuk (DFM4) is shown in Figure 49. This station's soil is similar to the South White Hills station, except that the soil appears to be more poorly drained. Water was observed to be very wet and was ponded in the bottom of the soil pit during sensor installation. At this station, soils have the highest soil-moisture content of the three reference stations, with the highest water content at the shallow 10 cm depth (which comprises the organic layer). Soil moisture at the deepest sensor (46 cm depth) is also high (as observed during the installation of soil sensors), but is more stable and has less year-to-year variability than the shallower sensors (likely near saturation all of the time). In 2007, we observe a decrease in soil moisture after the snowmelt period throughout the profile due to the dry summer (Figure 49). Starting in mid to late July of 2008 and 2009, there is a clear increase in soil moisture at 10 and 20 cm depths in response to widespread rain events.

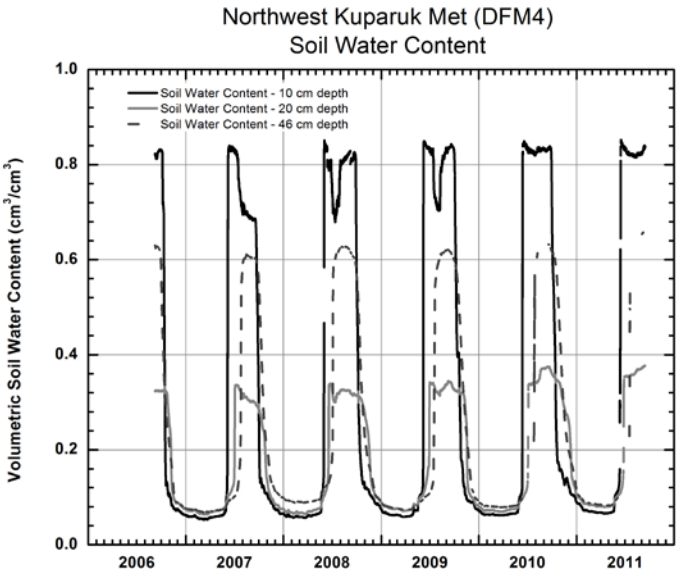

Figure 49. Soil moisture at Northwest Kuparuk (DFM4) station, 2006–2011.

Soil moisture records for the seasons of 2007 and 2009 at Northwest Kuparuk (DFM4) station are presented in Figure 50 and Figure 51. The unfrozen soil moisture content at the 10 cm depth increases in early June, at the 20 cm depth in early July, and at the deepest in late July, well beyond the end of spring runoff for the Kuparuk River. In 2007, the unfrozen soil moisture content decreased throughout the summer at the shallower depths, but remained stable at the 46 cm depth. In 2009, soil moisture decreased after the spring runoff period at the 10 and 20 cm depths, but increased in response to a rain event in early August.

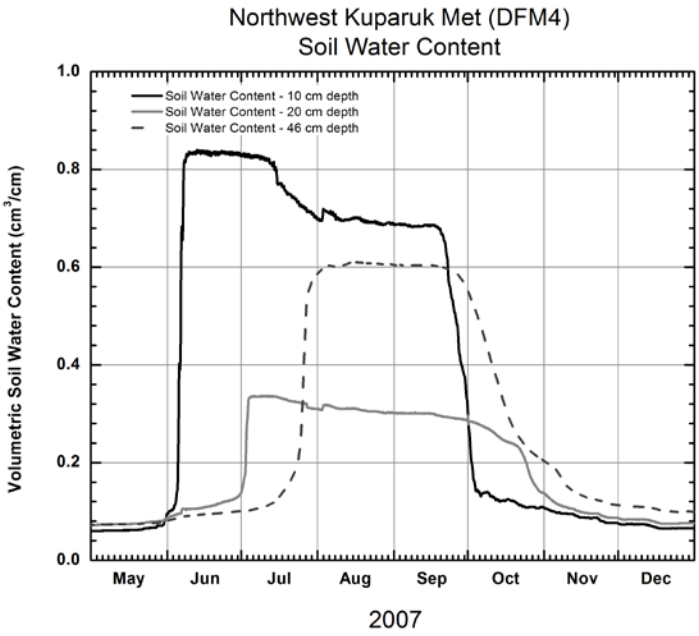

Figure 50. Northwest Kuparuk (DFM4) soil moisture record for summer/fall 2007.

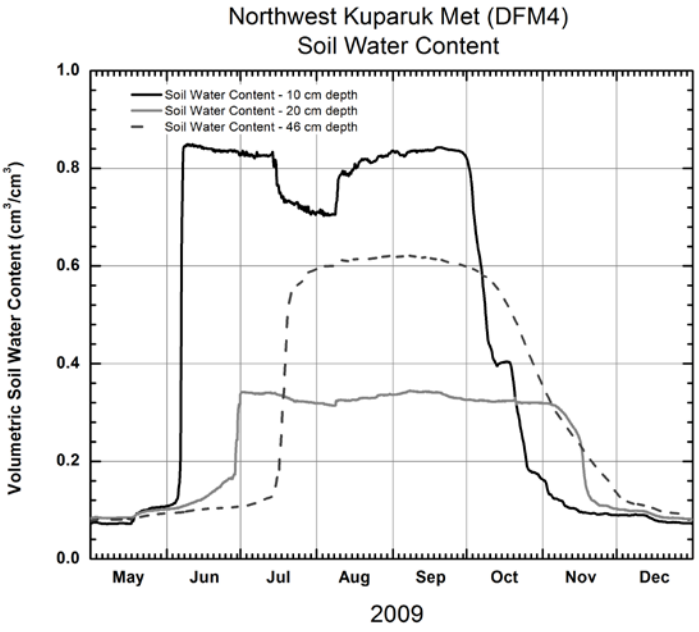

Figure 51. Northwest Kuparuk (DFM4) soil moisture record for summer/fall 2009.

4.10 Surface Water Hydrology

Hydrological stations on No Name (U1), Shaviovik, Kadleroshilik, Itkillik, Anaktuvuk, and Chandler Rivers were installed in early spring 2009 to capture the spring snowmelt and summer runoff events. Water levels are monitored in all watersheds during most of the spring break-up period and summer. Since 2009, point discharge measurements are made several times during snowmelt and a few times during summer on the No Name (U1), Shaviovik, Kadleroshilik, and Anaktuvuk Rivers, and beginning in summer 2010, on the Itkillik and Chandler Rivers. In August 2010, the surface water observation stations in the DNR Bullen project (No Name, Shaviovik, Kadleroshilik) were removed. Continuous recording of water levels and discharge measurements will likely continue on the Itkillik, Anaktuvuk, and Chandler Rivers until fall 2012. To document the hydrologic activity more completely, we also have cameras, pointed at the river, at all hydrological stations.

The purpose of this section is to present the water level and discharge results of the spring and summer runoff period for 2009 through 2011 on the rivers studied for the Umiat Corridor and Bullen projects. Preliminary hydrologic results for the Itkillik, Anaktuvuk, and Chandler Rivers were presented in a 2011 data report (Youcha et al., 2011) to ADOT&PF. The present report provides updated data and the most recent findings.

4.10.1 Kadleroshilik River

East of the Sagavanirktok River is the Kadleroshilik River Basin (approximately 1,500 km^2), which drains north mostly from the Coastal Plain, although a small percentage of the upper basin lies in the foothills to the south. There are two UAF meteorological stations within this basin (Upper Kadleroshilik DBM5 and Lower Kadleroshilik DBM7). In spring 2009, UAF/WERC installed a surface water gauging station approximately 8 km (5 mi) from the river outlet into the Beaufort Sea, near the proposed DNR “north” route crossing above the left (west) bank. Water levels are measured continuously at this location. However, discharge was measured both at the pipeline crossing during high flow and at the station during summer low flow. This section summarizes our observations during the spring 2009 through summer 2010 study period.

Figure 52 shows continuous and manual water level measurements at the station for 2009 and 2010. The Kadleroshilik River began flowing at the observation station on May 25, 2009. Water levels were initially very high due to ice in the channel (Figure 53). Water levels dropped from May 27 to 31 and then began to rise until the peak of 349 m^3/s (12,324 ft^3/s) on June 3 (Figure 52). Water levels were ice-affected until about June 3. The river went into recession immediately after the peak and had low flow conditions the majority of the summer. Slight increases in discharge occurred on June 12 due to an early summer rain event and in late August/early September due to fall precipitation.

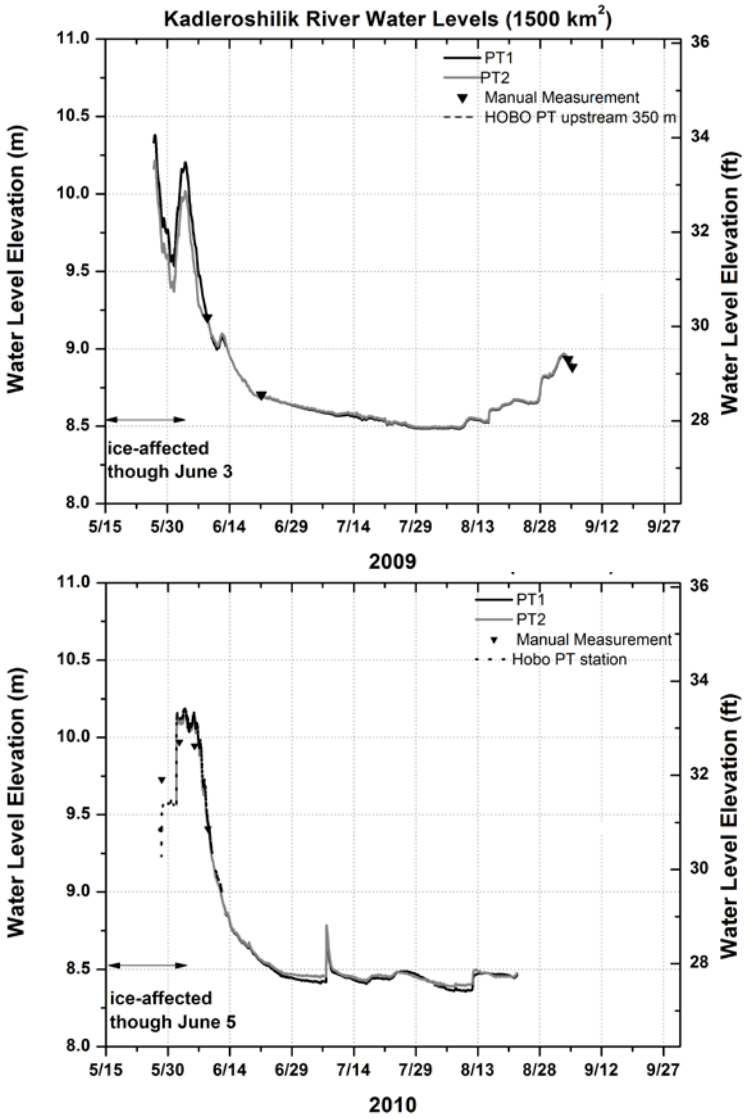

Figure 52. Continuous water levels at the Kadleroshilik station during the 2009 and 2010 warm seasons.

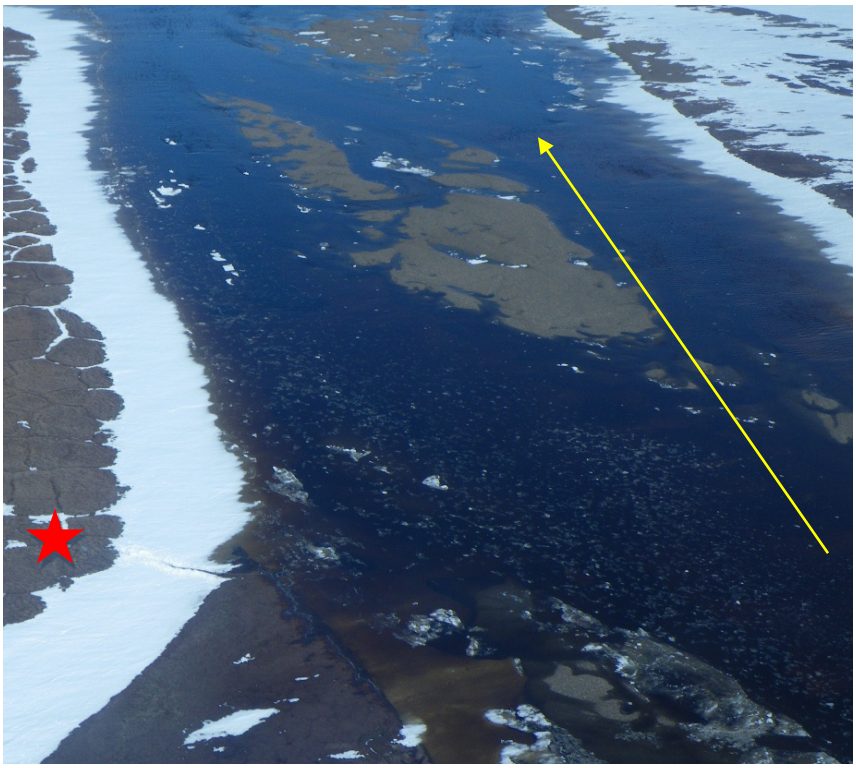

Figure 53. Kadleroshilik River initial flow on May 25, 2009, near the proposed "north" crossing location. The red star indicates the station location and the yellow arrow indicates the flow direction.

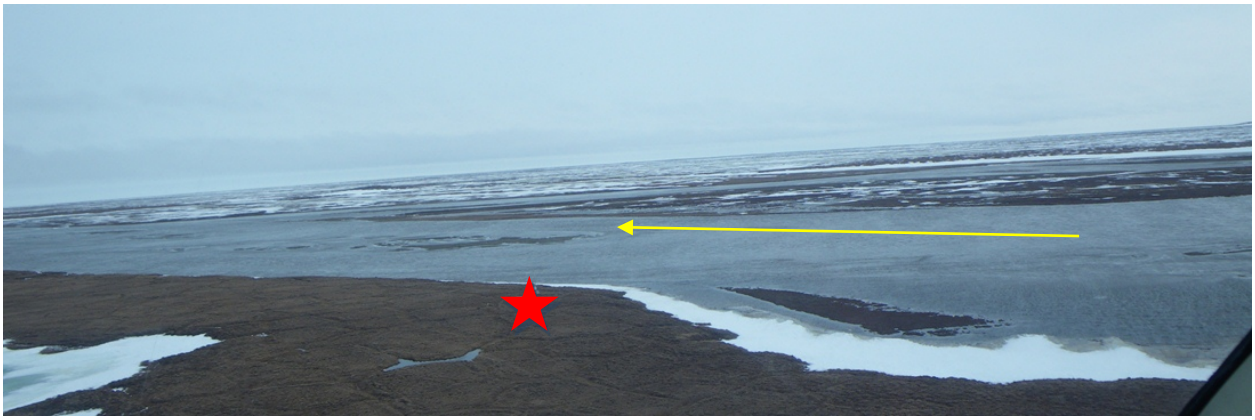

Figure 54. Kadleroshilik River on peak flow June 3, 2009, at proposed crossing location.

In 2010, the Kadleroshilik began flowing at the observation station on June 1. Due to site access limitations in poor weather, only three discharge measurements were made during 2010, after the

estimated peak flow (~322 m^3/s or 11,371 ft^3/s) occurred on June 5 (Figure 55). The river went into recession following the peak and remained at very low flow conditions throughout the summer. The difference between the highest stage during snowmelt and the low flow summer stage was 1.9 m (6.2 ft). The station was decommissioned on August 22, 2010.

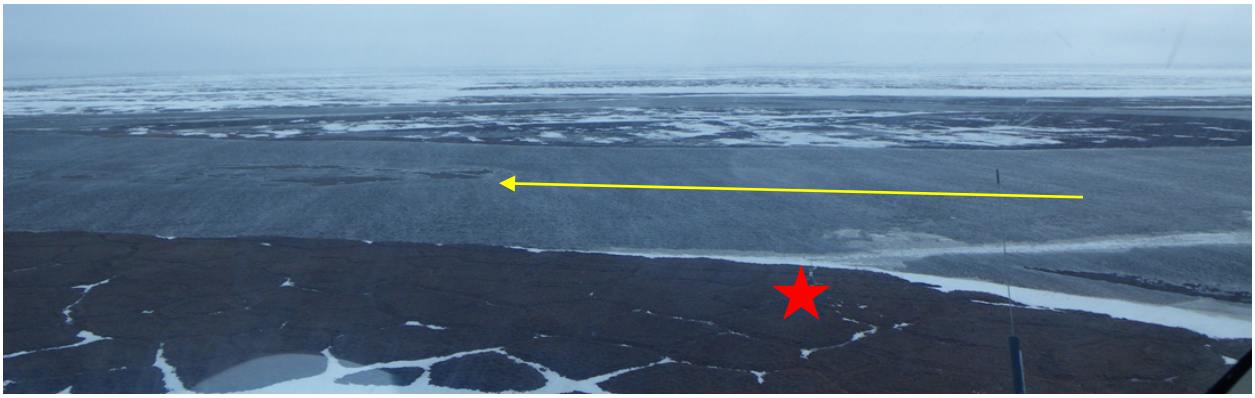

Figure 55. Kadleroshilik River on peak flow June 5, 2010, at proposed crossing location.

All individual discharge measurements are presented in Table 25. A preliminary rating curve was developed for Kadleroshilik River (Appendix D) based on individual discharge and stage measurements. The rating curve was then applied to continuous stage readings in order to estimate continuous discharge (Figure 56). This rating curve is very basic and does not include any shifts to the rating points. There is high uncertainty associated with the estimated continuous discharge, particularly at high and low stage (due to the lack of rating points at these extremes) and during spring, when the channel may be somewhat ice-affected. Appendix D contains the expanded rating table. The dates of estimated peak flows are presented in Table 26.

Table 25. Summary of discharge measurements at Kadleroshilik River 2009 and 2010 warm seasons.

Date	Measurement Number	Discharge m^3/ft	Discharge ft^3/s	Quality %	Notes	Stage m	Stage ft	Location WGS84
5/28/2009 13:00	1	94	3320	10	ice	9.87	32.37	70 10 41.19, 147 38 20.69
5/31/2009 19:00	2	85	3002	10	ice	9.62	31.55	70 10 41.19, 147 38 20.69
6/2/2009 14:00	3	305	10771	10	ice	10.16	33.33	70 10 41.19, 147 38 20.69
6/4/2009 17:00	4	228	8052	10		9.87	32.37	70 10 41.19, 147 38 20.69
6/6/2009 12:30	5	115	4061	10		9.49	31.12	70 10 41.19, 147 38 20.69
6/7/2009 15:00	6	83	2931	10		9.33	30.60	70 10 41.19, 147 38 20.69
9/3/2009 16:30	7	17	600	10		8.95	29.35	70 8 17.64, 147 38 27.40
6/7/2010 14:15	8	182	6427	10	ice	9.63	31.60	70 10 41.19, 147 38 20.69
6/9/2010 12:15	9	97	3426	10	ice	9.25	30.34	70 10 41.19, 147 38 20.69
6/10/2010 14:45	10	63	2225	2		9.09	29.83	70 10 41.19, 147 38 20.69

Nearly all of the Kadleroshilik basin lies in the Coastal Plain and the hydrograph is similar to other Coastal Plain rivers such as the Putuligayuk, where peak discharge and the majority of runoff volume occurs during snowmelt. Little flow occurs the remainder of the year, because summer rainfall on the Coastal Plain is very low and the percentage of basin area in the Foothills (where rainfall is greater) is probably less than 15% of the drainage area. Additionally, most rain events are quite scattered and do not occur across the entire basin. Interestingly, parts of the Kadleroshilik River are braided, with several gravel bars visible during lower flows. It is hypothesized that the majority of bedload transport occurs during the snowmelt break-up period, after the bottom ice is removed from the channel. It is likely that the summer runoff events are not large enough to move significant bedload. During spring break-up, bottom ice is present in some locations of the channel, but is not widespread across the entire channel. Bottom ice was observed to be gone in most locations 3 to 5 days after the initial flows during the 2009 observation period. The majority of the ice observed being transported downstream was either ice chunks or smaller ice pans. Slush flows were observed during 2009 and 2010.

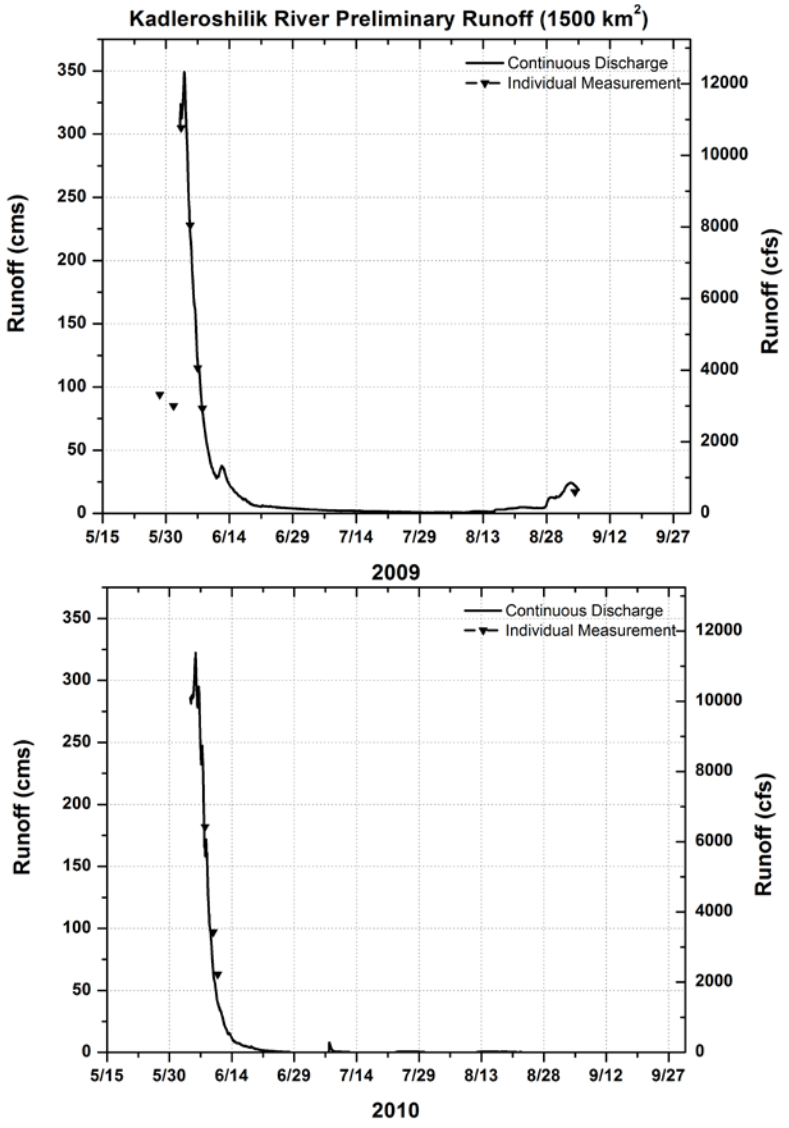

Figure 56. Continuous discharge at Kadleroshilik River 2009–2010.

Table 26. Summary of estimated peak flow for the Kadleroshilik River, 2009–2010.

Date	Peak Runoff (m^3/s)	Peak Runoff (ft^3/s)
Spring: 6/3/2009	349	12325
Summer: 6/12/2009*	37	1306
Spring: 6/5/2010	322	11371
Summer: 7/7/2010**	8	282

*combination of mixed snowmelt and rain-generated event
**period of record ended 8/22/2011. Summer runoff events after this date are unknown.

4.10.2 Shaviovik River

The Shaviovik River basin (approximately 4000 km^2) consists of the Shaviovik River in the west and the Kavik River in the east. This basin includes the Mountain, Foothills, and Coastal Plain regions. There are two meteorological stations within the basin (Juniper Creek DBM3 and Kavik DBM6) and one additional station nearby (Bullen Point DBM8). In spring 2009, UAF installed a surface water gauging station approximately 11 km (7 mi) from the river outlet into the Beaufort Sea, near the proposed DNR south route crossing. Discharge is measured either at the station, or within 4 km (2.5 mi) downstream of the station. This section summarizes our observations during the spring 2009 through summer 2010 study period.

Figure 57 shows the water level elevations for 2009 and 2010 at the Shaviovik River. In 2009, it was reported that the Kavik River at Kavik Camp (Kavik River flows into the Shaviovik) was flowing during a period of warm temperatures in late April. Upon arrival at the Shaviovik River site on May 21, the river was flowing less than an estimated 100 m^3/s (3500 ft^3/s), but much of the ice remained in the channel (Figure 58). It is likely that the river had been flowing since the early warm-up in late April. UAF began water level measurements on May 21 and discharge measurements on May 27, after it was safe to enter the river. Conditions were ice-affected until about May 29. Water levels were the highest during snowmelt runoff, and peak water level occurred on May 26 (ice-affected) (Figure 59). Water levels dropped when the ice was removed from the river, and then began to rise again on June 3 with another high water-level event. It is thought that the peak discharge during snowmelt (also peak for the entire year) of ~625 m^3/s (~22,071 ft^3/s) occurred on June 3 as well. Rain events throughout the summer caused the water levels to rise on July 14, and again in mid to late August. The difference between the highest stage during snowmelt and the low-flow stage in summer was 2.11 m (6.9 ft).

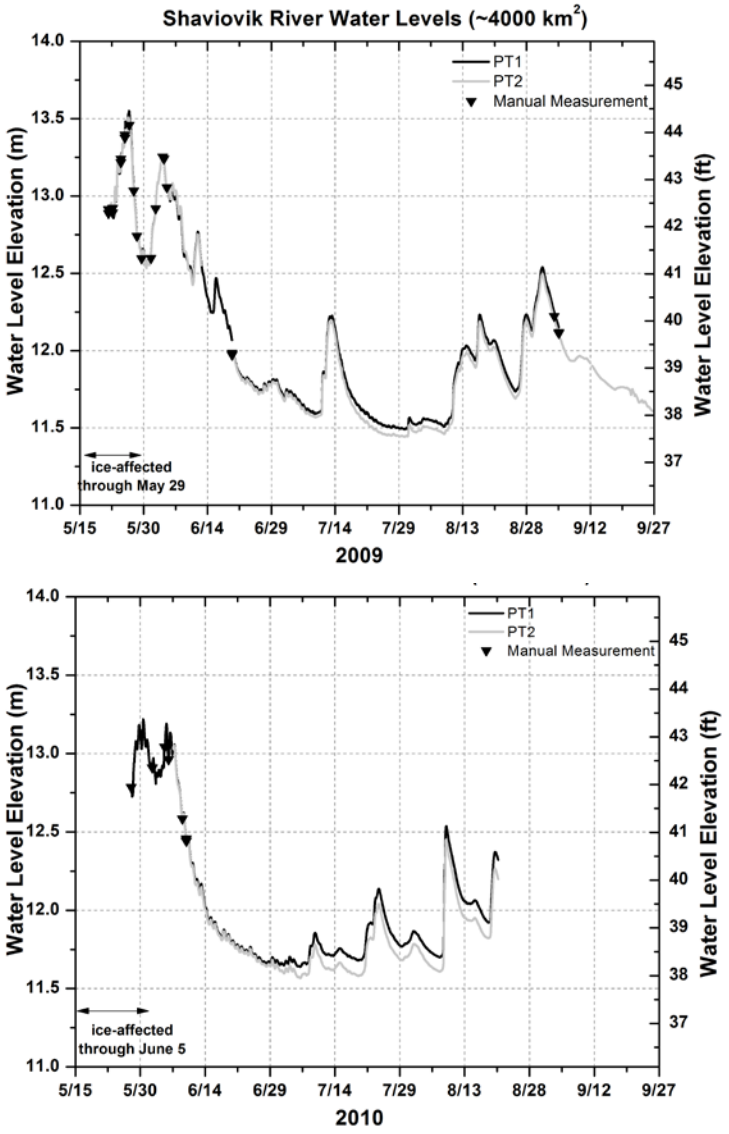

Figure 57. Shaviovik River water level elevations, 2009–2010.

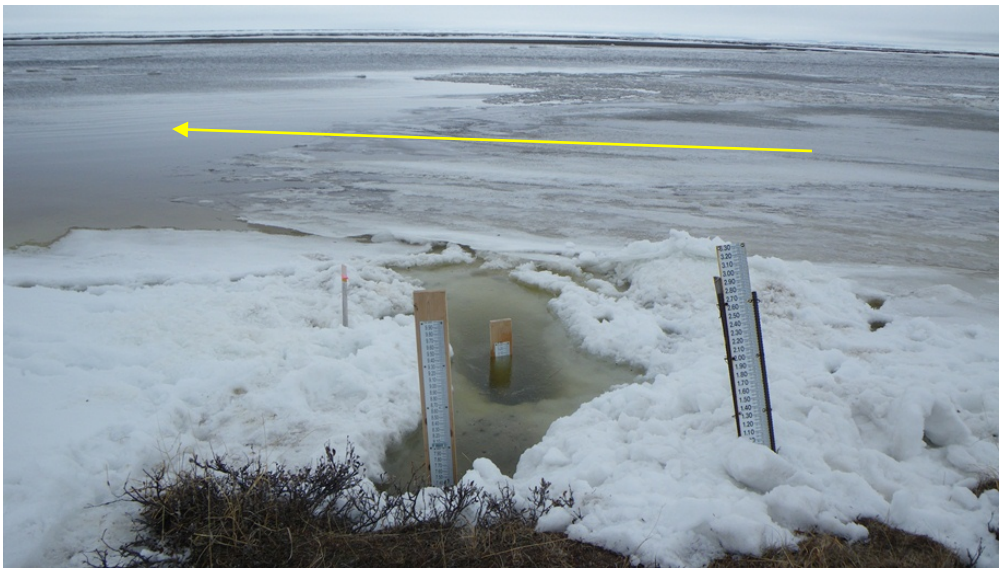

Figure 58. Shaviovik River on May 21, 2009. River was flowing upon arrival.

Figure 59. Shaviovik River on May 26, 2009, during the highest water level elevation at 1.6 km (1 mi) downstream from proposed southern crossing location. Ice in the channel causes water levels to reach bankfull conditions, and all channels are full of water. Peak flow occurs several days later.

In 2010, UAF recorded water levels and measured discharge again on the Shaviovik River. Only three discharge measurements were made due to poor weather conditions and limited site access via helicopter. The initial flow front reached the Shaviovik Station on the evening of May 25, 2010. Continuous water levels were recorded beginning on May 28, and water levels were ice-

affected through June 4 or 5. The peak water levels occurred on May 30 and June 5 (Figure 60). The first discharge measurement was made on June 6 of 465 m^3/s (16,419 ft^3/s), shortly after the peak flow on June 5. As with the previous year, rain events caused increases in water levels during July and mid-August, but the main runoff event occurred during snowmelt. The Shaviovik station was removed on August 22 after the Bullen Point project ended.

During spring break-up, larger ice chunks and pans were visible floating in the channel and stranded on gravel bars (Figure 61), and water became turbid after several days of runoff. It is hypothesized again that sediment may be tranpsorted during spring break-up after the ice is removed from the bed and shore. Additional sediment transport may occur during higher summer flow events as well. Figure 62 shows a large ice chunk floating downstream on the Shaviovik River one day after the peak discharge in 2010. Larger ice pans are observed earlier in the break-up period when anchor ice lifts off the riverbed.

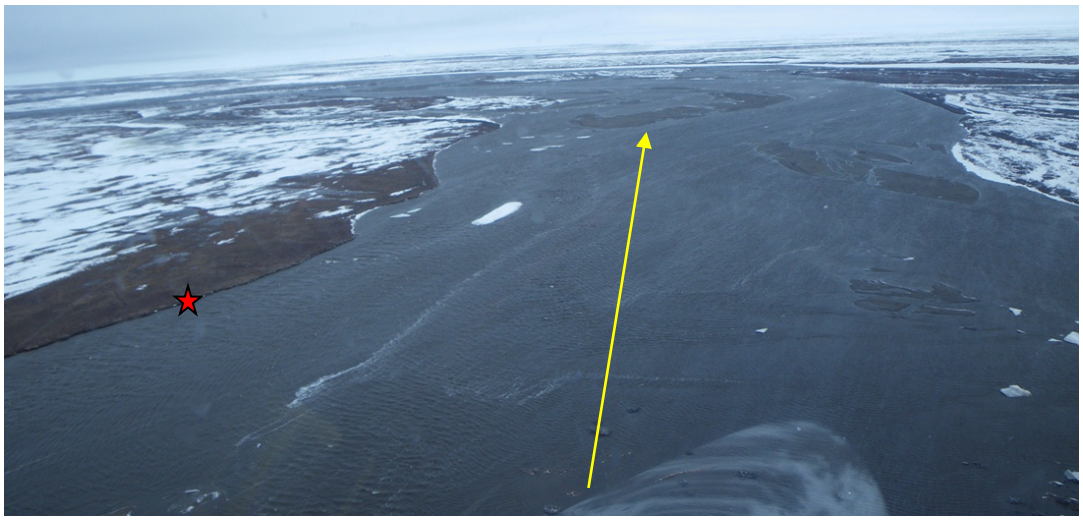

Figure 60. Shaviovik River during peak flow June 5, 2010, at proposed south route bridge-crossing location.

Figure 61. Stranded ice pans on a gravel bar on the Shaviovik River on May 31, 2009.

Figure 62. Ice chunk on the Shaviovik River on June 6, 2010. Dimension of ice chunk is approximately 10 ft long by 8 ft wide with a smaller ice chunk resting on top.

Table 27. Discharge measurements for the Shaviovik River (2009–2010).

Date	Measurement Number	Discharge		Quality	Notes	Stage		Location
		m^3/s	ft^3/s	%		m	ft	WGS84
5/27/2009 13:30	1	329	11617	8	Ice	13.99	45.87	70 06 07.02, 147 14 34.68
5/31/2009 16:00	2	141	4982	8	Ice	13.51	44.31	70 06 07.02, 147 14 34.68
6/1/2009 17:00	3	254	8969	8		13.79	45.25	70 06 07.02, 147 14 34.68
6/3/2009 16:00	4	587	20727	8	Estimated*	14.16	46.46	70 06 07.02, 147 14 34.68
6/6/2009 18:45	5	362	12782	5		13.91	45.64	70 05 46.95, 147 15 51.05
9/4/2009 11:00	6	66	2330	8		13.03	42.74	70 04 14.57, 147 16 59.49
6/6/2010 18:00	7	465	16419	8	Ice	14.01	45.94	70 05 46.95, 147 15 51.05
6/8/2010 16:00	8	213	7528	8		13.55	44.43	70 06 07.02, 147 14 34.68
6/10/2010 12:40	9	128	4520	8		13.29	43.60	70 06 07.02, 147 14 34.68

*Main western channel measured with ADCP, and smaller eastern channel estimated.

Individual discharge measurements on the Shaviovik River are presented in Table 27. A preliminary rating curve was developed for the Shaviovik River (Appendix D) based on

individual discharge and stage measurements. The rating curve was then applied to continuous stage readings in order to estimate continuous discharge (Figure 63). This rating curve is preliminary and does not include any shifts to the rating points. There is high uncertainty associated with the estimated continuous discharge, particularly at high and low stage (due to the lack of rating points) and during spring, when the channel may be somewhat ice-affected. Appendix D contains the expanded rating table. Table 28 indicates the estimated peak discharge for both spring and summer runoff events for 2009 and 2010.

Unlike the Kadleroshilik and Putuligayuk River, the Shaviovik River shows more response to summer rain events (Figure 63) because a high percentage of the basin area is within the Foothills and Mountain regions. Runoff events due to early June rainfall are observed in the hydrograph, and discharge increases several times throughout the summer, correlating with high intensity rain events that occur throughout the uplands region of the basin. The greatest amounts of rainfall occur in the upper part of the basin (Mountain and Foothills regions) according to rainfall data collected at the meteorological stations in the Bullen/Sagavanirktok region.

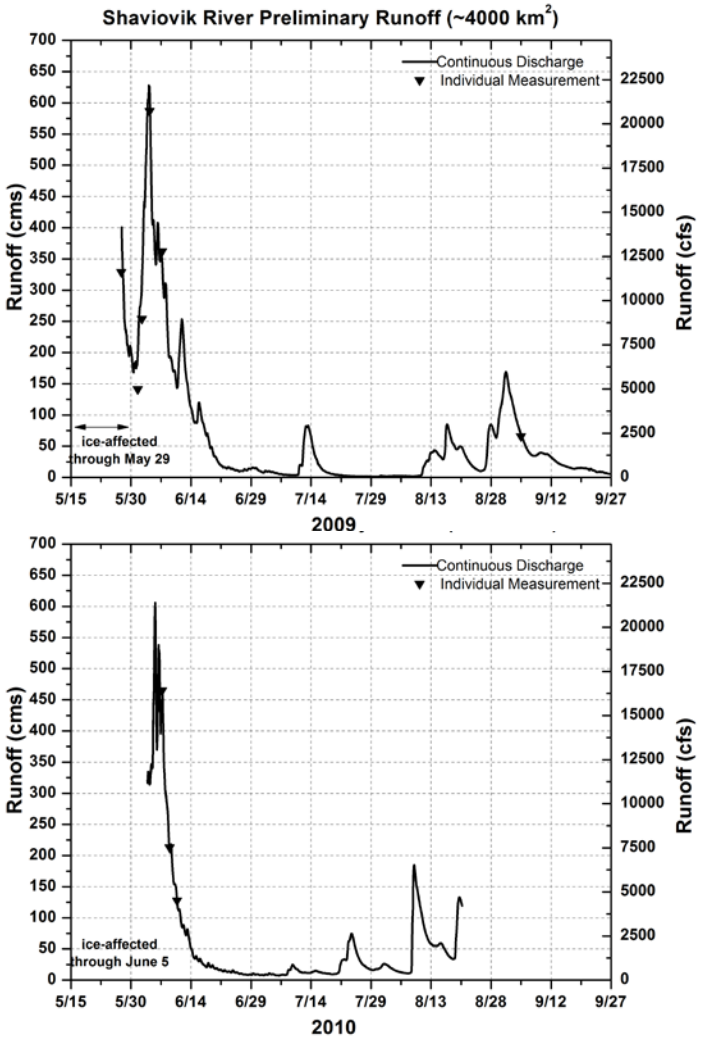

Figure 63. Continuous discharge during the warm season for the Shaviovik River 2009–2010.

Table 28. Estimated peak discharge for Shaviovik River, 2009–2010.

Date	Peak Runoff (m^3/s)	Peak Runoff (ft^3/s)
Spring: 6/3/2009	628	22177
Summer: 6/11/2009*	250	8828
Spring: 6/5/2010	604	21330
Summer: 8/8/2010**	185	6533

*combination of snowmelt and rain-generated event
**period of record ended 8/22/2011. Summer runoff events after this date are unknown.

4.10.3 No Name River (Unnamed Creek 1)

Also included in the Bullen study is No Name River (also called Unnamed Creek 1 or U1), a smaller basin of approximately 350 km^2, located 3.2 km (2 mi) to the east of the Shaviovik River, lying within both the Coastal Plain and the Foothills (small extent in headwaters) regions and draining north into the Beaufort Sea. In spring 2009, UAF installed a surface water station 11 km (7 mi) upstream from the outlet into the Beaufort Sea (near the proposed south route). Discharge measurements are made at the station. No meteorological stations are installed in the basin; however, two stations (Bullen Point, DBM8; Kavik, DBM6) are located nearby. This section summarizes our observations during the spring 2009 through summer 2010 study period.

Figure 64 shows the water levels measured with continuous-recording pressure transducers for 2009 and 2010. In 2009, the No Name River began flowing on May 26, with the water flowing over extensive bottom ice (Figure 65). Water levels increased until the peak on June 2 and 3; peak discharge probably occurred on June 3 (Figure 66), similar to other nearby rivers in the Bullen Point study area. Bottom ice mostly seemed to melt in place rather than mechanically break apart. Shore ice remained in the channel until June 2 at the earliest. During a discharge measurement on June 2, the gravel streambed was observed to be moving, and flows were unsteady. The water did not appear turbid during spring break-up. A large rain event in early June caused an increase in water levels and discharge during snowmelt recession. Little flow occurred during the summer months of late June and July, but discharge increased in mid-August through early September in response to fall season rain.

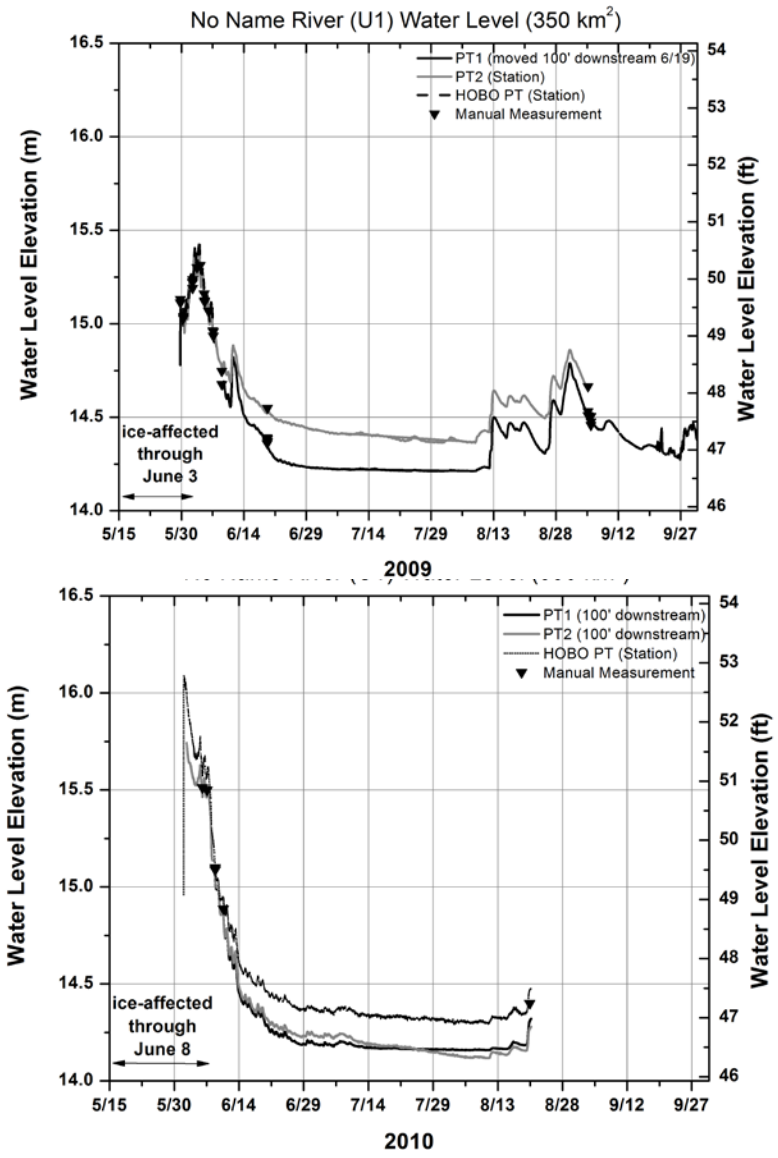

Figure 64. Continuous water level measurements on the No Name River (U1), 2009–2010.

Figure 65. No Name River on May 27, 2009, near proposed south crossing location. Bottom ice is visible in the channel and it remains in the channel for at least 5–6 days after initial flows over the top of the ice.

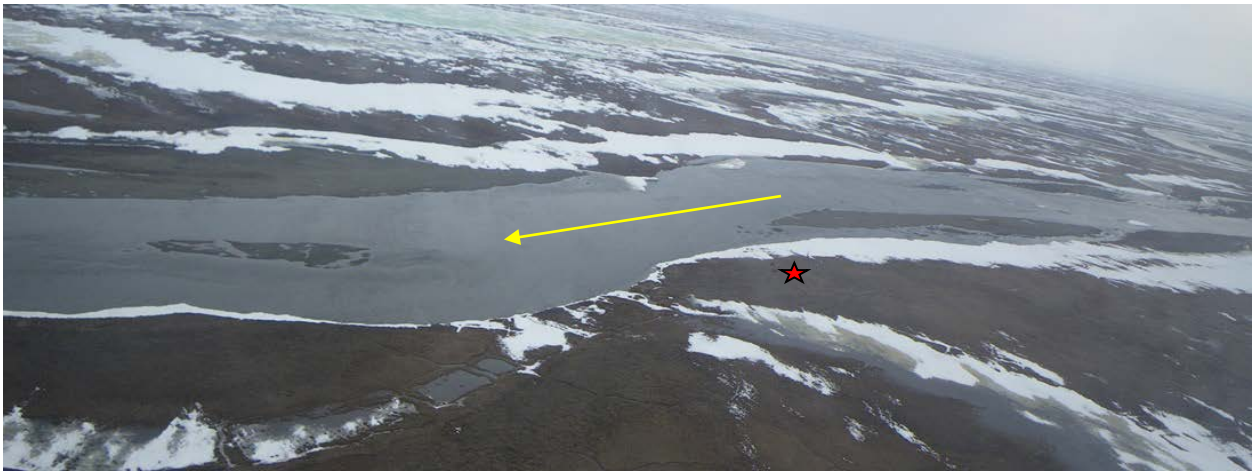

Figure 66. No Name (U1) River on June 3, 2009 during peak flow at proposed southern crossing location.

In 2010, water began flowing at the station on the morning of June 1, with water flowing above extensive bottom ice. Site access was limited in 2010 due to poor weather conditions, and only two discharge measurements were made during spring runoff. Water levels appeared higher than 2009, and the channel was probably ice-affected during the peak discharge, which occurred sometime between June 5 and 7. Estimates of peak flow based on the rating curve are at least 85 m^3/s (3000 ft^3/s), although the estimate is uncertain due to the possibility of snow and ice-affected conditions present through about June 7 or 8. Runoff was very low through the rest of summer, and the station was removed on August 22, 2010. It is probable that discharge increased slightly in late August due to fall rainfall. The maximum difference between water levels of 1.78

m (5.8 ft) occurred between the peak water level during snowmelt and the low-flow water level in summer.

Table 29 presents all individual discharge measurements made by UAF/WERC on No Name River. A preliminary rating curve was developed for No Name River (Appendix D) based on individual discharge and stage measurements collected by UAF. The rating curve was then applied to continuous stage readings in order to estimate continuous discharge (Figure 67). This rating curve is very basic and does not include any shifts to the rating points. There is high uncertainty associated with the estimated continuous discharge, particularly at high and low stage (due to the lack of rating points) and during spring, when the channel may be somewhat ice-affected. Appendix D contains the expanded rating table.

Table 29. Discharge measurements on No Name River (U1) 2009–2010.

Date	Measurement Number	Discharge m^3/s	Discharge ft^3/s	Quality %	Notes	Stage m	Stage ft	Location WGS84
5/31/2009 12:00	1	16	554	8	ice	15.11	49.57	70 3 44.58 N, 147 11 35.91 W
6/2/2009 18:00	2	58	2041	8	ice	15.30	50.20	70 3 44.58 N, 147 11 35.91 W
6/4/2009 12:30	3	40	1423	8		15.13	49.64	70 3 44.58 N, 147 11 35.91 W
6/6/2009 13:50	4	23	808	8		14.96	49.08	70 3 44.58 N, 147 11 35.91 W
6/19/2009 15:30	5	1.5	54	8		14.55	47.73	70 3 44.58 N, 147 11 35.91 W
6/8/2010 12:20	6	41	1441	5	ice	15.08	49.46	70 3 44.58 N, 147 11 35.91 W
6/10/2010 9:45	7	24	858	5		14.87	48.78	70 3 44.58 N, 147 11 35.91 W

No Name River is similar to nearby Coastal Plain rivers in that the primary runoff event of the year is during snowmelt. However, No Name River may get some relatively high streamflow events during the summer if rainfall in the upper part of the basin (Foothills region) is high, as shown in the 2009 hydrograph (Figure 67). Based on field observations, bed sediment may be moved during snowmelt runoff in areas of the river that no longer have anchor ice. Table 30 presents annual snowmelt and summer peak discharges. The 2010 peak spring and summer runoff events are unknown due to lack of individual discharge measurements and ice-affected stages during snowmelt runoff; the highest discharge measurement (41 m^3/s) during 2010 was about two-thirds the highest estimated flow (58 m^3/s) in 2009. Additionally, sensors were removed on August 22, and it is possible that runoff increased in early fall due to rain events.

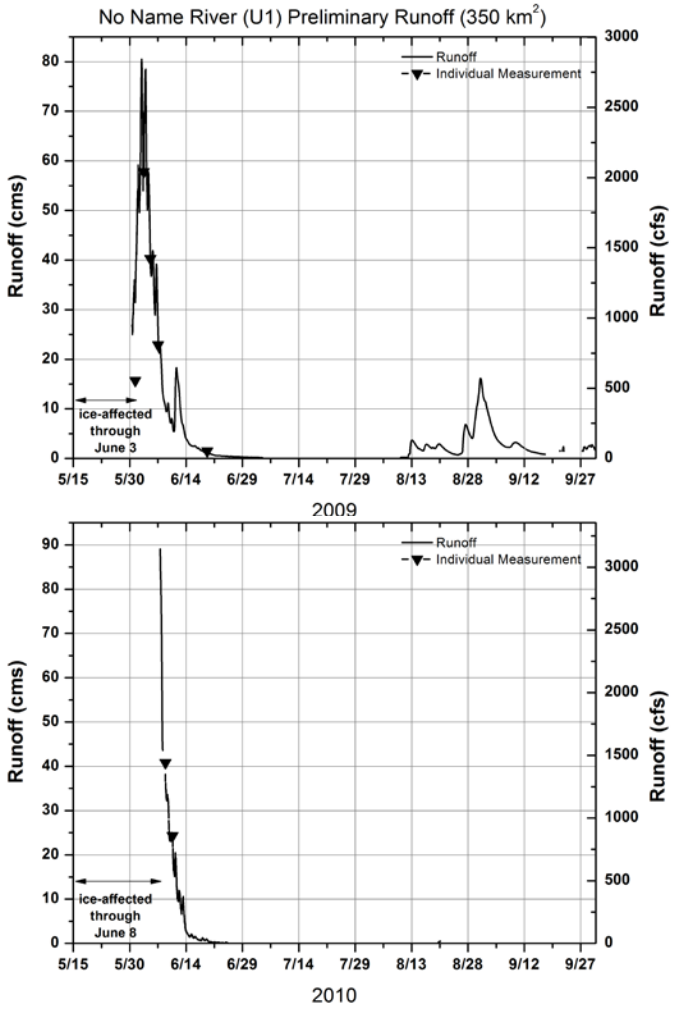

Figure 67. Continuous discharge for No Name River (U1) 2009-2010. Note that the station was decommissioned on August 22, 2010 and no information is available after that date.

Table 30. Estimated peak discharge for the No Name River.

Date	Peak Runoff (m^3/s)	Peak Runoff (ft^3/s)
Spring: 6/3/2009	79	2790
Summer: 8/31/2009	16	565
Spring: 6/5/2010	unknown	unknown
Summer: n/a***	n/a	n/a

*period of record ended 8/22/2011. Summer runoff events after this date are unknown.

4.10.4 Itkillik River

The Itkillik River is a long, narrow basin that originates at a few small glaciers in the Endicott Mountains (up to 2000 m elevation). The upper Itkillik has a basin area of approximately 1900

km^2 and is 153 km long (above our gauging site, which is located in the upper part of the basin near the proposed bridge crossing). The Itkillik eventually flows into the Colville River near the Colville delta on the Coastal Plain. Aufeis is typically observed within the stream channel near the station and in other locations upstream of the station in late April during snow surveys. In early May 2009, UAF installed an observation station approximately 5.5 km (3.4 mi) to the south (upstream) of the ADOT&PF proposed bridge-crossing location. The station records water levels continuously. In fall 2010, UAF began making discharge measurements on the river. This section summarizes the results from spring 2009 through September 2011.

Shore ice was present throughout the channel, and low flows occurred on May 15, 2009, as the river was probably flowing from the unseasonal late April/early May warm-up that year. Little anchor ice was present likely due to the earlier flows causing the anchor ice to mechanically break free or thermally melt. Interestingly, after drilling about 20–25 cm (8–10 in.) into the frozen river cutbank during station installation, water began flowing out of the drill hole, several meters above the river water surface. Beginning on May 18, water levels rapidly began to rise. Much of the shore ice was absent from the channel by May 25. Based on our pressure transducer data and camera images, peak water levels and probably the peak discharge for snowmelt occurred around May 25 or 26. After the peak, water levels dramatically dropped and flows were low. Water levels began rising again on June 1 and a series of peaks occurred June 1 through 15, likely due to a mix of snowmelt in the mountains and early June rain events. The peak water level occurred on July 10 from a rain event, and this peak exceeded the highest water level recorded during snowmelt. Water levels continued to decline the rest of the summer, and very little response was observed during late August rains. The maximum difference in water levels since we began observations occurred in 2009 (from lowest to highest stage difference) and reached 1.8 m (~6 ft).

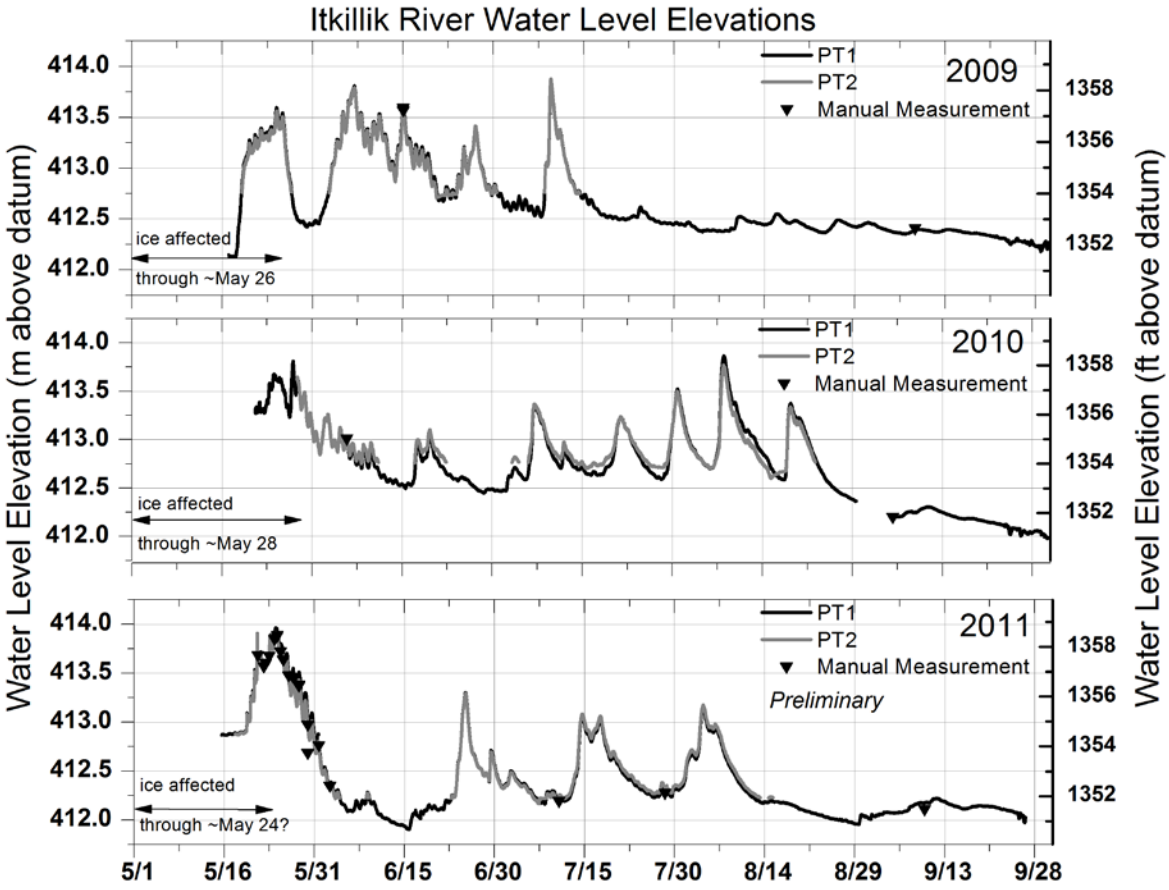

Figure 68. Manual and continuous water levels at the Itkillik River Station, 2009–2011.

In 2010, extensive ice was visible at the station prior to flow on the Itkillik River, but was confined to within the channel. The Itkillik River began flowing on May 17, 2010, with water flowing on top of the ice. Anchor and shore ice were still present during a site visit on May 21, and the region was still 100% snow covered. Most of the river ice floating in the Itkillik was smaller-sized chunks due to the river's high velocities and rocky streambed, which mechanically break the ice. However, when anchor ice initially lifts off the bottom in blocks, the ice may be up to several meters in length. Turbidity increases as snowmelt progresses, and turbidity remains high through the snowmelt period. In 2010, water levels remained steady and high throughout break-up, even as ice was removed from the channel. The peak water level occurred around May 27. It is estimated that most of the river ice was gone by May 27 or 28. Water levels gradually receded through early June. A series of rain events occurred in July and August of 2010, and the

flood event on August 7 was the summer peak for the Itkillik River. The lowest flows occurred in early October, and the river (at the station location) was covered in ice by mid-October according to camera images.

Snow surveys in the Kuparuk basin region (adjacent to the Itkillik basin) conducted in spring 2011 indicated that the snowpack was higher than the previous two years, so it was expected that a large runoff event could occur during snowmelt. In 2011, the Itkillik River began flowing at the station on the evening of May 19, with water flowing over the ice. During the early part of break-up, ice lifted off the bottom, and ice pans up to 3 m (9.8 ft) were observed floating downstream. An ice jam occurred on May 21 downstream of the bridge-crossing location, causing water levels to rise 0.3 m (1 ft) in 1.5 hours at the Itkillik River station (5 km or 3 mi upstream of crossing). Two hours later, the water levels dropped to their original level. Peak water level and flow likely occurred on May 24. Water levels were probably ice-affected until May 24, and turbidity remained high through the last site visit on June 1. Ice chunks up to 2 m × 2 m × 0.5 m in size were observed to be floating downstream May 22–23, and ice chunks of various sizes floated down the river each afternoon as water levels fluctuated diurnally (Figure 69 and Figure 70). On May 29, stranded ice chunks on a gravel bar were measured approximately 1 m thick. High water marks were not observed above either the left or right bank at the proposed crossing location during spring break-up. After spring break-up, several rain events occurred that caused an increase in flow (June 25, July 14, and August 3), but runoff was less than at break-up. Table 31 presents the estimated peak water levels for each year.

Figure 69. Ice chunks on the Itkillik River on May 21, 2011, at the proposed bridge-crossing location.

Figure 70. Ice chunks at the Itkillik River proposed crossing on May 22, 2011.

Table 31. Estimated peak spring break-up and summer water-level events for the Itkillik River 2009–2010.

Date	Peak Water Level Elevation (m)	Peak Water Level Elevation (ft)
Spring: May 25, 2009	413.60	1356.95
Summer: July 10, 2009	413.87	1357.84
Spring: May 27, 2010	413.81	1357.64
Summer: August 7, 2010	413.86	1357.80
Spring: May 24, 2011	413.96	1358.13
Summer: June 25, 2011	413.30	1355.97

Table 32. Discharge measurements for the Itkillik River, 2010. The stage is reported in units above the datum (GEOID09AK).

Date	No.	Discharge (m^3/s)	Discharge (ft^3/s)	Stage (m)	Stage (ft)	Quality (%)	Mean Velocity (m/s)	Mean Depth (m)	Approx. Width (m)	Location
7/15/2010 14:00	1	38	1359	412.65*	1353.8*	10	1.4	0.78	35	Nr. bridge crossing
9/4/2010 13:00	2	20	710	412.21	1352.4	5	0.9	0.73	32	Station
5/25/2011 18:30	5	230	8121	413.75	1357.44	20	2.5	1.55	61	Bridge crossing
5/26/2011 14:15	6	170	6003	413.51	1356.66	10	2.3	1.31	78	Bridge crossing
5/27/2011 15:00	7	169	5967	413.47	1356.52	10	2.0	1.22	71	Bridge crossing
5/28/2011 13:00	9	156	5508	413.43	1356.39	10	1.9	1.15	70	Bridge crossing
5/29/2011 20:10	10	111	3919	413.26	1355.83	10	1.6	1.04	65	Bridge crossing
5/31/2011 12:15	11	70	2472	412.87	1354.56	10	1.3	0.85	70	Bridge crossing
7/6/2011 16:15	12	29	1024	412.65	1353.83	5	0.9	0.68	50	Bridge crossing
9/9/2011 17:22	13	26	918	412.11	1352.06	5	0.8	0.65	50	Bridge crossing

*Stage based on pressure transducer data, no stage available at time of measurement

Table 32 presents all ADCP discharge measurements by UAF at the Itkillik River. Most measurements were made near the bridge-crossing location, approximately 5 km (3 mi) downstream from the station. Experiments with dye trace measurements to estimate discharge during ice-affected conditions are presented in Section 4.10.4.1. A preliminary rating curve was developed for the Itkillik River (Appendix D) based on individual discharge (using ADCP measurements) and stage collected by UAF. The rating curve was then applied to continuous stage readings in order to estimate continuous discharge (Figure 71). This rating curve is very basic and does not include any shifts to the rating points. There is high uncertainty associated with the estimated continuous discharge, particularly at high and low stage (due to the lack of rating points) and during spring, when the channel may be somewhat ice affected. Appendix D contains the expanded rating table.

The Itkillik River hydrograph (Figure 71) shows the estimated discharge for 2009, 2010, and 2011. The 2009 record has no discharge measurements to verify the estimated flow. For each year, early spring data have higher uncertainty due to the possibility of ice in the channel, which results in higher stages and overestimated discharge. This early data are not presented; however, the exact date at which the ice no longer affects the channel is not precise, as this varies along the channel. The spring runoff event is a large event each year in terms of peak and total volume of water. Large events may also occur during summer months, as observed in 2009 and 2010 when several rain events had very high discharge that probably equaled the snowmelt peak discharge. However, these events are of shorter duration (and less total volume) than the annual snowmelt event. In 2011, snowmelt was the peak flow of the year, with discharge likely exceeding 250 m^3/s (8800 ft^3/s). Table 33 shows the estimated peak flows for the snowmelt and summer period for each year.

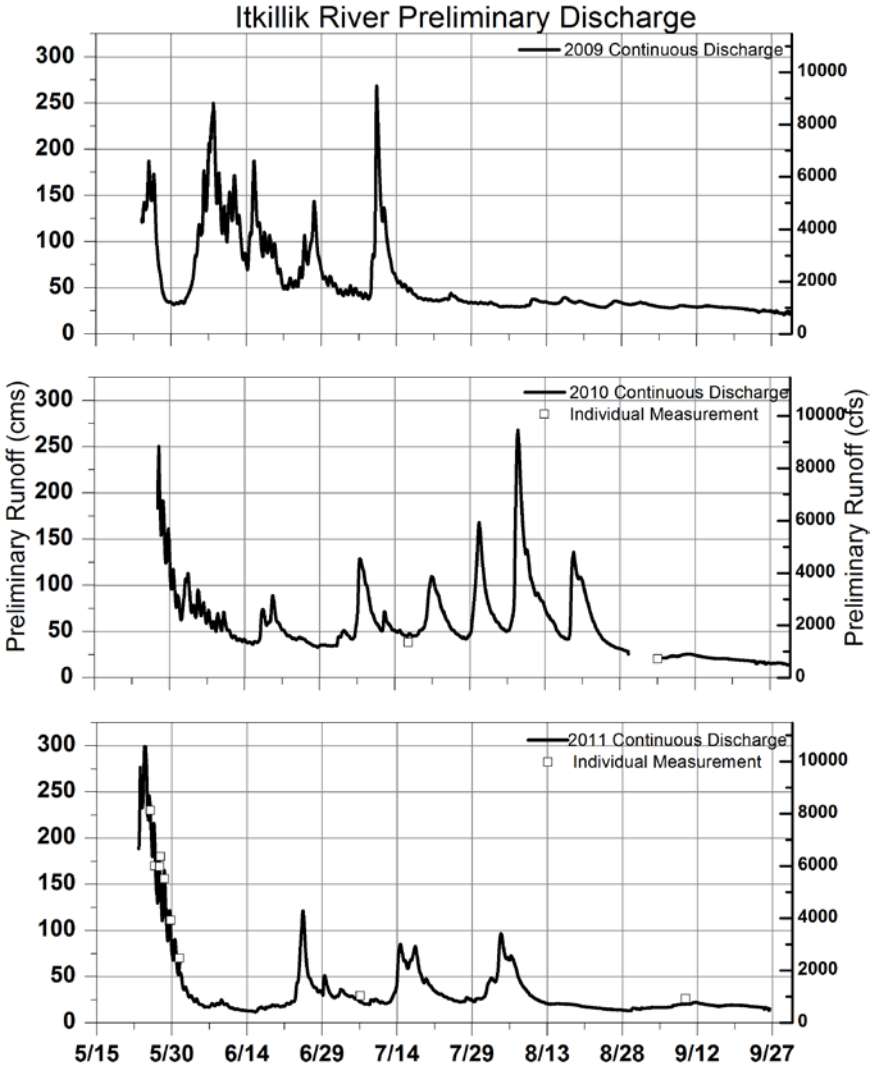

Figure 71. Estimated preliminary discharge for the Itkillik River, 2009–2011.

Table 33. Estimated peak runoff for the Itkillik River.

Date	Peak Runoff (m^3/s)	Peak Runoff (ft^3/s)
Spring: May 25, 2009	183	6462
Summer: July 10, 2009	268	9464
Spring: May 27, 2010	250*	8829
Summer: August 7, 2010	268	9464
Spring: May 24, 2011	300*	10594
Summer: June 25, 2011	120	4237

*High uncertainty due to possibility of channel ice affecting rating curve

4.10.4.1 Itkillik River Dye Trace Results

Due to relatively high flows and the presence of moving ice in the channel, the collection of break-up discharge measurements from small watercraft can be hazardous. Consequently, we are developing methodologies to collect flow information on the Itkillik River from the banks using a dye tracer technique. The methodologies and experimental setup are described in Section 3.9.2. The results of the tests are described below.

4.10.4.1.1 Mixing Distance

As discussed in Section 3.9.2, the tracer technique requires that the dye be thoroughly mixed across the river in order to produce reliable results. When that condition is met, the areas under the recovery curves for each lateral sampling interval will be the same, regardless of the shape of the curve. As discharge is calculated as an inversely proportional function of curve area, comparison of calculated discharge is a convenient mechanism for evaluating lateral mixing. In order to evaluate lateral mixing on the reach in question, samples were collected in parallel from the right bank, midstream, and left bank sections of the river during T1. These resulting recovery curves are presented in Figure 72.

As illustrated in Figure 72, the recovery curves for the three lateral sections were similar to one another. The calculated discharge in the three sections was 103 m^3/s, 108 m^3/s, and 137 m^3/s for the right bank, midstream, and left bank sections, respectively. While the left bank section resulted in a calculated discharge larger than the right bank and midstream sections, sampling for the left bank section did not begin until after the dye had already begun to pass through the sampling reach. Hence, a portion of the left bank curve was not sampled, leading to a diminished curve area and an overestimate of discharge compared with the right bank and midstream sections. We presume, based upon the similar shapes and magnitudes of the three curves as well as the numerical agreement between right bank and midstream discharge calculations, that lateral mixing was complete for T1. Due to logistical constraints, sampling for all remaining trials was limited to the right bank and midstream river sections.

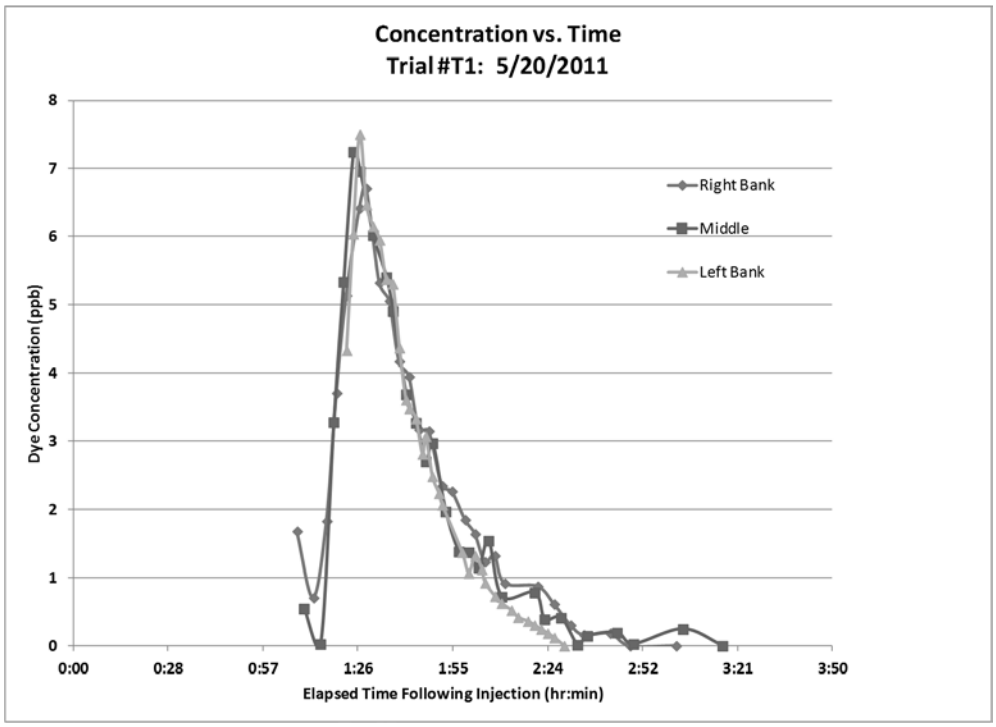

Figure 72. Dye recovery curves for right bank, midstream, and left banks samples during Trial #T1.

4.10.4.1.2 Dye Recovery/Discharge

As discussed, river discharge is inversely proportional to the area underneath the dye recovery curve. This relationship is given by the following formula:

$$Discharge\ \left(\frac{volume}{time}\right) = \frac{Mass\ Injected\ (mass)}{\sum_{i=0}^{n}(Recovery\ Concentration\left(\frac{mass}{volume}\right) \times Time\ Interval\ (time))} \qquad (2)$$

Thus, by plotting dye concentration versus time, and summing the area within each time interval, a calculation of reach discharge can be made. In a reach long enough to promote complete lateral mixing, the calculated discharge will be the same regardless of the lateral section of river from which the samples were obtained. However, the method assumes that the discharge at the point of injection is the same as the discharge at the sampling point. If a side channel entered the main flow at a point just upstream of the sampling reach, for instance, the addition of clean water from one side of the river would confound the mixing assumption. Moreover, the method assumes that the added tracer is conservative within the river reach, and is not lost to sorption, photo-degradation, entrapment in stationary snow or ice in channel, or other mechanisms. Common

loss mechanisms reported for Rhodamine WT include sorptive losses associated with high levels of total suspended solids (TSS) and/or turbidity (Kilpatrick and Cobb, 1985).

During the spring melt event, side channel contributions were unavoidable between the injection and sampling points. Moreover, TSS and turbidity were generally high and somewhat variable in the vicinity of the peak flows. As a consequence of the uncertainty associated with these confounding factors, we intended for the tracer results to provide estimates of discharge, but did not intend to integrate the estimates into the ADCP-derived stage-discharge curve.

Recovery curves for all dye tracer trials are presented in Figure 73. To more clearly illustrate the shapes of the curves, only the sample results from the midstream interval are provided in this figure. However, in most instances, the shape and area of the recovery curves from all sampled sections were similar for any given trial. The discharge results presented in Figure 73 are based on the average area of all river sections. In order to compare dye-based discharge results with river stage and ADCP measurements, the dye- and ADCP-based discharge results are presented along with the continuous stage observations in Figure 74. Following is a brief overview and discussion of each trial (Figure 73):

T0 (9/4/2010): The recovery curve from the low-flow autumn trial (T0) is indicated in Figure 73. The dye-calculated discharge in this trial was 19m^3/s, as confirmed by a simultaneous ADCP measurement of 20 m^3/s. Consequently, we considered T0 results to be exemplary, and the shape of the curve to be indicative of a successful dye measurement in this reach. The T0 results support the notion that the dye tracer technique is fundamentally sound under the appropriate conditions.

T1 (5/20/2011): T1 was completed on the day following the initiation of surface flow in the Itkillik. The estimated discharge was 106 m^3/s. The shape of the recovery curve was similar to that of the T0 trial, thus lending some credence to the calculated estimate. Stage measurements observed during T1 were similar to the river stage associated with a discharge of approximately 100 m^3/s (Figure 74), based upon ADCP data obtained during ice-free conditions. However, the river was clearly ice-affected during T1. As a channel at a specified stage will produce a lower

discharge under ice-affected conditions as compared with ice-free conditions, T1 is likely an overestimate of the actual discharge. However, due to our inability to safely collect an ADCP measurement or rely upon a stage-discharge curve during the initial break-up, we could not determine the degree of overestimation. While neither TSS nor turbidity was measured at the time of T1, field observations indicated that the water was significantly clearer during this trial than during later trials. This point, in conjunction with the similarities of the T0 and T1 curve shapes, suggests that the T1 trial was likely our most reliable tracer estimate of the spring break-up discharge.

T2 (5/22/2011): T2 occurred during the rising limb of the break-up flood (Figure 73c). As indicated in the figure, the T2 dye recovery was intermittent over time, and the curve shape was markedly different from T0 and T1. This could have resulted from a change in the longitudinal mixing characteristics of the reach (e.g., differential holding times associated with new channels), or could have been an indicator of an emerging problem with the dye recovery and analysis methods. Regardless, the lack of a smooth recovery curve leads us to question the results, and the discharge measurement of 274 m^3/s appears to be inconsistent with the expected discharge at that river stage. Again, while the T2 stage results presented in Figure 74 cannot be directly associated with a discharge due to the presence of ice, Figure 74 does indicate that T2 was likely an overestimate of the actual discharge.

T3 (5/25/2011): T3 took place near the time of peak break-up flow (Figure 73d). The T3 measurement was confounded by high turbidity and suspended sediment load, and resulted in a gross overestimate of discharge (Q=3,975 m^3/s). A simultaneous ADCP measurement provided an approximate discharge value of 230 m^3/s (Figure 74). The T3 overestimate was due in part to a change in our analytical procedures in response to the high TSS. During sample analysis, we noted that the measured concentration of each sample varied wildly following insertion into the fluorometer. Moreover, the measured concentration tended to decrease with time spent in the fluorometer, presumably as the suspended sediments settled to the bottom of the vial. This indicated that a significant fraction of the dye was likely sorbed to the suspended sediments. In order to obtain a consistent reading, we allowed the samples to settle overnight, and read them the following morning without shaking the samples. Thus, a significant fraction of the dye was

likely absent from our readings, leading to an overestimate. Due to the inconsistency in our analytical technique, we consider T3 to be an invalid discharge measurement. We present it here only to inform future modifications of the analytical methodology. However, as the dye velocities discussed in Section 4.10.4.1.3 are based upon the shape of the recovery curve rather than the numeric concentration values, we consider the calculated T3 dye velocity to be valid.

T4 (5/29/2011): T4 occurred during the falling limb of the spring flood, under channel conditions that were not considered ice-affected (Figure 73e). As was the case in T3, we noted fluctuations in the fluorometer readings due to suspended sediment. However, the fluctuations were not as severe as those noted during T3, and we were able to obtain reasonably consistent readings. The dye-based T4 discharge measurement, 246 m^3/s, was roughly double that of a simultaneous ADCP measurement (Figure 74). Again, this overestimate was likely attributable to dye loss resulting from sorption to TSS.

T5 (5/31/2011): The final measurement, T5, again resulted in an overestimate of discharge likely due to sorption (Figure 73f). The dye-measured discharge was approximately three times that of a simultaneous ADCP measurement (Figure 74). Moreover, there was a 41% relative difference between the dye recovered from the T5 MS and RB sampling intervals, indicating that lateral mixing was not complete for this trial. This incomplete lateral mixing was likely due to the injection method. Whereas all other trials were injected via distributed methods or point injections from midstream, the T5 slug was injected as a slug from the right bank.

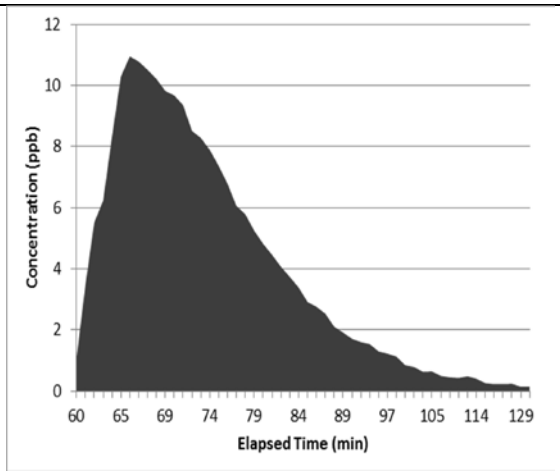

A: T0 Recovery Curve; Q=19 m^3/s, 9/4/2010.

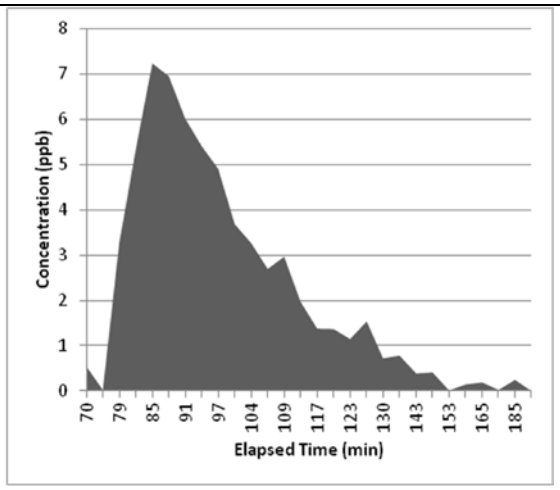

B: T1 Recovery Curve; Q=106 m^3/s, 5/20/2011.

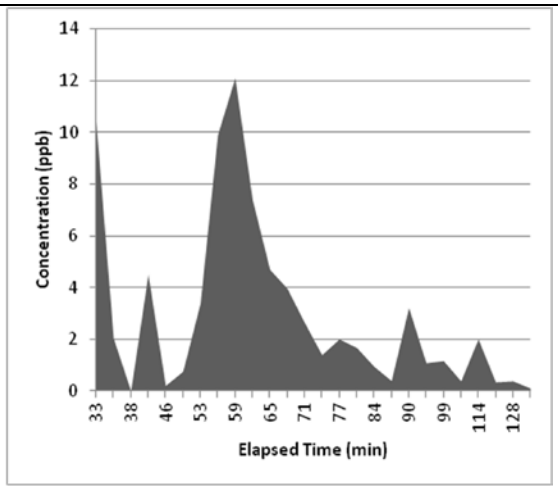

C: T2 Recovery Curve; Q=274 m^3/s, 5/22/2011.

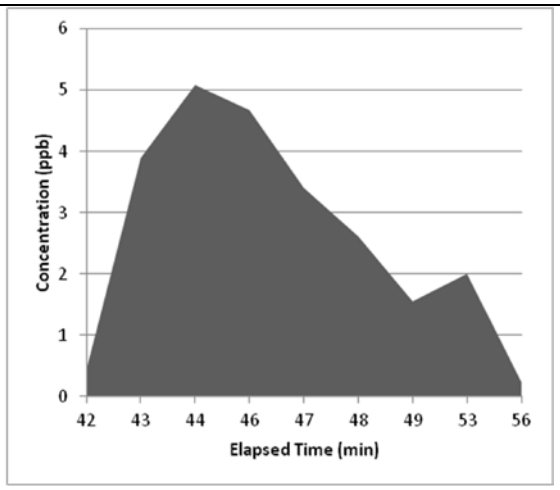

D: T3 Recovery Curve; 5/25/2011, Invalid Q Measurement.

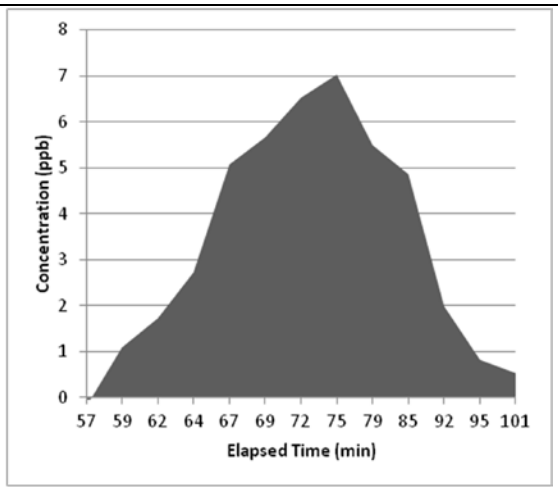

E: T4 Recovery Curve; Q=246 m^3/s, 5/29/2011.

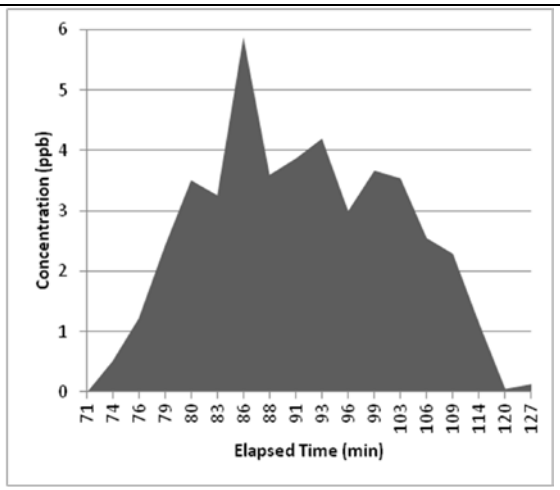

F: T5 Recovery Curve; Q=245 m^3/s, 5/31/2011.

Figure 73. Recovery curves for all dye injection trials.

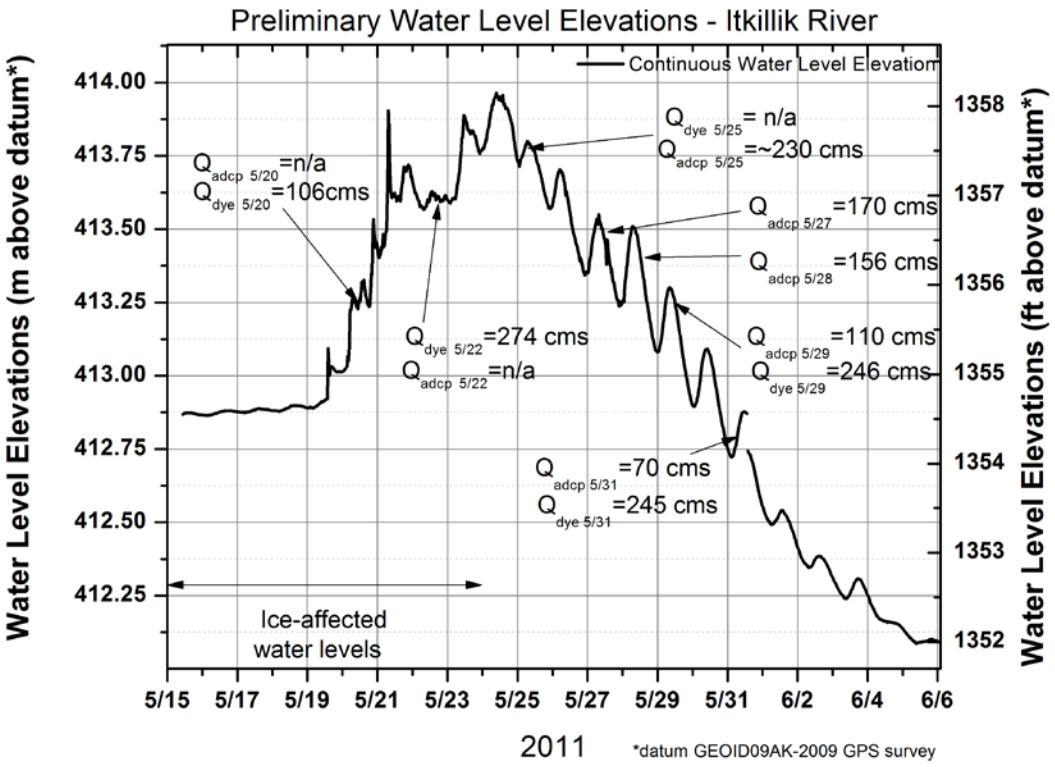

Figure 74. Preliminary spring 2011 Itkillik stage observations with dye- and ADCP-based discharge measurements included.

4.10.4.1.3 Dye Velocity

While the high TSS and turbidity associated with break-up flows hindered the interpretation of dye recovery results with respect to discharge calculations, the time of peak flow was readily apparent in every trial (Figure 73). As the reach length between dye injection and sample recovery was known, a dye velocity value could be calculated for all trials. We define dye velocity as the time required for the peak concentration to travel to the sampling point, divided by the reach length. The dye velocities for each trial, as well as the ADCP-derived average water velocities are presented in Table 34:

Table 34. Dye velocity results for Spring 2011 trials.

Trial	Dye Velocity (m/s)	ADCP Reach Avg. Velocity (m/s)	Relative Percent Difference (%)
T1	1.29	n/a	n/a
T2	2.10	n/a	n/a
T3	2.49	2.51	1.0%
T4	1.48	1.70	14.1%
T5	1.24	1.26	1.7%

As indicated in Table 34, the measured dye velocities integrated over the ≈7 km tracer reach were representative of the average water velocities measured via ADCP in the sampling reach. This relationship, which is somewhat fortuitous, indicates that the cross section at the sampling reach was representative of the average cross section over the entire reach between the injection and sampling points. As the springtime samples were collected at the proposed Itkillik bridge-crossing site, this indicates that dye tracers likely constitute an effective method for determining average crossing-site water velocities during periods when ADCP measurements are not feasible.

While supplying estimates of the crossing-site average water velocity is a useful outcome of the dye tracer method, additional information can be inferred by comparing the ADCP-derived maximum velocities to the ADCP-derived average water velocities for the crossing site. Based upon evaluation of the ADCP data, the maximum water velocity in the channel was approximately 1.6 times the average velocity of the cross section. This estimate is based upon observed data, and is applicable only to the cross section at the crossing location. Consequently, we estimate that the upper-limit velocity of floating ice at the crossing site during the dye tracer tests was approximately 1.6 times the measured dye velocity. In the case of T3, this value was approximately 4 m/s. During the upcoming season, we plan to further develop and test our dye-based velocity estimates, and to ground-truth those estimates against visual measurements of ice flowing through the crossing reach.

4.10.4.1.4 Conclusions/Recommendations

The dye tracer methodology can be a useful tool for measuring river characteristics under conditions when ADCP measurements are not feasible. However, the method still requires additional evaluation, and future dye measurements should be accompanied by simultaneous ADCP measurements when possible.

The single trial in which we employed the point slug injection method from the right bank (T5) appeared to result in incomplete lateral mixing. The remaining trials, employing either midstream point slug injections or distributed slug injections, appeared to demonstrate sufficient

lateral mixing. Consequently, bank-based point slug injections should be avoided in future trials conducted along the same reach.

Tracer-based discharge calculations for the spring flood were severely hampered by high TSS and turbidity in the flow. Potential solutions for future trials could include the use of an alternate dye formulation, or the development of a calibration technique designed to account for the sorption of Rhodamine WT onto suspended particulates. Future testing should also be performed to investigate the role of snow and ice in attenuating the dye signal.

Based upon data collected thus far, the peak concentration time of travel provides reasonable estimates of the average water velocity at the crossing site. Thus, tracer-based velocity measurements could prove to be vital during periods when river conditions prevent the safe collection of ADCP-based measurements.

Future dye studies should also incorporate the use of dye at the crossing site for visual evaluation of ice velocities. While we attempted in this study to measure the ice velocity by visually tracking floating ice over a measured distance, individual ice chunks were difficult to track in the turbulent flow. Subsequent observations could be enhanced by using a dye-dispersing mechanism such as a fire hose or a paintball gun to tag individual ice chunks as they flow through the crossing reach.

4.10.5 Anaktuvuk River

The Anaktuvuk River, which is approximately 215 km long and has a drainage area of 7100 km^2, flows from the Endicott Mountains (~2000 m elevation) to the Colville River near Umiat (elevation ~90 m). Included in the Anaktuvuk basin drainage network are the Nanushuk and Tuluga Rivers. In early May 2009, UAF installed an observation station approximately 15 km (9.4 mi) to the north (downstream) of the ADOT&PF proposed bridge-crossing location. The station records water levels continuously, and discharge measurements are made near the station. This section summarizes the results from spring 2009 through September 2011.

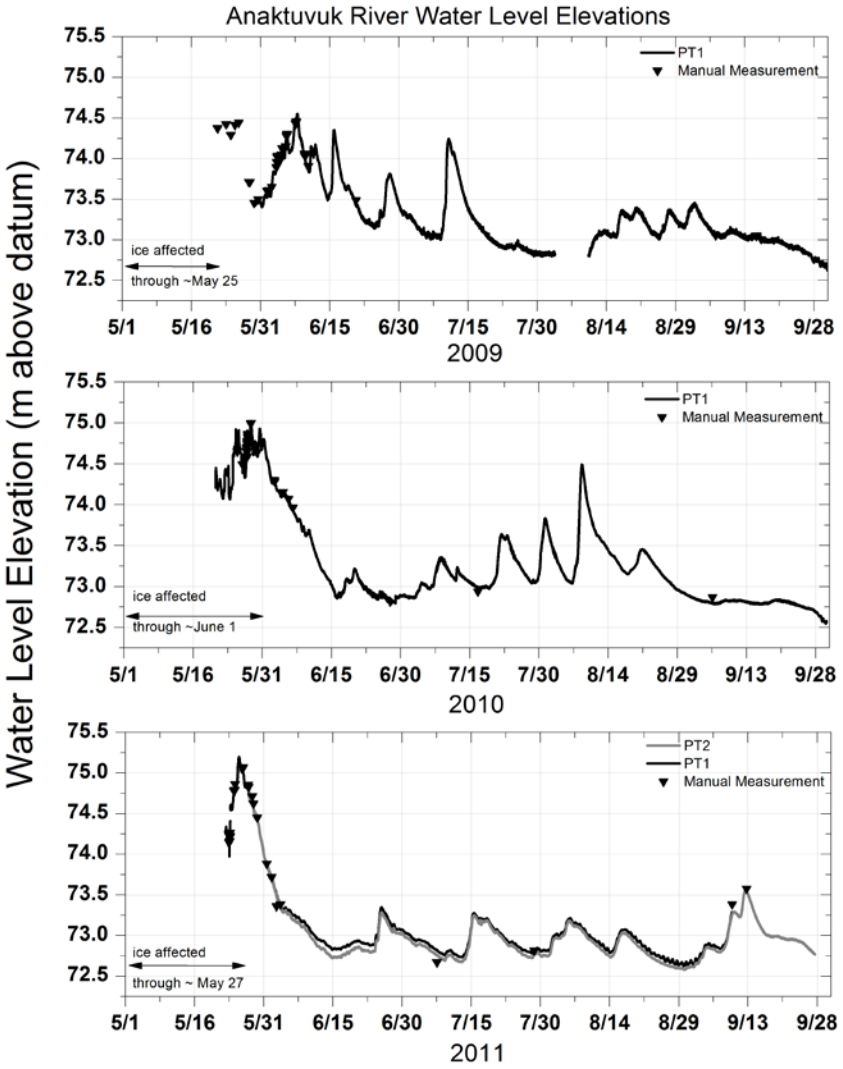

Figure 75. Manual and continuous water levels at the Anaktuvuk River station, 2009–2011.

Water levels were recorded at the Anaktuvuk River station from 2009 to 2011, as shown in Figure 75. Table 35 shows the peak water level events for each year. Upon our arrival on May 18, 2009, flow had already begun on the Anaktuvuk River due to the unseasonal April warm-up, and water levels were rising. Water levels and discharge were not measured prior to May 22 and the stage was ice-affected, so no discharge data are available prior to May 24. Some shore and anchor ice remained in the channel, and stranded ice blocks remained on gravel bars, indicating that water levels were previously higher. From May 22 to 25, water levels remained steady and high, and the estimated snowmelt peak flow (~767 m^3/s or 27,086 ft^3/s) occurred on May 26.

Water levels rapidly declined after May 26 (about 2 m or 6.5 ft) and began rising again around June 1. Water levels continued to rise until a peak on June 7, which was probably a result of a combination of the last snowmelt from the higher elevations of the basin and widespread rain events in early June. This second peak had almost the same estimated discharge (797 m^3/s or 28,145 ft^3/s) as the estimated May 26 spring runoff peak. Suspended sediment samples collected at the Anaktuvuk River beginning on June 3 show sediment concentrations generally increasing as discharge increases and decreasing during periods of lower flows. Additional high-flow events occurred in June and early July of 2009 as a result of rainfall events. In August, water levels rose slightly due to rain, but not nearly as much as the June and July flow events. The lack of significant streamflow response in late August is likely due to a dry period in July and early August (when evapotranspiration is greater than precipitation), resulting in a soil moisture deficit.

Table 35. Peak spring break-up and summer water level events for the Anaktuvuk River 2009–2011.

Date	Peak Water Level Elevation (m)	Peak Water Level Elevation (ft)
Spring: May 26, 2009	74.44	244.22
Summer: June 7, 2009	74.55	244.58
Spring: May 28, 2010*	75.02	246.13
Summer: August 8, 2010	74.49	244.39
Spring: May 25, 2011	75.20	246.72
Summer: September 12, 2011	73.58	241.40

*Ice-affected water level. Peak discharge probably occurred around May 31, 2010.

The Anaktuvuk River began flowing on May 21 in 2010, but discharge measurements on the Anaktuvuk were not made until June 2 because of poor weather that restricted site access and safety issues. Initially, clear water flowed on top of the ice and above the lower bank at the station. The majority of the flowing ice was chunks and pans up to several meters (5+ m) in length. On May 26, an ice jam occurred on one of the channels in a braided reach near the station. Water levels remained high throughout the break-up period until the peak water-level elevation around May 28, which was still slightly ice-affected. The water was increasingly turbid as runoff increased, and bottom ice was removed from the channel. The estimated peak discharge probably occurred on May 31 (1091 m^3/s or 38,528 ft^3/s). By June 2, water levels had dropped about 0.6 m (2 ft). Recession occurred during the first half of June, and several runoff events occurred in response to large rain events July 21 to 23, July 31, and finally August 8, the highest

summer flow event (estimated at 636 m^3/s or 22,460 ft^3/s). With little rainfall going into winter, the lowest water levels occurred in September and October.

During snow surveys in late April 2011, flow was visible approximately 1.6 km (1 mi) upstream (69.31987, -151.00152, WGS84) from the proposed bridge crossing. Aufeis was visible, but it was not extensive across the entire channel. In spring 2011, the river began flowing on May 22 at 09:15 AST at the station. On May 21 at 19:25 AST, the flow front on the Anaktuvuk was approximately 18 km (11 mi) upstream from the bridge crossing and ~35 river km (22 mi) upstream of the station, giving an initial average velocity of 0.7 m/s (1.6 mi/hr or 2.3 ft/s). The flow front on the Nanushuk River was not observed. Initially water flowed over the ice and turbidity was very low. On May 22 and 24, large ice chunks and ice pans 15+ m (50+ ft) in size were observed lifting off the bottom of the river and floating downstream (Figure 76) and were also observed to be stranded on gravel bars. On May 24, water levels continued to rise and a large number of ice chunks were carried downstream, making it impossible to make a discharge measurement. Flows continued to increase, and the channel probably became bankfull on May 24 and over bankfull by May 25 (Figure 77). Water bagan flowing through parts of the floodplain and across several gravel bar islands. In 2011, measurements began on May 25 when it was safe to enter the river, even though the river began flowing at the station on May 22. However, the measurement on May 25 was of very poor quality due to significant floating ice in the channel that affected boat navigation, technical issues with equipment, and difficulty capturing the entire channel flow (due to extensive river braiding). Water levels continued to rise until the peak flow (estimated at 1476 m^3/s or 52,124 ft^3/s) on the evening of May 26, and the river remained over bankfull until May 27. After May 26, the river went into recession through about June 15. High water marks were located above the right (east) cutbank at the proposed bridge crossing location.

The rest of the summer was mostly uneventful, with generally less than average rainfall. The peak summer discharge (175 m^3/s or 6180 ft^3/s) occurred in mid-September after a rainy period between September 2 and 11. The greatest seasonal difference in water levels occurred in 2011 (from lowest to highest recorded); it was 2.56 m (8.4 ft). Water levels were higher during spring

break-up in 2010 and 2011, as compared with 2009, and this is verified by field personnel observations.

Figure 76. Photograph of the Anaktuvuk River on May 23, 2011. Ice pans were observed floating downstream. The 3 m (10 ft) length red boat on shore (indicated with black arrow) is used for scale.

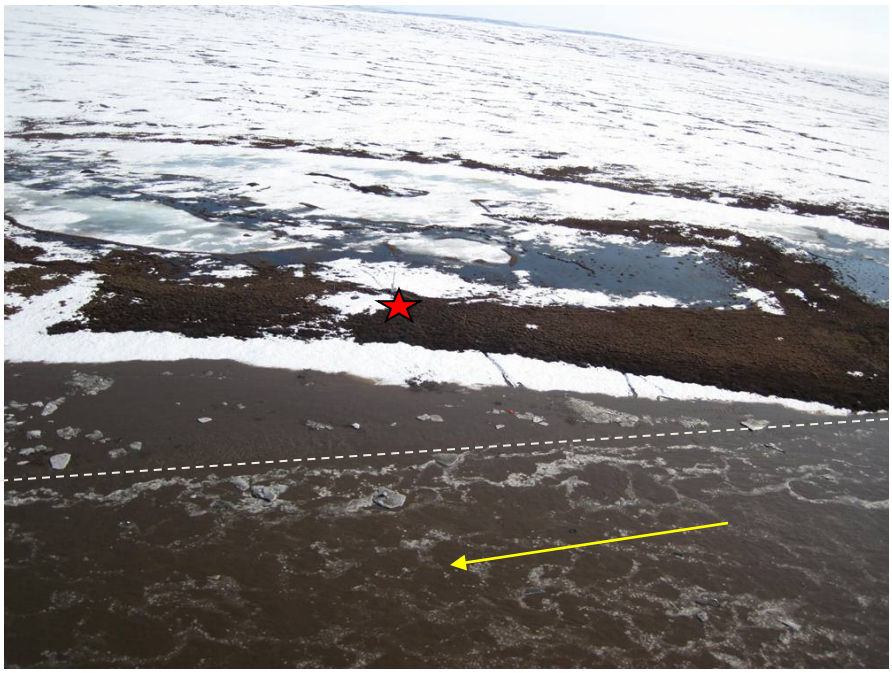

Figure 77. Anaktuvuk River on May 25, 2011, with water flowing over the lower terrace (indicated with dashed white line) near the station (red star).

The individual discharge measurements for the Anaktuvuk River are shown in Table 36. A few early measurements in 2011 were ice-affected. Measurements were collected across a wide range of stages. All measurements during the highest flows were made at the station, and lower-flow measurements were made within 1 mi of the station. Appendix D contains the expanded rating table. Shifts to the curve have not yet been applied to the rating curve/continuous discharge. We use the continuous water level data and the rating curve to estimate a continuous record of discharge. Continuous discharge data are presented for the Anaktuvuk River for 2009, 2010, and 2011 in Figure 78. A large degree of error is associated with the computed high discharges due to the uncertainty in the rating curve at high stages, a lack of measurements, and uncertainty in the channel geometry (i.e., over bankfull conditions).

Table 36. Discharge measurements for the Anaktuvuk River, 2009–2011. The stage is reported in units above the datum (GEOID09AK).

Date	No.	Discharge (m^3/s)	Discharge (ft^3/s)	Stage (m)	Stage (ft)	Quality (%)	Mean Velocity (m/s)	Mean Depth (m)	Approx. Width (m)	Location
5/25/2009 16:30	1	532	18,787	74.46	244.2	10	1.5	1.40	275	Station
5/28/2009 13:00	2	206	7,275	73.71	241.8	10	1.0	1.24	160	Station
5/30/2009 12:00	3	162	5,721	73.50	241.1	10	1.0	1.09	145	Station
6/1/2009 14:00	4	184	6,498	73.63	241.5	10	1.0	1.14	145	Station
6/3/2009 13:00	5	326	11,513	74.04	242.9	8	1.4	1.41	160	Station
6/4/2009 12:45	6	374	13,207	74.05	242.9	8	1.3	1.47	190	Station
6/5/2009 16:45	7	504	17,798	74.30	243.7	8	1.6	1.54	200	Station
6/7/2009 15:00	8	574	20,270	74.43	244.1	8	1.4	1.52	265	Station
6/9/2009 13:45	9	356	12,572	74.32	243.8	10	1.6	1.37	165	Station
9/16/2009 11:00	10	66	2,331	73.01	239.5	10	0.9	0.65	95	¼ mile d.s.*
6/2/2010 13:40	11	512	18,081	74.28	243.7	10	1.4	2.04	180	Station
6/4/2010 14:00	12	388	13,702	74.15	243.3	8	1.4	1.66	165	Station
6/5/2010 13:30	13	339	11,971	74.06	243.0	8	1.4	1.54	160	Station
6/6/2010 12:00	14	290	10,241	73.96	242.6	8	1.2	1.47	160	Station
7/16/2010 12:00	15	54	1,907	72.95	239.3	5	0.7	1.12	65	¼ mile d.s. station
9/3/2010 17:00	16	45	1,554	72.88	239.1	8	1.2	0.69	50	¼ mile d.s. station
5/25/2011 12:00	17	580	20,480	75.14	246.5	20	n/a	n/a	n/a	Station
5/27/2011 21:00	18	1100	38,841	74.73	245.2	10	1.8	1.93	315	Station
5/28/2011 18:54	19	830	29,307	74.62	244.8	20	1.4	2.19	265	Station
5/29/2011 13:00	20	729	25,741	74.45	244.3	10	1.6	1.45	321	Station
6/2/2011 14:00	21	191	6,744	73.55	241.3	5	1.0	1.11	160	Station
7/7/2011 14:00	22	48	1,695	72.77	238.7	5	0.5	1.01	95	Station
9/12/2011 12:45	23	212	7,486	73.58	241.4	5	1.1	1.27	150	1 mile d.s. station

*d.s.=downstream

The estimated snowmelt peak for both 2010 and 2011 likely exceeded 1000 m^3/s (35,000 ft^3/s) (Figure 78, Table 35). In 2009, an early warm-up in late April probably resulted in a lengthy spring runoff period, resulting in a lower magnitude of peak discharge. In 2009 and 2010, several summer runoff events estimated at over 600 m^3/s (21,000 ft^3/s) occurred, but summer 2011 was relatively dry with no large runoff events. The low-flow discharge on the Anaktuvuk River for each year is around 35 m^3/s (1200 ft^3/s).

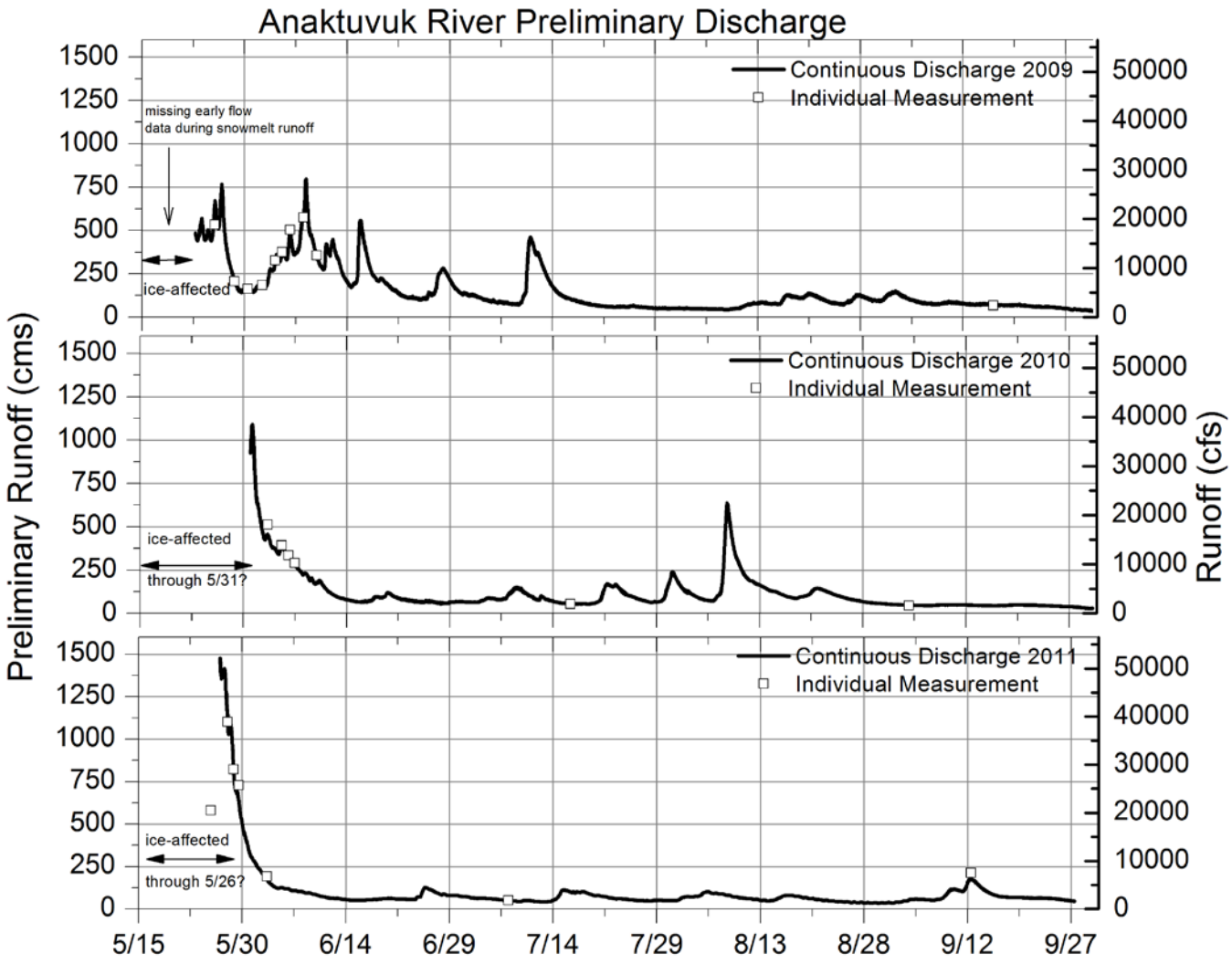

Figure 78. Continuous (and individual measurements for comparison) discharge for the Anaktuvuk River 2009 to 2011 based on initial rating curve.

Table 37. Estimated peak discharge events for the Anaktuvuk River.

Date	Peak Runoff (m^3/s)	Peak Runoff (ft^3/s)
Spring: May 26, 2009	767	27,086
Summer: June 7, 2009	797	28,145
Spring: May 31, 2010*	1091*	38,528
Summer: August 8, 2010	636	22,460
Spring: May 26, 2011*	1476*	52,124
Summer: September 12, 2011	175	6,180

*High uncertainty; channel may have been slightly ice-affected and flow was over bankfull.

4.10.6 Chandler River

The Chandler River, located in the far west of the study area, emanates from the high-elevation Chandler Lake in the Brooks Range and flows north to the Colville River near Umiat (elevation ~90 m). The Chandler River is approximately 225 km long with a drainage area of 5800 km^2. The Chandler basin also includes the Siksikpuk and the Ayiyak drainages. In early May 2009, UAF installed an observation station approximately 15 km (9.4 mi) to the south (upstream) of the ADOT&PF proposed bridge-crossing location. Located on a bluff above the river, the station recorded water levels in 2009. In 2010, the station was expanded, becoming a full meteorological station. In spring 2011, because of difficulties accessing the river from the bluff and sensor damage due to bank erosion, a new water level observation station was established within the floodplain approximately 2.4 km (1.5 mi) downstream from the original station. Discharge measurements are typically made downstream from the bluff station about 1.3 km (0.75 mi). This section summarizes the results from spring 2009 through September 2011.

Upon arrival at the Chandler River on May 18, 2009, the river was already flowing due to an early warm-up in late April, and most of the ice was removed from the Chandler River. Water levels were rising when we arrived; however, the presence of ice chunks on gravel bars indicated that water levels were previously elevated. Manual water-level measurements were made prior to the installation of continuously recording pressure transducers on May 31 (Figure 79). On May 19 and 20, water levels (and discharge) were rising, and ice blocks that were stranded on gravel bars were carried downstream. Shore ice was no longer present and the water was turbid. Based on visual observations, the peak water level probably occurred on May 20 and the river appeared to be close to bankfull. Water levels dropped 2.5 m (8.2 ft) very quickly after the peak. Water levels began to rise again on June 3 and peaked on June 7 in response to the widespread rain event in the basin. Another high water level event occurred on July 10 from a rain event, and water levels rose 2 m (5 ft) in a 24-hour period. The rest of July and early August were very dry. Water levels rose due to several rain events in mid to late August. The highest water levels for 2009 occurred during snowmelt, but it is unknown if this was the annual peak event because water levels were ice-affected during this time and discharge was not measured.

Table 38 shows the peak water level measurements for each year. In 2009, water levels were ice-affected through May 23. The highest recorded water level of 85.59 m (280.8 ft above datum) occurred on May 20 and was ice-affected. It is not known what happened prior to the first water level measurement on May 20, but it is assumed that water levels were relatively high due to the number of ice blocks remaining on the gravel bars. It is interesting to note that the timing of the break-up peak on the Chandler was earlier than the Itkillik and Anaktuvuk Rivers (which occurred ~May 25 or 26), but the general patterns were the same. The second highest water level on the Chandler occurred on June 7 in 2009 (84.93 m or 278.6 ft above datum) due to area-wide rainfall. Water levels likely were at their lowest in late September and October. The difference in water levels (from the highest on May 20 to the lowest in August) was 3.4 m (11.1 ft) in 2009.

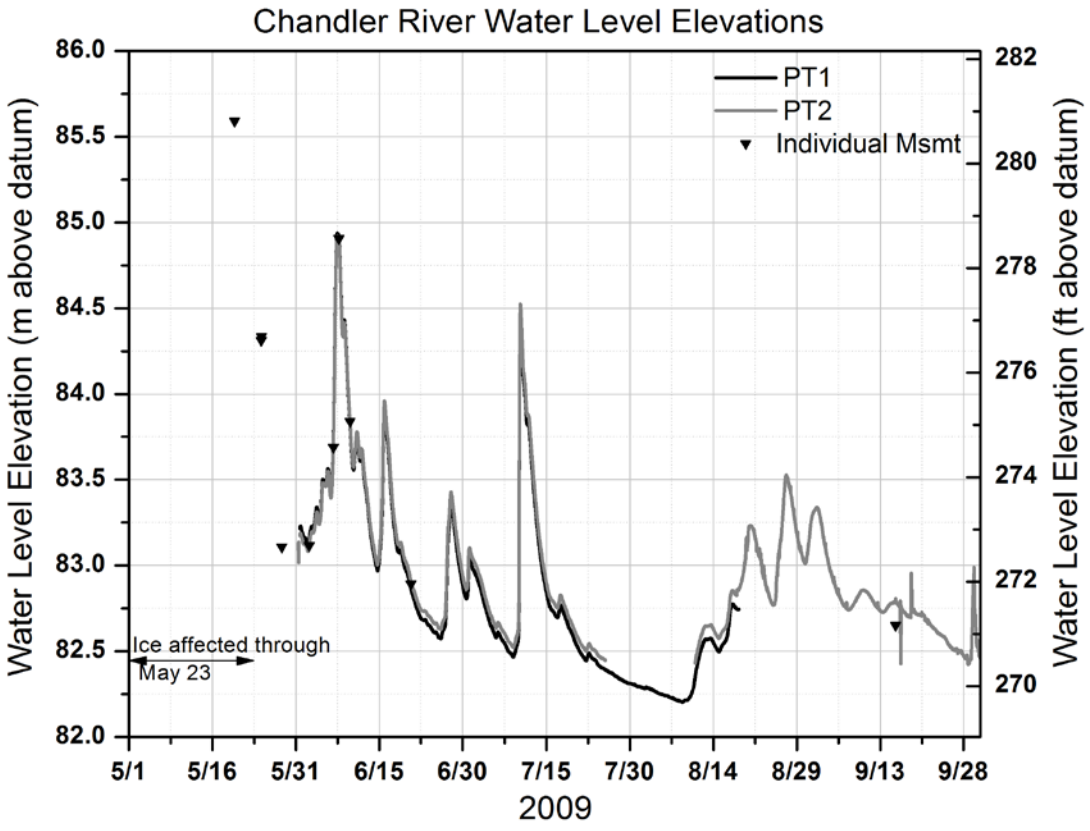

Figure 79. Manual and continuous water levels at the Chandler River Bluff station, 2009. Note that the datum is arbitrary. This station was discontinued as a water level station in fall 2010 and moved to a new location.

The Chandler River began flowing on May 21, 2010. Initially, water flowed on top of the ice, and large ice chunks and pans were observed floating downstream on May 22. By May 27, most of the bottom ice was gone and turbidity had increased. The snowmelt peak likely occurred on the morning of May 31 (according to station camera photographs). Water levels were declining by June 2. Most of the ice was no longer in the active channel and turbidity remained high. Attempts to collect a continuous water level record in 2010 were unsuccessful due to faulty pressure transducers, erosion of the bank, which damaged our sensors, and a lack of manual water-level readings at the station staff gauges, which are required to calibrate the water depth to a vertical datum. Additionally, one of our backup pressure transducers was lost during break-up. Based on the webcam images, the river had high flows during summer events on July 22, July 31, and August 8, similar to the other rivers.

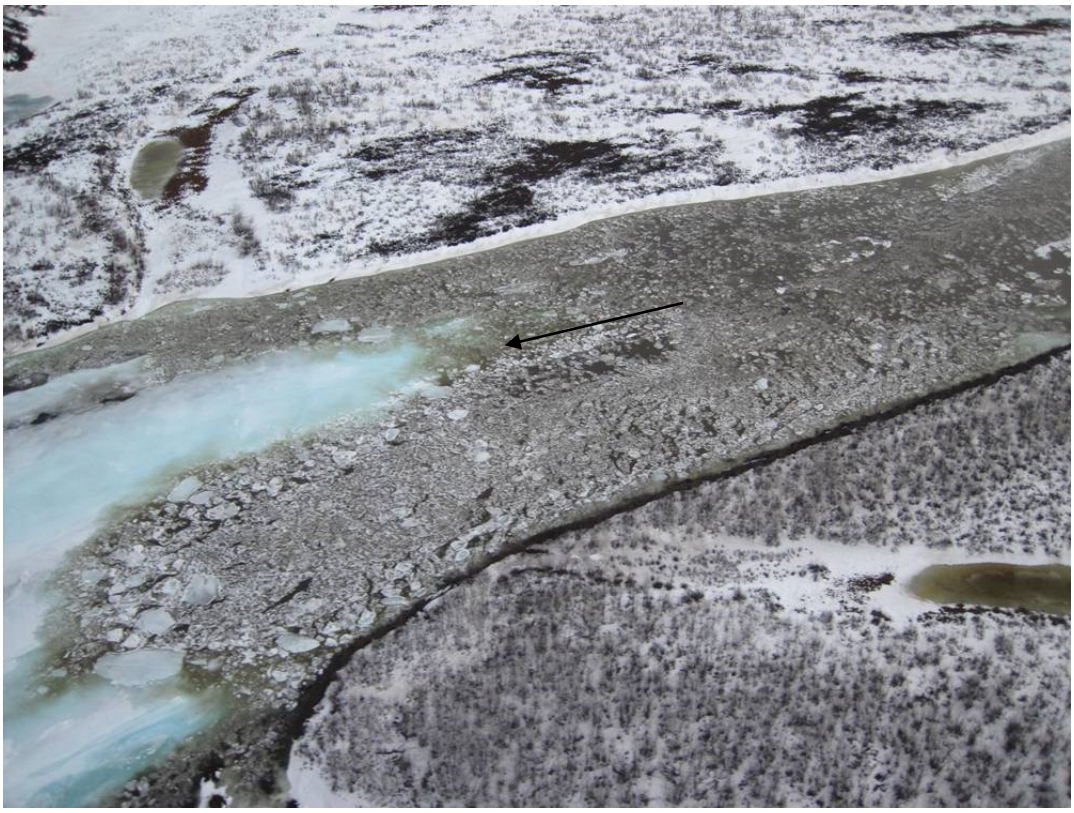

Figure 80. Chandler River flow front, approximately 28 km (17.2 mi) upstream from station on May 22, 2011.

On May 21 2011, at 18:00 AST, the flow front was located approximately 28 km (17.2 mi) upstream of the station (69.11434, -151.80127). On May 22 at 10:30 AST, the flow front arrived at the Chandler River Bluff meteorological station (according to camera images), resulting in an average velocity 0.53 m/s (1.18 mi/hr or 1.73 ft/s). The initial flow front was dramatic, with most of the flow concentrated within one channel (Figure 80) and river ice mechanically breaking up into chunks and pans as the flow progressed. Large ice pans were visible throughout the river, with sizes over 20+ m. Several ice runs were visible throughout the river, and on the afternoon of May 22, an ice jam formed approximately 0.4 km (¼ mi) downstream from the newly established water level station (Figure 81 through Figure 84). Water levels rose 0.9 m in 40 minutes as the water backed up in the channel. On the morning of May 23, another ice jam was observed approximately 2.4 km (1.5 mi) upstream from proposed bridge crossing on a tight bend in the river. Water levels were high in the vicinity of this ice jam, and water levels appeared much lower downstream of the bend at the proposed bridge crossing. On the evening of May 23, a few ice blocks were located on a gravel bar on the right bank at the proposed bridge crossing. Snow remained visible on the gravel bar, and no high water marks were visible to indicate over bankfull conditions.

Figure 81. Location of old Chandler River observation station (DUS3) (which remains a meteorological station) on the bluff and the location of the new hydrologic station established in 2011 (DUS3w). An ice jam formed just downstream from the newly established station on May 22. Flow direction is from the bottom of the photo to the top of the photo (to the north).

Figure 82. View of Chandler River from new water-level observation station on May 22, 2011, 14:52 ADT.

Figure 83. View from the new water-level station of the Chandler River full of ice, after the river ice backed up due to an ice jam on May 22, 2011, at 15:34 AST.

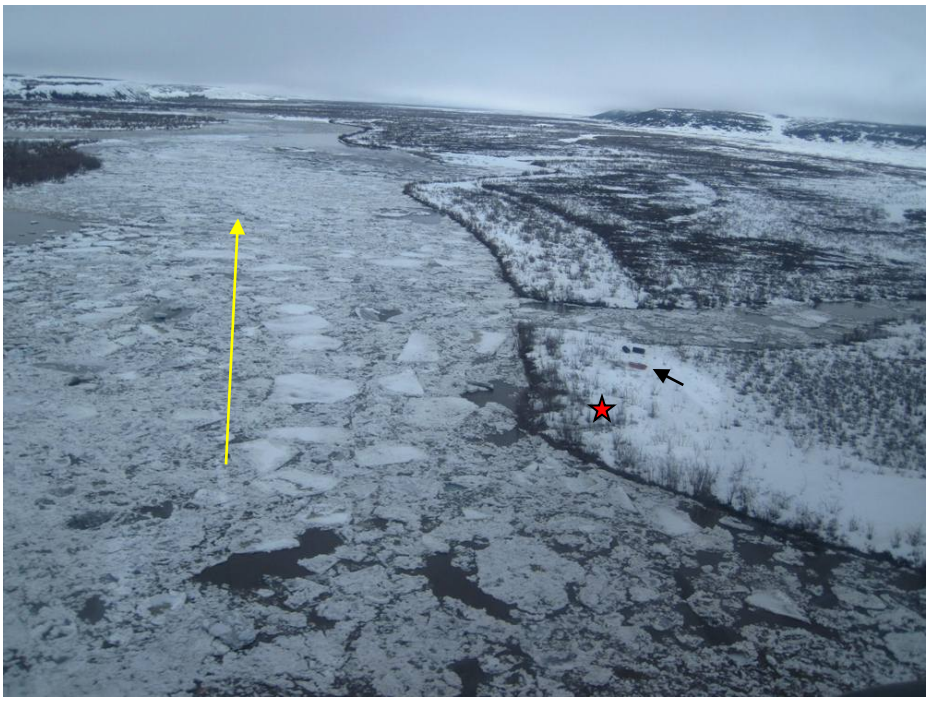

Figure 84. Ice jam at Chandler River station (red star), May 22, 2011. For scale, the black culverts in the photo are 7 ft long. Ice pans 30 m in length were visible.

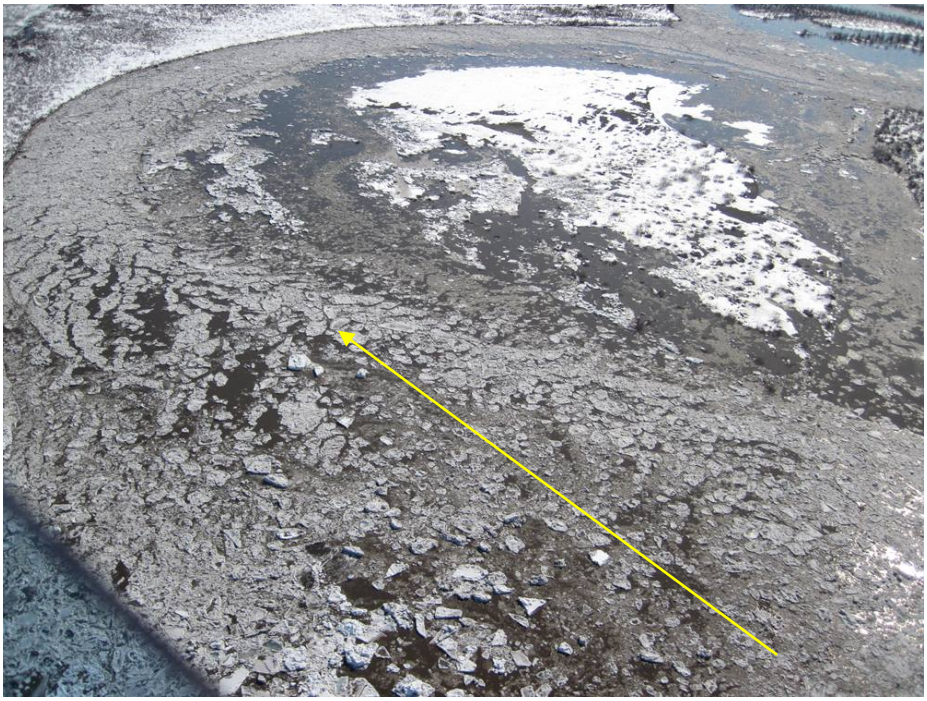

Figure 85. Ice run or jam approximately 2.4 km (1.5 mi) upstream from the proposed bridge crossing on May 23 (2011). Water levels appeared much higher in this area than downstream at the proposed bridge crossing.

Water levels continued to rise an additional 1 m during the ice jam at the new observation station, and this lasted until May 25. An ice pan approximately 12 m × 6 m × 0.8 m was deposited on top of the bank next to the new station, causing our pressure transducers to shift their position. Water was flowing over bankfull at most locations in the vicinity of the station from May 22 through May 26. On May 25, water levels were very high, and a large amount of ice was transported downstream.

Water levels remained high at the station until May 25, as shown in Figure 86, when the ice jam near the new station went out. Peak discharge was estimated to occur on May 26 (~1160 m^3/s or 40,960 ft^3/s), and the first discharge measurement was made on this day. The river remained over bankfull until May 27. As the water levels began to drop, ice chunks and pans were visible above the bank (Figure 87). After the peak flow, water levels rapidly declined until June 3, when the river flow was slightly above low flow conditions. During break-up considerable bank erosion occurred at the new observation station (several meters of bank collapsed), and severe undercutting of the bank (up to 3+ m) was visible at the discharge measurement reach (Figure 88). At the proposed bridge crossing location, high water marks were located above the left (west) cutbank (also see photographs of high stages in Appendix E). No major runoff events occurred the rest of summer until a small event occurred on September 12 (291 m^3/s or 10,276 ft^3/s) in response to early September rainfall. The difference between the highest stage (during spring runoff) and lowest stage (during low flow conditions) was 3.6 m (11.8 ft).

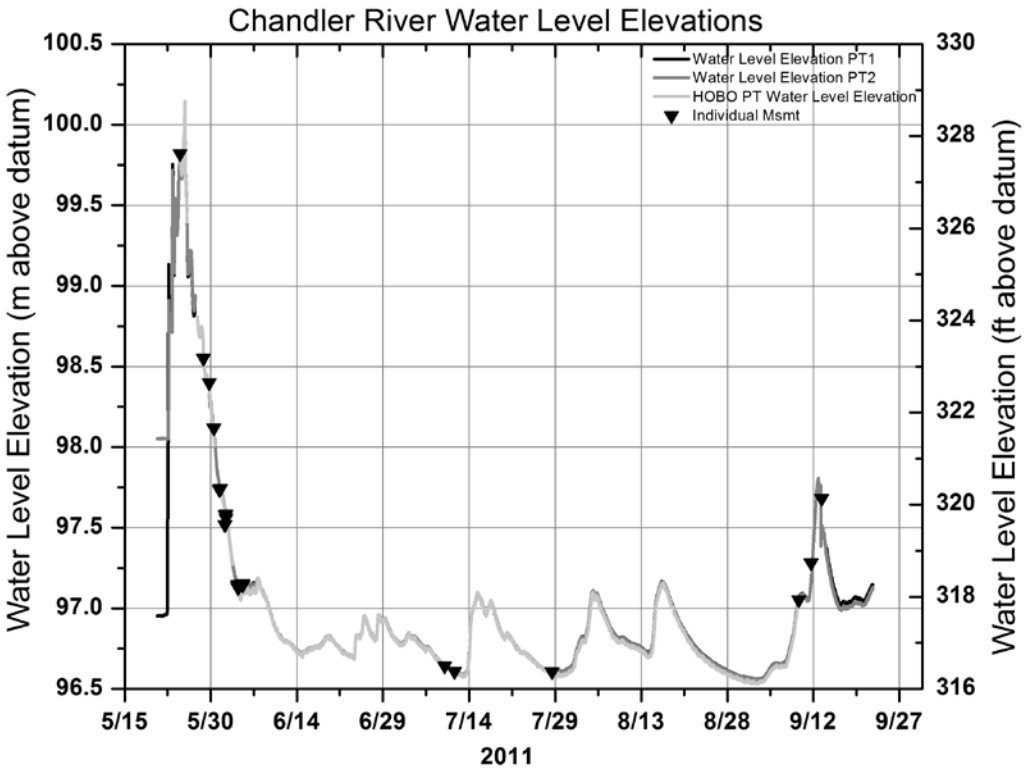

Figure 86. Chandler River water level elevations, 2011. Station was newly established in 2011, relocated approximately 1.6 km (1 mi) downstream from original station. Note that the datum is arbitrary.

Figure 87. Ice chunks and pans on top of the Chandler River cutbank on May 28, 2011, after water level declined.

Figure 88. Undercutting of the Chandler River bank at gauge site after spring break-up 2011.

Table 38 presents the peak water-level elevations for each year, and Table 39 presents all discharge measurements made at the Chandler River. Discharge measurements made in 2010 are not yet correlated to a stage because of the use of arbitrary datums at two different locations. In 2009, water levels were recorded at the Chandler River Bluff meteorological station, and in 2010, water levels were not recorded due to technical difficulties. In 2011, a new station for recording water levels was established 2.5 km downstream from the bluff station. Currently the reference datums for the 2009 and 2011 water-level measurements are arbitrary and water-level elevations cannot be compared with each other. After differential GPS survey results are available, all the water level data will be adjusted relative to the GEOID09AK vertical datum.

Table 38. Peak spring break-up and summer water level events for the Chandler River 2009–2010..

Date	Peak Water Level Elevation (m)	Peak Water Level Elevation (ft)
Spring: May 20, 2009	85.59	280.81
Summer: June 7, 2009	84.93	278.64
Spring: May 31, 2010	n/a	n/a
Summer: August 8, 2010	n/a	n/a
Spring: May 25, 2011	n/a	n/a
Summer: September 12, 2011	n/a	n/a

Table 39. Discharge measurements for the Chandler River, 2010–2011. Stage datum is arbitrary.

Date	No.	Discharge (m^3/s)	Discharge (ft^3/s)	Stage (m)	Stage (ft)	Quality (%)	Mean Velocity (m/s)	Mean Depth (m)	Approx. Width (m)	Location
7/16/2010 14:00	1	15	544	n/a	n/a	10	0.2	1.91	50	Bluff Station
9/3/2010 14:00	2	30	1,080	-	-	5	0.8	0.53	70	500 m d.s.* station
5/26/2011 16:50	3	1029	36,339	99.08	325.06	10	2.3	2.18	210	500 m d.s. station
5/28/2011 12:25	4	729	25,744	98.55	323.33	10	2.1	1.68	210	500 m d.s. station
5/29/2011 11:45	5	424	14,973	98.40	322.83	5	1.7	1.78	145	500 m d.s. station
5/31/2011 15:00	6	268	9,464	97.74	320.66	5	1.3	1.71	130	500 m d.s. station
6/1/2011 11:10	7	242	8,546	97.52	319.94	5	1.1	1.84	120	500 m d.s. station
6/3/2011 14:15	8	112	3,955	97.14	318.69	8	1.5	1.19	65	500 m d.s. station
7/9/2011 16:30	9	25	883	96.64	317.07	5	1.2	0.52	42	500 m d.s. station
9/11/2011 15:25	10	118	4,167	97.28	319.17	5	1.5	0.80	120	500 m d.s. station
9/13/2011 11:15	11	258	9,111	97.68	320.48	10	1.6	1.11	145	500 m d.s. station

*d.s.=downstream

A preliminary rating curve was developed for the Chandler River (Appendix D) based on individual discharge and stage measurements collected by UAF/WERC in 2011. This rating curve is very basic and does not include any shifts to the rating points. The rating curve is applied to continuous stage measurements in order to estimate continuous discharge (Figure 89). There is high uncertainty associated with the estimated continuous discharge, particularly at high and low stage (due to the lack of rating points) and during spring, when the channel may be somewhat ice-affected. For now, only data from 2011 are presented. We expect to estimate the 2009 continuous discharge data after water levels are adjusted to the datum.

The hydrograph presented in Figure 89 and Table 40 show an estimated peak discharge for the Chandler River of nearly 1200 m^3/s (41,000 ft^3/s) occurring during snowmelt runoff and the low-flow discharge of around 22 m^3/s (775 ft^3/s) occurring in mid-July for 2011. The summer of 2011 was relatively dry until September rain events caused a fall increase in discharge. This year was different from 2009 and 2010 in that there were no large summer events.

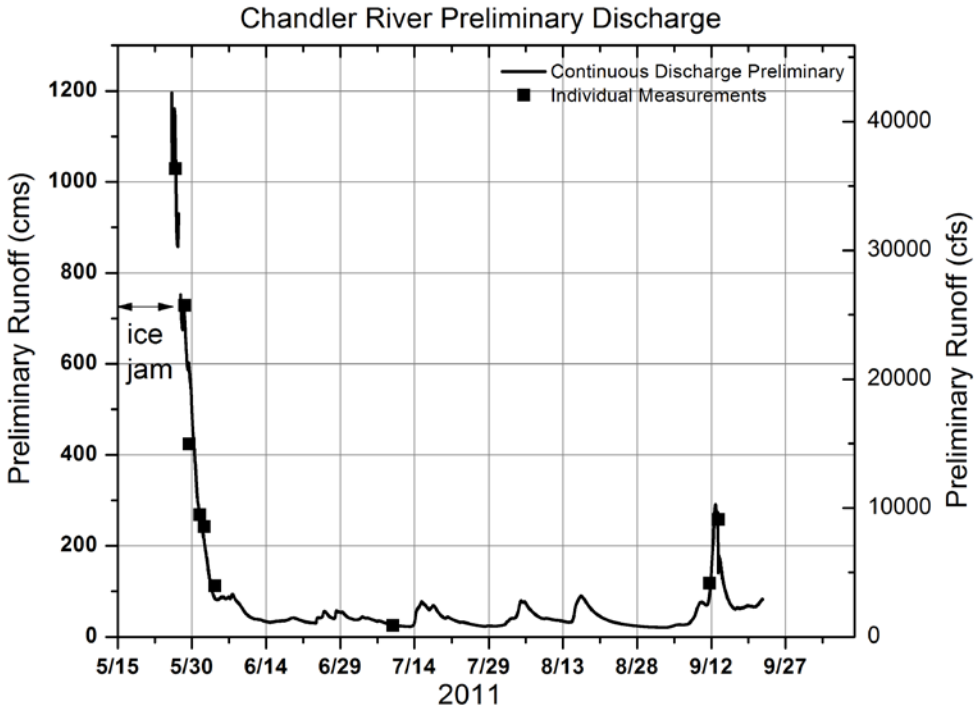

Figure 89. Estimated Chandler River preliminary discharge, 2011.

Table 40. Estimated peak discharge, Chandler River.

Date	Peak Runoff (m^3/s)	Peak Runoff (ft^3/s)
Spring: May 26, 2011*	1160	40,965
Summer: September 12, 2011	291	10,276

4.10.7 Additional Field Observations

In addition to meteorological and hydrologic measurements for the Umiat Corridor project, aerial photographs were taken at the Itkillik, Anaktuvuk, and Chandler River proposed bridge-crossing locations to document the progression of spring break-up river conditions in spring 2011. Appendix E contains daily photographs at each river.

UAF and the USGS also measure runoff in several other rivers within or near the study region. This section presents runoff measurements from 2007 through 2011 on the Upper Sagavanirktok (USGS), Upper Kuparuk (UAF), Kuparuk at Prudhoe Bay (USGS), and Putuligayuk at Prudhoe Bay (UAF) Rivers. We can use these data to examine relationships between basins with long-term runoff records and basins with short-term runoff records.

The Upper Sagavanirktok River originates in the Brooks Range and flows north into the Arctic Ocean near Deadhorse. The basin area at the USGS gauge site is 4100 km^2 (the entire basin is approximately 14,000 km^2) and runoff is measured in the Sagavanirktok before the confluence with the Ivishak River. Above the gauge site, the majority of the basin area lies in the Mountain region and a smaller percentage is within the Foothills region. Figure 90 presents hydrographs for the Upper Sagavanirktok River from 2007 through 2011. Runoff during spring is generally not measured due to ice conditions; it is typically estimated and reported as mean daily discharge. For this reason, it is not possible to do flood-frequency analysis for the spring snowmelt period; it is also not possible to do a spring water balance because the cumulative spring runoff is unavailable. Spring runoff is the largest event of the year in terms of cumulative runoff volume, but summer rainfall also contributes to high runoff events and may produce the annual peak flow. The timing and magnitude of the highest flow events on the Upper Sagavanirktok generally correlate with observations on the Itkillik, Anaktuvuk, and Chandler Rivers due to similar basin characteristics. For example, in 2009, the early summer high runoff event on June 7 was also observed on the Itkillik, Anaktuvuk, and Chandler Rivers. The runoff events on the nearby Itkillik River (Figure 71) appear to be the most similar to the Upper Sagavanirktok in terms of peak and timing of not only the summer events, but also the snowmelt recession period. The Itkillik River is smaller than the Upper Sagavanirktok (in terms of basin area above the gauge site), but it is similar in gradient and the percentage of basin area within the Mountain and Foothills regions. According to Stuefer et al. (2011), the Sagavanirktok basin average snow water equivalent was 187% higher in 2011 than 2010, but this great increase is not clearly visible in the hydrographs when comparing the two years. The hydrograph for 2008, however, does reflect the low snowpack of 2008 (and previous years' drought) with very little runoff response.

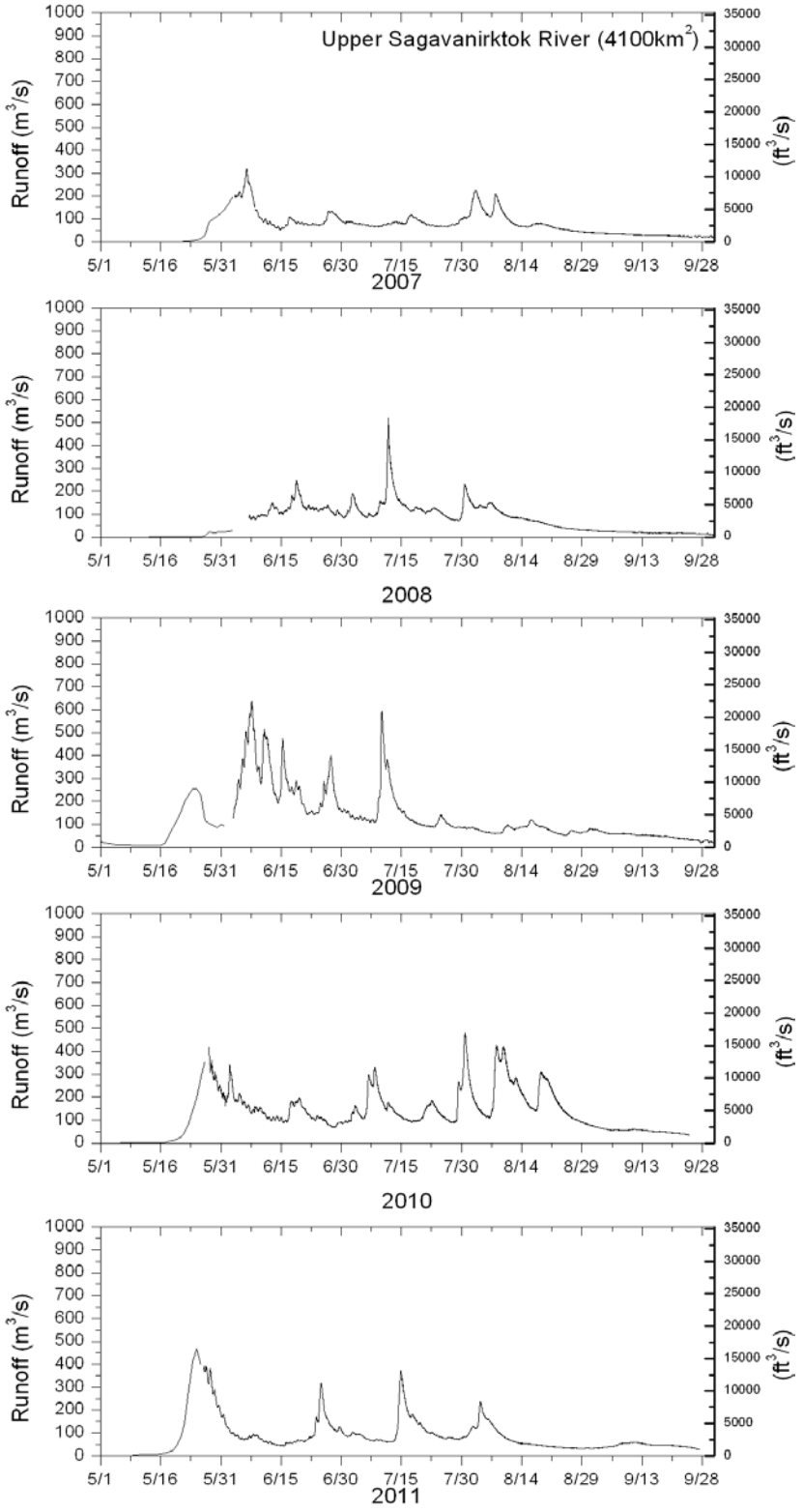

Figure 90. Upper Sagavanirktok River runoff, 2007 to 2011 (USGS, 2011). Note that data during peak spring runoff are generally estimated due to ice, and that runoff data are mean daily values. For that reason, we do not conduct flood frequency analysis during spring runoff because it would be inaccurate.

The Upper Kuparuk River (142 km^2 above the gauge site) is a small basin that originates in the foothills of the Brooks Range and is the headwaters of the Kuparuk River basin. Runoff in the Upper Kuparuk River is measured by UAF at the Dalton Highway road crossing, just northeast of Toolik Field Station. Runoff is manually measured twice daily during the spring runoff period in order to capture discharge when the channel is ice-affected, and once or twice per summer to verify and improve the station rating curve. Runoff for the Upper Kuparuk from 2007 to 2011 is presented in Figure 91. Annual peak flow may be due to snowmelt runoff or summer runoff. Floods of record will always be rainfall generated (Kane et al., 2008a). The summer floods of 1999 and 2002 are the largest floods during the 19-year period of record. In 2011, we believe the largest snowmelt runoff event on record occurred, but unfortunately the peak discharge was not measured. The timing of peak flow events correlates well with other small nearby basins (such as the Atigun and Oksrukuyik Rivers that used to be gauged by the USGS). Summer events that occur in the Upper Kuparuk also occur most of the time on the nearby upper Itkillik and Sagavanirktok Rivers.

The Kuparuk River originates in the foothills of the Brooks Range and flows north through the Coastal Plain to the Arctic Ocean. It is a medium-gradient basin of relatively large size (8100 km^2). Approximately 62% of the basin area is within the Foothills region and 38% is within the Coastal Plain. Runoff is measured by the USGS near Prudhoe Bay, and this data (2007 through 2011) are presented in Figure 92. Since runoff observations began in 1971, the largest event (in terms of total volume of runoff and annual peak flow) always occurs during snowmelt runoff. For the early part of snowmelt runoff, the runoff presented in Figure 92 may be estimated (or reported as mean daily values) if the channel is still ice-affected. Although smaller in basin size, the Kadleroshilik River (Figure 56), which flows through both the Foothills and Coastal Plain regions, has a similar hydrograph to the Kuparuk River, where the majority of the runoff occurs during snowmelt, but responses to rainfall also occur during the late summer. In 2007, the peak snowmelt runoff on the Kuparuk was the highest of the 2007–2011 study period; however, the total volume of snowmelt runoff is the lowest and is comparable to 2008.

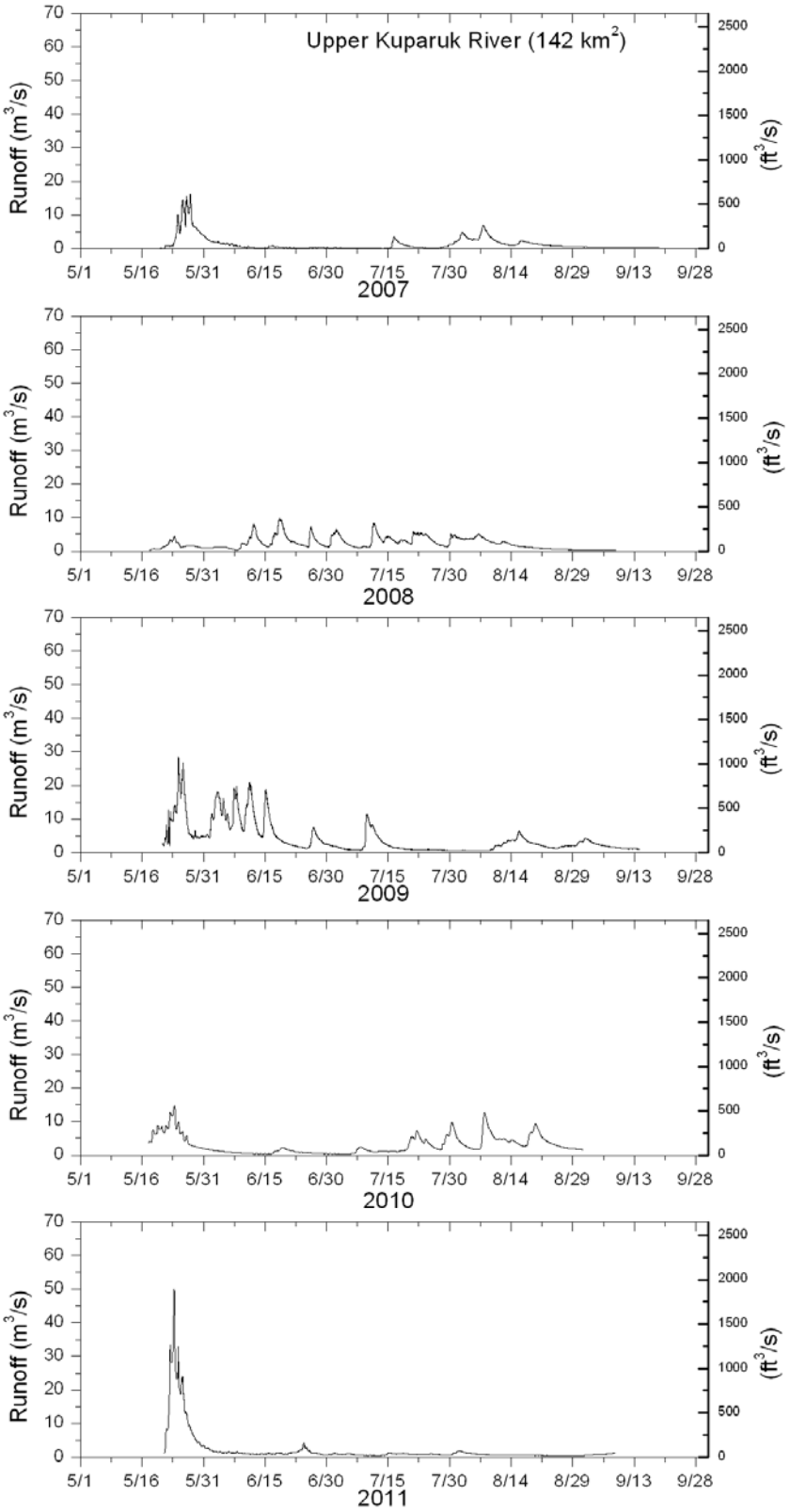

Figure 91. Upper Kuparuk River hydrographs, 2007–2011. The peak flow for spring 2011 is estimated.

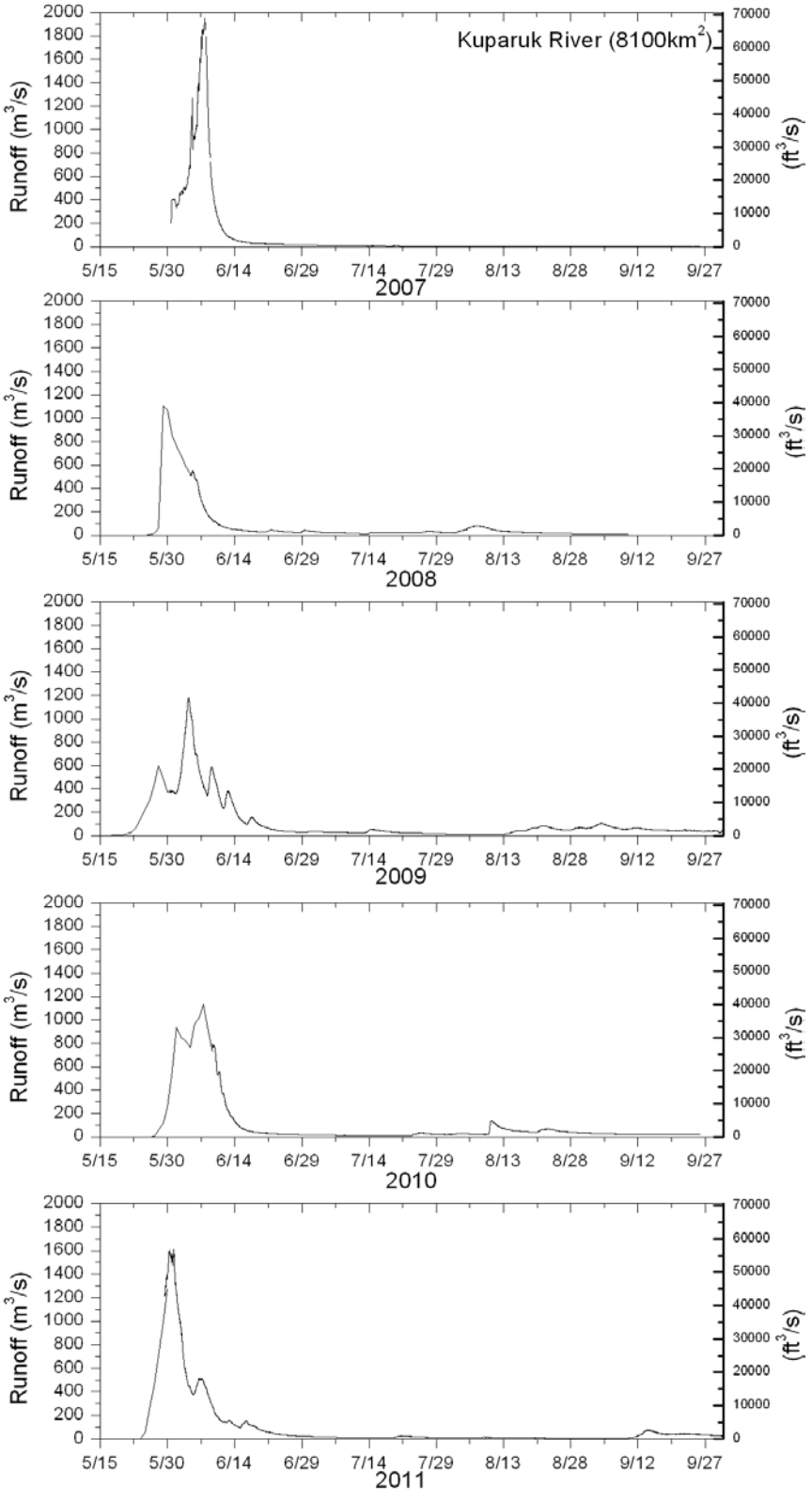

Figure 92. Kuparuk River (at Prudhoe Bay) hydrographs, 2007 to 2011 (USGS, 2011). Note that early data during spring runoff may be estimated due to ice in the channel.

The Putuligayuk River (471 km^2) is a low-gradient basin contained entirely within the Coastal Plain and constrained by the Kuparuk to the west and the Sagavanirktok to the east. Snowmelt runoff is the only significant runoff event of the year, because what little precipitation that occurs during summer goes into deficit storage in the numerous lakes and wetlands within the basin. Figure 93 presents the hydrographs for the Putuligayuk River. The Putuligayuk is measured twice daily by UAF/WERC during snowmelt runoff and once or twice during the summer months during low flow conditions. The years 2007 and 2008 had lower magnitudes and lower total volumes of runoff. In 2010, the highest peak runoff was recorded; however, the total volume of runoff was less than 2009 and similar to 2011. As with the other basins in the region, the shape of the hydrograph during snowmelt may be very different each year, depending not only on the basin snow water equivalent, but also on local meteorology, which can prolong the snowmelt runoff period during cold periods.

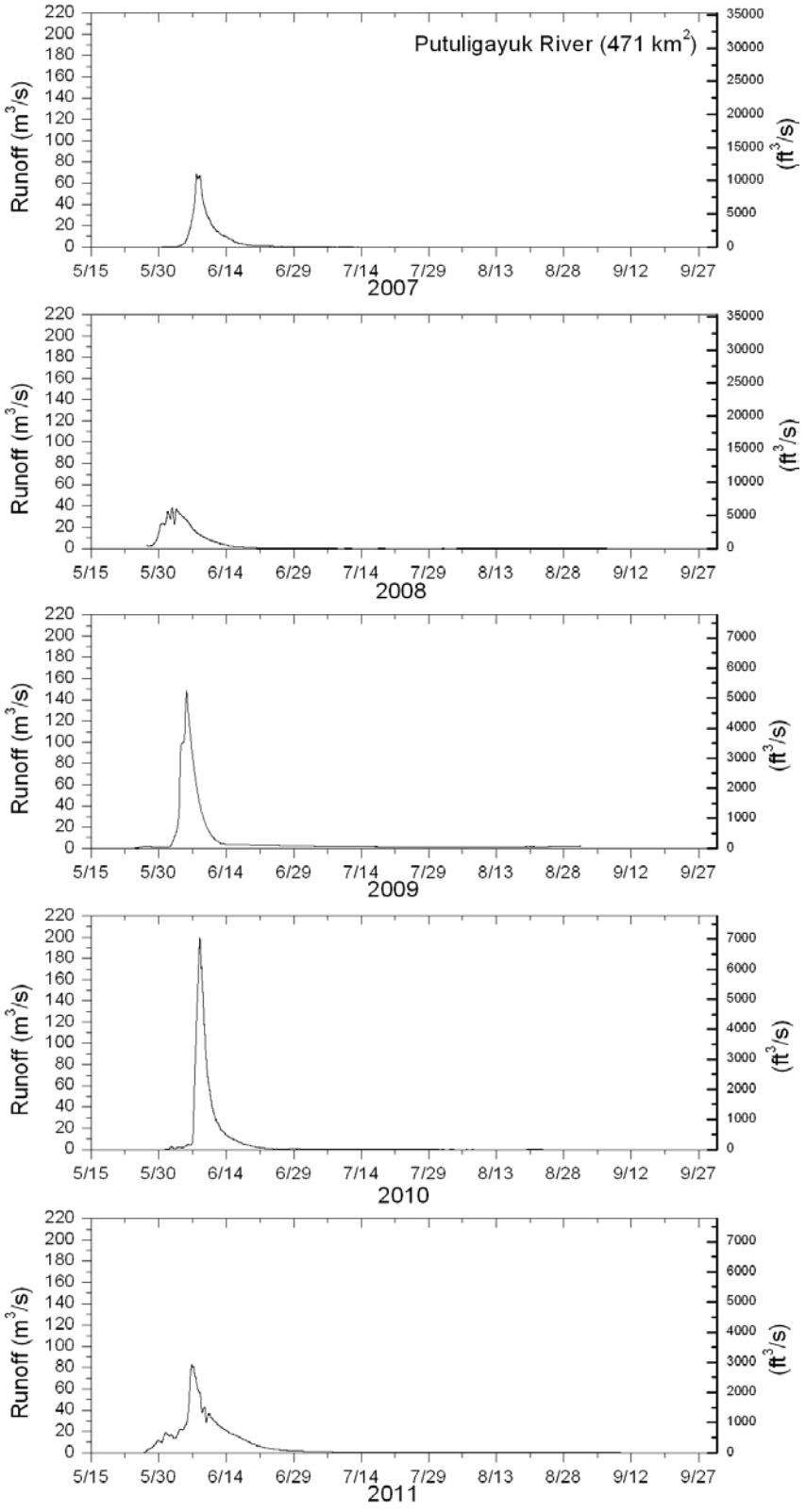

Figure 93. Putuligayuk hydrographs, 2007–2011.

4.11 River Sediment Results

4.11.1 Suspended Sediment

Sediment concentration is a key hydraulic parameter when considering the overall character of a river. While fairly extensive research has been done on the sediment transport regimes of gravel rivers in temperate climates (Parker et al., 2007), our understanding of these processes is less complete in arctic systems. For larger rivers in the Arctic, the spring break-up is the major hydrologic event of the year. The presence of snow and ice for almost eight months of the year, coupled with rivers that may freeze to the bed, clearly differentiates the sediment transport regimes of arctic rivers from their temperate brethren. The impact of bed ice on bedload transport has been studied on the Kuparuk River (Oatley, 2002; Best et al., 2005), where it was observed that the presence of ice on the bed during the spring flood significantly reduced bedload transport. Clearly, the occurrence of ice during spring melt will also affect the suspended-sediment transport in a river; in the Canadian Arctic, this effect was seen to vary between rivers, depending on channel size and discharge rates (Forbes and Lamoureux, 2005).

The amount of suspended sediment in each river varied dramatically throughout the summer. Using samples from the Isco autosamplers, the temporal variation of total suspended solids (TSS) can be seen on each river; discharge is plotted as well for reference (Figure 94 through Figure 96).

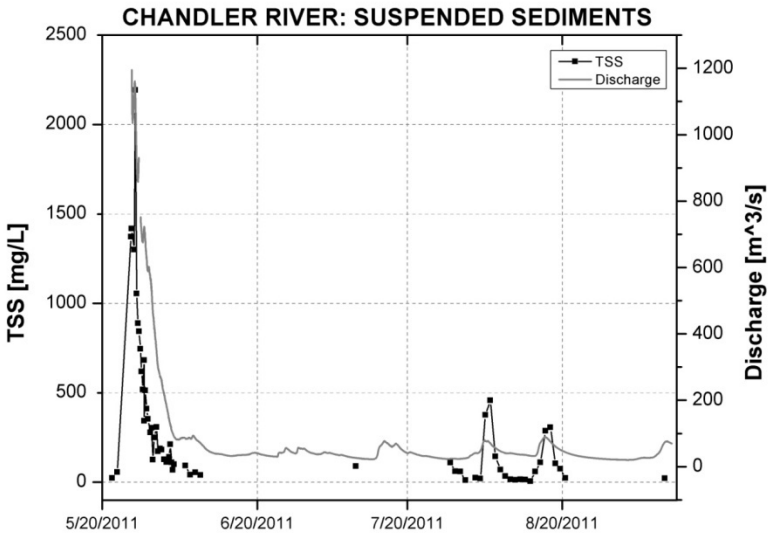

Figure 94. Suspended-sediment load and discharge for the Chandler River during the summer of 2011.

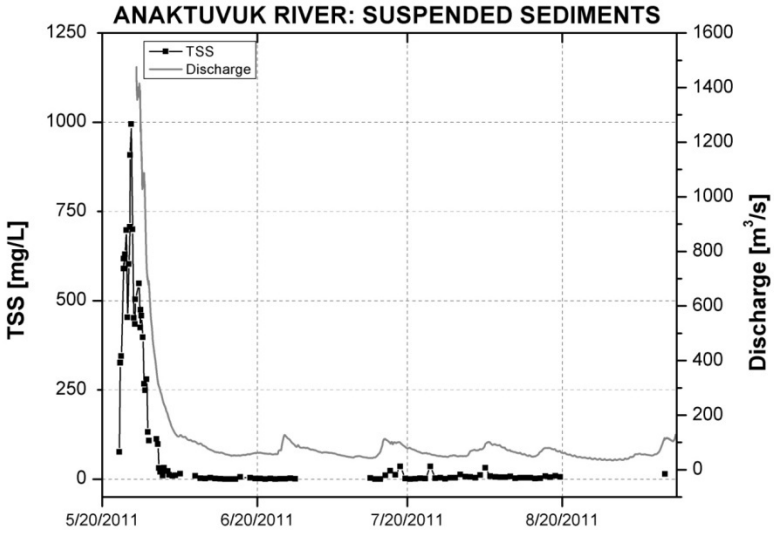

Figure 95. Suspended-sediment load and discharge for the Anaktuvuk River during the summer of 2011.

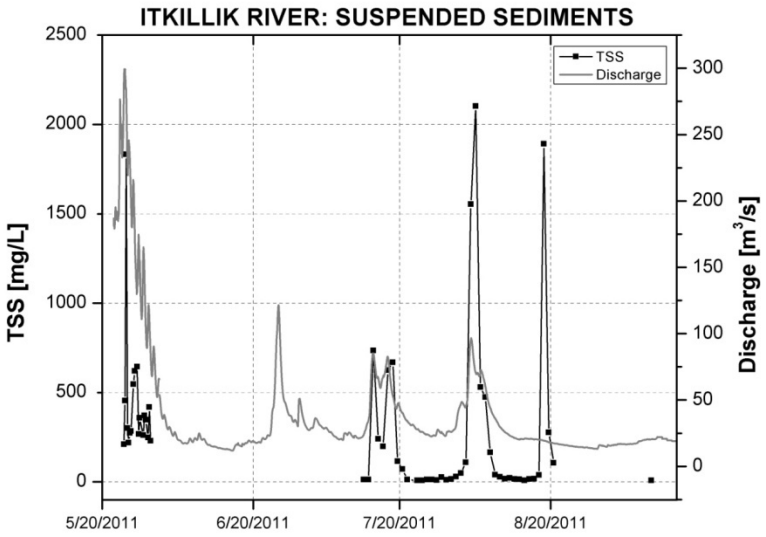

Figure 96. Suspended-sediment load and discharge for the Itkillik River during the summer of 2011.

Table 41. Summary of total suspended solids for the Chandler, Anaktuvuk, and Itkillik Rivers, 2011. Note that the TSS data sets (Figures 93, 94, and 95) are not continuous and there are large runoff events with no TSS measurements that potentially could produce a maximum or minimum value different from that shown in this table.

	Maximum TSS [mg/L]		Minimum TSS [mg/L]	
Chandler	2193	5/26/2011 15:00	5	8/13/2011 15:00
Anaktuvuk	1075	5/25/2011 13:40	0.01	6/4/2011 15:00
Itkillik	2019	8/5/2011 15:00	4	9/9/2011 16:15

On the Chandler and Anaktuvuk Rivers, the peak in suspended sediments came during the spring flood (see Table 41); on the Itkillik, however, the peak was during a flood event in early August. An explanation for this observation probably has to do with the Itkillik basin being smaller and the potential for rain events covering most of the basin. While TSS did rise in the Itkillik to a level of 1755 mg/L on May 24, 2011, the late summer event had a TSS 265 mg/L greater than in the spring, which is most likely related to characteristics of the watersheds. The Anaktuvuk and Chandler watersheds are considerably larger upstream of the gauging stations than the Itkillik, which also has a very narrow shape. As a result, the Anaktuvuk and Chandler Rivers generally did not respond to summer storms with the same magnitude of change as the Itkillik (in 2011), which experienced large increases in both discharge and TSS. Again, this is related to both the

shape and size of the basin and the areal extent of summer precipitation. Minimum values for TSS came at varying points throughout the summer; the lowest for the Chandler River was a value of 5 mg/L on August 13, 2011. On the Anaktuvuk River, the minimum value for TSS was essentially zero, a value that first occurred on June 4, 2011, but was seen multiple times throughout the summer. The Itkillik River had a minimum TSS value of 4 mg/L, which was measured on the last day of sampling, September 9, 2011.

Because the Isco sampler was located on the bed during break-up and then 15 cm (6 in.) above the bed throughout the rest of the summer, it is expected that the TSS values obtained from the Isco will vary from those of the depth-integrated sampler. On the Anaktuvuk River, the integrated samples had a higher TSS than the Isco during break-up, and then became approximately equal once the Isco intake was elevated off the riverbed. The differences ranged from 10 mg/L to almost 100 mg/L, with the difference becoming smaller later in the spring. On the Chandler River the opposite effect is seen, where the Isco samples exhibited a higher TSS than the integrated samples throughout the entire sampling period. The integrated samples had TSS values 5 mg/L to 50 mg/L lower than the Isco samples. No such comparison can be made on the Itkillik River, as depth-integrated samples were not taken on this river.

All samples from the Isco samplers and the integrated samples were analyzed to determine the organic content. On the Anaktuvuk River, the average organic content was 2.9%, with a maximum of 6.5% and a minimum of 0.2%. On the Chandler River, the average organic content was 3.7%, with a maximum of 9.2% and a minimum of 1.1%. Finally, on the Itkillik River, the average organic content was 2.9%, with a maximum of 5.7% and a minimum of 0.9%. There was no discernible pattern of when organic content would be highest in the samples.

One interesting feature that can be seen especially clearly in Figure 94 and Figure 95 is that TSS are initially very low and do not begin to increase until after the initial peak in discharge has occurred. The most likely reason for this observation on the Chandler and Anaktuvuk Rivers is that the channel is ice-covered, suppressing sediment transport until the ice has cleared. It is expected that the same pattern occurs on the Itkillik River; however, sampling began later on that river and so the pattern could not be detected. More investigation is needed to determine if this

scheme occurs annually on all three rivers, and if it is dependent on channel and watershed characteristics. It would also be expected that the suspended sediment rating curve (Figure 97) would appear quite different for the time period before the hydrograph peaks with the spring flood and after, due to this suppression of sediment transport by ice in the channel. Increased grab sampling during the rising limb of the hydrograph in the spring of 2012 will improve the suspended sediment rating curves.

As seen in Figure 94 through Figure 96, there is a lag between when discharge peaks and when sediment peaks throughout the summer. On the Chandler River, for the event that occurs on August 4, 2011, the discharge peaks approximately twenty-five hours before TSS peaks. On the Itkillik, this lag varies between fifteen minutes for the July 14, 2011, event and eighteen hours for the event on August 4, 2011. The Anaktuvuk River did not experience summer floods of the same magnitude as the Chandler and Itkillik Rivers. However, for the event that had a peak in discharge on July 18, 2011, there is a rise in TSS, which also occurs on July 18, 2011. Increased sampling frequency would be necessary to accurately determine the true lag time on all three rivers. Turbidity sensors would potentially be able to capture this lag (see Methods Section 3.10.2 for further discussion on turbidimeters) by taking readings at the same time interval as the pressure sensors.

The suspended sediment load carried by each river was strongly related to the discharge, as expected, except when ice was in the channel. A suspended-sediment transport rating curve was determined for the Anaktuvuk and Chandler Rivers using the integrated suspended-sediment samples; no integrated suspended-sediment samples were taken on the Itkillik River in the summer of 2011, but a rating curve will be produced for the summer of 2012.

Figure 97 clearly shows that at the same discharge the Chandler carries a larger suspended sediment load than the Anaktuvuk. The exponent of the power function is also larger for the Chandler, indicating that for the same increase in discharge, the Chandler will show a larger increase in TSS than the Anaktuvuk.

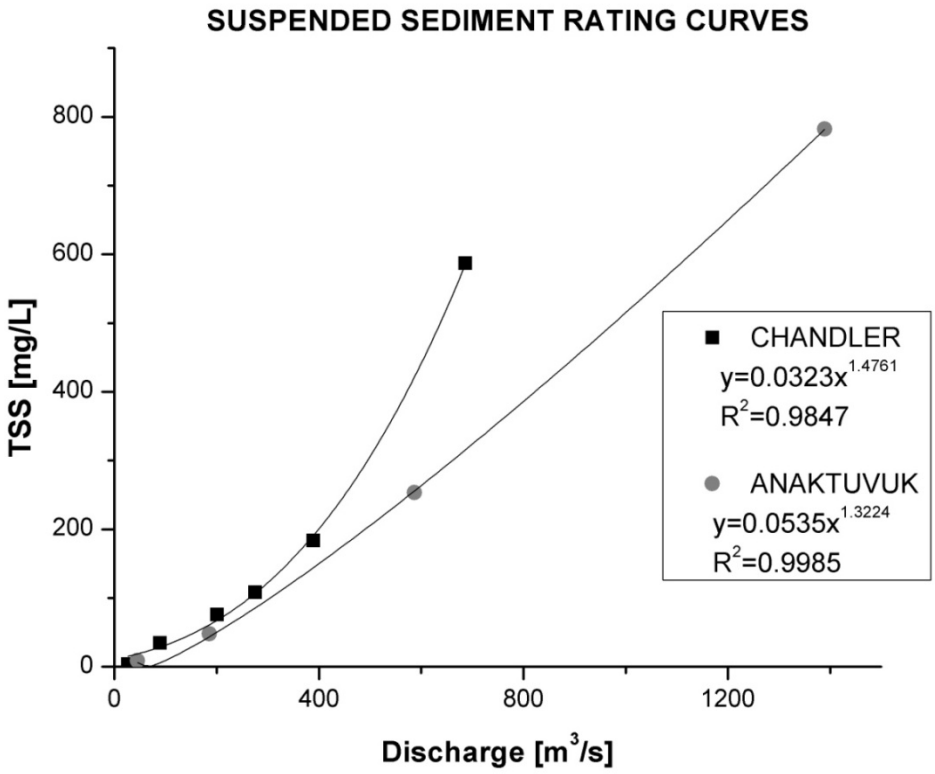

Figure 97. Rating curves of suspended sediments for the Chandler and Anaktuvuk Rivers for the period of May 25, 2011, through July 11, 2011.

4.11.2 Bed Sediment Distribution

Calculation of the bed sediment distribution in a river, and subsequent determination of the D_{50}, allows for the use of multiple equations to determine hydraulic parameters. Examples include calculation of the bankfull discharge, dimensionless bed shear stress, and Reynold's number (Parker *et al.* 2007). The ability to estimate these parameters increases our understanding of a river and its sediment transport regime.

Table 42. Bed sediment distribution by weight for the Chandler and Itkillik Rivers.

	% Finer by Weight		
Diameter [mm]	**Chandler [Coarse]**	**Chandler [Fine]**	**Itkillik**
7	0	0	0
9.5	4.5	0	0
13.5	10.0	3.9	2.0
19	18.7	11.8	8.2
27	33.1	49.9	16.8
38.4	55.1	76.2	29.9
54.5	72.2	93.0	44.2
77	90.1	97.7	56.5
109	98.5	100	72.1
154	100	100	88.6
218	100	100	96.3

Table 43. Bed sediment distribution for the Anaktuvuk River.

	% Finer by Weight
Diameter [mm]	**Anaktuvuk**
15.2	0
33.0	38.8
63.5	79.3
101.6	95.5
127.0	99.3

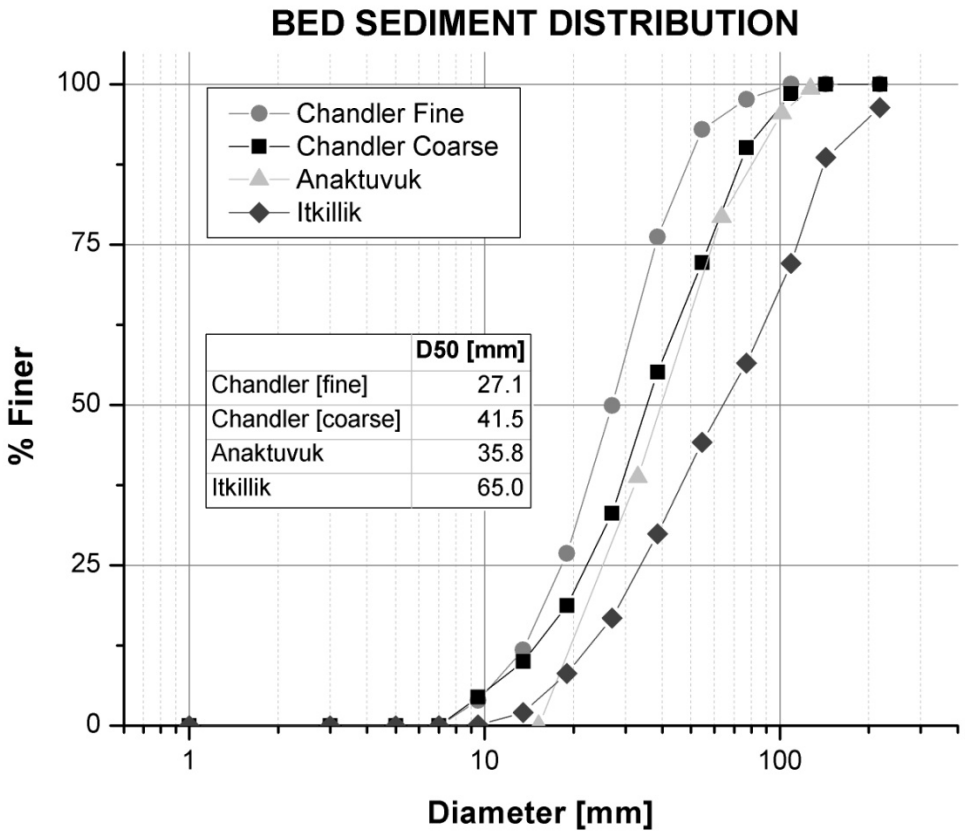

Figure 98. Bed sediment distribution for the Chandler, Itkillik, and Anaktuvuk Rivers. Bed sediment sampling was done at two locations in the Chandler River. Data indicates the variability of sediments in this river.

Looking at Figure 98, the Itkillik is the coarsest of all the rivers, with a D_{50} (65 mm) equivalent to very large gravel, almost small cobbles. On the Anaktuvuk, the D_{50} (35.8 mm) is also very large gravel, while on the Chandler it ranges between coarse gravel and very coarse gravel (27.1 to 41.5 mm). Two grids were measured on the Chandler; this was done due to the large variation in bed sediments that existed on the gravel bar chosen for study. It highlights the large spatial variation that occurs in sediment transport, even within relatively small regions, emphasizing the need for large data sets and increased sampling.

4.11.3 Turbidity

There is a large amount of “noise” in these graphs, and the results are not as clean as those of total suspended solids. This is due to organics and other matter building up on the optical

window of the turbidimeters, clouding the window and falsely raising turbidity. In fact, at times on the Chandler and Anaktuvuk Rivers, turbidity appears to increase while discharge is decreasing, and then decrease when discharge increases. This is the opposite result of what was found with the water samples analyzed in the lab. It appears that buildup on the optical windows happens during lower flows, and increases until flows are able to "clean" the window, thereby lowering the measured turbidity. This effect is not seen on the Itkillik to the same degree due to less organic debris in the river. As stated earlier, we plan to install wipers in the sensors in the spring of 2012. This should allow for more-accurate readings of turbidity. Figures 117 and 118 show the turbidity data for the Chandler and Itkillik Rivers; only data not affected by material on the optical window are shown.

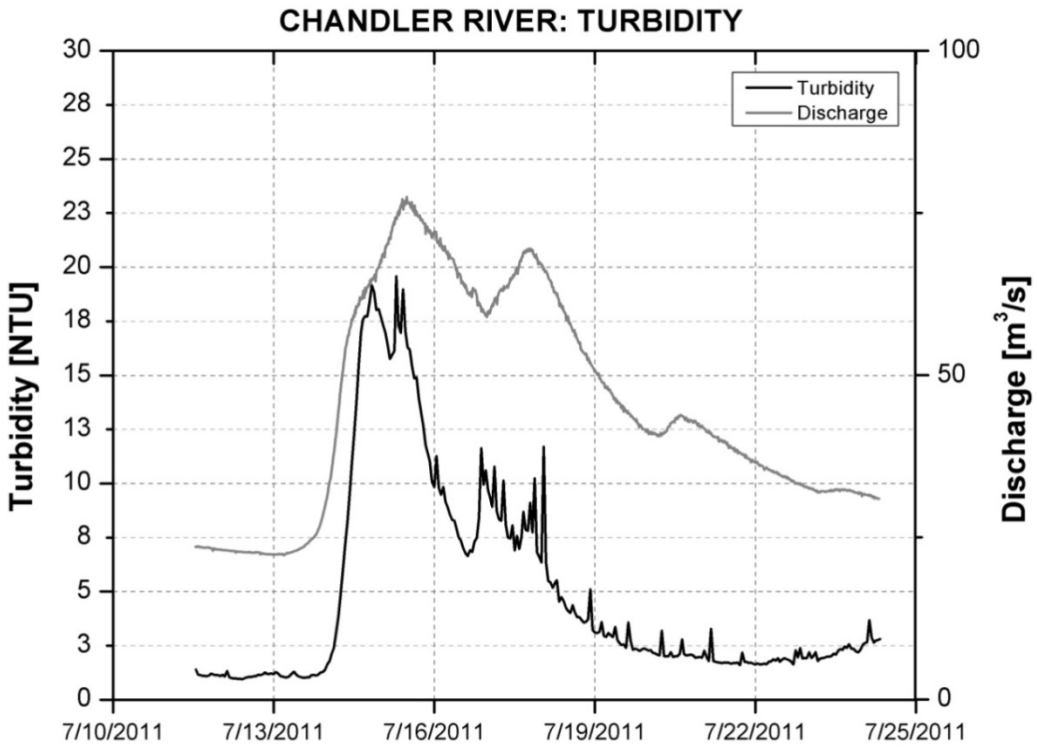

Figure 99. Chandler River turbidity, July 2011.

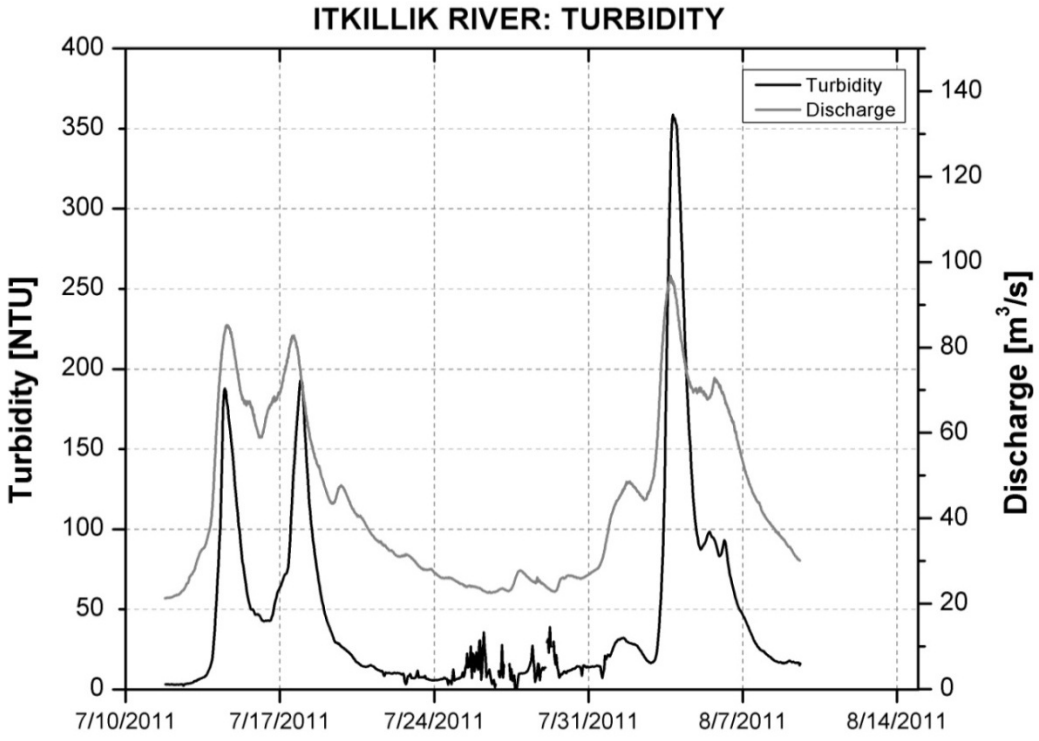

Figure 100. Itkillik River turbidity, July 2011.

4.11.4 Bedforms

Table 44 shows the temporal variation of steepness ratio in the Chandler River. Minimum, average, and maximum values are reported to represent the natural variability of bedforms in this river. The table indicates that the change in average values was approximately 350% in 4 days, which shows the river's capacity to adjust to different flow conditions.

A comparison of these values with the steepness values reported on the Tanana River near Nenana (Toniolo, under review) indicates that average values in the Chandler River are, in general, smaller than the average values in the Tanana River, indicating that form friction would play a smaller role on the total roughness coefficient in the Chandler River.

Table 44. Minimum, average, and maximum bedform steepness ratio for the Chandler River.

Date	Minimum	Average	Maximum
5/26/2011	0.004	0.008	0.016
5/28/2011	0.006	0.014	0.024
5/30/2011	0.009	0.013	0.021
5/31/2011	0.003	0.005	0.012
6/1/2011	0.002	0.004	0.006

4.12 Floodplain Surveys

In Fall 2011, floodplain surveys were conducted at the proposed bridge crossings for the Itkillik, Anaktuvuk, and Chandler Rivers. A Novatel Smart V1 GPS base station was set up at the crossing, and a Novatel Smart V1 rover GPS was used to walk across the floodplain in a single transect, collecting RTK DGPS horizontal and vertical GPS positions across it. Vegetation type and size was described and photographed along the transect. This section presents a summary of results for each transect in cross section. Geo-tagged photographs taken during the transect and more detailed vegetation field notes are available upon request.

4.12.1 Itkillik River

The Itkillik River floodplain survey, conducted on September 10, 2011, is indicated on the map in Figure 101. The transect is projected into a cross section in Figure 102. The main channel during nearly all flows is clearly delineated on the cross section with the river terrace at the crossing location. Vegetation in the floodplain (above the terraces) consists of areas of tussock tundra, sedges, and dense shrubs (particularly on the west side of the river near the crossing) between 0.25 and 2 m tall. Flow is confined to the main channel during all flows observed during the study period (Figure 103). The right bank (east side of the river) has a lower terrace than the left bank (west side of the river). During the spring 2011, water levels did not exceed the terrace on the right bank; however, signs of woody debris were visible above this terrace, indicating that previous floods probably exceeded this elevation. Woody debris is not visible above the left terrace, but historical channels are visible in the aerial photography and low-lying areas are observed in the field. At the proposed bridge-crossing location, the floodplain to the west of the

main channel is larger, with denser shrubs than the eastern floodplain. These features can be seen in the aerial image in Figure 101. The channel streambed in the vicinity of the proposed bridge crossing consists of sand, gravel, cobbles, and boulders, and is described in more detail in Section 4.11.2. Within the main channel, sparse shrubs 2–3 m tall are present (Figure 104). These tall shrubs are almost completely covered in flowing water at spring and summer flood stages. The estimated difference in water levels between annual low and high flow is approximately 2 m (6.6 ft).

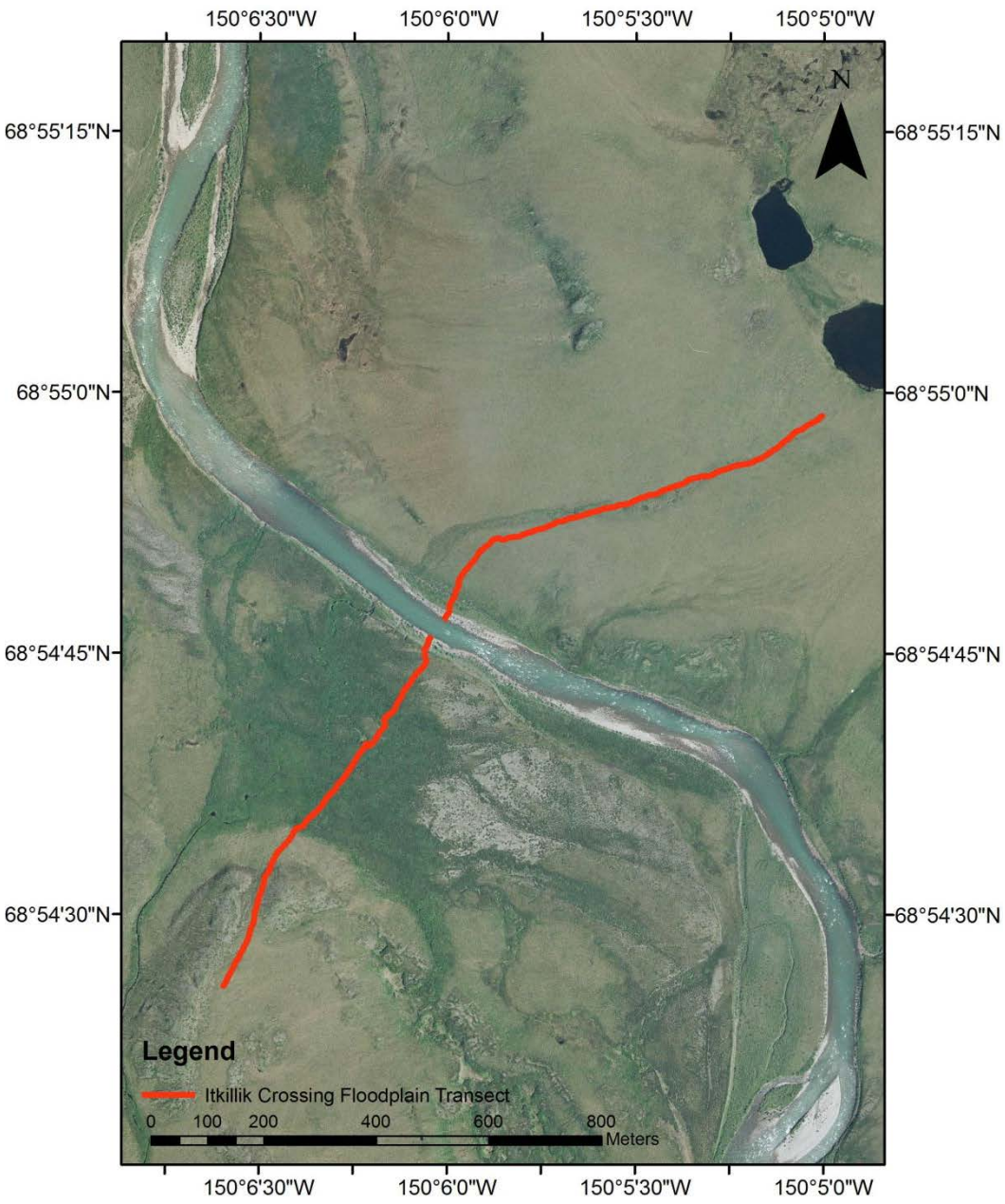

Figure 101. Itkillik River floodplain survey transect conducted on September 10, 2011. Transect location is at proposed bridge crossing, with the flow direction from the bottom to the top of the figure.

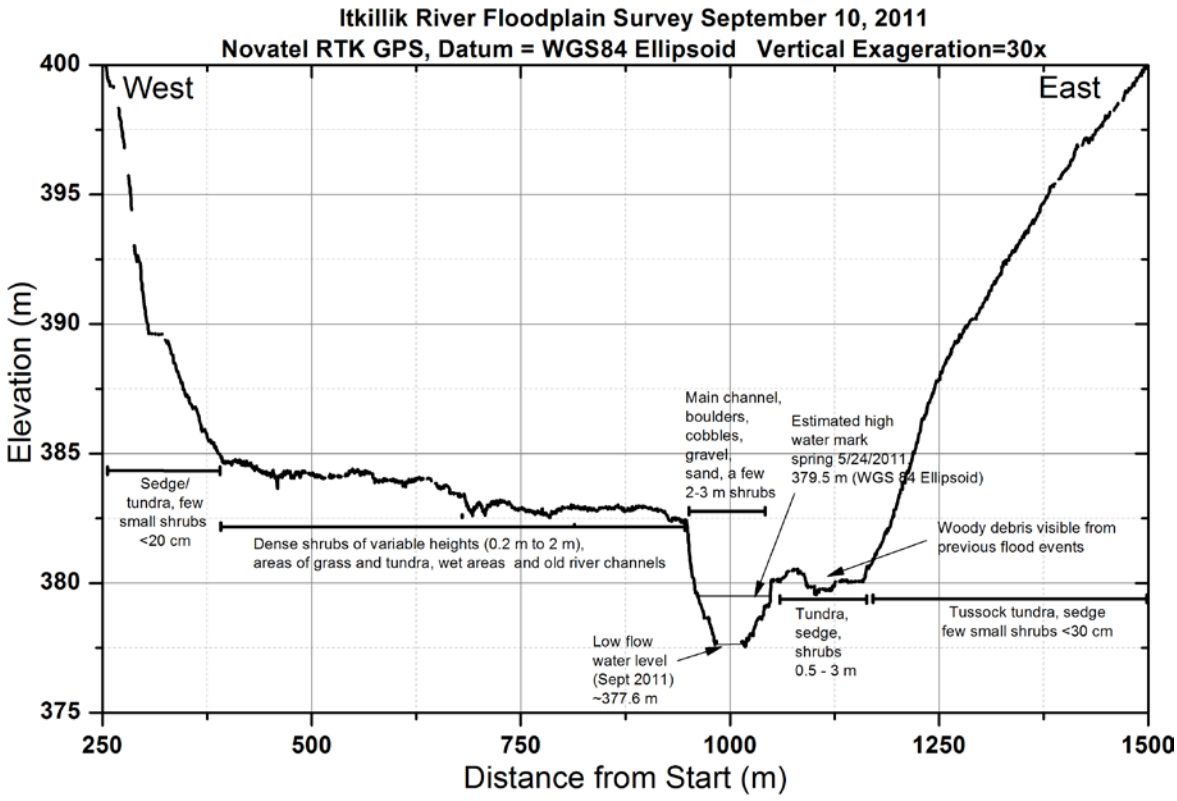

Figure 102. Itkillik River floodplain cross section looking downstream near the proposed stream crossing.

Figure 103. Photograph of the river at the Itkillik River proposed bridge crossing during higher flows on May 23, 2011 (facing south).

Figure 104. Photograph of Itkillik River main channel during low flows. Photograph taken on right bank looking downstream (~ north) showing shrubs 2–3 m in height and a sand, cobble, boulder bed.

4.12.2 Anaktuvuk River

The Anaktuvuk River floodplain survey, conducted on September 12, 2011, is shown on the map in (Figure 105). The transect is projected into a cross section shown in Figure 106. The Anaktuvuk River floodplain in the vicinity of the proposed bridge-crossing location is over 3 km (2 mi) wide. Vegetation within the floodplain consists of areas of tussock and sedge tundra, sparse and dense shrubs of 0.2 to 3 m height (as shown in Figure 107). The active channel consists of mostly sand and gravel, as discussed in Section 4.11.2. The active main river channel during flood stage is well over 500 m (1700 ft) wide, as observed in the photograph taken during high flow in Figure 108 and in aerial photographs. The main channel is braided during most flows, and gravel bar islands vegetated with shrubs are often visible. Flow may occur in multiple smaller side channels across the floodplain during periods of very high flow/stage. During spring 2011 runoff, a few vegetated islands remained free of flowing water, but most gravel bars were completely submerged (as shown in Figure 108) and flow was bankfull. During periods of summer low flows, the channel width may only be 50 m (106 ft) or less. The estimated water-level difference between annual low and high flows (at the proposed crossing) is over 2 m (6.6 ft).

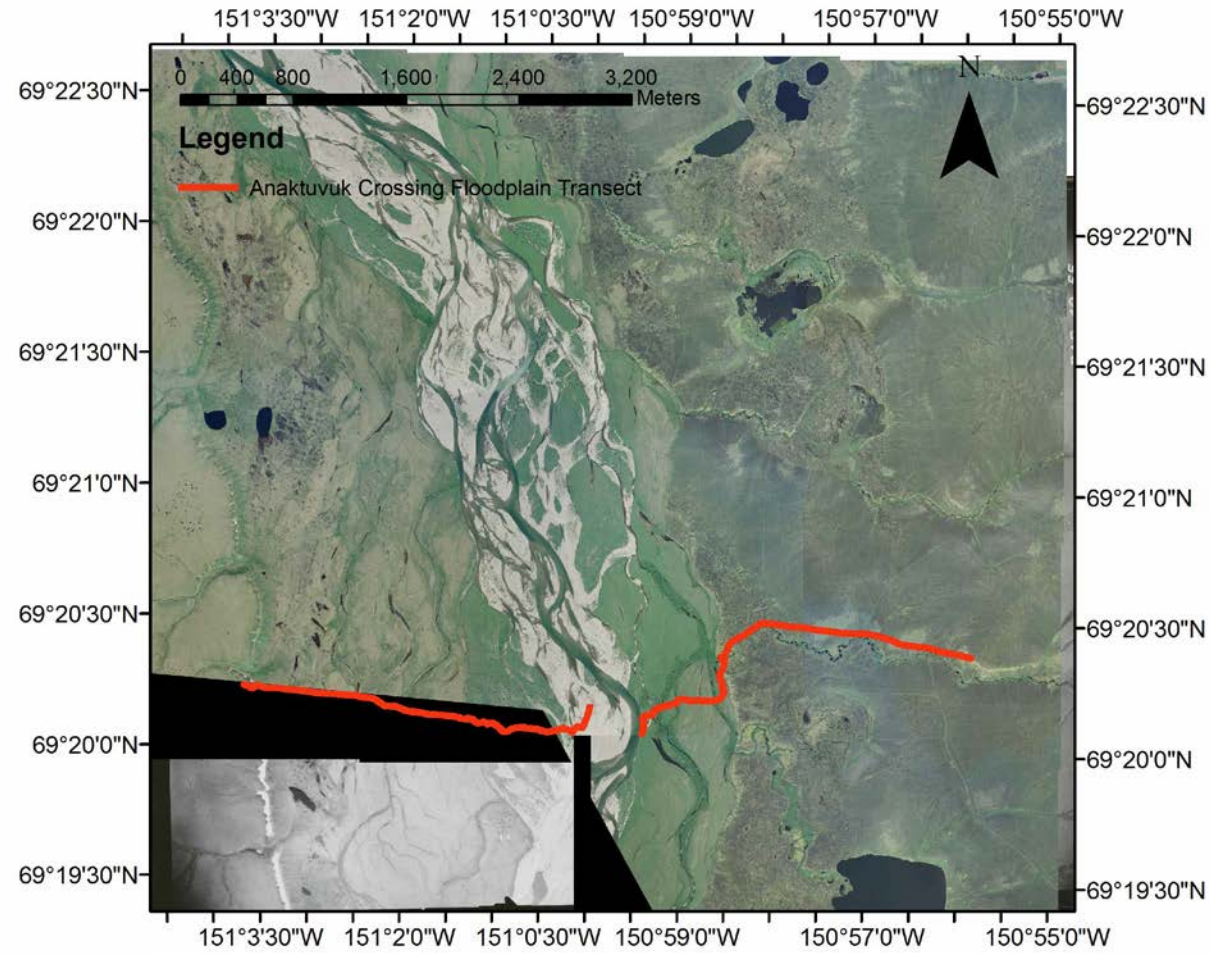

Figure 105. Anaktuvuk River floodplain survey transect. Transect location at proposed bridge crossing. Flow direction is from bottom to top of the figure.

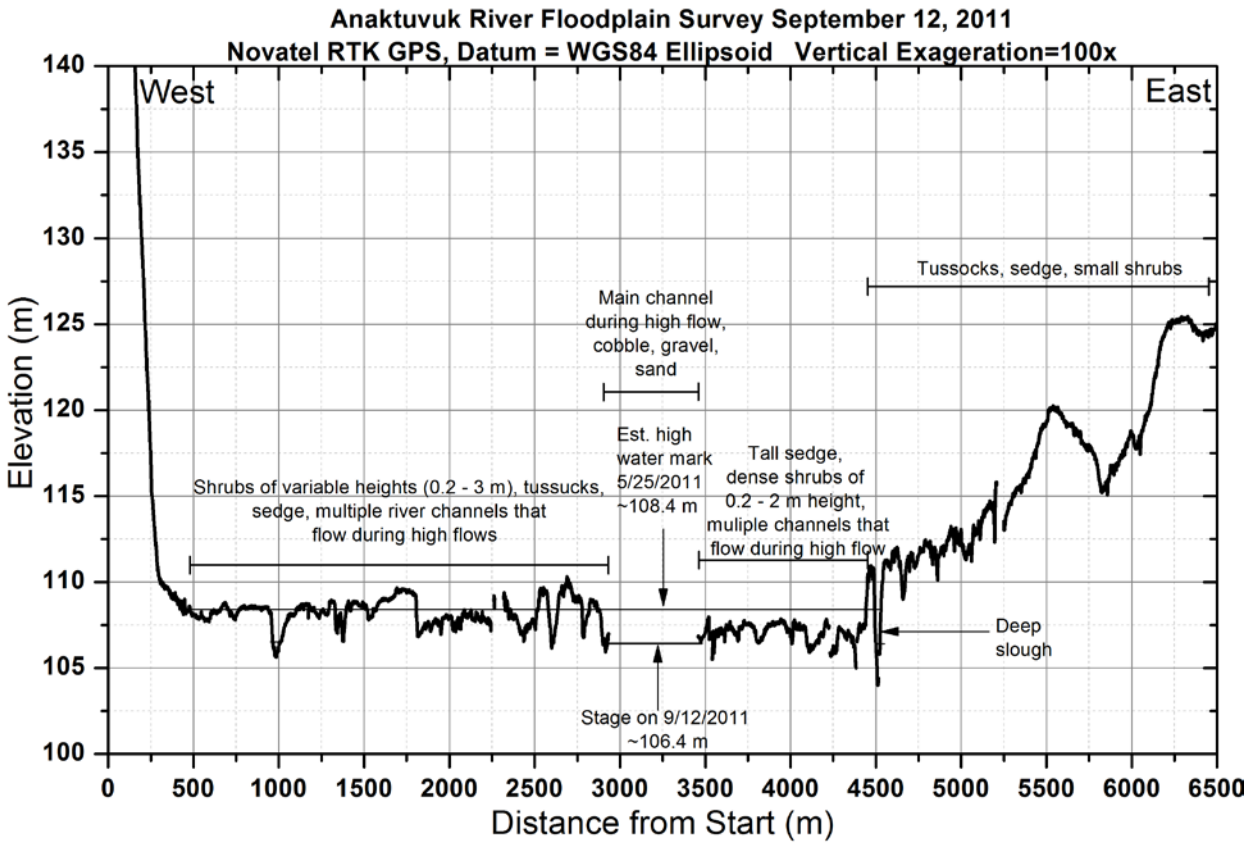

Figure 106. Anaktuvuk River floodplain cross section.

Figure 107. Tall shrubs over 3 m in height in the Anaktuvuk River floodplain.

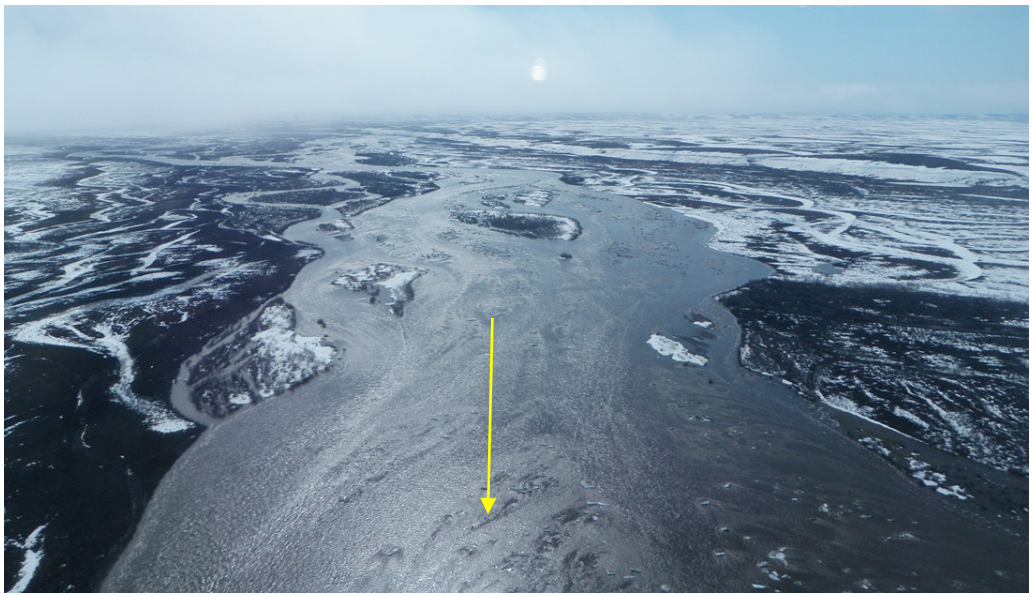

Figure 108. Photograph taken on May 26, 2011, of Anaktuvuk River during spring flood stage at proposed bridge crossing. Photograph taken facing south and yellow arrow indicates flow direction.

4.12.3 Chandler River

A floodplain survey near the proposed bridge crossing for the Chandler River was conducted on September 11, 2011, as shown on the map in Figure 109. The Chandler River floodplain in the vicinity of the crossing is over 3 km (2 mi) wide; a cross section is projected on Figure 110. Most of the flow is confined to a single channel over 300 m wide during high flows, but several side channels may also be flowing at the highest stages. Vegetation consists of sedge and tussock tundra and shrubs of variable height (up to ~3 m) and density. The riverbed sediments within the main channel consist of sand, gravel, and cobbles, and are further discussed in Section 4.11.2. Within the vicinity of the proposed bridge crossing, during higher flows there are two large channels upstream and to the south of the crossing (as observed in the photograph in Figure 111). During spring break-up, ice may accumulate on the inside bend (right/east bank) at the crossing area where the river depth is shallow. The floodplain on the eastern side of the river is lower in elevation and becomes over bankfull during high stages, as observed during spring 2011. During spring break-up in 2011, high water marks were observed over the left bank (west side) in the vicinity of the crossing. During lower flows, the river may be less than 60 m wide at the crossing.

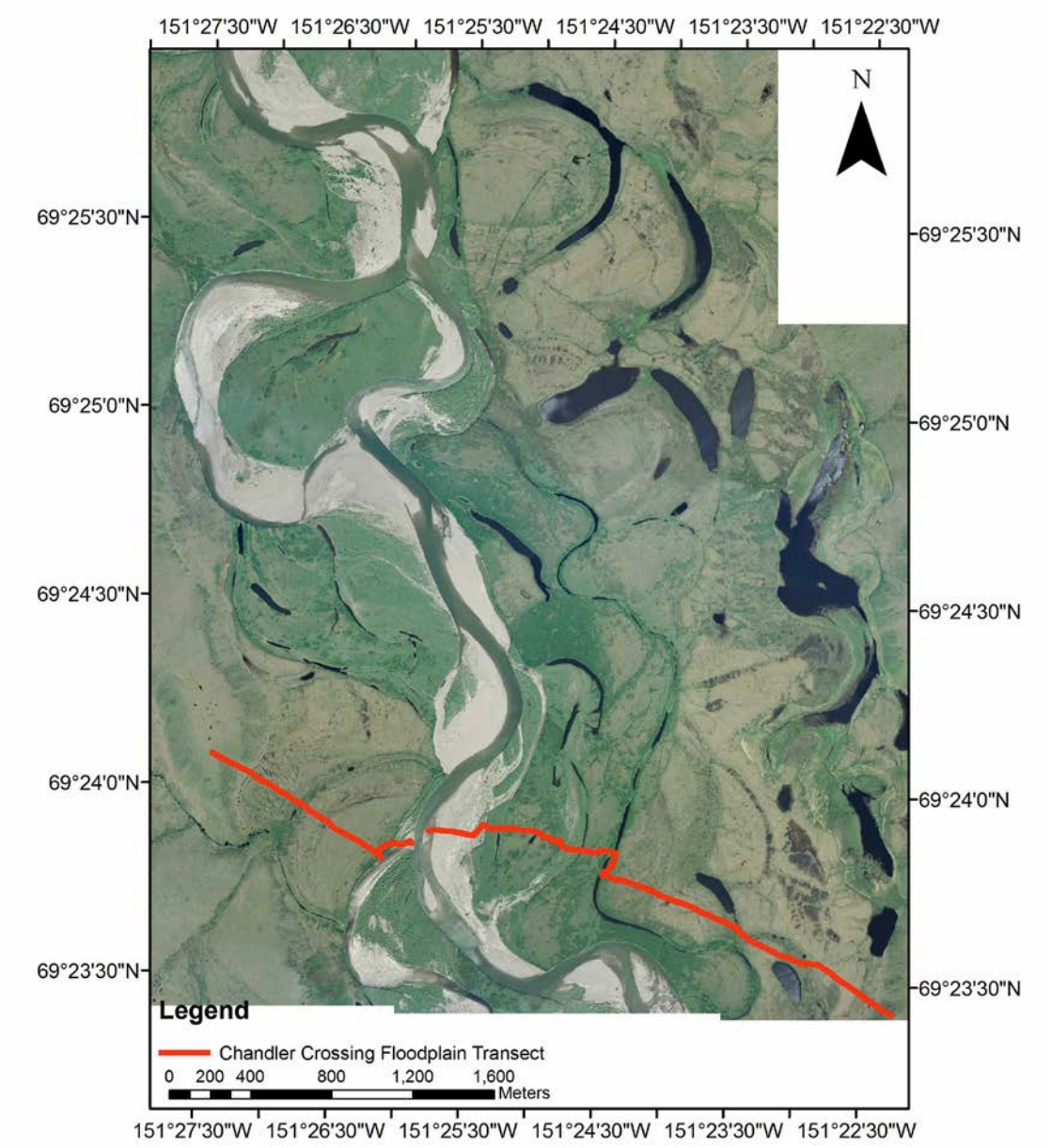

Figure 109. Chandler River floodplain survey transect. Transect location at proposed bridge crossing, with flow direction from the bottom to the top of the figure.

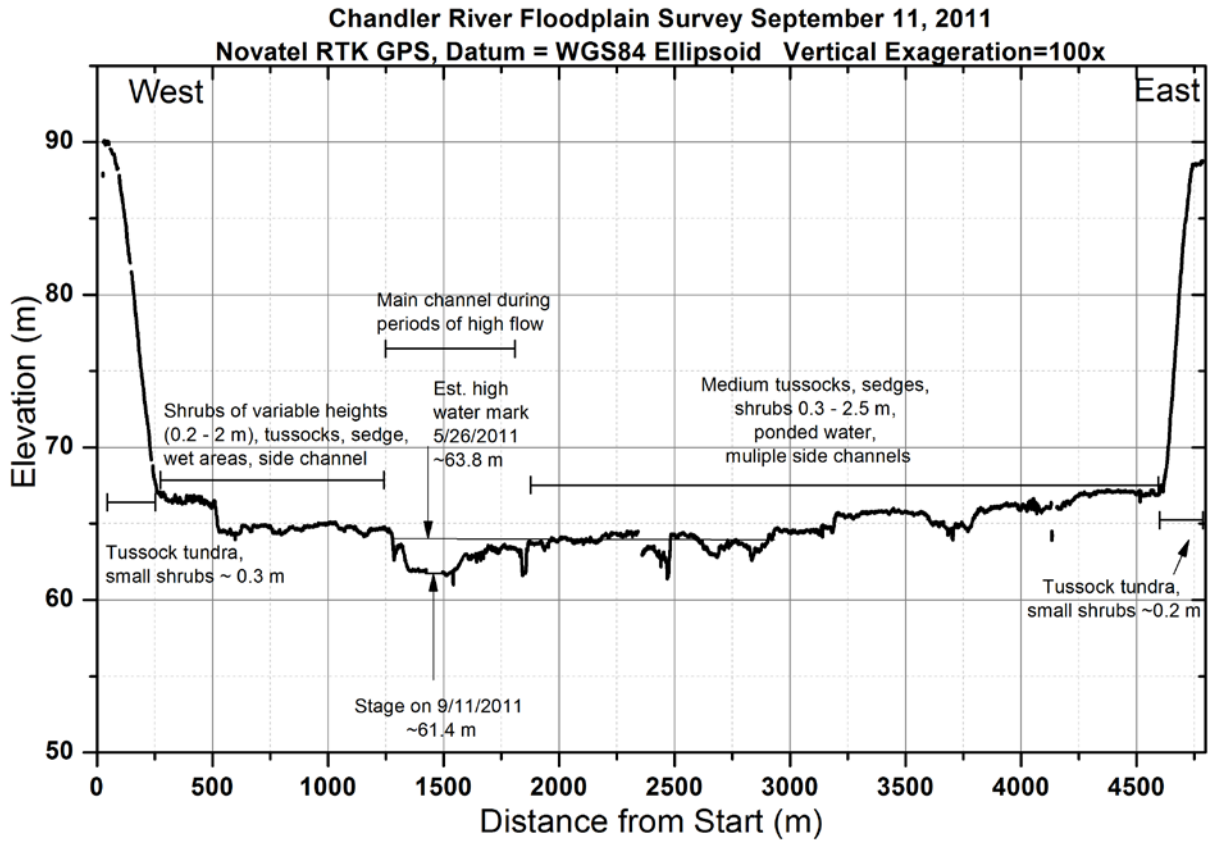

Figure 110. Chandler River floodplain cross section.

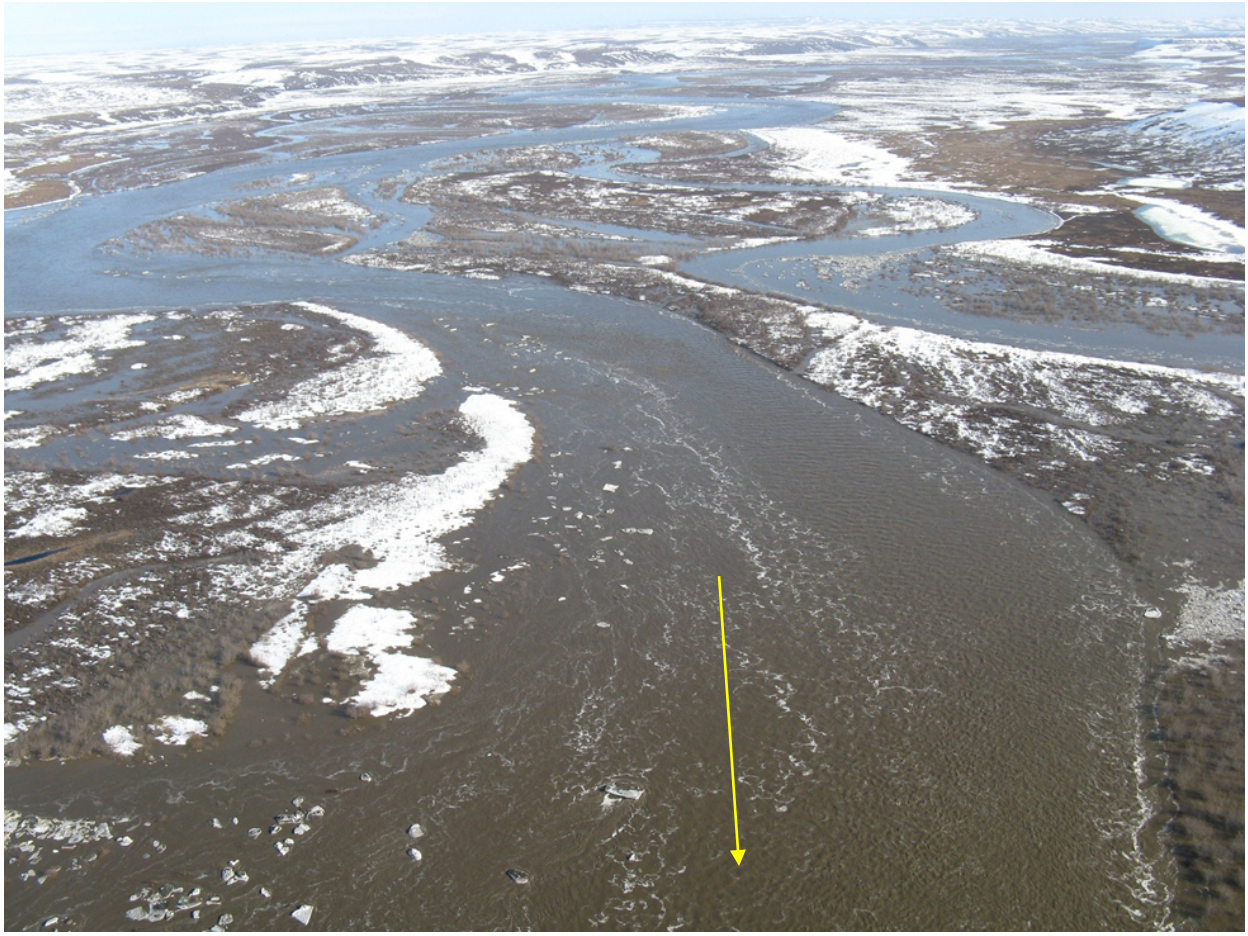

Figure 111. Chandler River on May 25, 2011, just south of the proposed bridge crossing (photograph taken toward the south) during the spring flood. Over-bank flow is visible, and significant flow occurs in side channels within the floodplain during very high stages.

4.13 North Slope Climatology

Alaska's Arctic Slope is a region that experiences large seasonal swings in net radiation and air temperature. The annual radiation balance totals a net loss (Polar Regions are the cooling engine for Earth). The imbalance in both hemispheres is compensated for by energy transferred northward and southward toward the poles by the oceans and atmosphere (Hinzman and Kane, 1992). The hydrologic cycle of cold regions is dominated by latent heat fluxes (i.e., sublimation, snowmelt, condensation, evaporation, transpiration, soil freezing and thawing, and formation and decay of rivers and lake ice). Wind is an important meteorological factor, too, in terms of its

redistribution of snow and its influence on sublimation in winter and evapotranspiration in summer.

Approximately 40% of the annual total precipitation is in the form of snow (Kane et al., 2008b) that accumulates over the eight- to nine-month-long cold season, which is accompanied by sub-freezing conditions that prevent mid-winter melt. Thus, snow is stored in the catchments until major hydrologic activity occurs over a three- to four-month-long warm season that begins with snowpack ablation (Benson et al., 1986). Snowmelt runoff often results in the largest stream discharge event of the year. However, floods of record for these watersheds can be either rainfall- or snowmelt-generated. The large north-draining river basins tend to have floods of record that are snowmelt-generated (like the Kuparuk and Colville River basins); this is also true for smaller low-gradient catchments along the coast (like the Putuligayuk River watershed). For smaller headwater streams, like the Upper Kuparuk River, floods of record are generally rainfall floods, because the spatial coverage of these storms results in rainfall over the entire basin.

Snow insulates and limits the transfer of heat between the atmosphere and ground (Stieglitz et al., 2003), directly influencing the timing and the rate of freezeback of the active layer. The soil moisture deficit at summer's end is a crucial component in the hydrologic cycle and influences the timing and amount of runoff during snow ablation the following spring.

Permafrost underlying the active layer is susceptible to long-term climate-warming trends, which may result in greater soil-water storage and greater downslope drainage, consequently changing the hydrologic response (Hinzman and Kane, 1992). The complex interrelationship of hydro-climatic variables results in considerable year-to-year variability in thermal and hydrologic processes.

4.13.1 Regional Climate Summary

The Arctic climate, combined with the topography difference from the inland Mountain region (2675 m, 8025 ft) to the Arctic Ocean, creates distinct physiographic regions. Because of orographic influences, the Mountain and Foothills regions receive substantially more summer precipitation than the Coastal Plain. For every 1 cm of precipitation on the Coastal Plain, there is

on average almost 2 cm in the Foothills region and 3 cm in the Mountain region. The Mountain region typically receives slightly less (or similar) solid precipitation during the winter season as both the Coastal Plain and Foothills regions. Logistically, it is challenging to make measurements of the snowpack in the Mountain environment. Most measurements in the Mountain region are made in valley bottoms; some are made on the few high flat spots where a helicopter can land. The Mountain region has warmer air temperatures during the winter months than both the Foothills and Coastal Plain regions and cooler temperatures than the Foothills region during summer. Adiabatic conditions, plus distance from the Beaufort Sea, result in the highest summer temperatures in the Foothills. Due to winter inversions, the Mountain and higher elevation Foothills areas do not experience the average extremely low temperatures of stations on the Coastal Plain. Low-lying stations on the Coastal Plain and valley bottoms in the Foothills region are prone to the coldest temperatures. From east to west along the coast, temperatures stay similar. Wind speed and direction is more variable at the Mountain stations, likely due to topographic channeling of winds and placement of the station (i.e., valley orientation). Wind directions in the Foothills region are mostly from the southwest and northeast. High winds occur more frequently along the Coastal Plain throughout the year and are the highest on average for the study area. The high-wind direction on the Coastal Plain is predominantly from the east-northeast.

Data from several long-term UAF/WERC-operated data collection stations can be compared with recent data collected in the Bullen, Kuparuk Foothills, and Umiat projects. The long-term stations include Imnavait, Upper Kuparuk, Sagwon Hill, West Kuparuk, Franklin Bluffs, Betty Pingo, and West Dock stations—all located in or near the Kuparuk basin. Examination of a long-term historical record is useful for understanding the range of possible hydrologic conditions that may be encountered in the study area. A summary of temperature, wind, and snow-cover data for the Kuparuk River basin for the five-year period spanning 1994 to 1998 can be found in Olsson et al. (2002).

4.13.2 Summer Precipitation

According to the historical summer precipitation records at Imnavait, Sagwon Hill, and Betty Pingo, most summer precipitation occurs in either July or August (occasionally June and

September are the wettest months). Understanding summer precipitation during the fall (August and early September) is useful for predicting what could happen during the following spring runoff period. For example, a dry August causing dry soils going into freeze-up will result in an increase in soil-moisture storage during spring snowmelt and less spring runoff, because soil-deficit storage must be satisfied first (fall 2007/spring 2008 is a good example) . Alternatively, a wet fall, which is common, may result in decreased subsurface storage the following spring, causing more spring runoff during snowmelt.

The average summer precipitation at Imnavait is approximately 205 mm (n=26), but there is considerable year-to-year variation, from 50 mm up to nearly 350 mm. Figure 112 shows the range of summer precipitation for the period of record at Imnavait Creek. The lowest recorded cumulative summer precipitation is in 2005 (~54 mm); the highest is in 1999 (~340 mm) at Imnavait basin. Figure 113 shows the monthly summer precipitation for each year. Historically, most of the summer precipitation at Imnavait station falls in July, followed by August and June. Both May and September are prone to receiving solid precipitation, which is not measured by our continuous recording gauges.

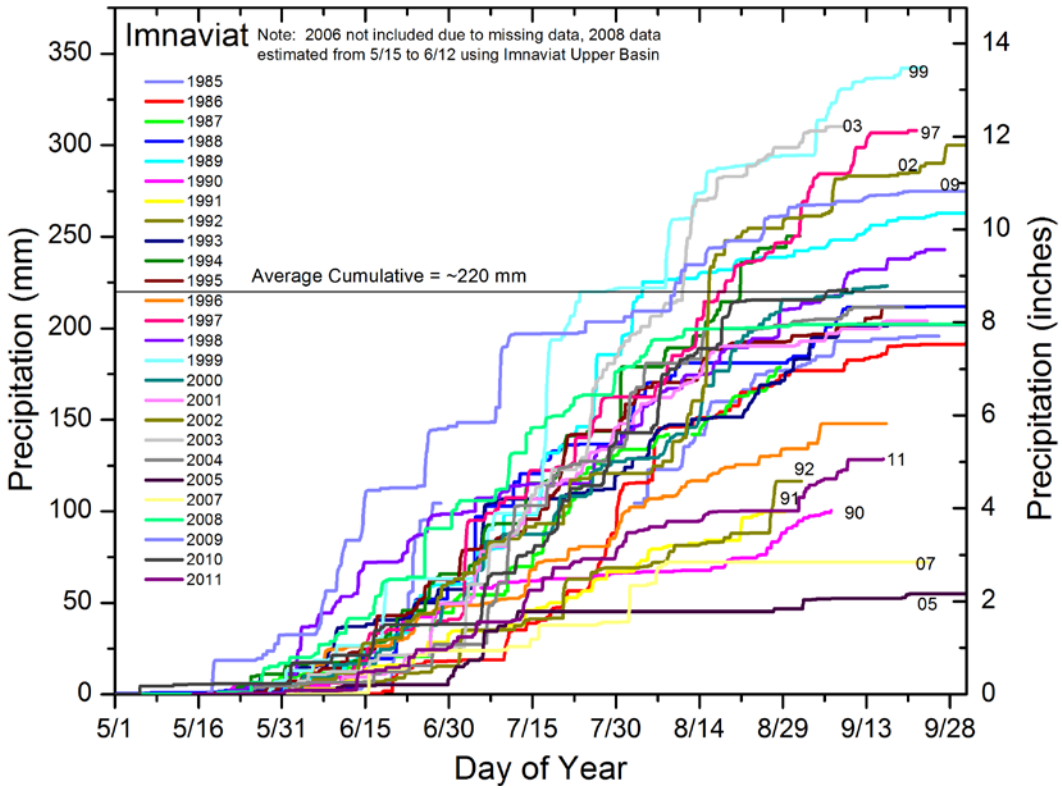

Figure 112. Historical summer cumulative precipitation at Imnavait Creek station, 1985–2011 during the warm season. The lowest cumulative summer precipitation in the record occurred in 2005 and 2007, while the highest was in 1999. Note: 2006 is missing.

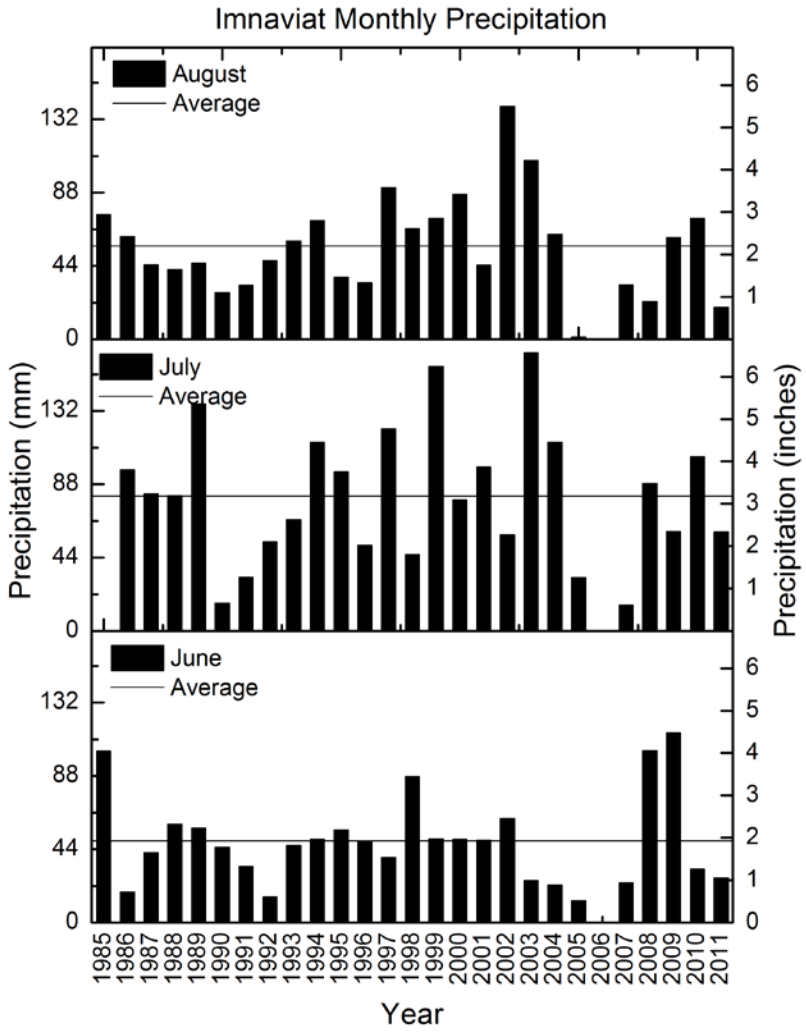

Figure 113. Historical monthly and monthly long-term average summer precipitation at Imnavait Creek catchment (1985 to 2011).

At Sagwon Hill, located in the Foothills region, the average cumulative precipitation is 116 cm (*n*=24) and ranges from 25 mm up to 155 mm. The cumulative summer precipitation at Sagwon Hill was highest in 2002 (155 mm), 2003 (151 mm), and 2006 (152 mm), and lowest in 2007 (27 mm; Figure 114). Figure 115 shows that most of the monthly summer precipitation falls in July and August at Sagwon Hill, with the monthly average for August the highest and July next highest.

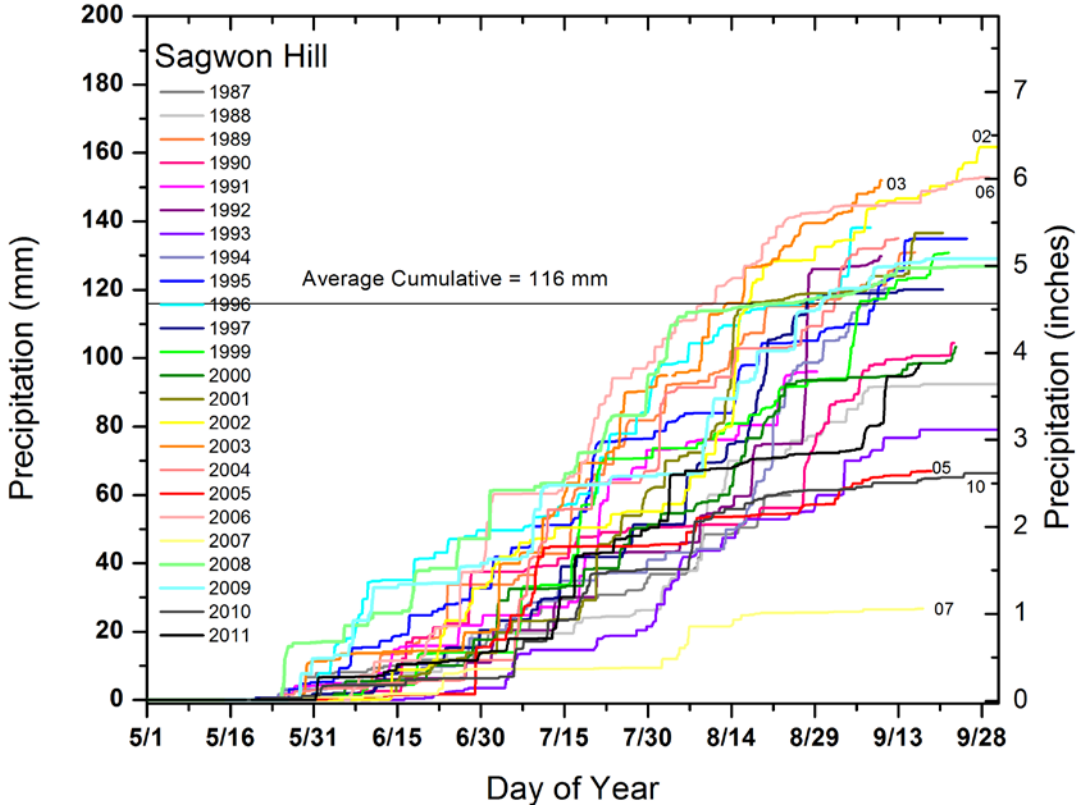

Figure 114. Historical summer cumulative precipitation at Sagwon Hill. Two of the lowest recorded cumulative summer precipitation amounts occurred in 2007 and 2010.

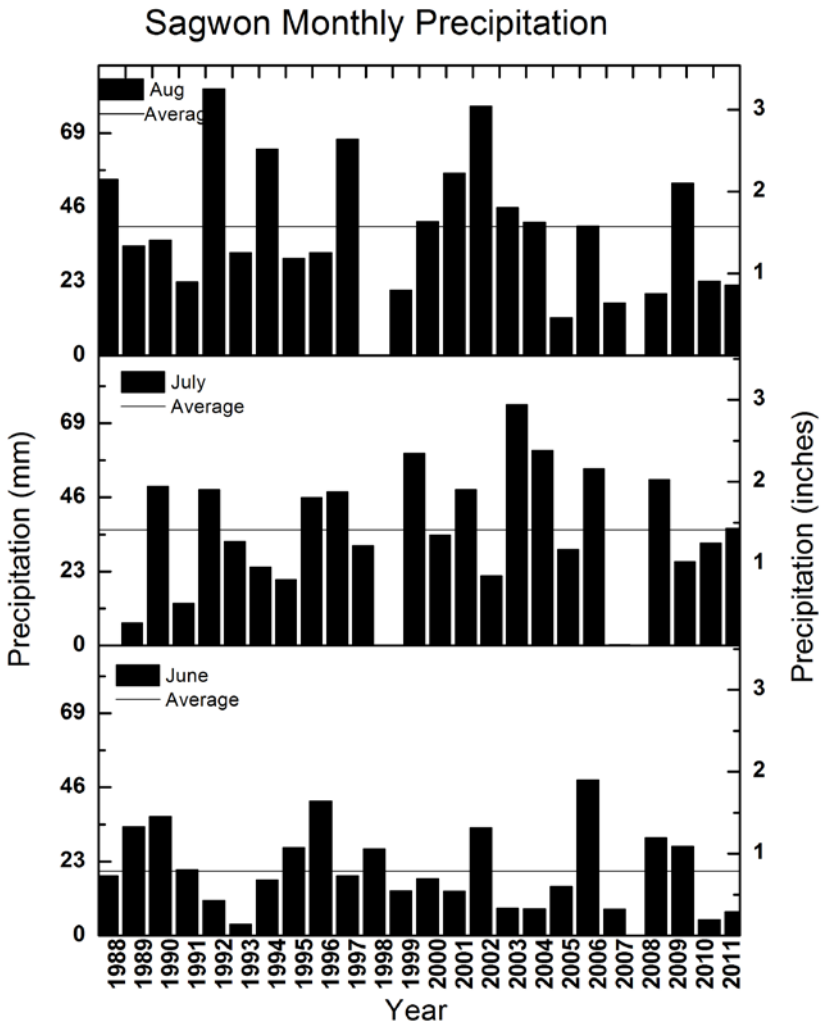

Figure 115. Historical monthly and long-term monthly average summer precipitation at Sagwon Hill (1988 to 2011).

The average cumulative precipitation at Betty Pingo, located on the Coastal Plain, is 82 mm (*n*=13) and ranges from 15 mm up to 140 mm (Figure 116). The years 1999 and 2002 were particularly rainy years at Betty Pingo. The lowest recorded precipitation at Betty Pingo was in 2007 (15 mm). Similar to Sagwon Hill, most summer precipitation falls in July and August at Betty Pingo, as shown in Figure 117; June is a rather dry month.

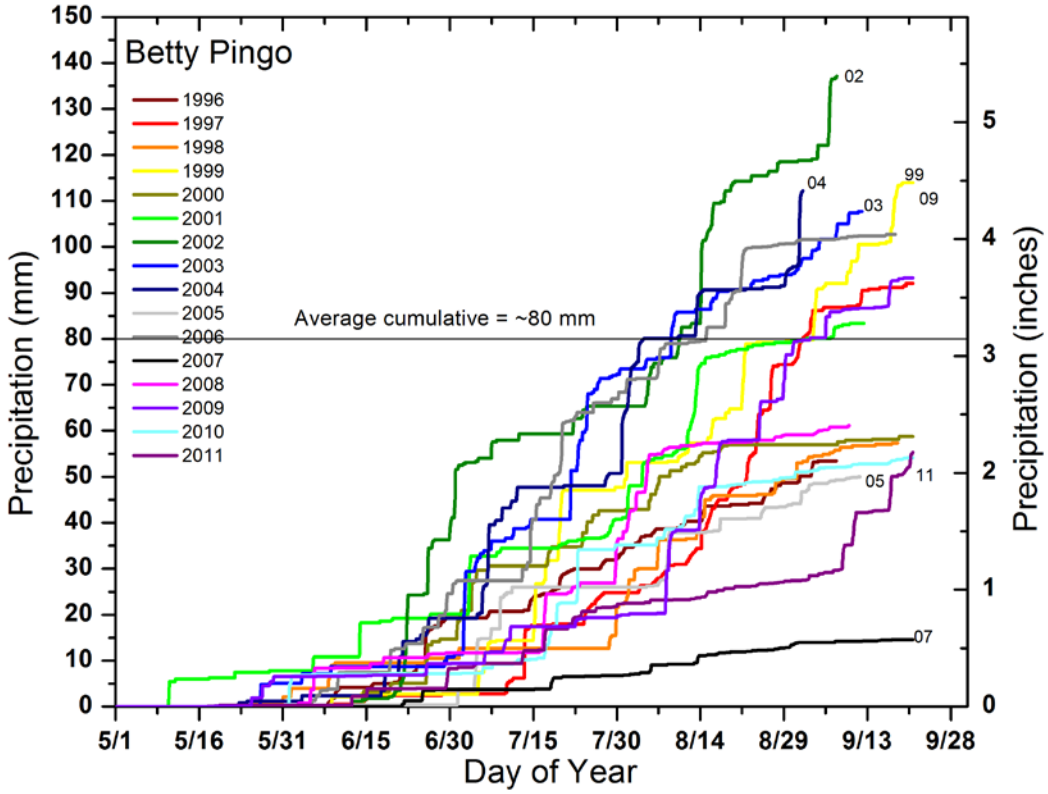

Figure 116. Historical summer cumulative precipitation at Betty Pingo, 1996–2011. Betty Pingo received less than 20 mm of summer precipitation in 2007, while in 2002, 140 mm of rain fell.

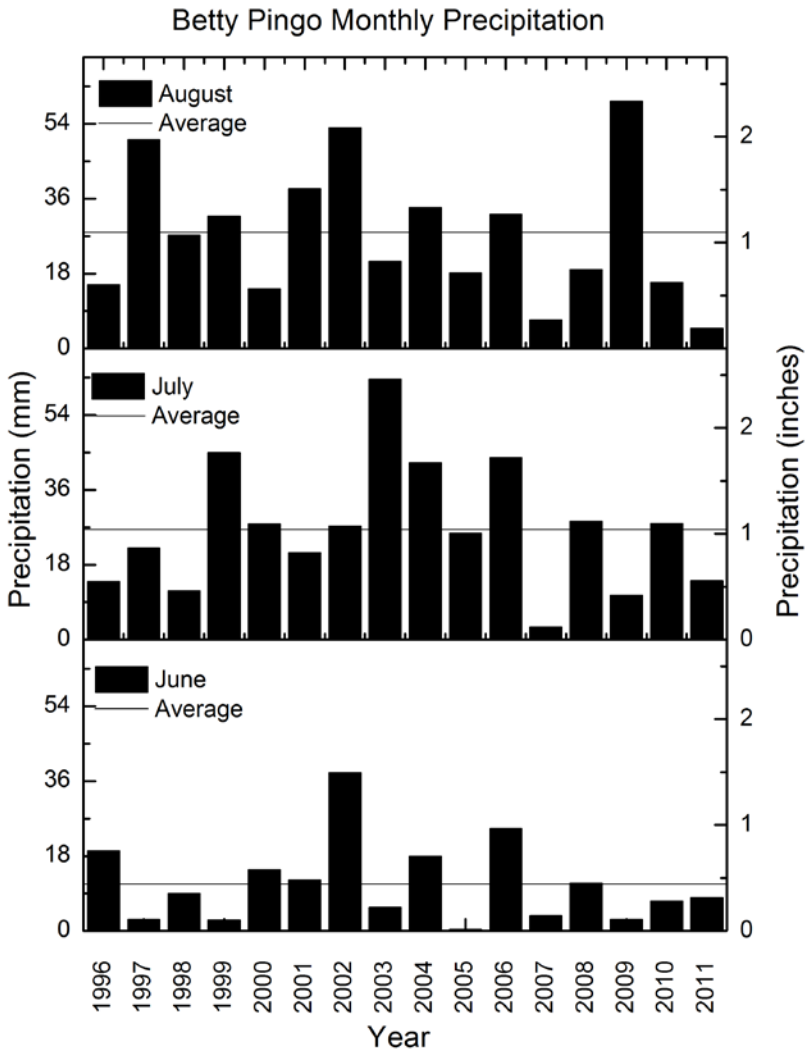

Figure 117. Historical monthly summer precipitation at Betty Pingo, 1996–2011.

All data collected at the newer Bullen, Kuparuk Foothills, and Umiat project stations were presented in Section 4.4. Data collection began in mid-summer 2006, so cumulative summer precipitation is not available for the new stations that year. Data from other long-term UAF/WERC-operated monitoring stations indicate that the 2006 cumulative rainfall was above average. In 2007, record-low precipitation was measured at all long-term stations throughout the study areas, except Imnavait (where it was the next lowest year, 72 mm versus 54 mm in 2005). The long-term Betty Pingo station recorded only 15 mm of precipitation over the 2007 summer, while the Lower Kadleroshilik station had 16 mm. It is reasonable to assume that all regions of the study area experienced record low 2007 precipitation. In 2008, summer precipitation was

average or slightly below average at most long-term stations. Rainfall was generally above average in 2009, with June being an unusually rainy month resulting in high runoff events in many rivers. The years 2010 and 2011 were below average for total rainfall at Betty Pingo and Sagwon Hill.

The timing of precipitation during the summers of 2007 and 2008 was different from the historical pattern of the majority of summer precipitation occurring in July and/or August. In both 2007 and 2008, August was relatively dry. Runoff response to summer precipitation is most important in the Mountain region, where the hydraulic gradients are steeper and more precipitation falls. In the Coastal Plain region, little runoff response is seen in the hydrograph from summer precipitation (partially because of low hydraulic gradients, substantial potential storage in lakes, ponds and wetlands, and generally the lowest amounts of summer precipitation).

4.13.3 Snow Water Equivalent

The Anaktuvuk and Itkillik River basins have 3 years of repeated snow survey data: 2009, 2010, and 2011. Snow survey observations in the Chandler River basin were initiated in 2010. The Sagavanirktok, Kadleroshilik, Shaviovik, and Kavik River basins had 5 years of repeated snow survey data, from 2006 to 2010. The Kuparuk, Sagavanirktok, and Putuligayuk River watersheds have snow survey data for each year from 2006 to 2011. Our snow observations show that in 2006 and 2008, the end-of-winter SWE was below average in these watersheds. In 2007, areal SWE initially appeared to be below average, but a large storm with strong winds followed by significant snowfall occurred in late spring, resulting in approximately normal SWE for the end of winter. In 2008, end-of-winter SWE was below normal; the lowest was found in the Mountain region, where many snow course sites were completely devoid of snow. The highest end-of-winter SWE was observed in 2009 and 2011.

4.13.4 Air Temperature

Air temperature data collected at Bullen, Kuparuk Foothills, and Umiat Corridor stations (2006 through 2011) were compared with the long-term historical averages from long-term stations.

Air temperature data are presented in Figure 118 through Figure 123 for the long-term stations on a north–south transect in the Kuparuk River basin.

Based on the historical data records, Betty Pingo (*n*=15) and West Kuparuk (*n*=15) have the coldest temperatures in winter, followed by Franklin Bluffs (*n*=22), Sagwon Hill (*n*=22), and Imnavait (*n*=23). Generally, temperatures are colder in the north and warmer to the south (Figure 118). During summer, the Foothills stations (Sagwon Hill, West Kuparuk) report the warmest temperatures. The next warmest summer temperatures are recorded at Franklin Bluffs (located on the Coastal Plain, slightly north of the Foothills region), followed by Imnavait (located at the border of the Foothills and Mountain region), and finally by Betty Pingo on the northern Coastal Plain. Interestingly, West Kuparuk station, located near the western boundary of the Kuparuk basin and at a similar latitude as Sagwon Hill station, reports some of the coldest temperatures in winter and warmest temperatures in summer. This is due, in large part, to the difference in elevation between the two sites. West Kuparuk station is lower in elevation (159 m, 522 ft) and located on a low ridge adjacent to the Kuparuk River (140 m, 458 ft). Sagwon Hill is located near the top of a hill (275 m, 902 ft) above the nearby Sagavanirktok River (183 m, 600 ft). The greatest temperature difference between the two stations occurs during winter. In autumn, all stations experience similar temperatures.

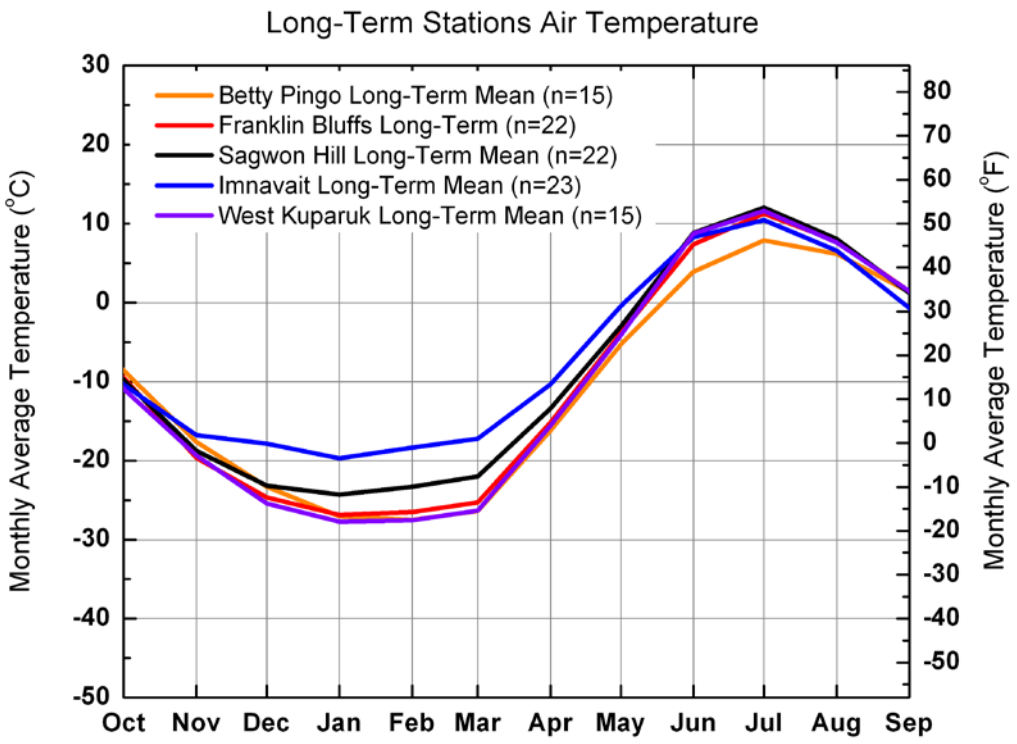

Figure 118. Comparison of monthly average air temperature for period of record for Betty Pingo (Coastal Plain), Franklin Bluffs (Coastal Plain), Sagwon Hill (northern edge of Foothills), Imnavait (border of Foothills and Mountain regions), and West Kuparuk (northern edge of Foothills) stations.

Summer air temperatures tended to be similar to the long-term average temperatures at all stations (Figure 119 through Figure 123). Winter temperatures differed from the long-term mean. Early to mid winter 2006-2007 temperatures were near normal or slightly above normal across the study area, and late winter 2006-2007 temperatures were below normal. Mid to late winter 2007-2008 temperatures were well below normal. Winter 2008-2009 air temperatures were also warmer than normal in early winter and colder than normal in late winter. Winter 2009-2010 was slightly warmer than normal near the coast (Betty Pingo and Franklin Bluffs). Sagwon Hill and Imnavait temperatures were warmer early and cooler later in the 2009-2010 winter season. Warmer than average temperatures occurred in the winter of 2010-2011. In general, however, the last few years have been normal from a temperature viewpoint.

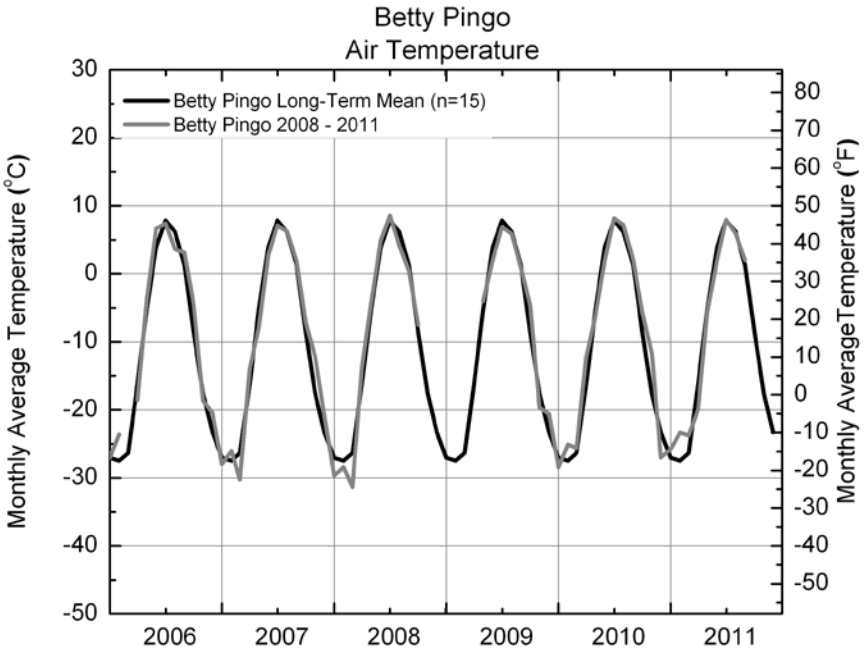

Figure 119. Comparison of Betty Pingo monthly average for period of record with Betty Pingo from 2006 to September 2011.

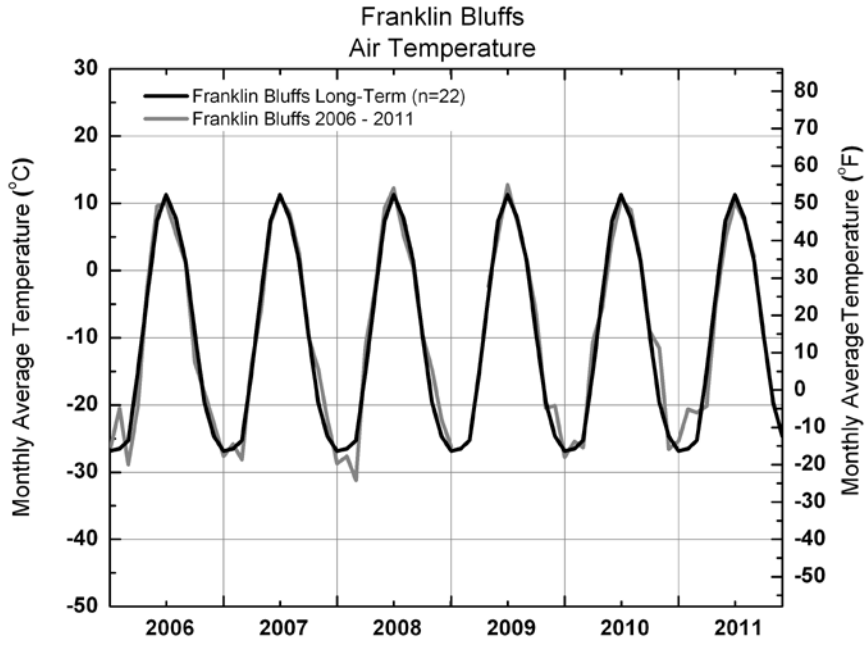

Figure 120. Comparison of Franklin Bluffs (Coastal Plain) station monthly average for period of record with monthly average from 2006 to September 2011.

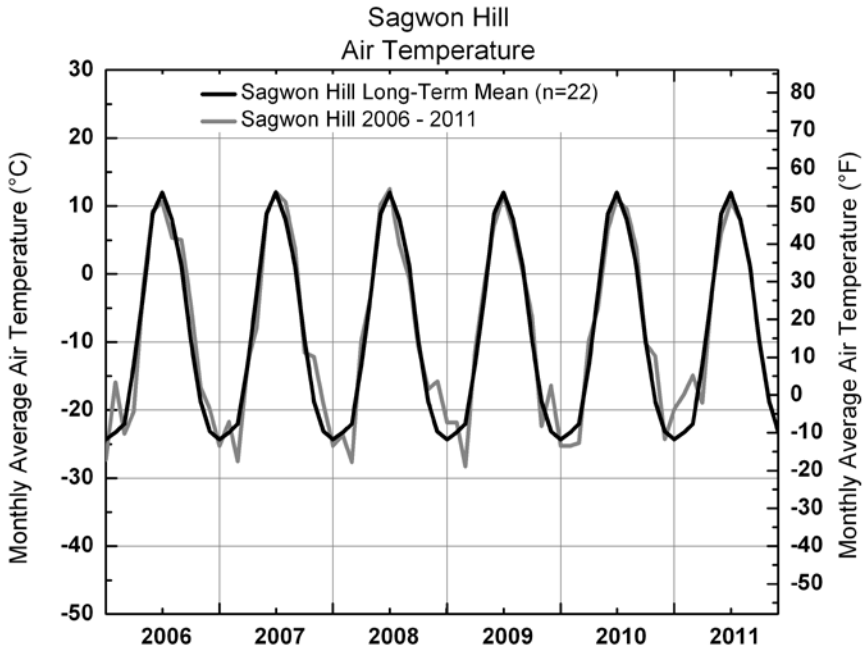

Figure 121. Comparison of Sagwon Hill (northern edge of Foothills) station monthly average for period of record with monthly average from 2006 to September 2011.

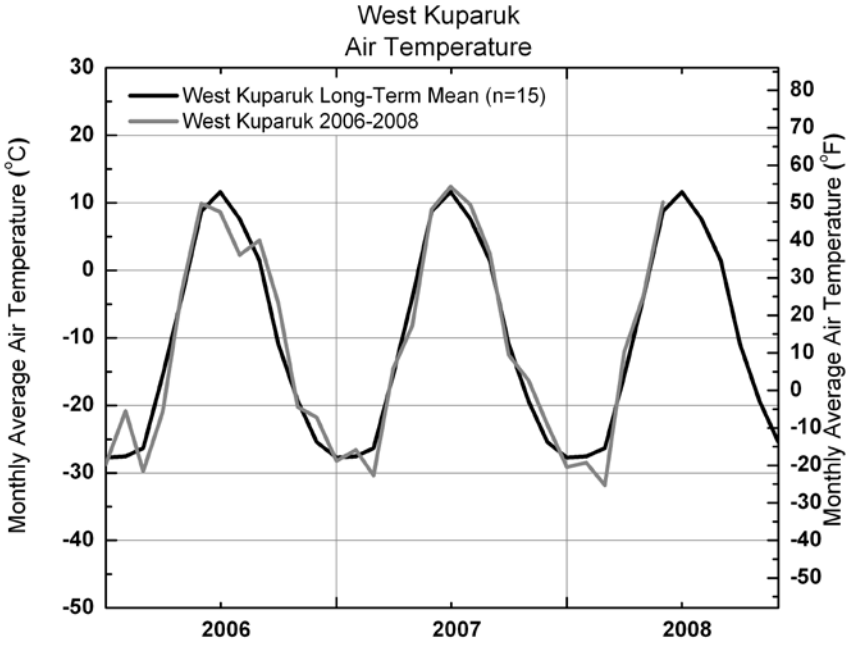

Figure 122. Comparison of West Kuparuk (Foothills) station monthly average for period of record with monthly average from 2006 through September 2008.

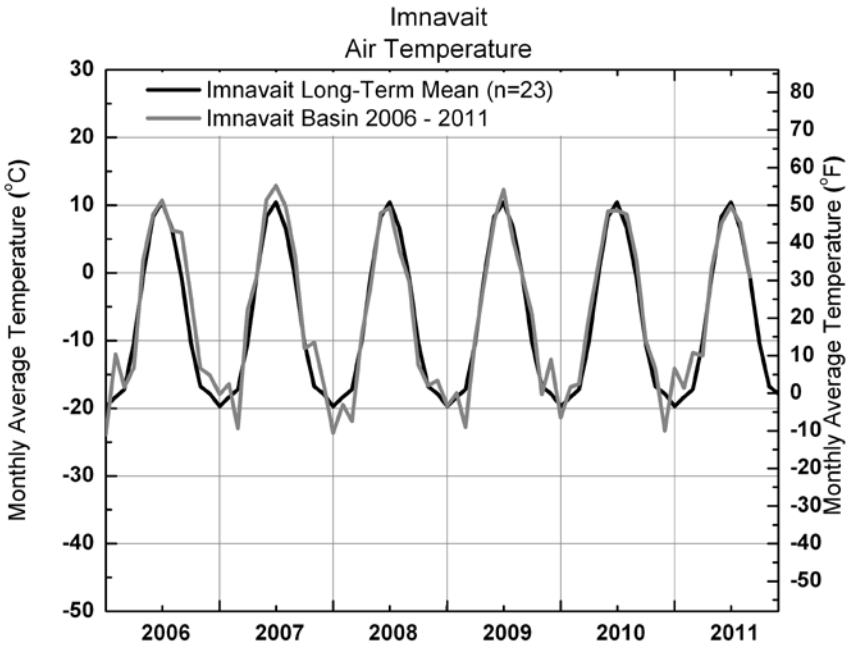

Figure 123. Comparison of Imnavait (Foothills) station monthly average for period of record with monthly average from 2006 to September 2011.

4.13.5 Net Radiation

Net radiation is a balance of incoming solar shortwave and atmospheric longwave against outgoing reflected shortwave and emitted terrestrial longwave radiation. The incoming components, incident solar shortwave and atmospheric longwave radiation, which vary regionally, are primarily tied to the season and cloudiness of an area. The outgoing components, reflected solar shortwave and emitted terrestrial radiation, can vary drastically over short distances. Low-lying areas with dark, cool soils absorb higher net radiation than well-drained, light-colored, warm soils. Two sites at Betty Pingo (upland and wetland) are less than 25 m apart, but the wetland site receives on average 56% more net radiation over the summer season (Section 4.3). The Coastal Plain region, which generally has fewer clouds, is dominated by wet poorly drained soils and has the highest absorbed net radiation (Figure 124). Mountain region stations have the lowest net radiation because of more cloudiness and well-drained warmer soils. Net radiation at the Foothills stations is less easily categorized and depends on site-specific conditions, but is generally higher than net radiation measured at stations in the Mountain region.

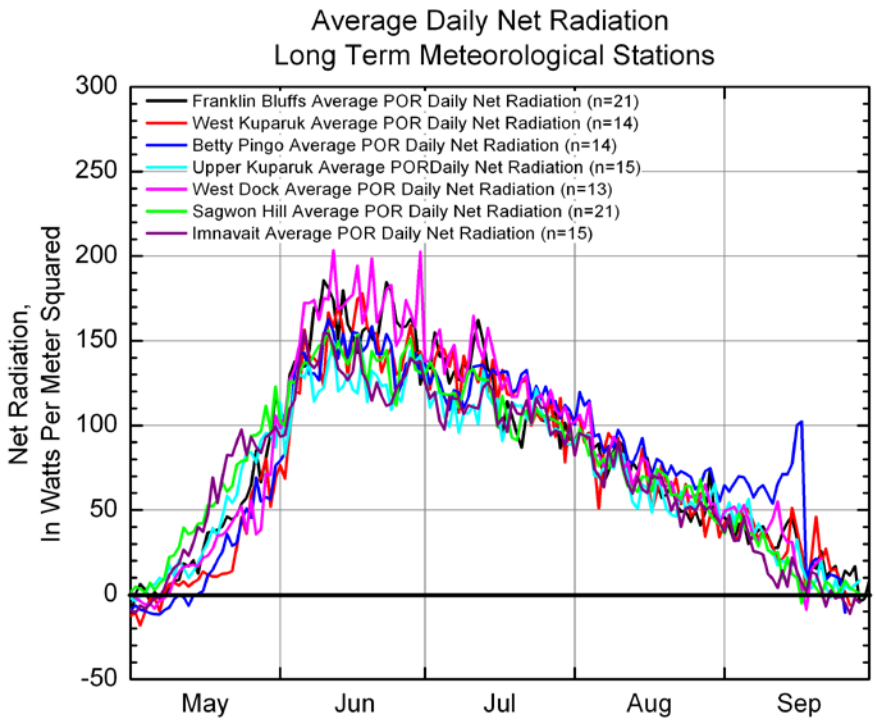

Figure 124. Daily average absorbed net radiation for Kuparuk basin stations (based on the period of record for the station).

5 HYDROLOGIC ANALYSIS

First, we present the results of the water balance for several basins where we collect meteorological and hydrological data as part of prior and ongoing investigations. The addition of the Bullen and Kuparuk Foothills/Umiat Corridor studies provides recent input to this process. Next, we present a flow-frequency analysis, using historical peak and low streamflow data collected by the USGS and UAF/WERC for the handful of stations gauged in this region. After this analysis, we present the results of runoff modeling with the HBV precipitation-runoff model. Lastly, we present the results of a historical floodplain analysis for the Itkillik, Anaktuvuk, Chandler, and Colville Rivers.

5.1 Water Balances

This section includes the results of water balances for the various watersheds where good-quality continuous discharge and meteorological data are available. Results from several catchments are

presented by Kane et al. (2008b) for the Putuligayuk basin (1999 to 2007) and Kane et al. (2004) for the Upper Kuparuk (1996 to 2002). In a previous report, Kane et al. (2009) presented water balance results for the Imnavait, Kuparuk, and Sagavanirktok Rivers through 2008. In this report, we performed water balance analysis on the Upper Kuparuk, Kuparuk, and Putuligayuk through 2011, but not for the Sagavanirktok River because of the difficulty associated with separating snowmelt and summer runoff periods, and the lack of a measured snowmelt peak during most years. Water balances are generally on an annual scale. In reality, for the Arctic, the various fluxes in the water balance are measured only during snowmelt and the warm season.

5.1.1 Methods

The water balance is defined as

$$(P_{snow}+P_{rain}) - (R_{snow}+R_{rain}) - ET - \Delta S = \eta \quad (3)$$

where *P* is precipitation from either snow or rain, *R is* runoff from snow or rain, *ET* is evapotranspiration, ΔS is change in storage, and η is the closure error. The storage term in the Arctic includes water in the active layer and surface storage (lakes, ponds and wetlands, glaciers, aufeis and snowfields). Subpermafrost groundwater is usually not a large factor in Arctic watersheds; however, there are some special cases. Springs located throughout this region of the Alaska Arctic derive water from both above and below the permafrost. For example, springs in the headwater drainage of the Sagavanirktok River are of subpermafrost origin, while some springs in the headwater drainage of the Kuparuk River are of suprapermafrost origin.

Most of the water balance components used are measured directly in the hydrometeorological network. Hourly summer precipitation, winter precipitation (end-of-winter SWE), and hourly runoff data are collected within the Upper Kuparuk and Putuligayuk basins.

Runoff data from WERC-operated gauging stations at the Upper Kuparuk and the Putuligayuk Rivers are used in the analysis. Hydrographs are presented for both rivers in Figure 125 and Figure 126 in the following sections. Although not presented in the report, the hydrographs for

the streams were analyzed on a log scale in order to separate the spring runoff period from the summer runoff period.

Snow water equivalent is measured at the end of winter during snow surveys throughout the Bullen and Kuparuk Foothills/Umiat Corridor study areas. With this data, an average end-of-winter SWE is determined for each basin. Summer precipitation is measured with UAF/WERC-shielded tipping-bucket rain gauges at the meteorological stations throughout the study areas. Any precipitation (measured in the tipping buckets) that fell before the summer flow period was added to the end-of-winter SWE, although it was always much less than the measured SWE on the ground. For example, a wide-scale precipitation event occurred in late May 2008, and the tipping buckets recorded precipitation due to either rain or wet snow, depending on location and elevation. This precipitation was added to the end-of-winter SWE. Unfortunately, there is no way of quantifying the undercatch of these gauges for these mixed precipitation events.

The only measurements of evaporation we have are at Imnavait basin, where pan evaporation is measured during the warm season (Table 45). For 19 years of water balance data from Imnavait Creek, the ratio of evapotranspiration estimated from water balance over the pan evaporation was 0.55. We have used the Priestley-Taylor method to estimate potential evapotranspiration at Betty Pingo (for the Putuligayuk water balance) and Imnavait station in the past, but potential evapotranspiration has not been determined yet at the new Bullen and Kuparuk Foothills stations. Using a Priestley-Taylor empirical alpha coefficient value of $\alpha = 0.95$ (determined from literature) for Imnavait, we get a similar average ratio (of Priestley-Taylor evapotranspiration over pan evaporation) to the 0.55 value above. It should be noted that there is considerable year-to-year variation between the two ratios. In the past, we calculated evapotranspiration as the residual in the water balance computation (assumes no closure error). However, this may not be entirely accurate because changes in storage and any errors in the measurement of precipitation and runoff are then included in this evapotranspiration term. It is likely that the majority of the error is in the precipitation term due to the poor spatial coverage of gauges and/or snow survey sites and the undercatch when measuring precipitation. In some cases, however, the high error may be due to changes in storage.

Table 45. Pan evaporation compared with Priestley-Taylor calculations at Imnavait.

	Potential Pan Evaporation (mm)	Priestley-Taylor Evapotranspiration (mm)
2000	335	168
2001	285	179
2002	285	216
2003	327	172
2004	384	231
2005	378	165
2006	n/a	174
2007	391	244
2008	329	224

5.1.2 Upper Kuparuk River

The Upper Kuparuk River (142 km^2 drainage area) is located adjacent to the long-term research watershed Imnavait Creek in the headwaters of the Kuparuk River. The elevation of the basin is between 798 m and 1464 m. The upper reaches of the Upper Kuparuk originate in a mountainous area to the south, and the river flows north where it is gauged near the Dalton Highway Bridge. The Upper Kuparuk basin consists of both water tracks and rocky stream channels; it is somewhat similar to the Imnavait catchment, in that it responds quickly to snowmelt and rain events. Peak annual flow may occur in either spring or summer. WERC has collected runoff data since 1993, and the historical data are presented in Figure 125.

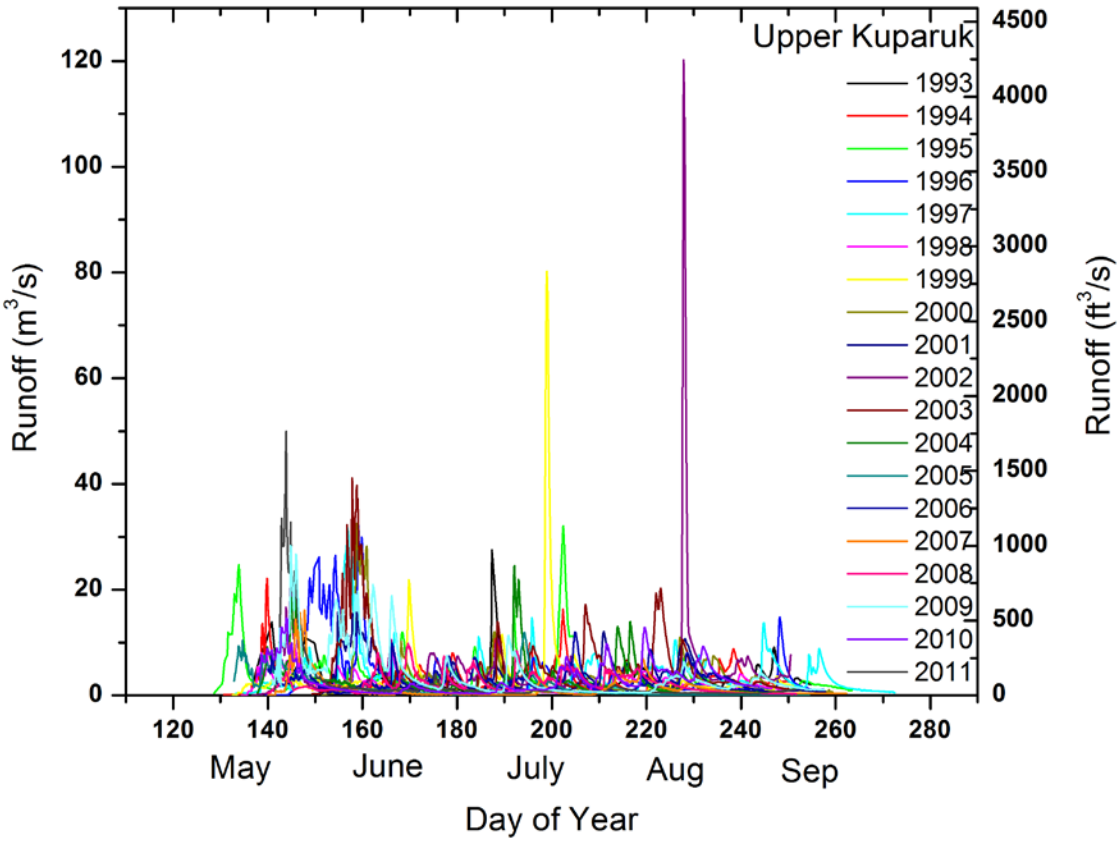

Figure 125. Historical runoff at Upper Kuparuk River (1993 to 2011). Note the two large peaks, 1999 (yellow, rain) and 2002 (purple, mixed rain/snow)

The water balance for Upper Kuparuk was previously published through 2002 in Kane et al. (2004) and has been updated for this report (Table 46). For the Upper Kuparuk Basin, an average snow water equivalent was calculated based on snow surveys in the Upper Kuparuk each year. Summer precipitation data from East Headwaters, West Headwaters, North Headwaters, Upper Kuparuk, Imnavait, Upper Headwaters, and Green Cabin Lakes were averaged for the basin.

Table 46. Upper Kuparuk basin water balance.

Year	P_{snow}	P_{rain}	P_{tot}	ET_{WB}	R_{snow}	R_{rain}	R_{total}	R_{snow}/P_{snow}	R_{rain}/P_{rain}	R_{tot}/P_{tot}	R_{snow}/R_{tot}	P_{snow}/P_{tot}
1996	147	242	389	143	71	175	246	0.48	0.72	0.63	0.29	0.38
1997	150	310	460	156	89	215	304	0.59	0.69	0.66	0.29	0.33
1998	81	236	317	153	35	129	164	0.43	0.55	0.52	0.21	0.26
1999	54	324	378	175	27	176	203	0.50	0.54	0.54	0.13	0.14
2000	148	205	353	142	72	139	211	0.49	0.68	0.60	0.34	0.42
2001	117	222	339	123	68	148	216	0.58	0.67	0.64	0.31	0.35
2002	105	294	399	87	38	274	312	0.36	0.93	0.78	0.12	0.26
2003	152	278	429	106	104	220	324	0.68	0.79	0.75	0.32	0.35
2004	109	188	296	120	46	134	180	0.42	0.71	0.61	0.25	0.37
2005	119	98	217	114	50	54	103	0.42	0.55	0.48	0.48	0.55
2006	79	198	276	100	27	150	177	0.34	0.76	0.64	0.15	0.29
2007	90	107	198	104	36	58	94	0.40	0.55	0.48	0.38	0.45
2008	58	185	243	88	7	148	155	0.13	0.80	0.64	0.05	0.24
2009	114	238	352	74	46	232	278	0.41	0.98	0.79	0.17	0.32
2010	72	205	277	90	45	141	187	0.63	0.69	0.67	0.24	0.26
2011	124	101	225	91	85	50	134	0.68	0.49	0.60	0.63	0.55
Overall Average	**107**	**214**	**322**	**117**	**53**	**153**	**206**	**0.47**	**0.69**	**0.63**	**0.27**	**0.35**
SD	**33**	**70**	**79**	**30**	**26**	**64**	**71**	**0.14**	**0.14**	**0.10**	**0.15**	**0.11**
Max	**152**	**324**	**460**	**175**	**104**	**274**	**324**	**0.68**	**0.98**	**0.79**	**0.63**	**0.55**
Min	**54**	**98**	**198**	**74**	**7**	**50**	**94**	**0.13**	**0.49**	**0.48**	**0.05**	**0.14**

Both 2005 and 2007 were dry summers in the Upper Kuparuk watershed (similar to the rest of the North Slope region). In 2008, Upper Kuparuk had a low spring runoff ratio due to dry soils from the previous fall and the record-low SWE. Additionally, only 5% of the total runoff for 2008 was from snowmelt, compared with the average of 27%. Interestingly, the Upper Kuparuk basin summer-runoff ratio is always higher than the spring runoff ratio, which is the opposite for the entire Kuparuk and Imnavait basins. The combination of increased precipitation in the uppermost reaches and the steep mountainous slopes probably accounts for such a high runoff ratio in the summer (Lilly et al., 1998). The exception is in 2011, where the runoff ratio for spring was the highest on record and the first time the spring runoff ratio was higher than the summer runoff ratio. Additionally, in 2011, 55% of the total annual precipitation was in the form of snow, compared with the average of 35%.

5.1.3 Putuligayuk River

The Putuligayuk River is a low-gradient watershed located on the Coastal Plain in the Prudhoe Bay area. Runoff records for the Putuligayuk River exist from the 1970s to present, with some years in the 1980s and 1990s missing. WERC assumed operation of the gauging station from the USGS in 1999. A high percentage (83%) of the basin consists of lakes, ponds, and wetlands. Runoff in the Putuligayuk River is dominated by snowmelt. Little runoff occurs during the

summer because basin storage increases (evapotranspiration often exceeds precipitation). As the watershed dries out in the summer, the drainage network also becomes fragmented. Snowmelt runoff begins generally in late May or early June and continues until the end of June or early July, as shown in the historical record (Figure 126). The annual peak is produced from snowmelt, and low flow conditions occur the rest of the year, with slight fall increases some years due to fall rain events.

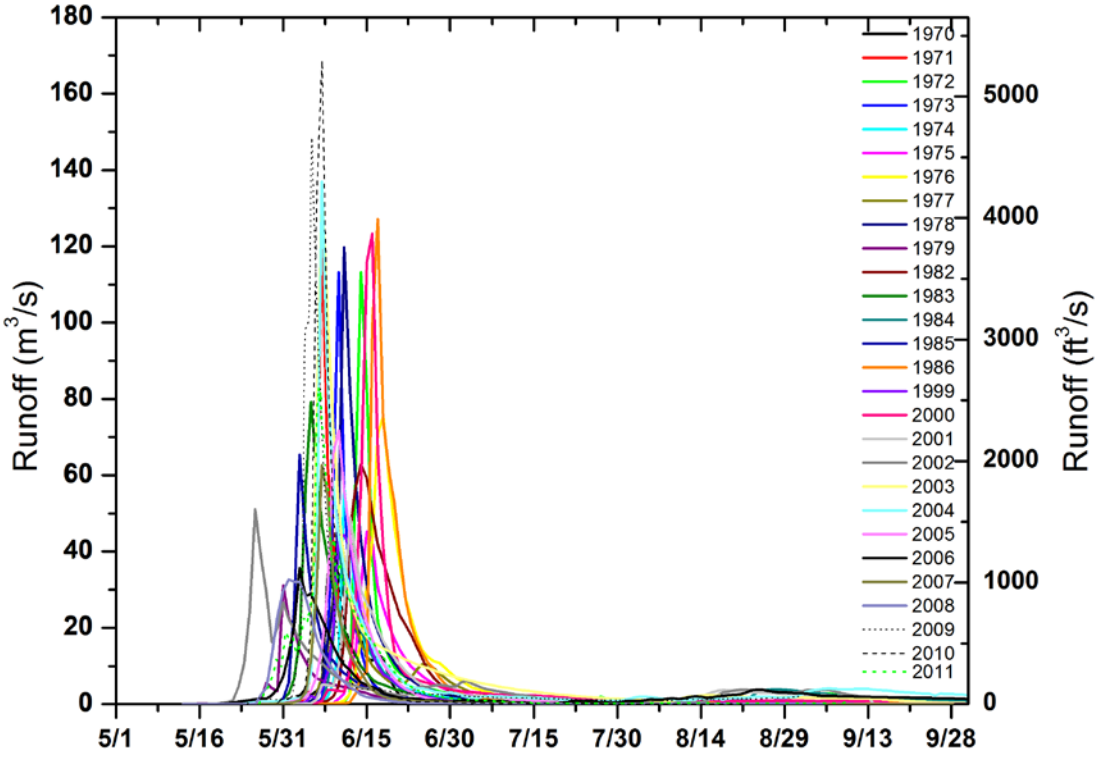

Figure 126. Historical Putuligayuk River runoff 1970–2011.

The Putuligayuk water balance, shown in Table 47, is updated through 2011 (previously presented in Kane et al. [2008b]). The average snow water equivalent for the basin, reported in Berezovskaya et al. (2007a, 2007b, 2008a, 2008b, 2009, 2010) and Stuefer et al. (2011) is used to calculate spring precipitation. Summer rainfall is measured by a tipping bucket at Betty Pingo and Franklin Bluffs meteorological stations. Evapotranspiration is calculated by the Priestley-Taylor method using meteorological data collected at Betty Pingo, Franklin Bluffs and/or West Dock stations. The complete balance is not updated for 2008–2011 due to the lack of good-quality meteorological data at Betty Pingo and West Dock after the stations lost funding for

maintenance. The Putuligayuk River basin has a high runoff ratio during spring and a relatively low runoff ratio in the summer because summer precipitation goes mostly into storage. In recent years over 90% of the total runoff was from snowmelt, compared with the average of 77%. In 2008, the spring runoff ratio was one of the lowest on record, 0.56 (compared with an average of 0.81), due to the record-dry summer and fall in 2007 and low SWE during the 2007/2008 winter. The calculated snowmelt runoff ratio in 2010 is above 1.0, indicating an error in the measurement of runoff or basin average snow water equivalent. The snowmelt runoff ratio averages 0.81; often it is reported in the 0.9 or above range. One notable difference is the year-to-year change in the number of SWE measurements to calculate the basin average SWE. In 2010, the number of measurements decreased from 41 to 21.

Table 47. Putuligayuk water balance, 1999–2011.

Year	P_{snow}	P_{rain}	P_{tot}	P-T ET	R_{snow}	R_{rain}	R_{tot}	ΔS	R_{snow}/P_{snow}	R_{rain}/P_{rain}	R_{tot}/P_{tot}	R_{snow}/R_{tot}	P_{snow}/P_{tot}
	mm	mm	mm	mm	mm	mm	mm	mm	Ratio	Ratio	Ratio	Ratio	Ratio
1999	104	100	204	56	51	16	67	81	0.49	0.16	0.33	0.76	0.51
2000	99	60	159	58	97	28	125	-24	0.98	0.47	0.79	0.78	0.62
2001	84	75	159	54	68	23	91	14	0.81	0.31	0.57	0.75	0.53
2002	94	137	231	63	74	63	137	31	0.79	0.46	0.59	0.54	0.41
2003	112	108	220	54	105	68	173	-7	0.94	0.63	0.79	0.61	0.51
2004	92	111	203	63	76	71	147	-7	0.83	0.64	0.72	0.52	0.45
2005	89	50	139	50	84	5	89	0	0.94	0.10	0.64	0.94	0.64
2006	95	107	202	80	55	28	83	39	0.58	0.26	0.41	0.66	0.47
2007	82	15	97	66	52	3	55	-24	0.63	0.20	0.57	0.95	0.85
2008	96	61	157	48	54	3	57	52	0.56	0.05	0.36	0.95	0.61
2009	134	87	221	n/a	125	27	152	n/a	0.93	0.31	0.69	0.82	0.61
2010	101	53	154	n/a	111	21	132	n/a	**1.10**	0.40	0.86	0.84	0.66
2011	129	55	184	n/a	119	8	127	n/a	0.92	0.15	0.69	0.94	0.70
Max.	134	137	231	80	125	71	173	81	1.10	0.64	0.86	0.95	0.85
Min.	82	15	97	48	51	3	55	-24	0.49	0.05	0.33	0.52	0.41
Ave.	101	78	179	59	82	28	110	16	0.81	0.32	0.62	0.77	0.58
Std. Dev.	16	33	39	9	27	24	39	35	0.19	0.19	0.17	0.15	0.12

5.1.4 Kuparuk River

The entire Kuparuk basin is a relatively large drainage (8140 km^2) that originates in the Brooks Range in the south and flows north through the Foothills and across the Coastal Plain. The river has been gauged at Deadhorse by the USGS since 1971, the longest measurement period of any river on the North Slope. The majority of runoff on the Kuparuk River occurs during the spring snowmelt period, from late May to mid-June (Figure 127), although summer runoff events (like August 2002) do appear in the hydrograph. Peak flows for the year are during the snowmelt runoff period.

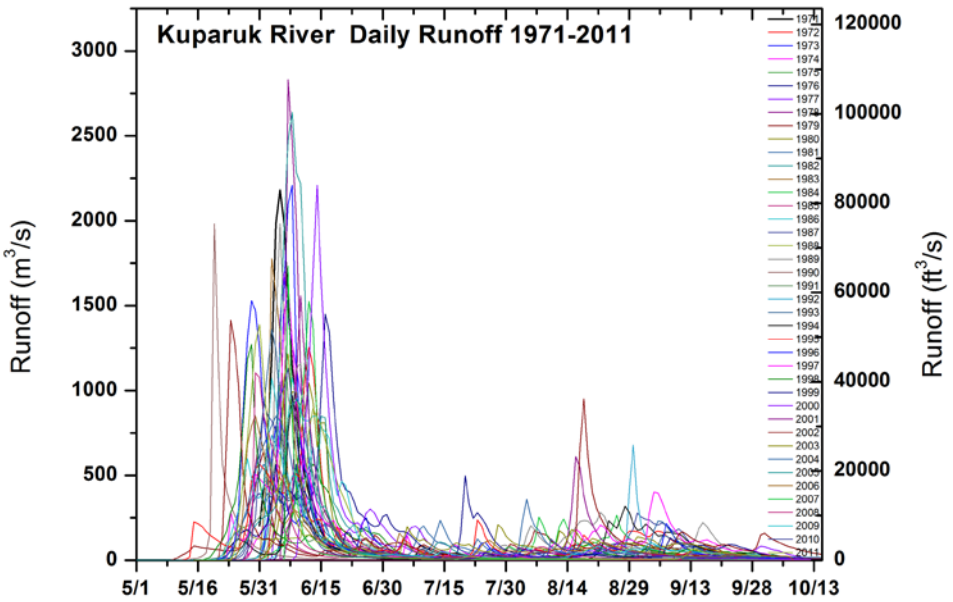

Figure 127. Daily historical runoff 1971–2011 at Kuparuk River at Deadhorse. Most of the runoff occurs during the spring snowmelt period in late May and early June.

A study by Lilly et al. (1998) reported on the water balance for the Kuparuk River from 1993–1997. In the present report, we update the water balance for 2007 to 2011. For the Kuparuk basin water balance 2007 to 2011, summer precipitation data from the following stations are used when data are available to calculate a basin average with Thiessen polygons: South White Hills (DFM1), White Hills (DFM2), North White Hills (DFM3), Northwest Kuparuk (DFM4), Betty Pingo, Sagwon Hill, West Kuparuk, and Upper Kuparuk. The average snow water equivalent for the basin, reported in Berezovskaya et al. (2007a, 2007b, 2008a, 2008b, 2009, 2010) and Stuefer et al. (2011) is used to calculate spring precipitation. In the future, we plan to test and compare other methods of determining the large basin's average precipitation, because it is likely that some spatial trends are not represented in these averages.

The water balance (Table 48) shows that the Kuparuk River has a high runoff ratio for spring and a low runoff ratio for summer. The high runoff ratio in spring is due to permafrost and frozen subsurface conditions of the active layer. The low runoff ratio for the summer months is partially due to evapotranspiration (ET) over the basin and more surface storage availability on the Coastal Plain, where there are many ponds and lakes and a lack of summer runoff contribution.

Results from the water balance of the early 1990s (Table 49) can be compared with the recent water balance calculation (Table 48) and the overall statistics (Table 50). Snow precipitation and spring runoff from snow has been lower in recent years than in the 1990s. In 2007, low summer precipitation resulted in only 12% of the total runoff that occurred in the summer. This can be compared with the average in the 1990s, where 32% of the total runoff occurred in the summer months. As with the Putuligayuk water balance, the 2010 snowmelt runoff ratio of 1.11 indicates a problem with the measured basin average snow water equivalent or the measured runoff. The number of SWE measurements decreased beginning in 2010, from 41 to 21 samples within the basin. The number of SWE measurements used to calculate basin average in the 1993–1997 water balance is much lower than the number used in the 2007–2011 calculation.

Table 48. Kuparuk River basin water balance, 2007 to 2011.

Year	P_{snow}	P_{rain}	P_{tot}	ET_{WB}	R_{snow}	R_{rain}	R_{tot}	R_{snow}/P_{snow}	R_{rain}/P_{rain}	R_{tot}/P_{tot}	R_{snow}/R_{tot}	P_{snow}/P_{tot}
	mm	mm	mm	mm	mm	mm	mm	mm	mm	mm	mm	mm
2007	90	44	134	55	69	10	79	0.77	0.22	0.59	0.88	0.67
2008	96	113	208	107	75	25	100	0.79	0.22	0.48	0.75	0.46
2009	123	160	283	158	91	34	125	0.74	0.21	0.44	0.73	0.43
2010	102	107	209	66	113	30	143	**1.11**	0.28	0.68	0.79	0.49
2011	126	95	221	83	120	18	138	0.95	0.19	0.62	0.87	0.57
Avg	107	104	211	94	94	23	117	0.87	0.23	0.56	0.80	0.52
sd	16	41	53	41	22	10	27	0.16	0.03	0.10	0.07	0.10
max	126	160	283	158	120	34	143	1.11	0.28	0.68	0.88	0.67
min	90	45	134	55	69	10	79	0.74	0.19	0.44	0.73	0.43

Table 49. Kuparuk River basin water balance 1993 to 1997 (Lilly et al., 1998).

Year	P_{snow}	P_{rain}	P_{tot}	ET_{WB}	R_{snow}	R_{rain}	R_{tot}	R_{snow}/P_{snow}	R_{rain}/P_{rain}	R_{tot}/P_{tot}	R_{snow}/R_{tot}	P_{snow}/P_{tot}
	mm	mm	mm	mm	mm	mm	mm	mm	mm	mm	mm	mm
1993	135	114	249	108	113	28	141	0.84	0.25	0.57	0.80	0.54
1994	74	157	231	113	61	57	118	0.82	0.36	0.51	0.52	0.32
1995	139	144	283	124	110	49	159	0.79	0.34	0.56	0.69	0.49
1996	136	130	266	88	133	45	178	0.98	0.35	0.67	0.75	0.51
1997	n/a	182	-	-	152	87	239	-	0.48	-	0.64	-
Avg	121	145	257	108	114	53	167	0.86	0.35	0.58	0.68	0.47
sd	31	26	22	15	34	22	46	0.07	0.08	0.08	0.11	0.10
max	139	182	283	124	152	87	239	0.67	0.98	0.48	0.80	0.54
min	74	114	231	88	61	28	118	0.51	0.79	0.25	0.52	0.32

Table 50. Kuparuk River basin water balance overall statistics (1993 to 1997, 2007 to 2011).

Year	P_{snow}	P_{rain}	P_{tot}	ET_{WB}	R_{snow}	R_{rain}	R_{tot}	R_{snow}/P_{snow}	R_{rain}/P_{rain}	R_{tot}/P_{tot}	R_{snow}/R_{tot}	P_{snow}/P_{tot}
	Mm	mm	mm	mm	mm	mm	mm	mm	mm	mm	mm	mm
Avg	113	125	232	100	98	38	142	0.87	0.29	0.57	0.74	0.50
sd	24	39	47	31	29	22	44	0.12	0.07	0.08	0.11	0.10
max	139	182	283	158	152	87	239	1.11	0.48	0.68	0.88	0.67
min	74	45	134	55	61	10	79	0.74	0.19	0.44	0.52	0.32

5.1.5 Comparison of Water Balances

Table 51 compares the ratios of runoff and precipitation for the four catchment water balances presented in the previous section. The Coastal Plain region basins (Putuligayuk and Kuparuk River) both have high spring runoff ratios and receive more of the annual precipitation as snow, while the smaller Foothills region basins (Imnavait and Upper Kuparuk) have relatively low spring runoff ratios (although all are high when compared with more temperate watersheds). Most of the Putuligayuk and Kuparuk runoff occurs during the spring. It was anticipated that the Upper Kuparuk would have a higher runoff ratio during snowmelt.

The Imnavait and Upper Kuparuk basins have a higher percentage of annual precipitation that falls as rain rather than snow. Total winter precipitation is surprisingly uniform over the study area; however, total summer precipitation increases significantly from the Coastal Plain region to the Foothills region to the Mountain region. The Upper Kuparuk has a higher percentage of runoff that occurs from rain rather than snow. This may be due to (1) more summer precipitation in the higher elevations of the basin, (2) steep terrain with rocky surface conditions, and (3) snowpack in the upper reaches of the basin that is diminished during winter because of sublimation caused by high winds.

Table 51. Comparison of average ratios of various hydrologic components for four basins.

Basin	R_{snow}/P_{snow}	R_{rain}/P_{rain}	R_{tot}/P_{tot}	R_{snow}/R_{tot}	P_{snow}/P_{tot}
Imnavait (n=24, 1985-2008)	0.64	0.47	0.53	0.46	0.36
Upper Kuparuk (n=16, 1993-2011)	0.47	0.69	0.63	0.27	0.35
Putuligayuk (n=13, 1999-2011)	0.81	0.32	0.62	0.77	0.58
Kuparuk (n=10, 1993-1997, 2007-2011)	0.87	0.27	0.56	0.75	0.50

5.2 Flow Frequency Analysis

A flow frequency analysis was conducted to examine the frequency of peak and low flow events on Arctic streams. All analyses were completed according to the Interagency Advisory Committee on Water Data, Hydrology Subcommittee, Bulletin 17B (Log Pearson III distribution) using HEC software. The results of the flood frequency analysis for Imnavait Creek (through 2007), Upper Kuparuk River (through 2011), and Putuligayuk River (through 2011) are

summarized in this section. The results of additional analyses of the Upper Sagavanirktok, the Atigun River, and the Oksrukuyik River (also known as "Ox Creek") for this report are also included. The frequency analyses by Kane et al. (2008a) were separated into spring (snowmelt) and summer (rain) peak flow, and a third analysis was completed for low flow. Flood frequency analyses for the Upper Sagavanirktok River near Pump Station 3 (USGS 15908000), Atigun River near Pump Station 4 (15904800), and Sagavanirktok River Tributary (Oksrukuyik [Ox] River 15906000) presented in this report were completed using summer data based on USGS records. The annual peak on these rivers may occur during either spring or summer runoff, but snowmelt analyses are not conducted due to data-quality issues. Table 52 and Table 53 summarize the number of events and period of record for the analysis.

Table 52. Number of events in analysis.

Basin	Number of Events Snow	Number of Events Summer	Number of Events Low Flow
Imnavait Creek	23	22	n/a
Upper Kuparuk River	19	19	19
Kuparuk River	41	41	41
Putuligayuk River	38	n/a	28
Upper Sagavanirktok River	n/a	28	n/a
Sagavanirktok Tributary (Oksrukuyik Creek)	n/a	22	n/a
Atigun River nr Pump 4	n/a	9	n/a

Table 53. Period of record in analysis.

Basin	Period of Record Snow	Period of Record Summer	Period of Record Low Flow
Imnavait Creek	1985–2007	1986–2007	n/a
Upper Kuparuk River	1993–2011	1993–2011	1993–2011
Kuparuk River Deadhorse	1971–2011	1971–2011	1971–2011
Putuligayuk River	1970–80, 1982–1995, 1999–2011	n/a	1970–1979, 1982–1986, 1999–2011
Upper Sagavanirktok River	n/a	1984-2011	n/a
Sagavanirktok Tributary (Oksrukuyik Creek)	1979-2007	1997-2007	n/a
Atigun River nr Pump 4	2001, 2003, 2005	1992-1994, 2002,2004,2006-2009	n/a

The calculated station coefficient of skewness for each river is presented in Table 54. The generalized skew reported in the USGS tables by Curran et al. (2003) for Region 7 (based on only 7 stations with at least 25 systematic annual peaks) is -0.52, but the range we calculated is -1.759 to +1.062 and differs depending on the use of a spring or summer peak. Therefore, a regional skewness coefficient was not applied to the analysis; the station skewness was calculated for each site.

Table 54. Coefficient of skewness.

Basin	Coefficient of Skewness Snow	Coefficient of Skewness Rain	Coefficient of Skewness Low Flow
Imnavait Creek	-0.668	1.062	n/a
Upper Kuparuk River	-0.726	0.863	-1.759
Kuparuk River	-0.070	-0.774	0.233
Putuligayuk River	-0.438	n/a	-0.846
Upper Sagavanirktok River	n/a	0.420	n/a
Sagavanirktok Tributary (Oksrukuyik Creek)	n/a	0.254	n/a
Atigun River nr Pump 4	n/a	0.989	n/a

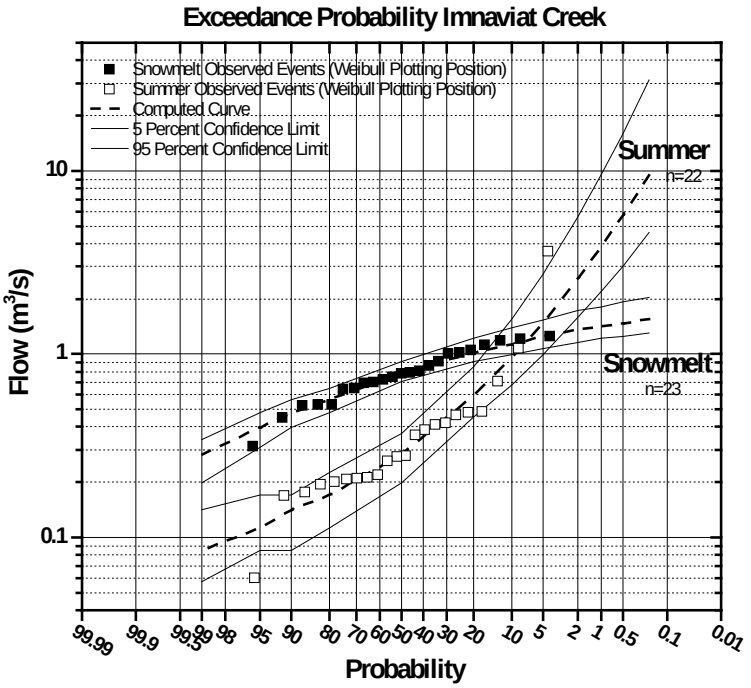

Figure 128. Exceedance probabilities for Imnavait Creek (2.2 km^2).

A flood frequency analysis for Imnavait Creek was performed by Kane et al. (2008a) for both snowmelt and summer runoff (Figure 128) with data through 2007. The coefficient of skewness for the snowmelt runoff is negative, while the skewness for summer runoff is positive. Kane et al. (2008a) concluded that floods of high probability (low return period) will be from snowmelt, but floods of low probability (floods of record) will be from summer precipitation. This conclusion is easy to draw from the diverging predicted flows for low probabilities or high return periods. No low-flow analysis was performed because there is a very high probability that the flow in this creek often actually ceases each year during the summer.

For the Upper Kuparuk River (Figure 129), in addition to snowmelt and summer runoff analyses, a low-flow analysis was performed and updated through 2011. Again, it was found that the coefficient of skewness for snowmelt was negative, and for summer runoff, it was positive. The floods of low probability would be due to summer precipitation, as the predicted flows diverge at high return periods. The low-flow frequency analysis for the Upper Kuparuk indicates that at low probabilities (high return periods), the flow approaches the "no flow" case (Kane et al., 2008a).

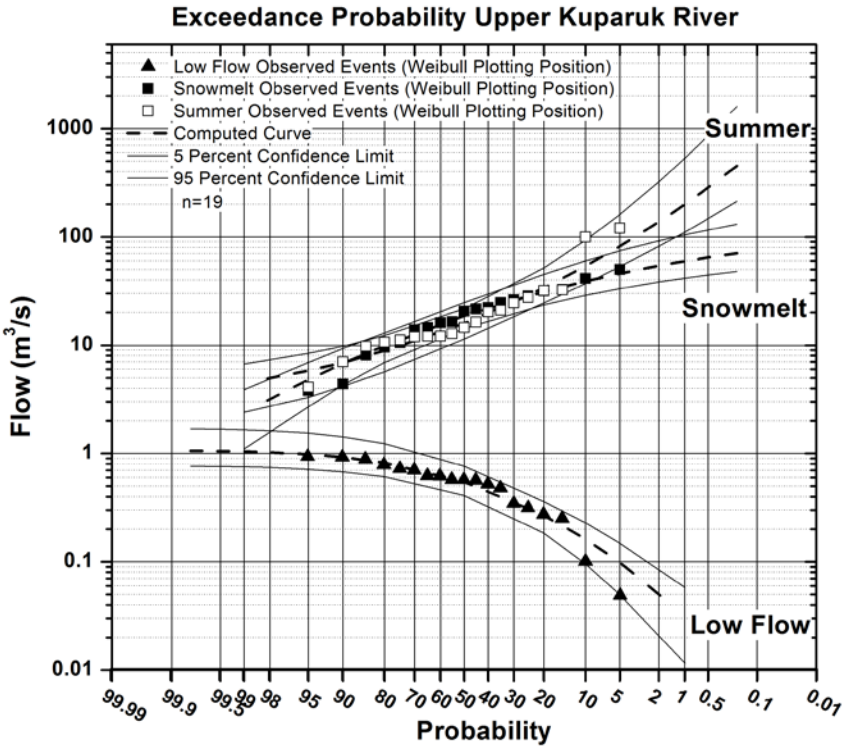

Figure 129. Exceedance probabilities for the Upper Kuparuk River (142 km^2).

The Putuligayuk is completely dominated by snowmelt runoff (all annual floods are snowmelt); thus, Kane et al. (2008a) did not perform an analysis for summer events (Figure 130). The computed curve for snowmelt runoff had a negative skew, similar to the Upper Kuparuk River and Imnavait Creek. The computed curve for low flow was steeper than that for the Upper Kuparuk, indicating that the streamflow on the Putuligayuk has a higher probability of very low flow conditions. Note that three of the four lowest flow events (which are predicted to have a low

probability) occurred in 2007, 2008, and 2010. Additionally, the spring flood of 2010 was the highest recorded peak, although the cumulative volumetric flow for the spring runoff period was not the highest (see water balance in Table 47).

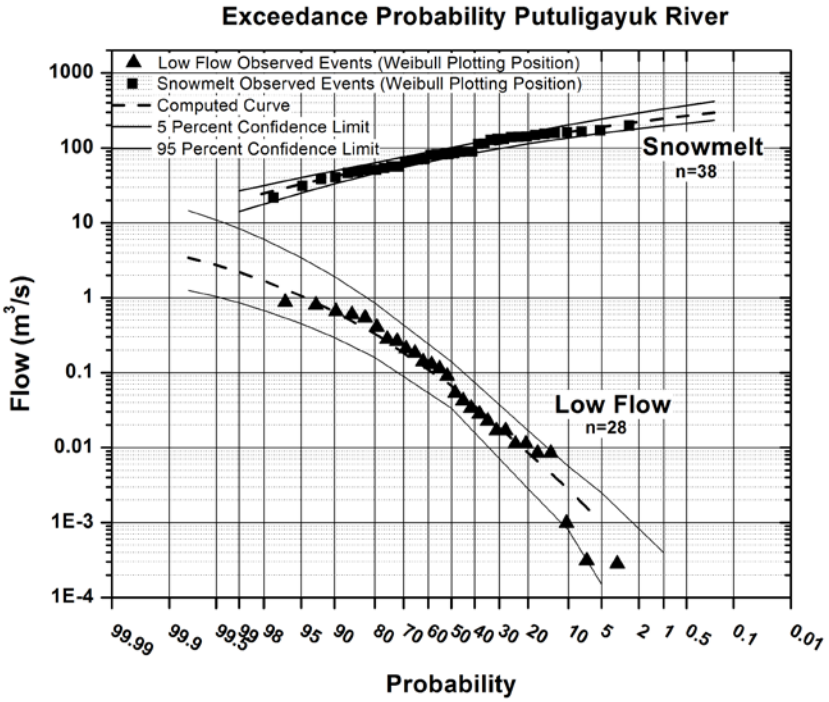

Figure 130. Exceedance probabilities for the Putuligayuk River (471 km^2).

The flow-frequency analysis for the Kuparuk River produced different results (Figure 131) than the three drainages described above. Kane et al. (2008a) found that the computed curve for snowmelt was negative, similar to the other streams examined; however, the computed curve for summer was also negative. Additionally, the snowmelt curve plots significantly higher than the summer curve, meaning that all low-probability floods of record are probably generated by snowmelt. Kane et al. (2008a) concluded that this occurs because there are no basin-wide summer precipitation events that would contribute to runoff over the whole of the basin (while this is not true during snowmelt). The low-flow analysis on the Kuparuk did not produce a highly skewed curve of predicted flows, and the curve is positively skewed (slightly) compared with the negative skew of the Upper Kuparuk and Putuligayuk Rivers.

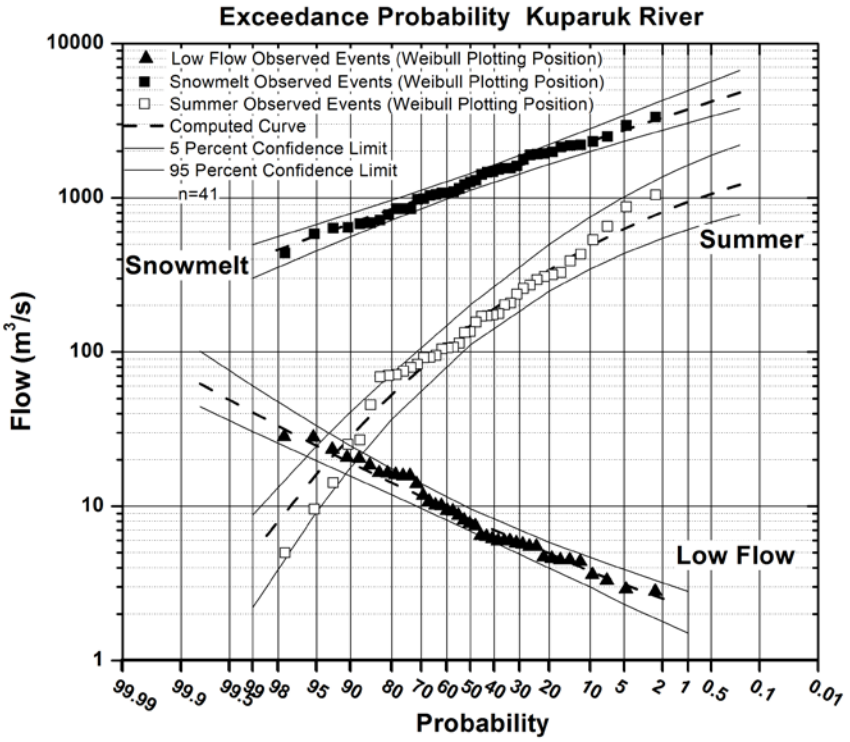

Figure 131. Exceedance probability for the entire Kuparuk River (8140 km^2).

Additional flood-frequency analysis was performed for this report on the Atigun River, Oksrukuyik River, and Upper Sagavanirktok River. For the Atigun River, the analysis was only conducted for the summer period due to the lack of availability of snowmelt peak data. The station skew was positive (Figure 132) and the results look similar to the Upper Kuparuk summer curve.

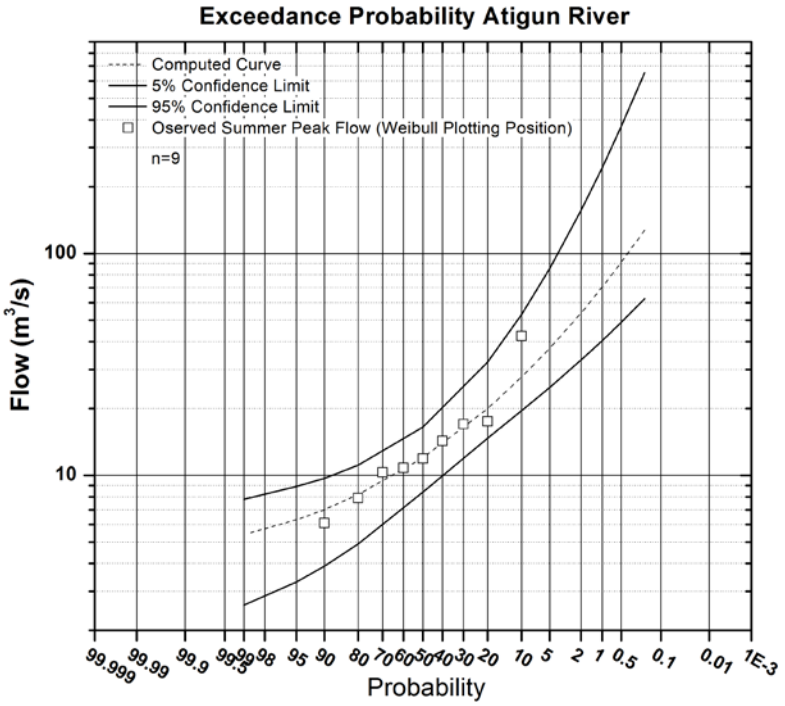

Figure 132. Exceedance probabilities for the Atigun River (126 km^2). Only summer peak events are plotted due to lack of available snowmelt runoff data. The skewness is 0.254.

The results of the Oksrukuyik, a tributary to the Sagavanirktok River, indicate an overall negative skewness (Figure 133) when just using one annual peak in the analysis. However, this analysis produces a positive skew for summer events when separately analyzed (Figure 134). Due to a lack of snowmelt peak-flow data, the analysis is not completed for the snowmelt period alone. This watershed differs from other watersheds because of the many lakes (some large) in this headwater drainage.

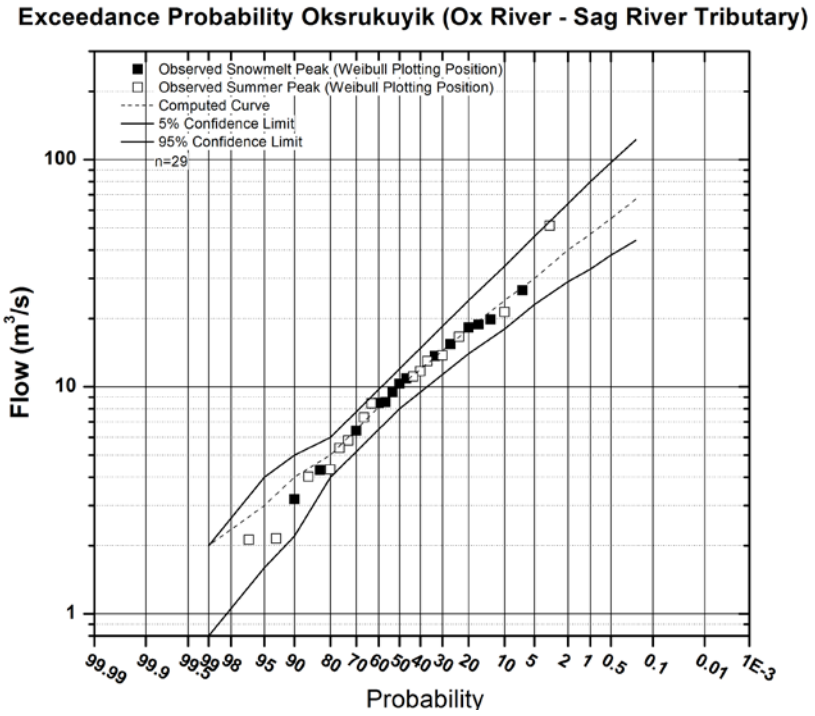

Figure 133. Exceedance probabilities for the Oksrukuyik based on annual peak flow (73 km^2). The skewness is -0.153 for annual peak flow analysis.

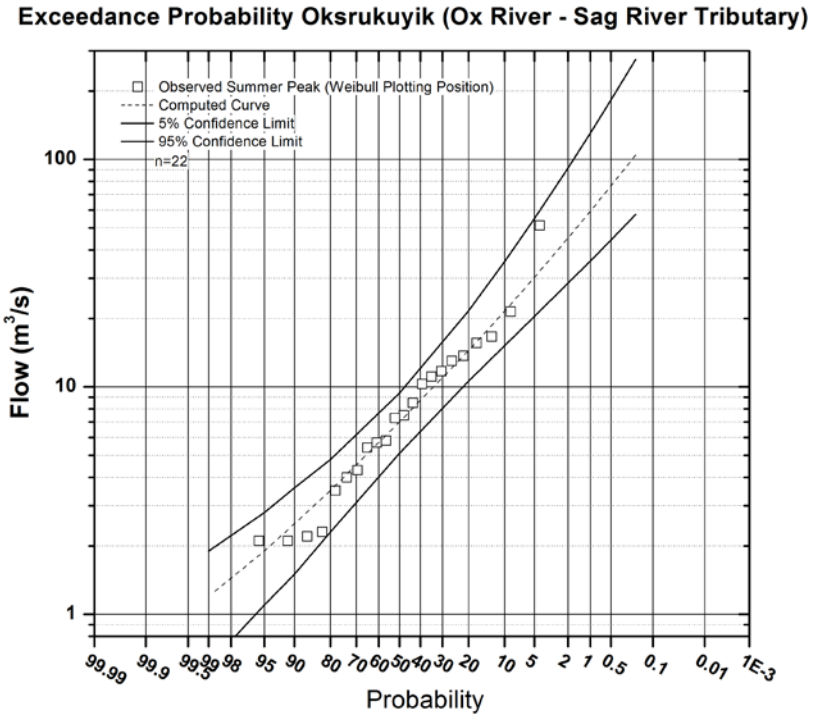

Figure 134. Exceedance probabilities for the Oksrukuyik based on summer peak flow events (73 km^2).

The flood-frequency analysis for the Upper Sagavanirktok is performed on the summer peak flow data only, due to the lack of a measured snowmelt peak for most years. If snowmelt peak data were available, we would likely see a different curve for spring (versus the summer results). The results of the flood-frequency analysis for summer produce a predicted curve with a positive coefficient of skewness (Figure 135).

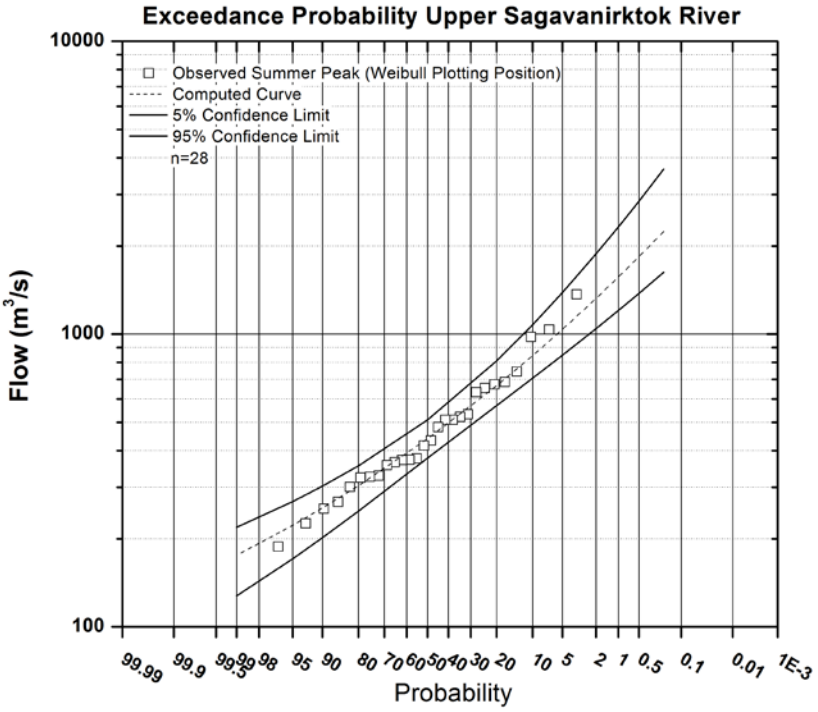

Figure 135. Exceedance probability for the Upper Sagavanirktok River (4817 km^2) for summer events.

The record length for the Chandler, Anaktuvuk, and Itkillik Rivers is too short to do customary flood-frequency analyses. By doing flood-frequency analyses on North Slope rivers with a long record, it was rationalized that we could look at the runoff response of those watersheds with only a few years of observation and make some conclusion about the probability of the flood magnitude for a specific year. For example, if the snowmelt peak on the Upper Kuparuk in 2011 was approximately a 20-year flood, then maybe the 2011 snowmelt flood on the Itkillik would be approximately a 20-year flood. So, we are using data from streams with long-term records as indices for streams with short-term records. This approach is sounder for snowmelt-generated

floods than for rainfall-generated floods because of the more-uniform areal distribution of solid precipitation.

The spring and summer peak runoff events for 2007 through 2011 are examined for the Upper Kuparuk, Kuparuk, Putuligayuk, and Upper Sagavanirktok Rivers as shown Table 55–Table 58. The Upper Kuparuk experienced a 20-year summer flood in 2002 and possibly a 20-year or greater snowmelt flood in 2011 (Table 55), during the study period. According to the flood-frequency analysis for the Kuparuk River, a 5-year snowmelt flood occurred in 2007, although the total volume of runoff during the flood was actually below average. In 2010, the Putuligayuk River experienced a 39-year high-flow event, although the total volume of runoff during the period was not the highest on record. Once spring runoff initiated on the Putuligayuk in 2010, air temperature warmed up rapidly and runoff for this period was short in duration but high in magnitude. For the Upper Sagavanirktok, it is not possible to examine the spring flood due to the limited data set. During the summer months of the study period from 2007 through 2011 for this river, no unusually large floods occurred.

Table 55. Upper Kuparuk River peak discharge, 2002 and 2007 to 2011.

Year	Spring Peak Runoff (m^3/s)	Summer Peak Runoff (m^3/s)	Spring Return Period (yr)	Summer Return Period (yr)
2002		120 on 8/16		20
2007	16 on 5/27	7 on 8/7	1.7	1.1
2008	4 on 5/23	10 on 6/18	1.1	1.3
2009	28 on 5/24	21 on 6/11	4.0	2.9
2010	14 on 5/23	13 on 8/7	1.4	1.8
2011	50 on 5/23	4 on 6/24	20	1.1

Table 56. Kuparuk River peak discharge, 2007 to 2011.

Year	Spring Peak Runoff (m^3/s)	Summer Peak Runoff (m^3/s)	Spring Return Period (yr)	Summer Return Period (yr)
2007	1951 on 6/7	n/a	5.0	
2008	850 on 5/31	79 on 8/7	1.4	1.4
2009	1073 on 6/3	106 on 9/3	1.6	1.7
2010	1262 on 6/7	135 on 8/10	2.0	2
2011	1608 on 5/31	72 on 9/14	3.2	1.3

Table 57. Putuligayuk River peak discharge, 2007 to 2011.

Year	Spring Peak Runoff (m^3/s)	Spring Return Period (yr)
2007	69 on 6/7	1.6
2008	38 on 6/2	1.1
2009	148 on 6/5	5.6
2010	199 on 6/8	39
2011	83 on 6/6	2.0

Table 58. Upper Sagavanirktok peak discharge, 2007 to 2011.
Spring peak runoff data are incomplete for this station.

Year	Summer Peak Runoff (m^3/s)	Summer Return Period (yr)
2007	226 on 8/2	1.1
2008	521 on 7/11	2.9
2009	634 on 6/7	3.6
2010	481 on 7/30	2.2
2011	371 on 7/14	1.7

There are challenges with comparing the results of the flood frequency of rivers with long-term data with the runoff in rivers with only short-term data in 2009–2011 (Table 59 through Table 64). Since spring runoff peak-flow data are limited for the Upper Sagavanirktok River, it is only possible to examine the summer peak data for basins such as the Itkillik (Table 59), Anaktuvuk (Table 60), and Chandler (Table 61) Rivers, which are most similar in basin characteristics (such as basin area, latitude, and gradient) to the nearby Sagavanirktok. The Kuparuk has peak snowmelt runoff data, but the basin characteristics are not entirely similar (the Kuparuk basin lacks extensive mountain area in the headwaters) to the Itkillik, Anaktuvuk, and Chandler Rivers. Additionally, a large percentage of the Kuparuk River basin area is within the Coastal Plain region, which is colder than the southern Foothills and Mountain regions during the month of May. Colder May temperatures may result in a longer, prolonged runoff period for the Kuparuk River, which decreases the magnitude of the peak spring discharge. The upper Itkillik, Anaktuvuk, and Chandler basins experience warmer air temperatures due to their southern location and tend to peak earlier and more quickly than the Kuparuk. The No Name (Table 62), Shaviovik (Table 63), and Kadleroshilik (Table 64) Rivers, although smaller in size than the Kuparuk, have a large percentage of basin area within the Coastal Plain, and a lesser percentage in the Foothills and Mountain regions, similar to the Kuparuk River. In 2009, the date of peak discharge for all three rivers was the same as the Kuparuk. The Putuligayuk is entirely contained within the Coastal Plain and may not compare well with any of the basins (except maybe No Name) in this study because they all have contributing areas in the Foothills and/or Mountain regions.

In summary, most of the summer floods observed so far on the Itkillik, Anaktuvuk, and Chandler Rivers are probably less than 5-year events. While we do not have a stream for good comparison

of snowmelt floods, the Upper Kuparuk 2011 snowmelt flood was estimated at a 20-year event. The highest snowmelt floods observed for all three Umiat rivers was the 2011 event.

Table 59. Itkillik River peak discharge, 2009 to 2011. Estimated return period based on Sagavanirktok River flood frequency.

Year	Spring Peak Runoff (m^3/s)	Summer Peak Runoff (m^3/s)	Spring Return Period (yr)	Summer Return Period (yr)
2009	~180 on 5/25	270 on 7/10	unknown	3-4
2010	~250 on 5/27	270 on 8/10	unknown	1-3
2011	~300 on 5/24	120 on 6/25	unknown	1-2

Table 60. Anaktuvuk River peak discharge, 2009 to 2011. Estimated return period based on Sagavanirktok River flood frequency.

Year	Spring Peak Runoff (m^3/s)	Summer Peak Runoff (m^3/s)	Spring Return Period (yr)	Summer Return Period (yr)
2009	770 on 5/26	800 6/7	unknown	3-4
2010	1090 on 5/31	640 on 8/8	unknown	1-3
2011	~1475 on 5/26	175 on 9/12	unknown	1-2

Table 61. Chandler River peak discharge, 2011. Estimated return period based on Sagavanirktok River flood frequency.

Year	Spring Peak Runoff	Summer Peak Runoff (m^3/s)	Spring Return Period (yr)	Summer Return Period (yr)
2011	~1160 on 5/26	290 on 9/12	unknown	1-2

Table 62. No Name River peak discharge, 2009. Estimated return period based on Kuparuk River flood frequency.

Year	Spring Peak Runoff (m^3/s)	Summer Peak Runoff (m^3/s)	Spring Return Period (yr)	Summer Return Period (yr)
2009	~80 on 6/3	16 on 8/31	1-2	1-2

Table 63. Shaviovik River peak discharge, 2009 to 2010. Estimated return period based on Kuparuk River flood frequency.

Year	Spring Peak Runoff (m^3/s)	Summer Peak Runoff (m^3/s)	Spring Return Period (yr)	Summer Return Period (yr)
2009	~630 on 6/3	250 on 6/11	1-2	1-2
2010	~600 on 6/5	n/a	1-2	1-2

Table 64. Kadleroshilik River peak discharge, 2009 to 2010. Estimated return period based on Kuparuk River flood frequency.

Year	Spring Peak Runoff (m^3/s)	Summer Peak Runoff (m^3/s)	Spring Return Period (yr)	Summer Return Period (yr)
2009	~350 on 6/3	37 on 6/12	1-2	1-2
2010	~320 on 6/5	n/a	1-2	1-2

5.3 Hydrological Modeling

To aid in the understanding of Arctic hydrology, we undertook a modeling exercise. The Swedish Meteorological and Hydrological Institute (SMHI) developed the HBV model, which was selected as a tool to understand the hydrologic cycle and the runoff response to precipitation events for Arctic rivers. The HBV model was selected because of its relative simplicity (minimum amount of measured field data required) and robustness. Additionally, it is a semi-distributed model, which is particularly important when simulating flow in large basins with non-uniform spatial processes. Currently we are applying the runoff model for the Anaktuvuk , Upper Kuparuk, Upper Sagavanirktok, Putuligayuk, Shaviovik, and Kadleroshilik Rivers. The purpose of the modeling effort is to develop an understanding of the processes controlling runoff in Arctic rivers. If we can develop HBV parameter sets that can adequately describe the runoff of gauged basins, we can test these parameter sets on ungauged basins to predict runoff in response to extreme events. This section is a brief summary of the HBV model and our progress.

5.3.1 HBV Model Description

The HBV model requirements include input data (hourly or daily precipitation, air temperature, and discharge, and daily or monthly evapotranspiration) and model parameters for the snow, soil moisture accounting, response, and transformation routines (Figure 136). Water enters the model simulation as either snow or rain; its form is determined by the model by setting a threshold temperature (TT) to separate the states. The water infiltrates the soil moisture routine, where overland flow is initiated if the soil moisture exceeds the maximum soil moisture (FC). The water is then routed through two separate but connected reservoirs: the upper and the lower. Runoff may only occur from the upper reservoir, but water may percolate to the lower zone (through the parameter PERC), which in traditional interpretations of the model represent contributions to groundwater levels. In the simulations, only the upper reservoir is used and PERC is turned off or assigned a very low value to simulate a continuous permafrost condition, where no deeper groundwater exists.

The snow routine uses input precipitation and temperature data and several parameters to determine the snowmelt. This routine uses the simple degree-day approach to calculate snowmelt.

$$Snowmelt = CFR * CFMAX * (T_a - TT)$$

where *CFMAX* is the degree-day melting factor (mm/°C – day), *TT* is the threshold temperature (°C), *CFR* is the refreezing factor, and T_a is the hourly air temperature.

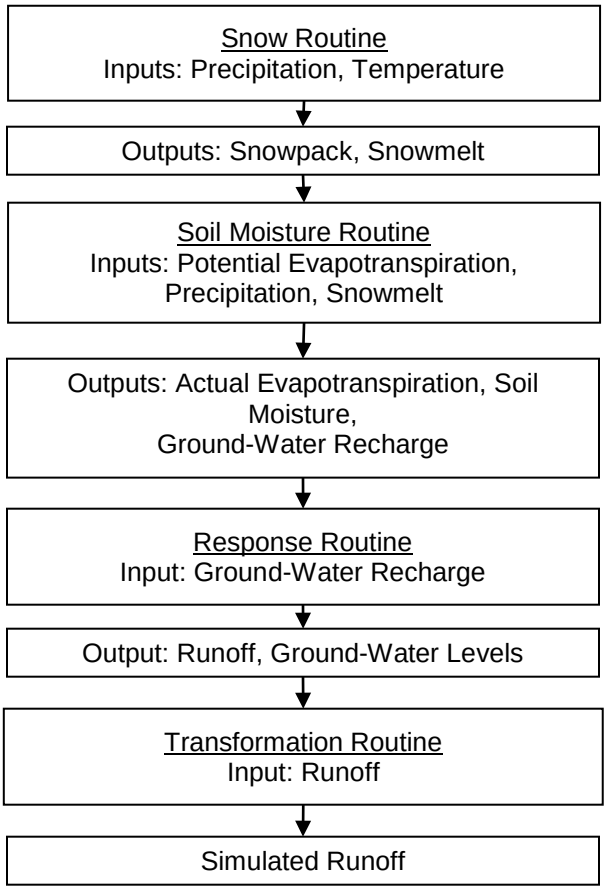

Figure 136. HBV routines and input data.

The soil moisture accounting routine takes the potential evapotranspiration (or pan evaporation), precipitation, and snowmelt to calculate actual evapotranspiration, soil moisture, and any groundwater recharge (Figure 137). The parameters needed to calculate these processes are limit

of potential evapotranspiration (LP), maximum soil moisture (FC), and beta, a shape coefficient that controls the contribution to the response function.

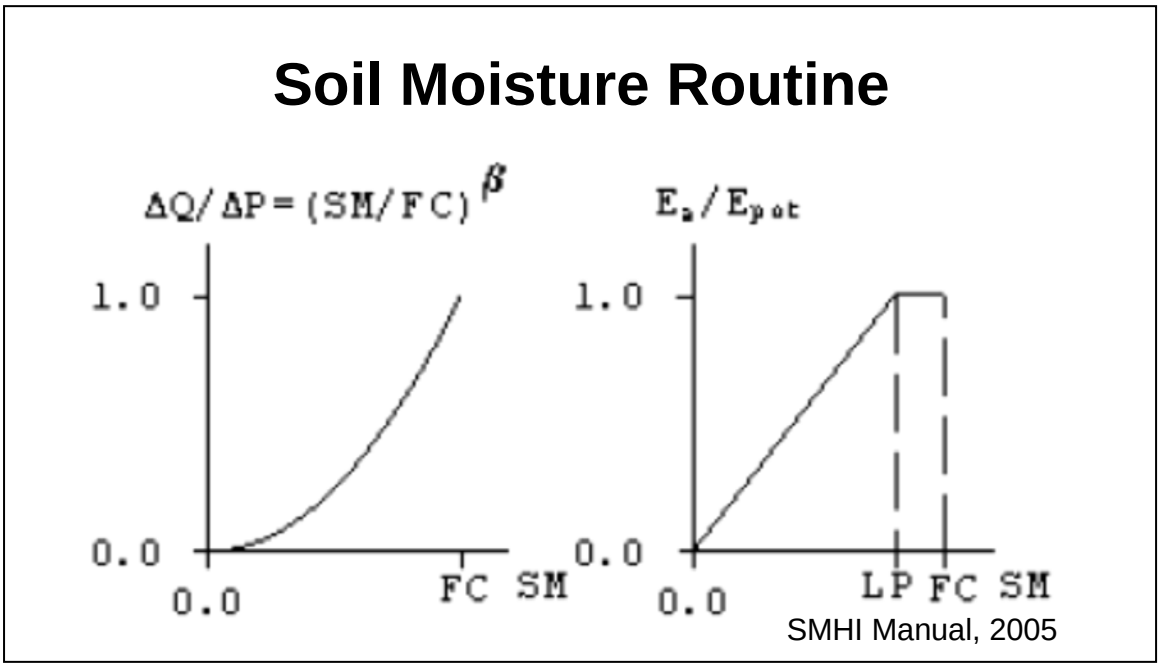

Figure 137. HBV soil moisture routine (SMHI, 2005).

The response routine transforms or routes excess water from the soil moisture zone to runoff (Figure 138 and Figure 139). In our simulations, we chose an upper reservoir with two outlets. Flow is controlled by recession constants (k). Again, for these simulations, no lower reservoir represents true groundwater base flow, so percolation to the lower response box (PERC) is set to zero or a very low value to represent continuous permafrost, blocking any percolation to a lower aquifer. The last routine in the simulation is the transformation routine to obtain the proper shape of the hydrograph. The parameter used is MAXBAS (units of days).

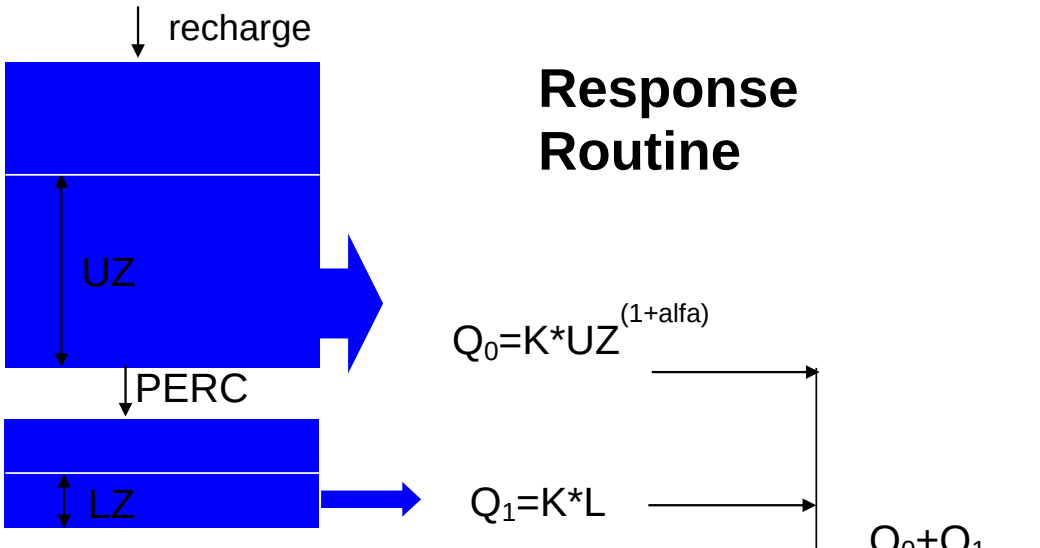

Recharge: input from soil routine (mm/day)
UZ,LZ:Threshold parameter
K: Recession coefficient (/day)
Qi: Runoff component (mm/day)
alfa: nonlinearity parameter
PERC: parameter to describe flow from upper (fast) to lower (slow) reservoir

Figure 138. Response routine (modified from Seibert, 2005).

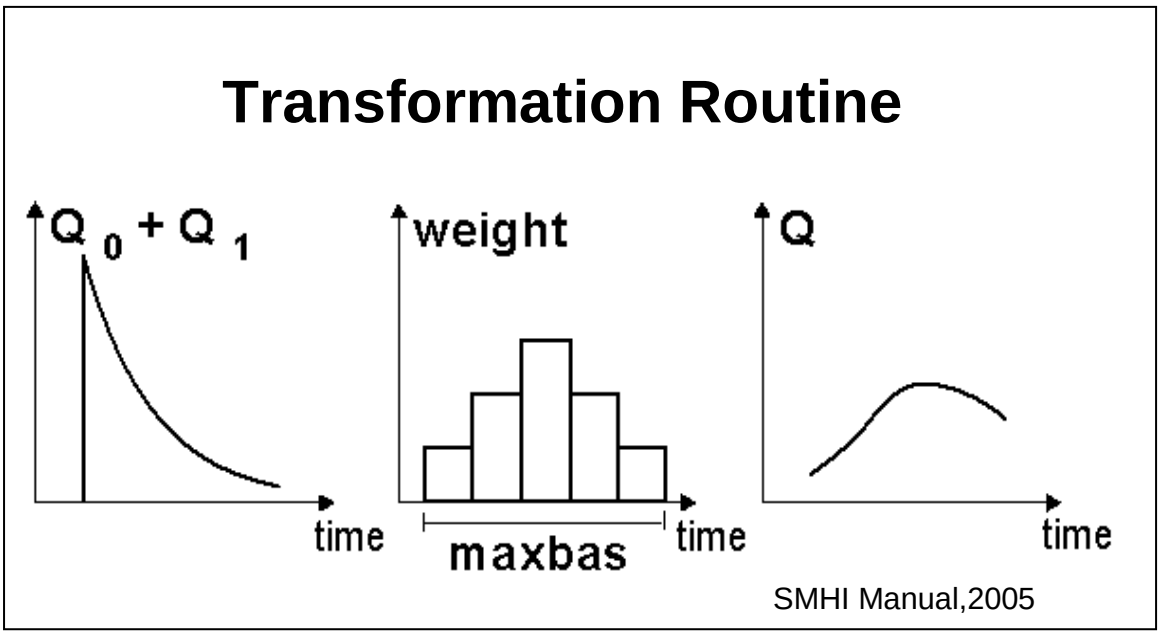

Figure 139. Transformation routine (SMHI, 2005).

5.3.2 HBV Model Calibration Approach

Initial parameter ranges were based on any known physical properties of the basin, ranges recommended by SMHI for use with the HBV model, and existing literature values (such as Hinzman,1990; Carr, 2003; Seibert, 2005). The purpose of this procedure was to determine if any parameters could be easily identifiable within the initial parameter ranges.

The goal is to minimize one or more objective functions. The objective functions we use are defined as:

1. The Nash-Sutcliffe coefficient, R-efficiency

$$\text{R-efficiency} = 1 - \frac{\sum (Qsim - Qobs)^2}{\sum (Qobs - \overline{Qobs})^2}$$

where 1 is a perfect fit and
Qsim = Simulated discharge
Qobs = Observed discharge.

2. Accumulated difference (mm)

$$\text{Accum. Diff} = \sum (Qsim - Qobs) * multiplier$$

where 0 is a perfect fit and the multiplier takes into account the drainage area.

3. Relative accumulated difference (%)

$$\text{Rel. Accum. Diff} = \frac{\sum (Qsim - Qobs)}{\sum Qobs} * 100$$

where 0 is a perfect fit.

HBV allows for a change in parameters with time; thus, some of the parameters may be different depending on whether it is spring or summer due to changing conditions (for example, thawing of active layer).

Our approach is to define a set of parameters that will apply to basins with similar characteristics. For example, one parameter set is developed for upland (high gradient) basins

such as Upper Kuparuk, Anaktuvuk, and the upper Sagavanirktok. Another parameter set is developed for the low-gradient basins, such as the Putuligayuk and Kadleroshilik. The model can be improved for each year; however, for this simulation, the goal is to find a unique set of parameters that can somewhat adequately simulate flow in any given year. The idea is that this set of parameters can be used in similar ungauged basins. Table 65 lists the HBV model parameter value or range used in each routine.

Table 65. HBV model parameters.

HBV Model Parameters			
Snow Routine		**Value**	**Units**
TT	Threshold Temperature	-0.7 to 2	°C
CFMAX	Snowmelt Factor	3 to 4	mm/C-day
CFR	Refreezing Factor	0.05	unitless
WHC	Water-holding capacity of snow	0.4	unitless
Soil Moisture Routine			
FC	Max Soil Moisture	10-50	mm
LP	Limit for potential ET	0.9	unitless
BETA	Shape Factor	0.2-2	unitless
Response Routine			
K4	Recession coefficient	0.01-0.2	/day
PERC	Controls flow from upper to lower reservoir	0-0.1	mm/day
Hq	Discharge at which recession coefficient Khq applies	River specific	mm/day
Khq	Recession coefficient	0.17-0.4	/day
alfa	Measure of non-linearity	0.9-1.1	unitless
Transformation Routine			
MAXBAS	Number of days in transformation	1.5	day

5.3.3 High-Gradient Arctic Rivers

The input data (precipitation and air temperature) are examined for data-quality issues, and the HBV model is applied to several years of data for the Anaktuvuk, Upper Kuparuk, and Upper Sagavanirktok. These high-gradient basins mostly lie in the Foothills and Mountain region of the

Brooks Range, up the 2500 m elevation. Annual peak flow may be snowmelt or rainfall, depending on basin size. Record peak discharge may be rainfall generated.

The Anaktuvuk River discharge has been measured by UAF since 2009, and the Upper Kuparuk has been measured by UAF since 1993. The Upper Sagavanirktok has been measured by the USGS since 1983; however, no complementary meteorological data (such as air temperature and precipitation) throughout the basin are available except for the years 2006–2010 (as part of the Bullen project).

HBV model parameters developed for the Upper Kuparuk (which has more years of available data) are applied to the other high-gradient basins. Attempts are made to use a unique parameter set that can adequately simulate all years of data for each basin. The years used in the simulation are selected based on the quality and availability of the data and the years that show a range of variability in hydrologic processes. The years presented in this section include 2009, when observations began at Anaktuvuk River as part of the Umiat project, along with the extreme-condition years of 2002 (high-flow summer events) and 2007 (dry year) for the Upper Kuparuk.

5.3.3.1 Results 2002

The year 2002 on the Upper Kuparuk is characterized by a normal snowmelt flow and a high summer flow due to a record precipitation event. Initially, winter precipitation data (end-of-winter maximum snow water equivalent and ablation) from the Upper Kuparuk station are used. These data are now augmented with additional snow survey data collected in the Upper Kuparuk, from North Headwaters, East Headwaters, Green Cabin Lake, Upper Headwaters, West Headwaters, and Imnavait. Hourly summer precipitation data from the Upper Kuparuk, North Headwaters, East Headwaters, Green Lake Cabin, Upper Headwaters, West Headwaters, and Imnavait station are used. Thiessen polygons are created to weight each station's summer precipitation data. Daily pan evaporation from Imnavait is used for potential evapotranspiration, and hourly air temperature and discharge from the Upper Kuparuk station and gauge are used.

In 2002 (Figure 140), spring and early summer runoff was relatively low, but an August storm (mixed rain and snow) caused a record high-flow event on many high-gradient rivers in the

region. The model did poorly at predicting the magnitude of this summer flood; it predicted a peak flow of 81 m^3/s (2860 ft^3/s), compared with the observed peak flow of 120 m^3/s (4240 ft^3/s). Clearly, we struggled to estimate the peak discharge and precipitation during this storm. Additionally, our precipitation gauges were inundated with snow, and our stilling well washed out 6 hours after the peak stage. As the peak flow was not physically measured, we used our stage-discharge relationship and the indirect method (Manning's equation) to estimate peak discharge. The precipitation entered into the model is only what was measured by the tipping buckets, which do not adequately measure snow.

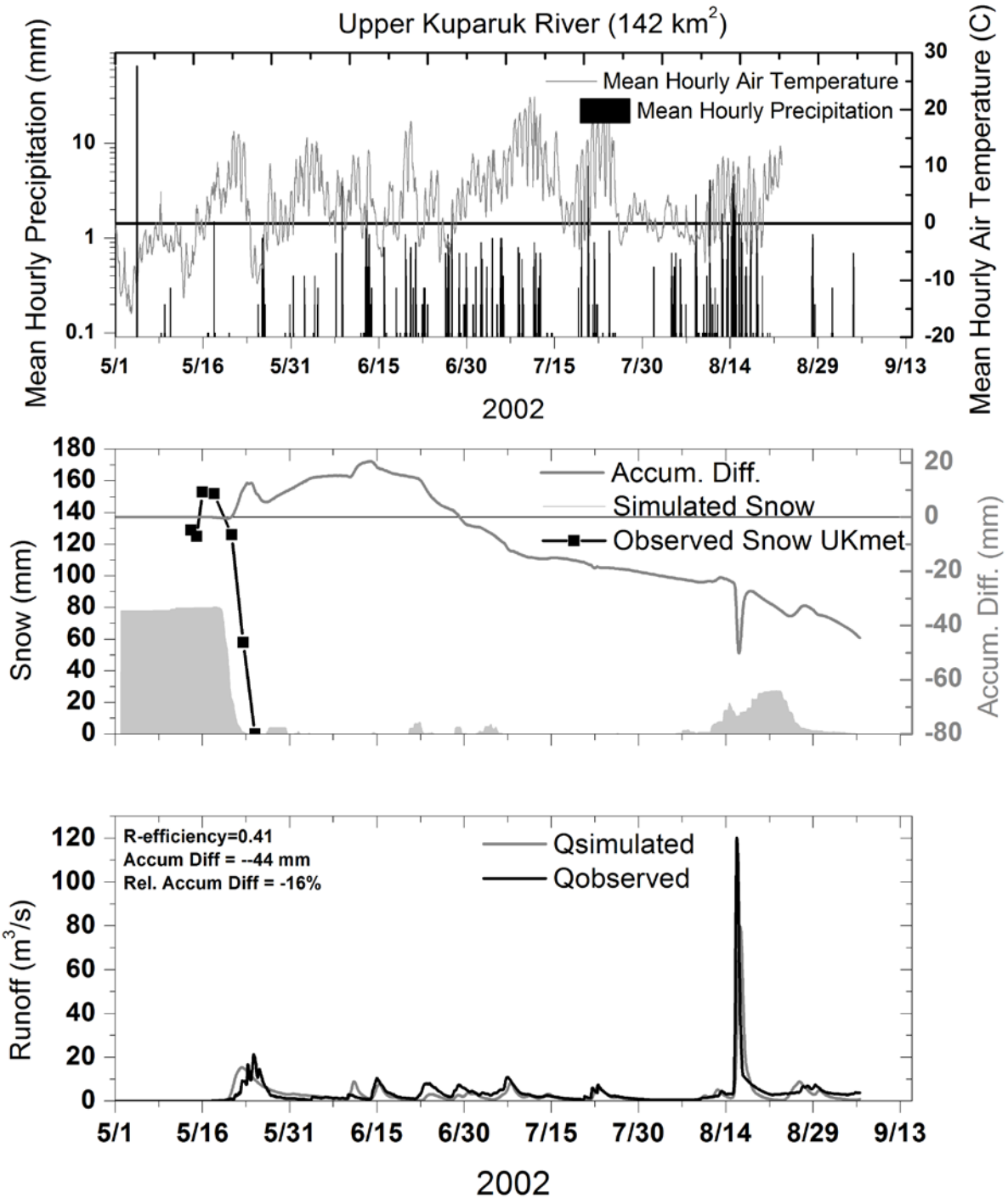

Figure 140. Upper Kuparuk HBV model results, 2002.

5.3.3.2 Results 2007

The year 2007 is a below average snowmelt year and a very dry summer (lowest summer precipitation on record, *n*=20 years at Upper Kuparuk station), with very few summer precipitation events causing runoff. Winter precipitation data (end-of-winter maximum snow water equivalent and ablation) from the Upper Kuparuk station are used. Again, additional snow survey data collected in the Upper Kuparuk, from North Headwaters, East Headwaters, Green Cabin Lake, Upper Headwaters, West Headwaters, and Imnavait are used. Hourly precipitation data from Upper Kuparuk, North Headwaters, East Headwaters, Green Lake Cabin, Upper Headwaters, West Headwaters, and Imnavait stations are used. Thiessen polygons are created to weight each station's summer precipitation data. Daily pan evaporation from Imnavait is used for potential evapotranspiration, and hourly air temperature and discharge from the Upper Kuparuk station and gauge are used.

The model predicted the timing and peak of the snowmelt event; however, the model slightly overpredicted the total volume of snowmelt runoff, as seen on the hydrograph during recession. An adjustment to the recession coefficients will likely resolve this issue, but our goal is to find a unique parameter set that may be applied to many basins during multiple years. The summer of 2007 was very dry, but the model did a good job of predicting the few late-summer runoff events (Figure 141) with a Nash-Sutcliffe coefficient of 0.82 during summer. Several very small runoff events in early June were predicted by the model that did not occur.

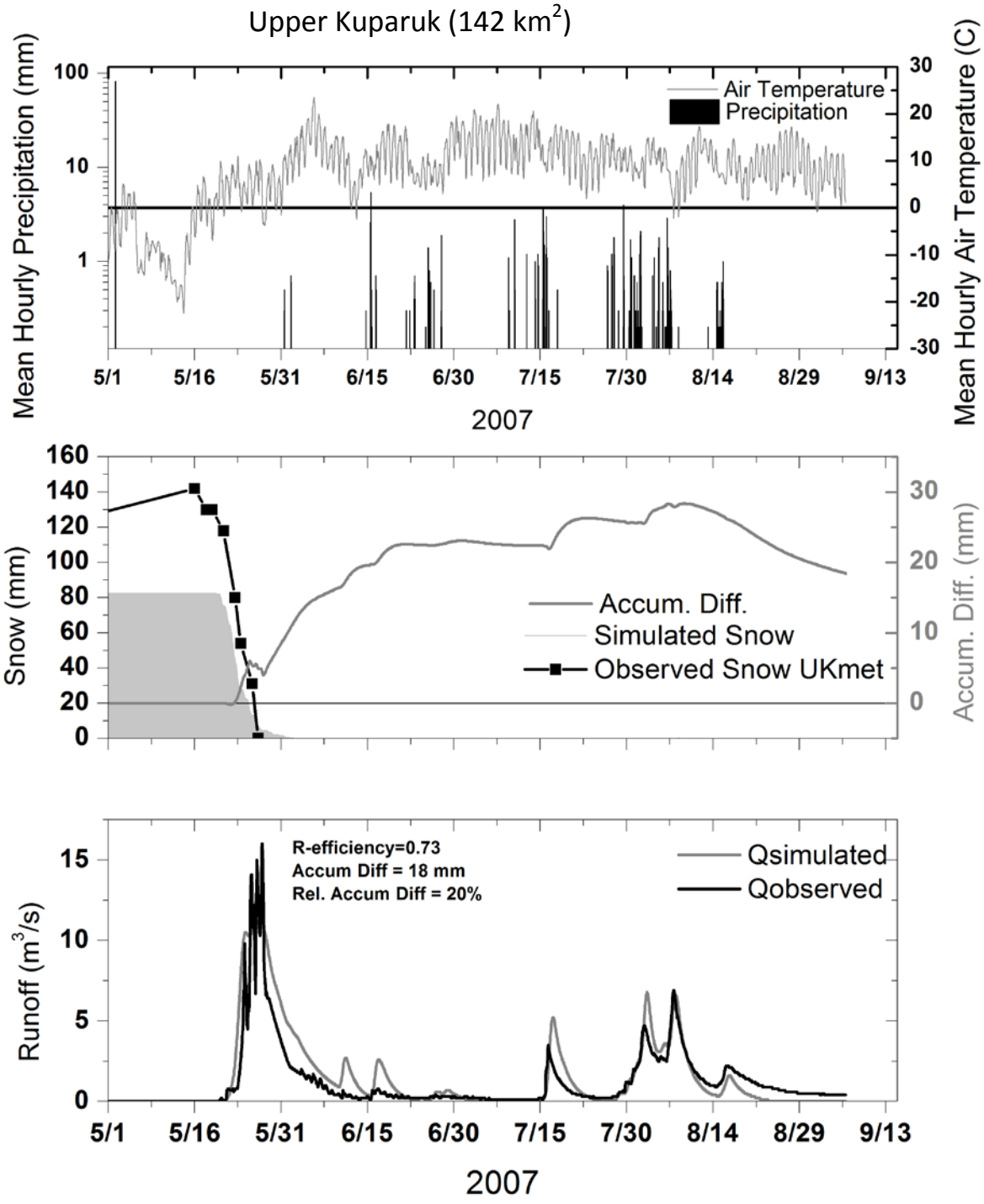

Figure 141. Upper Kuparuk HBV model results, 2007.

5.3.3.3 Results 2009

The year 2009 was an interesting year to observe hydrology on the North Slope. An unusual early warm-up in late April resulted in flow at many larger high-gradient rivers flowing out of the Mountain and Foothills regions. Additionally, an early-June widespread rainfall event caused very high flows on nearly all high-gradient rivers in the study area during snowmelt recession when the active layer has not yet developed. The year 2009 is the first year where flow and meteorologic data are available for the Anaktuvuk River basin.

For the Upper Kuparuk basin, winter precipitation data (end-of-winter maximum snow water equivalent and ablation) from the Upper Kuparuk station are used. Again, additional snow survey data collected in the Upper Kuparuk, from North Headwaters, East Headwaters, Green Cabin Lake, Upper Headwaters, West Headwaters, and Imnavait are used. Hourly precipitation data from Upper Kuparuk, North Headwaters, East Headwaters, Green Lake Cabin, Upper Headwaters, West Headwaters, and Imnavait stations are used. Thiessen polygons are created to weight each station's summer precipitation data. Daily pan evaporation from Imnavait is used for potential evapotranspiration, and hourly air temperature and discharge from the Upper Kuparuk station and gauge are used.

The model did not adequately simulate snowmelt on the Upper Kuparuk for 2009 (Figure 142), possibly due to the model's inability to simulate snow or ice damming. The observed discharge in 2009 had irregular fluctuations (in addition to diurnal fluctuations). The simulated discharge lacks fluctuation. Several peaks in early June (due to the early rain events) were not accurately simulated, likely because the parameter set during this time still applies to the snowmelt period (summer parameter set begins in mid-June). The model adequately predicted the timing of the summer peaks, but slightly over-predicted the magnitude of the flow.

The Upper Sagavanirktok, which is measured by the USGS, was simulated in 2009. Basin average end-of-winter snow water equivalent from snow survey sites in the Sagavanirktok basin are used. Actual ablation from the Upper Kuparuk station is compared with simulated ablation. Air temperature and rainfall from Accomplishment Creek, Sagwon Hill, Ribdon, Sag-Ivishak,

Upper Kuparuk, and Juniper Creek meteorological stations are used as input data. Potential evapotranspiration is estimated by the Priestley-Taylor method using Upper Kuparuk, Accomplishment, and Sag-Ivishak station data.

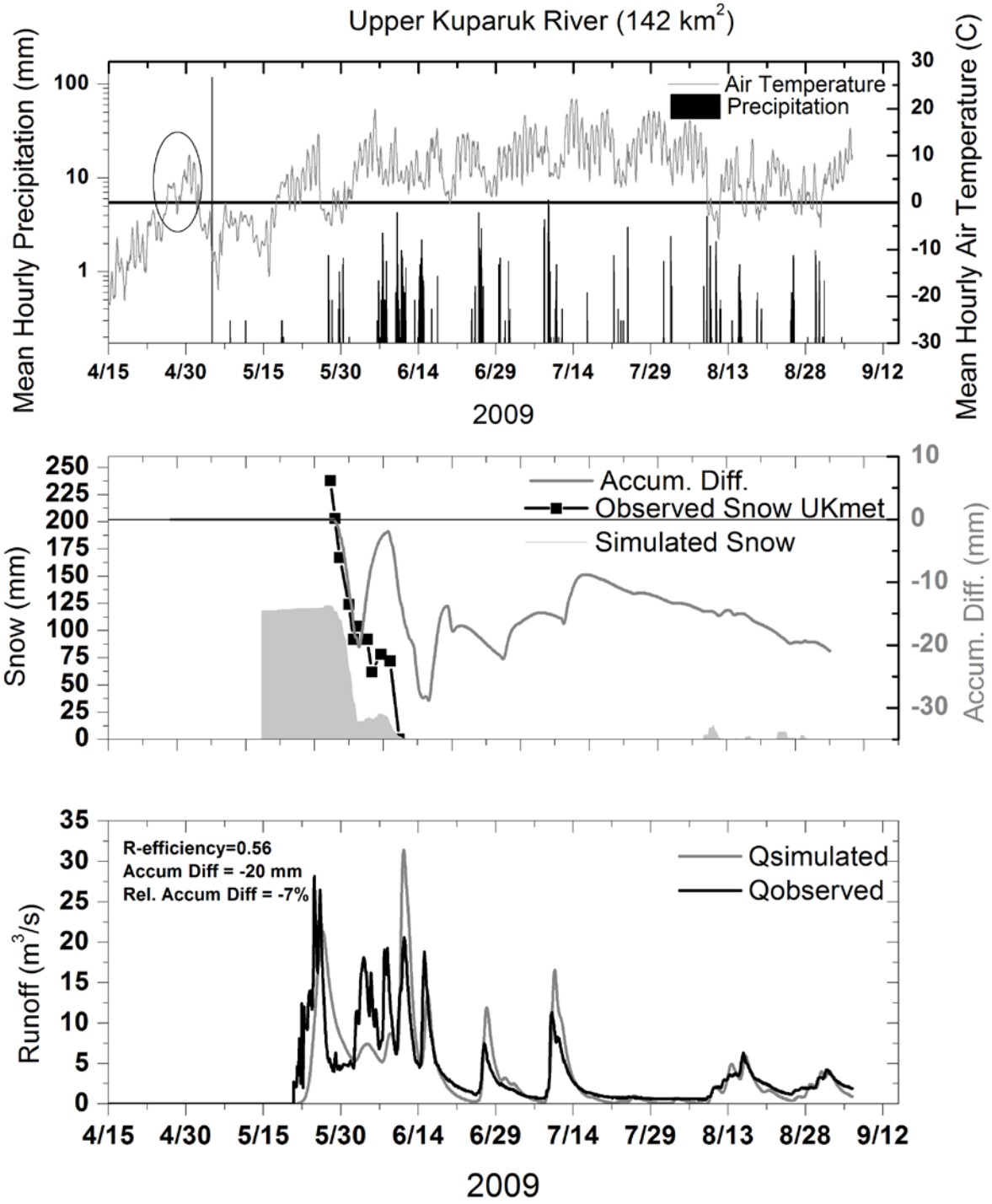

Figure 142. Upper Kuparuk HBV model results, 2009. The model did not predict an early warm-up due to forcing the model to begin all runoff in late May.

The Anaktuvuk River discharge measurements began in 2009. Basin average end-of-winter snow water equivalent is measured and used as input into the model. Only six measurements of snow water equivalent were used to calculate the basin average for the Anaktuvuk. Ablation data from the Upper Kuparuk are used for comparison with simulated ablation. Air temperature and rainfall from Anaktuvuk, Itikmalakpak, May Creek, Nanushuk, and Tuluga meteorological stations are used with equal weight factors. The Priestley-Taylor method is used to estimate potential evapotranspiration at each station.

Results for 2009 showed relatively good timing for most runoff events for both the Upper Sagavanirktok (Figure 143) and Anaktuvuk (Figure 144) Rivers. The Nash-Sutcliffe coefficient for the Sagavanirktok simulation is 0.79, and for the Anaktuvuk, 0.76. The simulation of peak snowmelt discharge may be acceptable, but good-quality continuously measured flow was not available for comparison and volume errors are likely for both rivers during snowmelt. An unusual early warm-up in late April results in the model predicting early runoff for both the Anaktuvuk and the Sagavanirktok. However, visual observations indicate that flow did occur during this warm-up period, but was not measured. The timing of summer peaks for the Sagavanirktok River was generally adequate; however, the simulation slightly underpredicted the magnitude for a few events. For the Anaktuvuk River, the simulation produced acceptable results for most of the summer events, as the timing and magnitude were generally simulated adequately.

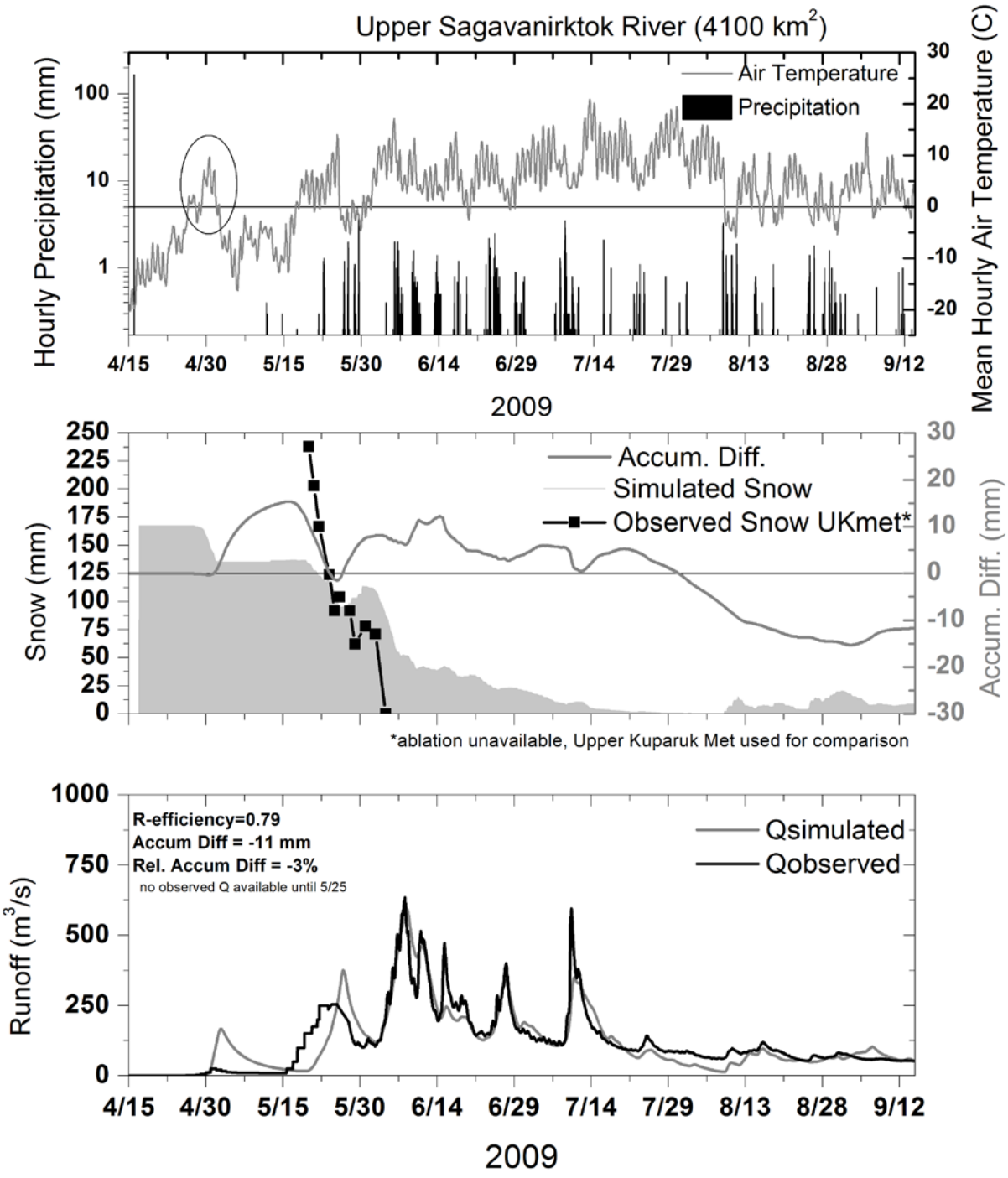

Figure 143. Upper Sagavanirktok HBV model results, 2009. An unusually early warm-up in late April resulted in the model predicting flow during late April/early May. No April/early May measurements were made to confirm model results but many high-gradient rivers in the region were observed to be flowing.

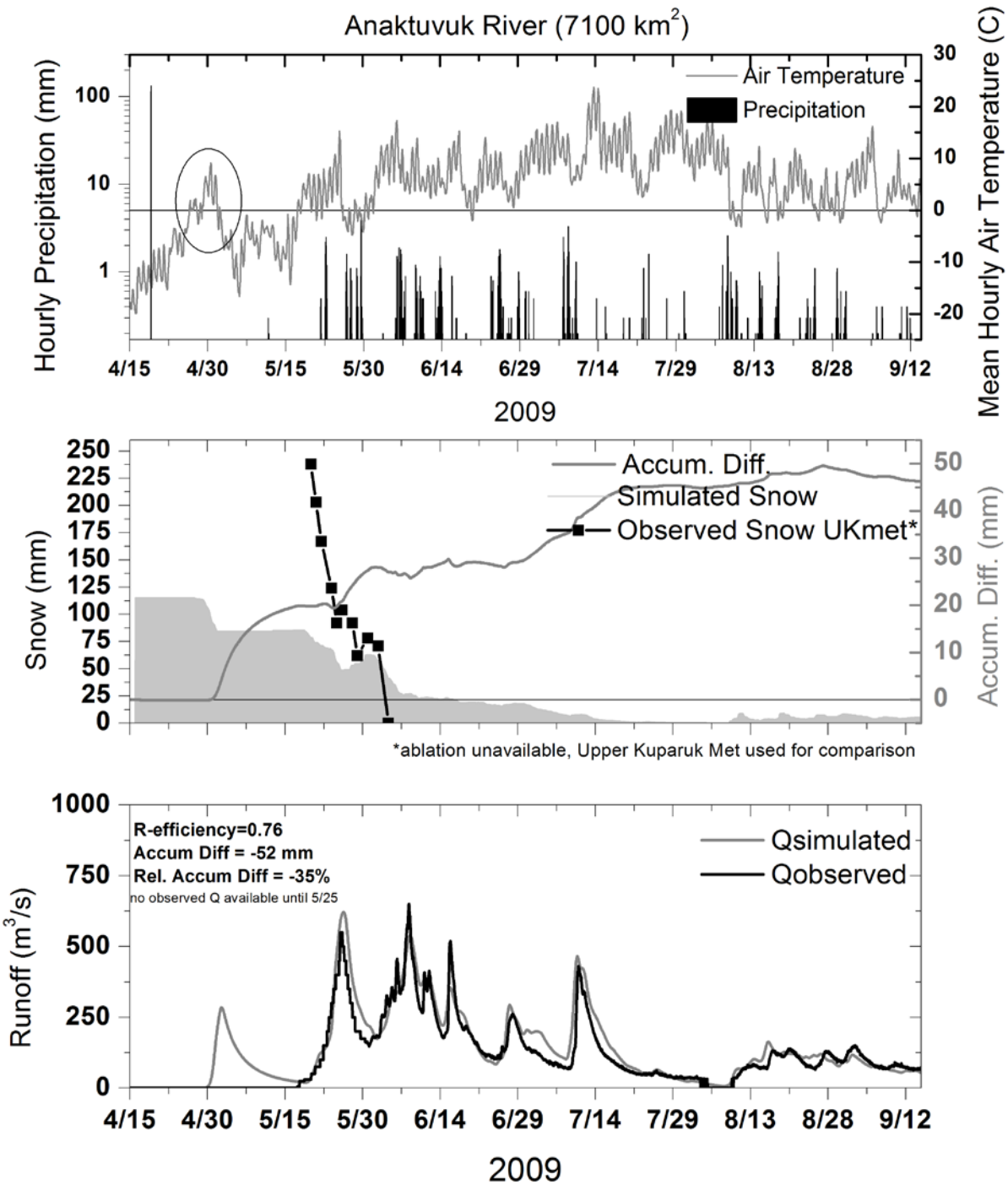

Figure 144. Anaktuvuk River HBV model results, 2009. An unsually early warm-up in late April resulted in the model predicting early flow. Early flows were observed; however, no early measurements were made to confirm the model results.

5.3.4 Low-Gradient Rivers

Snowmelt is the main factor governing the runoff response in the low-gradient Coastal Plain rivers, such as the Putuligayuk (471 km^2)and Kadleroshilik (1500 km^2) Rivers. Hydrographs shown previously (Figure 126) for the Putuligayuk indicate that summer flows are minimal (the river is mainly in recession after snowmelt) due to lack of rainfall, available surface storage, and high evaporation. The Putuligayuk, which lies entirely in the Coastal Plain region, has been measured by UAF since 1999. The Kadleroshilik River was measured by UAF in 2009 and 2010, and at least 75% of the basin is within the Coastal Plain, with the rest in the Foothills. In this section, we examine the Putuligayuk River during 2007 and 2008 and the Kadleroshilik River during 2009 and 2010. All simulations of the Putuligayuk and Kadleroshilik use a single parameter set. As shown in the results below, defining a unique parameter set for the Coastal Plain rivers that will produce acceptable results each year remains a challenge.

5.3.4.1 Putuligayuk River

The year 2007 was an average snowmelt flow year; discharge peak was close to 70 m^3/s (2470 ft^3/s). Winter precipitation data (end-of-winter maximum snow water equivalent) from West Dock, Betty Pingo, and Franklin Bluffs were used as precipitation inputs in the model. Hourly air temperatures from these stations also were used when available. Basin average end-of-winter maximum snow water equivalent was approximately 80 mm. Hourly river discharge at the UAF/WERC-operated gauge at the bridge on Spine Road was used. The results of the simulation are presented in Figure 145. The simulation is remarkably good, with a Nash-Sutcliffe coefficient of 0.90, and the timing and magnitude of the runoff peak are correct. Additionally, ablation appears to be properly simulated.

In 2008, the basin average end-of-winter average snow water equivalent was around 85 mm. The previous summer had record drought conditions, and as a result, the peak discharge was well below average at approximately 38 m^3/s (1342 ft^3/s). The results of the 2008 simulation are presented in Figure 146. The model did not predict the timing or magnitude of spring runoff accurately for this year. The predicted runoff occurred earlier and was greater than the actual runoff. This could be a result of data quality (air temperature), snow damming, or most likely the

inability of the model to simulate surface storage, an important component of the water budget in the basin. Because the previous summer was so dry, a larger-than-normal surface storage deficit developed.

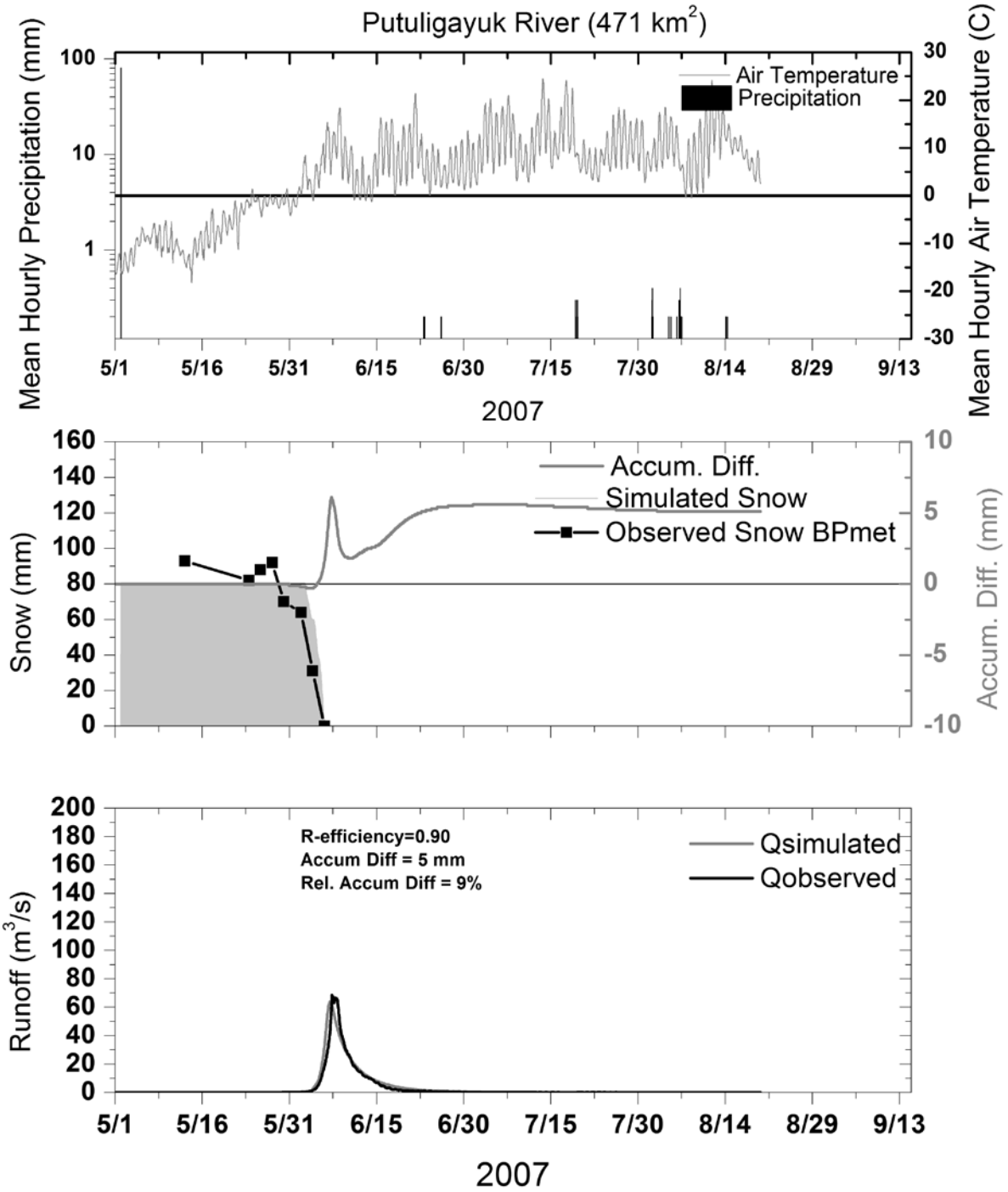

Figure 145. Putuligayuk River HBV model results, 2007.

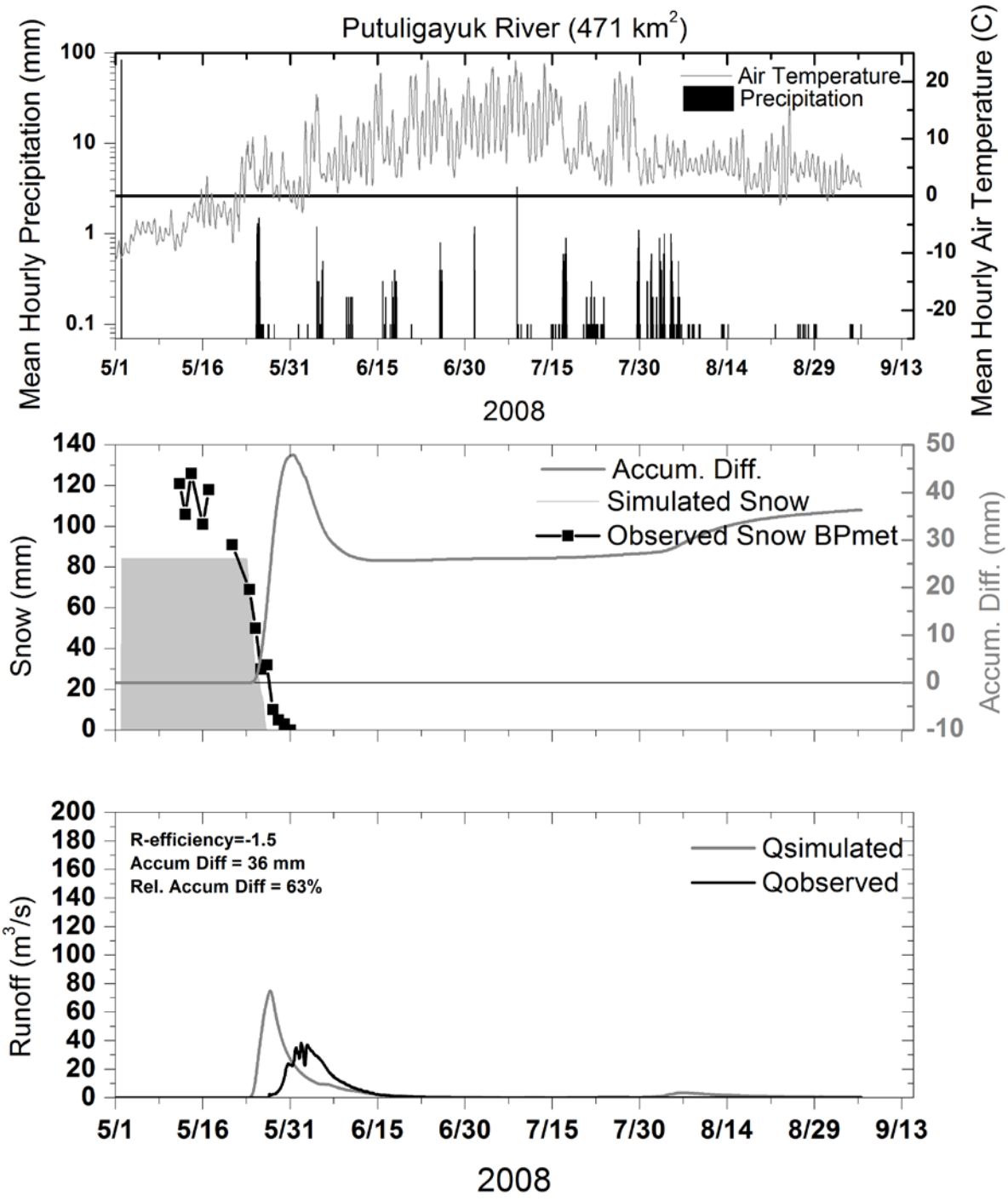

Figure 146. Putuligayuk River HBV model results, 2008.

5.3.4.2 Kadleroshilik River

Input meteorological data for the Kadleroshilik simulation were taken from the Upper and Lower Kadleroshilik stations, and flow data were observed at the Kadleroshilik River station in 2009 and 2010. Less meteorological and snow survey data are available in this basin compared with the Putuligayuk. The precipitation data for the basin are sparse, and the quality of the continuous discharge data is low due to such a short period of record and minimal discharge measurements. The identical parameters developed for the Putuligayuk were applied to the Kadleroshilik.

In 2009, an unusual early warm-up in late April resulted in early runoff at many of the larger high-gradient rivers. Temperatures were above freezing in the Kadleroshilik basin, but runoff did not begin until the end of May. The model predicted flow in the river in early May, so we forced the model to postpone runoff by delaying the input of precipitation until after the air temperatures dropped back to below freezing. By doing this, we were able to obtain good results with the timing and magnitude of the peak flow for 2009, and the Nash Sutcliffe coefficient was 0.85. Another solution would be to adjust the snow routine model parameters (such as threshold temperature, etc.).

In 2010, the simulation was poor in terms of the timing, but the magnitude of the peak runoff was well predicted. The simulated peak runoff occurred three days later than the actual peak. Additionally, the simulated ablation was also three days later than the observed ablation. This is likely due to the model parameter used in the snow routine. Additionally, some of the basin area lies in the Foothills region, which warms up earlier than the Coastal Plain region and may not be adequately captured by the set of model parameters. Distributing the basin into smaller areas (sub-basins) and assigning unique parameters for sub-basins may resolve this problem; however, there is a lack of data to do this satisfactorily.

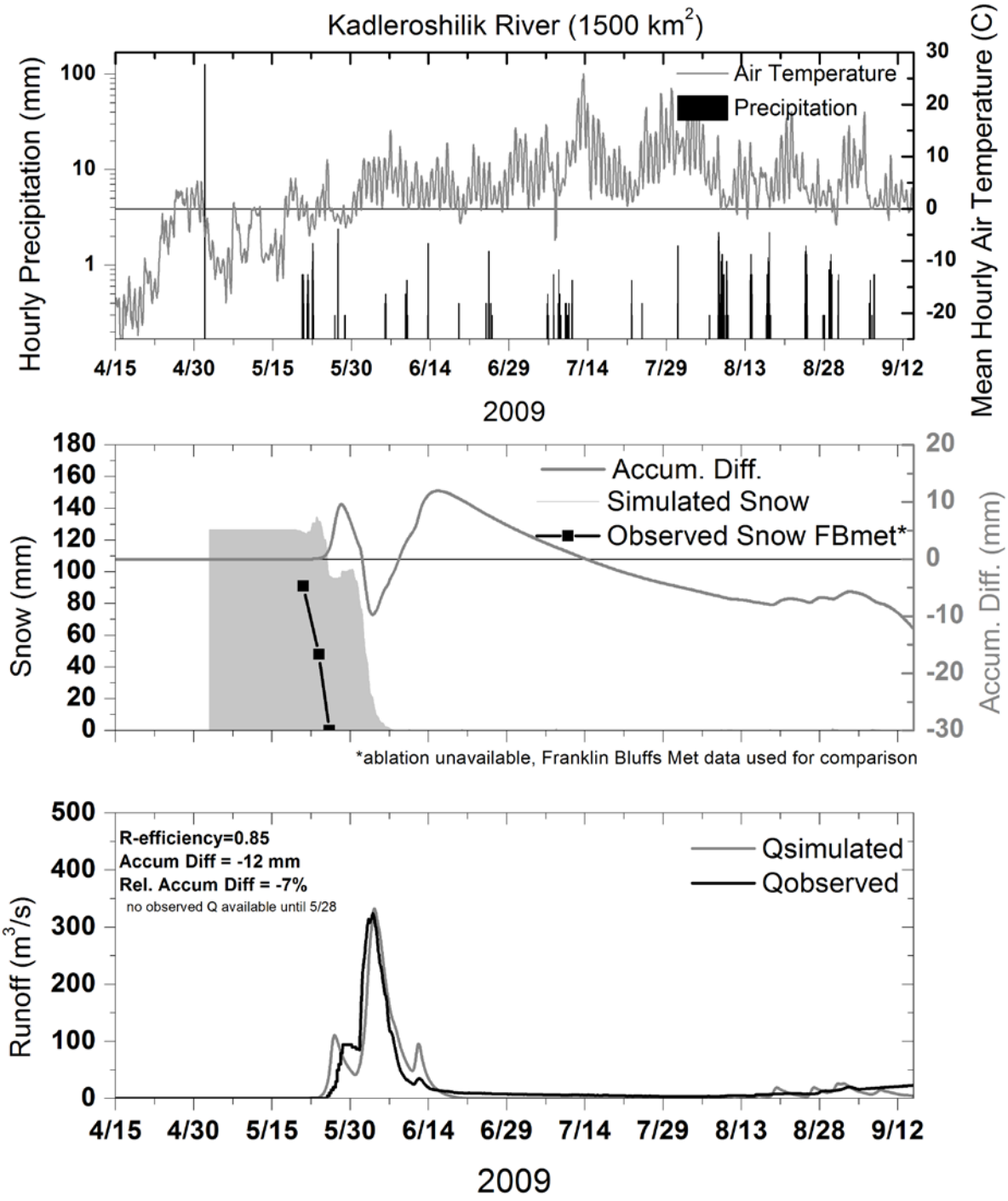

Figure 147. Kadleroshilik River HBV model results, 2009. Ablation data are unavailable for the basin, so Franklin Bluffs data are used.

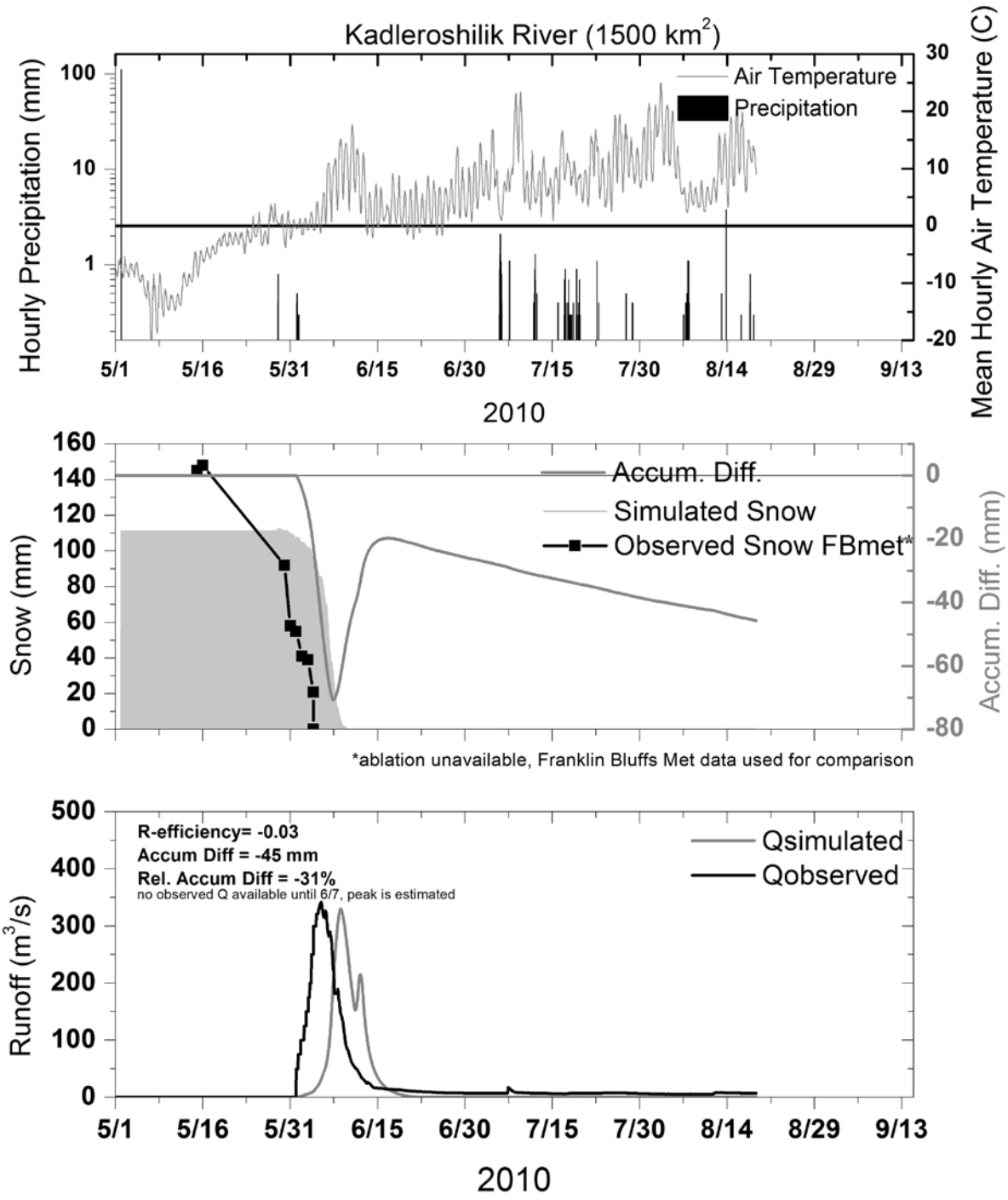

Figure 148. Kadleroshilik River HBV model results, 2010. Ablation data are unavailable for the basin, so Franklin Bluffs data are used.

5.3.5 Discussion

The model always overpredicted the volume of runoff during the spring runoff event, but it did a relatively good job at predicting the snowmelt peak and timing, which is partly controlled by the degree-day snowmelt factor and threshold temperature. We found that the model was sensitive to the average end-of-winter snow water equivalent for the basin, which impacts the peak and total volume of flow during the snowmelt runoff period. Improving the accuracy and precision of the end-of-winter snow water equivalent is a priority for accurate snowmelt runoff modeling, but it is not easy to quantify the spatial distribution of this heterogeneous snowpack, particularly over large basins.

The Nash-Sutcliffe coefficients were variable (ranging from less than 0 to over 0.90). A Nash-Sutcliffe coefficient less than 0 indicates that the mean discharge is a better predictor of flow than the simulation. An overall Nash-Sutcliffe coefficient was calculated for the entire year, and separate spring and summer coefficients were calculated.

For years with extreme flood events in the summer (such as 1999 and 2002), the model performs better, with a higher upper recession coefficient (k_0 closer to 1.0). However, for the flood event of 2002, the model does not perform well; the model predicts the timing of the runoff event, but cannot predict the peak discharge. This might be because at the beginning and end of this event, air temperatures were right around freezing and a significant amount of the precipitation fell as snow, which was not captured very well with our tipping-bucket precipitation gauges. Additionally, for flood events in both 1999 and 2002, a rainfall correction factor (RFCF) could be applied to improve model results for the peak, but doing so impacts the smaller flow events too much and should only be applied during an extreme event, which is not possible for prediction purposes. Currently the model is set up with only one set of snow routine parameters for the entire year. We could introduce a different set of parameters for the snow routine that only apply during the summer months, which may improve the results when we have summer mixed snow and rain events. In the summer when we have snow events, not only does the air temperature play a role in the melt, but also the heat stored in the active layer.

These results are promising, but it was found that the model could be improved with better input data (i.e., more spatially distributed data). When we added the snow water equivalent data from other snow-survey sites in the Upper Kuparuk basin, the snowmelt simulation improved. The Upper Kuparuk station, which has the highest snow water equivalent and snow depth in the basin, is not a good proxy for the basin-wide average ablation.

For two of the years the model performs poorly for the two Coastal Plain rivers. The main problem with poorly simulated years is the timing of snowmelt, which is mostly controlled by the threshold temperature for snowmelt parameter and the observed hourly air temperature. For the Putuligayuk, the model performs well with the threshold temperature below 0°C in some years, but other years the model predicts an early runoff, and the threshold temperature must be increased to above zero in order for the timing of runoff to match the observed flow. Additionally, the model is sensitive to the input of end-of-winter snow water equivalent. For the Putuligayuk River, runoff does not generally begin (snow damming delays runoff) until the snow cover has disappeared. However, for the Kadleroshilik, with about 20% of the basin in the Foothills region to the south (up to 375 m maximum basin elevation), runoff begins in the warmer upper part of the upper basin before the snow has melted in the lower basin. The 2010 simulated snowmelt peak runoff occurred a few days later than actually observed. The poor results of model timing may be due to significant year-to-year variability of the physical processes that affect snowmelt runoff in Coastal Plain basins and inadequate input of SWE data. Processes such as snow damming can delay runoff for many days (Kane et al, 2009). The conditions of the previous fall also greatly impact the spring runoff ratio and should be incorporated into the simulation. The snowpack also recharges the thousands of tundra lakes, ponds, and wetlands, and this process may not be adequately described in the HBV model. Lastly, the limited distribution of snow water equivalent measurements within the basin may result in a poor estimate of basin average snow water equivalent for the model.

We anticipate that this unique parameter set will have limitations (i.e., perform reasonably in some years and poorly in other years) due to our inability to track soil conditions during the year. As we gain an understanding of the soil moisture conditions with data from the Bullen and Foothills/Umiat projects, we can improve our input data (initial soil moisture conditions) and use

soil moisture to support model calibration. The use of runoff models in ungauged basins for predicting runoff in engineering applications should exercise an adequate safety factor for precipitation. Additionally, the model should always be validated in other basins of similar size and condition that are limited by lack of data.

5.4 Historical Floodplain Analysis

Historic imagery is used to examine potential floodplain changes between the date of the old imagery and the date of the modern imagery. The photos may show channel migration and vegetation changes, and knowing the dates of the photographs, we can calculate rates of change. Historic imagery is available in 1948 (Anaktuvuk 8/1/1948, Chandler 7/18/1948, and Colville 7/18/1948) and June 1978 (Itkillik). Modern imagery is available from ADOT&PF for June 2009. The figures below show the old and new imagery at each of the four proposed major bridge crossings in the Umiat road corridor. Modern imagery is already georeferenced (in State Plane Coordinate System), so old imagery is registered to the new imagery using tie-points. Both the historic and the modern images show the rivers at lower flow summer conditions, with the channel only partially filled with water and most gravel bars exposed. The approximate location of the historic "low flow" channel is outlined in each figure. The proposed bridge locations are denoted by a black straight line, when available. Arrows on the figures indicate channel migrations and/or encroachment of vegetation.

5.4.1 Itkillik River

Figure 149 shows the imagery of the Itkillik River historic (1978, Landsat/infrared) and Figure 150 shows the modern (2009) channel and floodplain. The 1978 infrared image indicates the main river channel as dark blue and lakes as black. The photos taken during low-flow summer conditions show that a small side channel (located approximately 0.62 km [0.4 mi] downstream from the proposed crossing) is not flowing. This small channel is typically flowing at discharges above ~70 m^3/s (2400 ft^3/s). When comparing the two photos, the channel geometry remains the same over 30 years in the vicinity of the proposed bridge crossing. The Itkillik River basin is a long and narrow basin and the river valley is narrow, with the channel incised at the location of the crossing. The cross section of the Itkillik River previously discussed in Section 4.12.1 and

Figure 102 demonstrate the narrow channel geometry. One difference between the two photographs is that a few of the smallest ponds within the floodplain appear to have dried up.

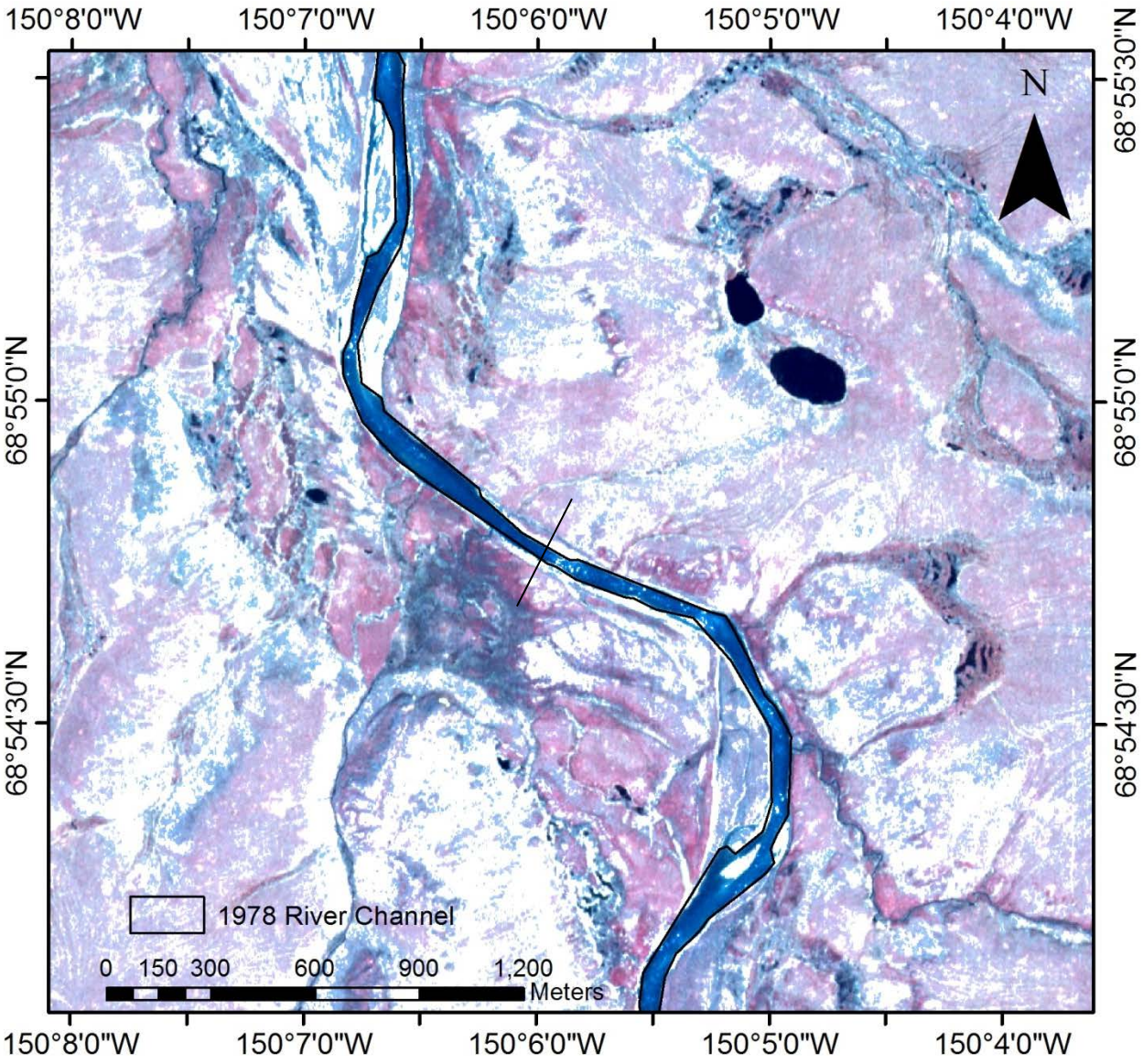

Figure 149. Itkillik River historic aerial imagery (June 1978). Black line is proposed bridge crossing.

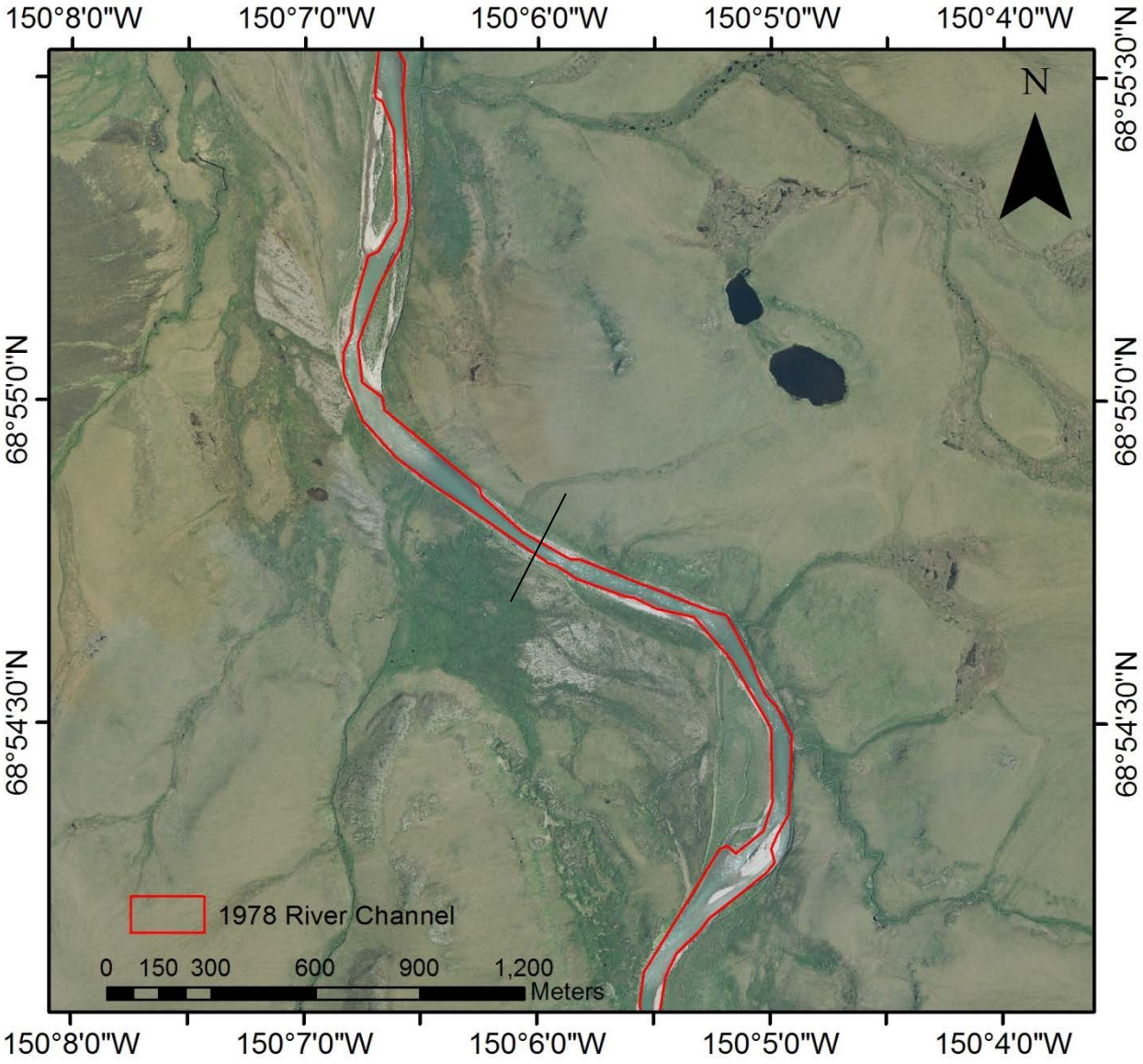

Figure 150. Modern Itkillik River aerial imagery (June 2009). Historic (June 1978) river outline appears in red. Black line is proposed bridge crossing.

5.4.2 Anaktuvuk River

Figure 151 shows the historic (1948) and Figure 152 shows the modern (2009) images for the Anaktuvuk River floodplain. Both images are taken at lower summer flows that are probably less than ~150 m^3/s (or 5200 ft^3/s). The Anaktuvuk River floodplain is very wide, up to 3 km (or 2 mi) in the vicinity of the proposed bridge crossing. There is a higher spatial coverage of shrubs within the floodplain and active channel in the modern image (2009) than in the old image

(1948), a change typical of the North Slope of Alaska (Tape et al., 2006). In the 2009 image, at the proposed crossing, the main active channel (during high flows) is up to 600 m wide, with several smaller channels that flow (during high flows) within the floodplain zone. In the 1948 image, the active main channel appears to be larger than it is today, due to the lack of shrubs and more-exposed gravel, particularly in the area north of the proposed crossing. At the proposed crossing location (at the large bend in the modern main channel), the main channel has migrated toward the east approximately 250 m (820 ft) through what was once dense shrubs in the 1948 image (as indicated by the white arrow in the photograph). Just south of the bend in the modern photograph, shrubs have expanded onto a gravel bar that was part of the historic main channel (as indicated by the black arrow in the photograph). The large lake in the northeast quadrant of the historic images appears to have decreased in area in the modern image.

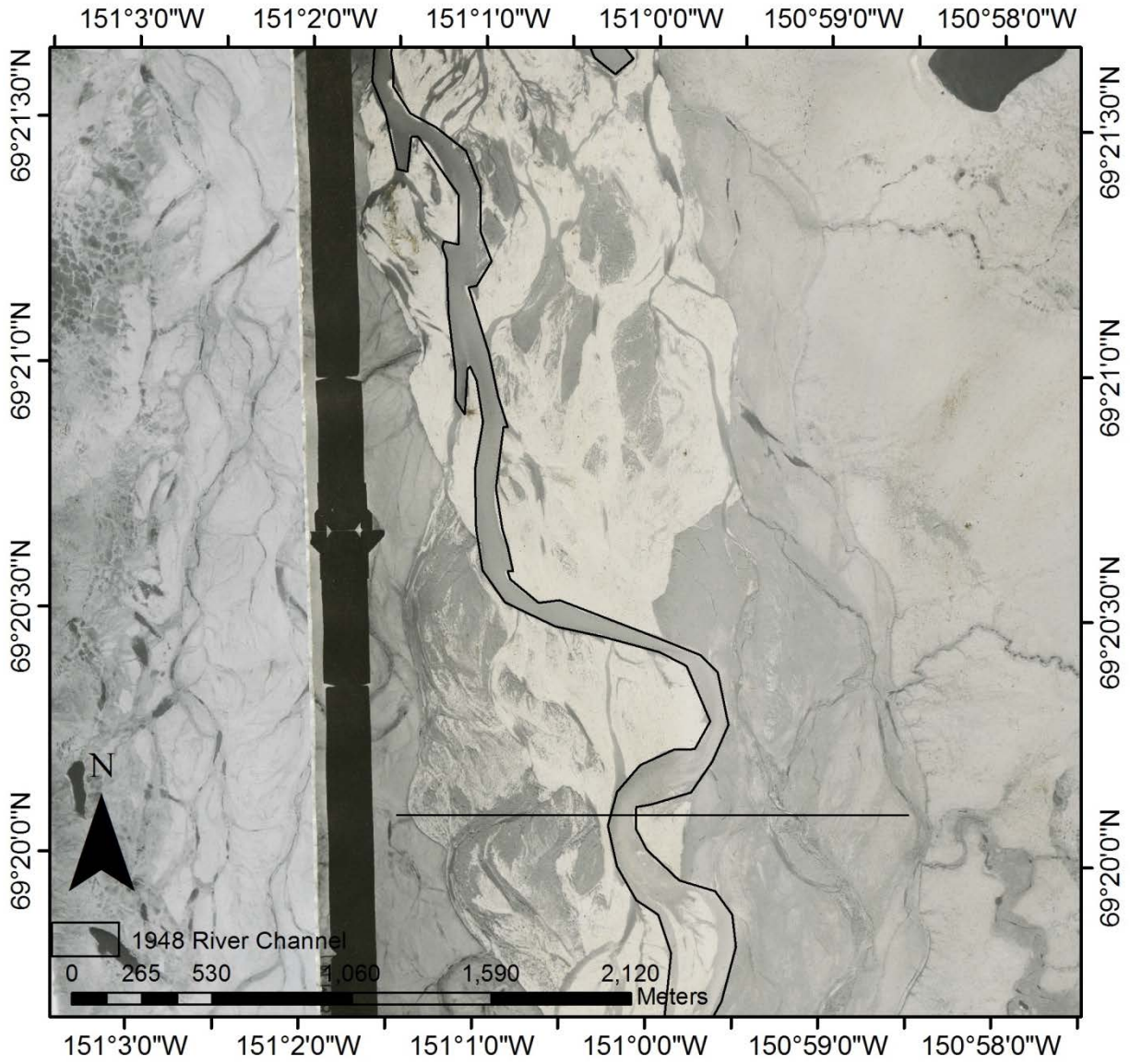

Figure 151. Historical Anaktuvuk River aerial photograph (August 1, 1948). Black line is proposed bridge crossing.

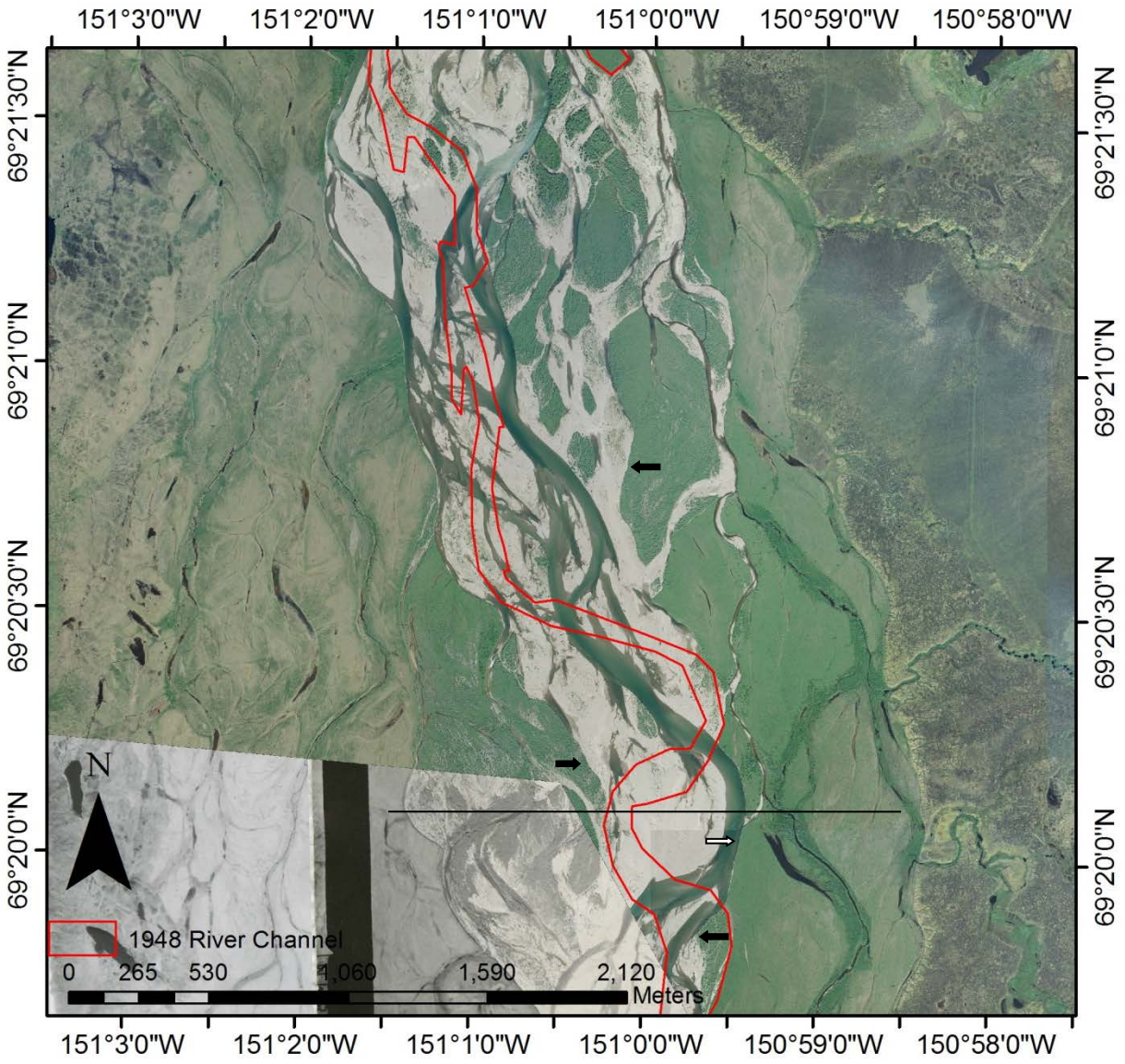

Figure 152. Modern Anaktuvuk River aerial photograph (June 2009). Historic (1948) river outline appears in red. Black line is proposed bridge crossing. White arrow indicates channel movement; black arrows indicate changing shrub coverage.

5.4.3 Chandler River

Figure 153 and Figure 154 show the historic (1948) and modern images (2009) for the Chandler River. Both photos are representative of lower-flow summer conditions (less than 150 m^3/s or 5200 ft^3/s). The floodplain is over 3 km (2 mi) wide. The channel width at the location of the proposed crossing appears to be roughly the same width (~325 m or ~1065 ft) in each photo. At

the proposed crossing location, the historic photographs indicate this was an area of braiding, with a large main channel to the left (west), a vegetated island, a smaller channel in the middle, a larger vegetated island, and a large side channel on the right (east). In the 2009 image, the large side channel on the east is now vegetated. The small middle channel is now the main channel and the historic (1948) main channel on the left is now covered in vegetation. However, during high flows, as observed during spring 2011, the old channel on the left side has flow in it. Just north of the proposed bridge crossing, on a straight reach, the channel has migrated to the east up to ~180 m (~590 ft). North of this, the main channel divides into two channels in both photographs, with a large vegetated island in the middle. Another notable difference between the two photos is the shrinking of the large lake to the east of the river.

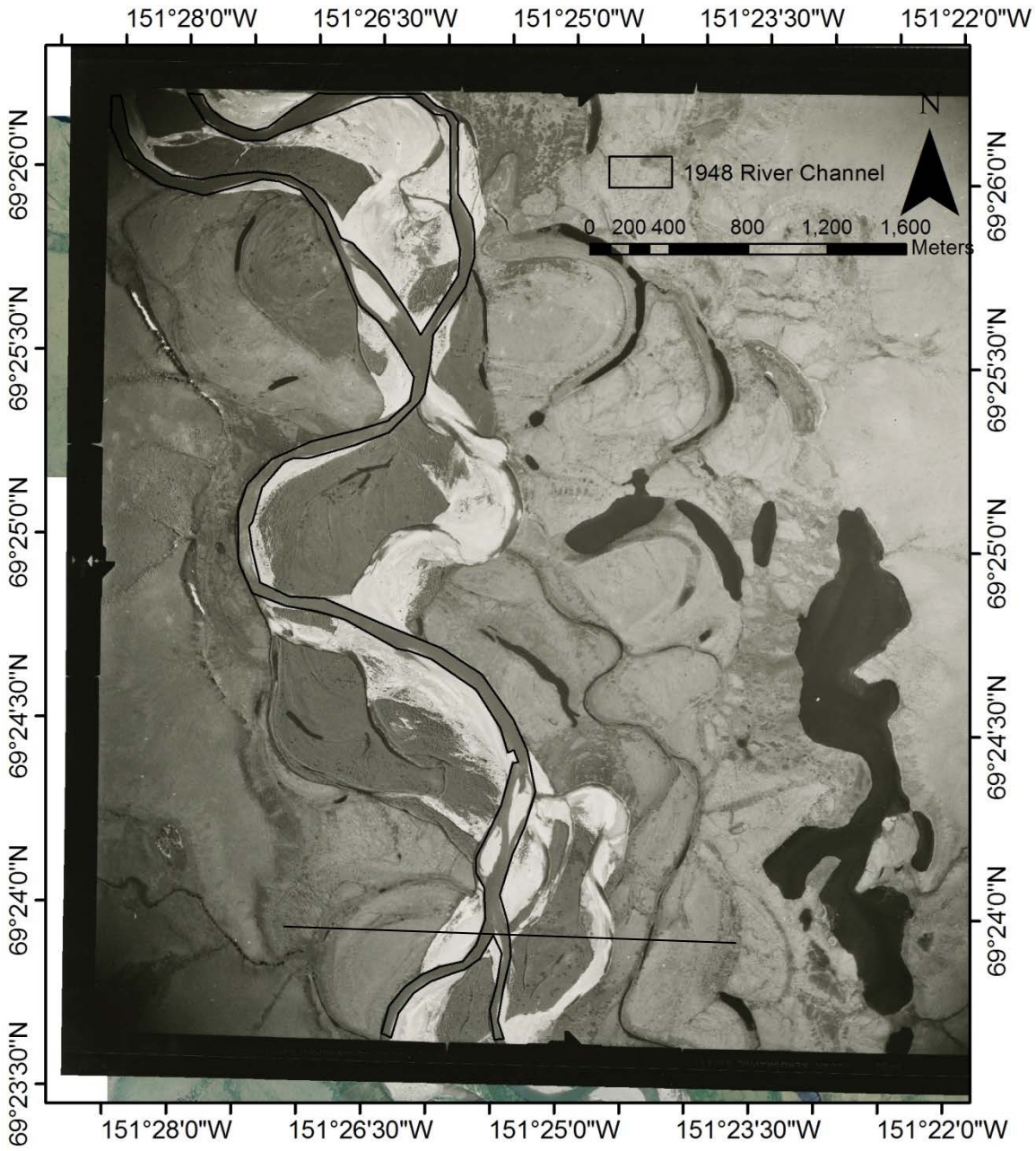

Figure 153. Chandler River historic (July 18, 1948) image. Black line indicates proposed bridge crossing.

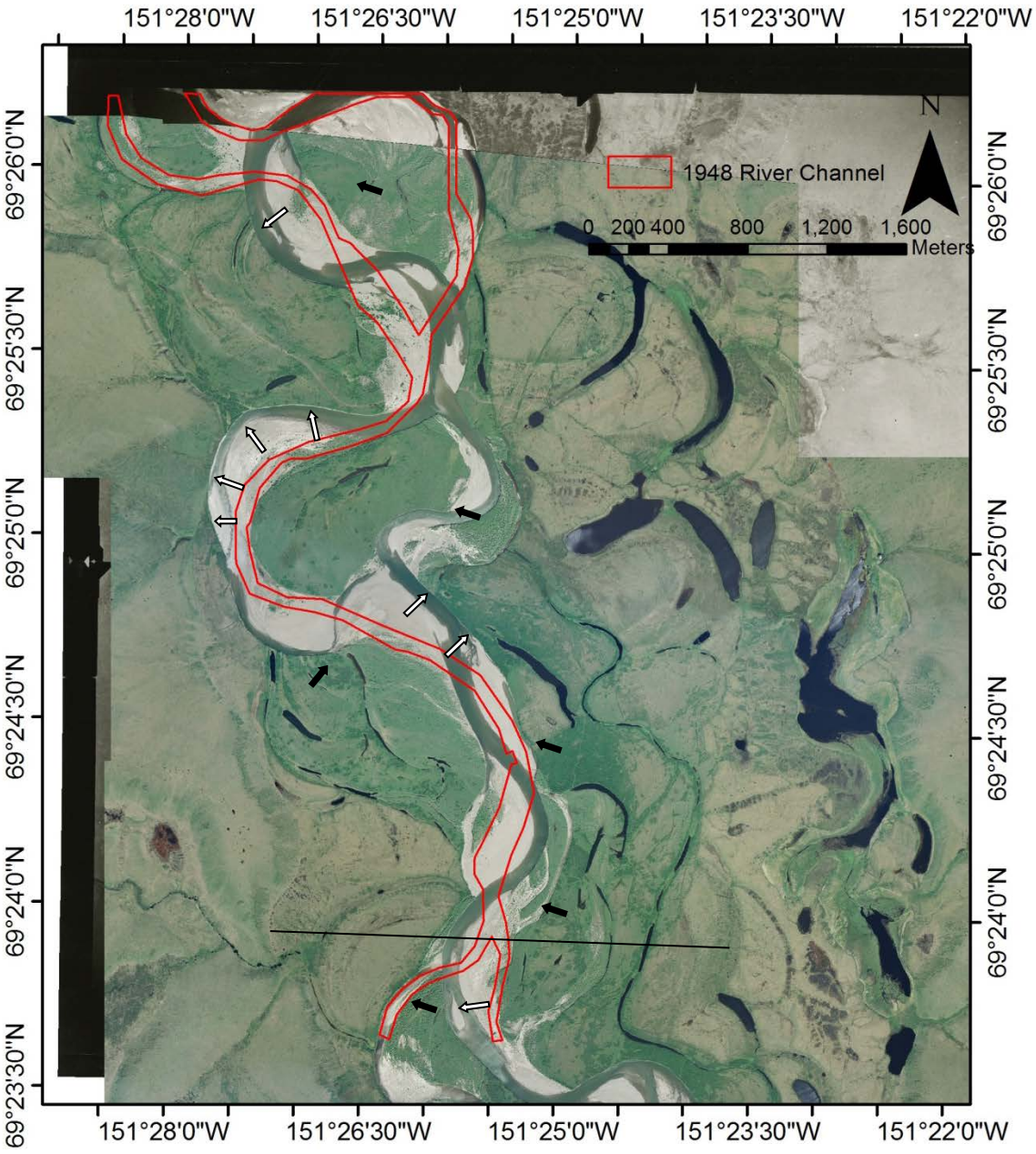

Figure 154. Chandler River modern image (June 2009). Historic (1948) river outline is indicated in red, and proposed bridge crossing is indicated with a black line. White arrows indicate where channel has migrated and black arrows indicate shrub changes since the 1948 image.

5.4.4 Colville River

Figure 155 shows the historic (1948) and Figure 156 modern images (2009) for the Colville River at Umiat, near the proposed crossing location. The Umiat camp and runway are visible in

the photograph. The floodplain is very wide near Umiat (over 2.5 mi or 6 km in places) and the entire floodplain is not shown in the image. Both photos are representative of lower-flow summer conditions. During high flow, the side channels are flowing and over-bank flow generally occurs. The density of shrubs has increased since the historic photograph, similar to the other rivers. The large gravel bar to the southeast of camp is free of vegetation in the 1948 photo, but in the 2009 photograph, vegetation covers at least half of this gravel bar. In this area, the river is shifting to the east. However, just downstream, to the east of the runway, the river is very slowly shifting to the west (toward the runway). To the south of the camp, the river has now migrated north, and is ~300 m (~985 ft) closer to camp.

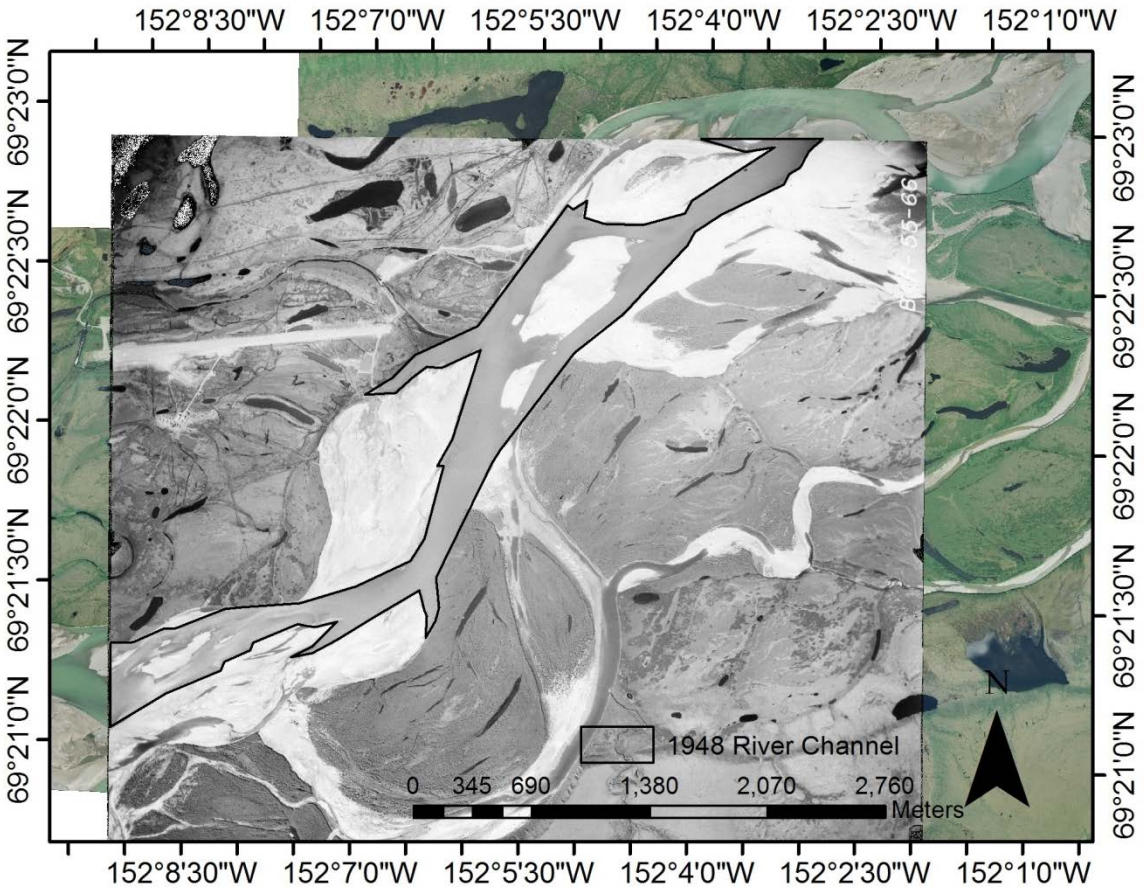

Figure 155. Colville River aerial photograph (July 18, 1948). The Umiat camp and runway are visible in the image.

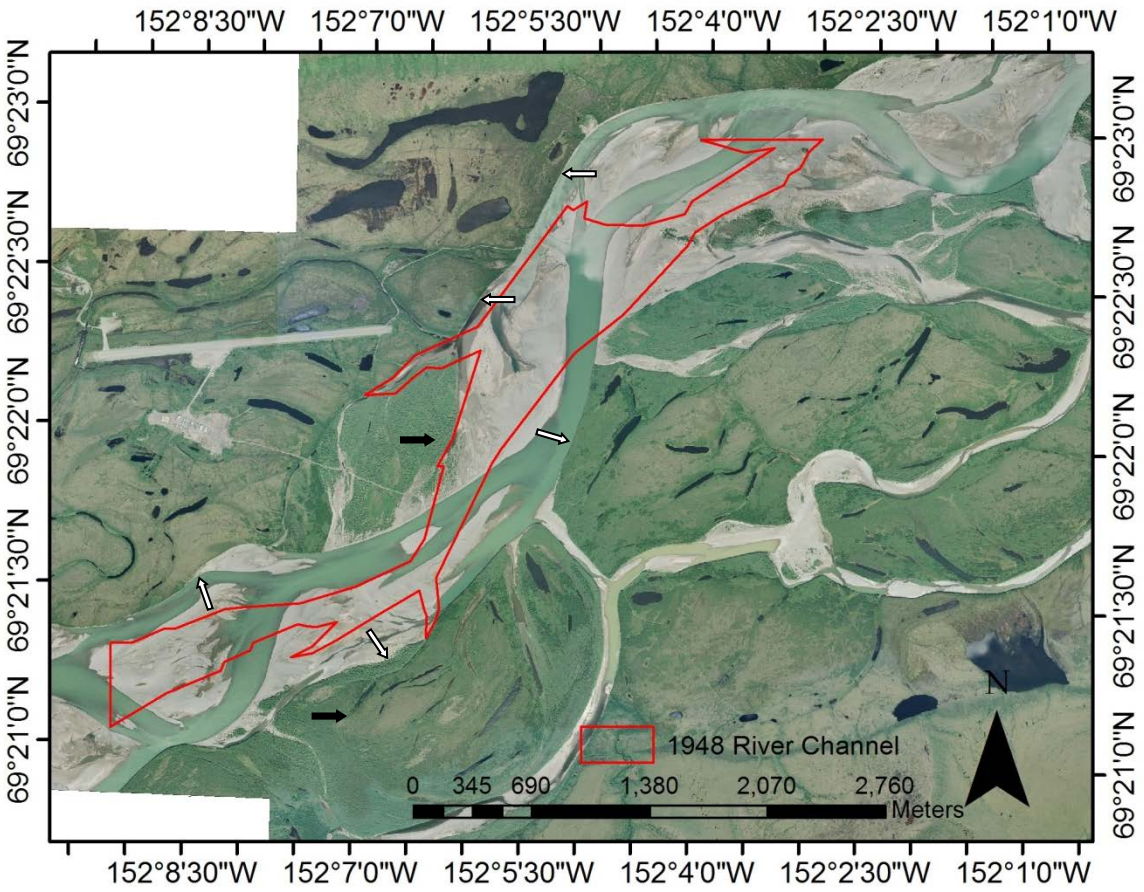

Figure 156. Colville River aerial photograph (June 2009). The Umiat camp and runway are visible in the image. White arrows indicate where the channel has migrated, and black arrows indicate where shrub areas have changed since 1948.

6 CONCLUSIONS TO DATE

UAF/WERC has been performing various research projects on the North Slope of Alaska since 1985. We initially looked at the hydrology of a small headwater drainage (Imnavait Creek) in the Kuparuk River basin. Gradually our studies expanded to the entire Kuparuk River basin (1993) and then included the Putuligayuk River catchment (1999). In 2006, we expanded both studies to the east (Bullen project funded by ADNR) and to the west (Umiat and Foothills projects funded by ADOT&PF). The thrust of most of our research projects was to establish spatially distributed meteorological stations in watersheds of interest and hydrological stations on the streams draining these watersheds. Along the way, we have collected substantial supporting data on these research projects: soil (active layer mostly) temperature and moisture data, longwave and shortwave radiation data, pan evaporation data, suspended and bedload sediment data, spatially distributed end-of-winter snow water equivalent, summer rainfall distribution, stream nutrient chemistry and many more. The sole purpose of these studies is to improve our understanding of Arctic hydrology, which prior to this course of research was severely lacking.

Our approach to enhancing our understanding of Arctic hydrology is to instrument a watershed so we can determine the water balance fluxes (incoming [P] and outgoing [Q, ET]) and changes in storage for that domain, whether it is a small catchment like Imnavait Creek or a large basin like the Kuparuk River. The overall strength of our research effort in the Alaska Arctic is that we have been able to carry forward what we have learned in earlier studies to the present studies, and at the same time have improved our understanding of the spatial and temporal variability of the Arctic hydrologic cycle.

To improve our understanding of Arctic hydrology, we need to document both the spatial and temporal variability. Because this study is too short to capture temporal variability, we rely on previous studies to give us an indication of the range of variability and to show how what we see now in the Itkillik, Anaktuvuk, and Chandler basins compares with what we see in basins like the Kuparuk. This study does allow us to examine spatial variability such as precipitation distribution in an area with no previous observations.

The following are summary conclusions (some are the same as in the earlier report) on what we have learned to date on the Bullen, Foothills, and Umiat projects based on the meteorological and hydrological data collected:

- During the warm season, the northern Foothills region is the warmest, while the Mountain and Coastal Plain regions are both cooler. The Coastal Plain region has the lowest average cold season, followed by the Foothills and then the Mountain regions.
- The highest average wind speeds are found on the Coastal Plain; however, very high individual wind events can occur anywhere on the North Slope. The dominant prevailing wind directions are from the northeast and southwest, but this varies in the Mountain region because of topographic channeling. For stations around the northern Foothills and Coastal Plain, there are seasonal differences in the wind direction with high-speed warm-season winds from the east-northeast or northeast and high winter winds coming from the opposite direction. These general seasonal trends were not observed at many stations in the far western part of the study area.
- Warm-season precipitation shows a strong increasing orographic trend from the Coastal Plain to the Mountain region. The Mountain region receives roughly three times more precipitation than the Coastal Plain region, and the Foothills region receives roughly two times more precipitation than the Coastal Plain region.
- From rainfall data collected at long-term sites, it is evident that there is considerable year-to-year variation in the cumulative rainfall over the warm season. In the years since we started the studies reported here, 2009 is the only year with above-average summer rainfall. Both the warm season of 2007 and the cold season of 2007/2008 were very dry; this is reflected in the low runoff responses from the watershed in summer 2007 and spring 2008. When there is drought, like in 2007, it impacts a much larger area than what would be covered by a low-pressure precipitation system; the 2007 drought covered all of the watersheds in the central North Slope and probably beyond, while rain events are never this extensive in coverage.
- Quantifying the snow depth and snow water equivalent is difficult because the snowpack is so heterogeneous, primarily due to wind events. While there is considerable variability from site to site, there is not much difference in the end-of-winter averages for the three regions: Mountain, Foothills, and Coastal Plain.

- Both SWE (with not much spatial variability) and warm season rainfall (with considerable spatial variability) demonstrate considerable year-to-year variability. While cumulative summer rainfall has varied by an order of magnitude at a station, cumulative winter SWE only varies by a factor of two or three.
- Snowmelt is the major hydrologic event of the year, with high flow volumes and substantial ice floes. Rainfall floods are possible, as the rainfall rate can (and has) exceed the rate of snowmelt. We have observed peak summer floods (for example, Upper Kuparuk, 1999 and 2002) from rainfall, but the question is whether rain can fall over an entire large watershed so that runoff is generated from the majority of the watershed. We have only documented storms with small areas of coverage high in the Foothills region and the northern edge of the Mountain region.
- Some preliminary sediment observations on the Itkillik, Anaktuvuk, and Chandler Rivers show that for these large rivers, there is considerable transport after the ice flushes out (usually before peak flow) of the channels. Earlier sediment studies on the Upper Kuparuk showed that for these smaller streams there was very little sediment transport during break-up. This is attributed to the ice staying in the smaller channels longer.
- Historic images (Itkillik, Anaktuvuk, Chandler, and Colville) from 1978 and 1948 show that the channel has moved laterally somewhat, but not drastically in the floodplain, and that revegetation has occurred on some of the gravel bars.
- Flood-frequency analysis of snowmelt-generated floods on the Upper Kuparuk revealed that the 2011 event had a predicted return period of 20 years. This is the only significant runoff event we have documented since we started to gauge the nearby Itkillik (2011), Anaktuvuk (2009), and Chandler (2011) Rivers. The maximum snowmelt floods for three years for the Anaktuvuk were measured in 2011.
- The HBV hydrologic model appears to work fairly well in a wide range of rivers that have a moderate to high hydraulic gradient (mainly in the Foothills and Mountain regions), but not as well for low-gradient streams in the Coastal Plain region. For the years that we applied the HBV model, a wide range of surface conditions on the Coastal Plain has occurred, from wet to very dry.

7 REFERENCES

ASCE (2008) “Sedimentation engineering: processes, measurements, modeling and practice”. Manual 110. *Edited by Marcelo Garcia*. 1132 pp.

Benson, C.S. (1982). Reassessment of winter precipitation on Alaska’s Arctic slope and measurement on the flux of wind blown snow. Report UAG R-288, Geophysical Institute, University of Alaska, 26 pp.

Benson, C.S., and M. Sturm (1993). Structure and wind transport of seasonal snow on the Arctic Slope of Alaska. Annals of Glaciol., 18: 261–267.

Berezovskaya, S.L., Derry, J.E., Kane, D.L., Geick, R.E., Lilly, M.R., and D.M. White (2007a). Snow survey data for the Sagavanirktok River / Bullen Point Hydrology Study: Spring 2007. July 2007, University of Alaska Fairbanks, Water and Environmental Research Center, Report INE/WERC 07.18, Fairbanks, Alaska, 17 pp.

Berezovskaya, S.L., Derry, J.E., Kane, D.L., Geick, R.E., Lilly, M.R., and D.M. White (2007b). Snow survey data for the Kuparuk Foothills Hydrology Study: Spring 2007. July 2007, University of Alaska Fairbanks, Water and Environmental Research Center, Report INE/WERC 07.17, Fairbanks, Alaska, 21 pp.

Berezovskaya, S.L., Derry, J.E., Kane, D.L., Gieck, R.E., Lilly, M.R., and D.M. White (2008a). Snow survey data for the Kuparuk Foothills Hydrology Study: Spring 2008. University of Alaska Fairbanks, Water and Environmental Research Center, Report INE/WERC 08.14, Fairbanks, Alaska, 40 pp.

Berezovskaya, S.L., Derry, J.E., Kane, D.L., Lilly, M.R., and D.M. White (2008b).. Snow survey data for the Sagavanirktok River / Bullen Point Hydrology Study: Spring 2008. June 2008, University of Alaska Fairbanks, Water and Environmental Research Center, Report INE/WERC 08.15, Fairbanks, Alaska, 30 pp.

Berezovskaya, S.L., Derry, J.E., Kane, D.L., Gieck, R.E., and M.R. Lilly (2009). Snow Survey Data for the Central North Slope Watersheds: Spring 2009. University of Alaska Fairbanks, Water and Environmental Research Center, Report INE/WERC 09.01, Fairbanks, Alaska, 45 pp.

Berezovskaya, S.L., Derry, J.E., Kane, D.L., Gieck, R.E., and M.R. Lilly (2010). Snow Survey Data for the Central North Slope Watersheds: Spring 2010. University of Alaska Fairbanks,

Water and Environmental Research Center, Report INE/WERC 10.01, Fairbanks, Alaska, 45 pp.

Best, H., J.P. McNamara, and L. Liberty (2005). Association of ice and river channel morphology determined using ground-penetrating radar in the Kuparuk River, Alaska. Arctic, Antarctic, and Alpine Research 37(2): 157-162.

Brown, R.D. and D.A. Robinson (2011). Northern Hemisphere spring snow cover variability and change over 1922–2010 including an assessment of uncertainty. The Cryosphere 5: 219-229.

Brazenec W.A. (2005). Evaluation of Ultrasonic Snow-depth Sensors for Automated Surface Observing Systems (ASOS). M.S. thesis, Colorado State University, 66 pp.

Campbell Scientific, Inc. (2006). CS616 and CS625 Water Content Reflectometers Instruction Manual, August 2006, Logan, Utah, 42 pp.

Carr, A. (2003). Hydrologic Comparisons and Model Simulations of Subarctic Watersheds Containing Continuous and Discontinuous Permafrost, Seward Peninsula, Alaska. M.S. thesis, University of Alaska Fairbanks, 123 pp.

Curran, J.H., Meyer, D.F., and G.D. Tasker (2003). Estimating the magnitude and frequency of peak streamflows for ungaged sites on streams in Alaska and conterminous basins in Canada. Water-Resources Investigations Report 03-4188, U.S. Geological Survey.

Derksen, C., Toose, P., Rees, A., Wang, L., English, M., Walker, A. and M. Sturm (2010). Development of a tundra-specific snow water equivalent retrieval algorithm for satellite passive microwave data Original Research Article. Remote Sensing of Environment 114: 8, 1699-1709.

Forbes, A.C. and S.F. Lamoureux (2005). Climatic controls on streamflow and suspended sediment transport in three large middle arctic catchments, Boothia Peninsula, Nunavut, Canada. Arctic, Antarctic, and Alpine Research 37(3): 304-315.

Groisman, P., and T.D. Davies (2002). Snow cover and the climate system. In: Snow Ecology (H.G. Jones, J.W. Pomeroy, D.A. Walker, and R.W. Homan, Eds.), Cambridge University Press, pp. 1–44.

Julien, P. (2002) “River mechanics”. Cambridge University Press. 433 pp.

Hinzman, L.D. (1990). The Interdependence of the Thermal and Hydrologic Processes of an Arctic Watershed and their Response to Climate Change. Ph.D. dissertation, University of Alaska Fairbanks.

Hinzman, L.D., D.L. Kane, R.E. Gieck, and K.R. Everett (1991). Hydrologic and thermal properties of the active layer in the Alaskan Arctic. Cold Regions Science and Technology, 19: 95–110.

Hinzman, L., and D.L. Kane (1992). Potential response of an Arctic watershed during a period of global warming. J. Geophys. Res., 97: 2811–2820.

Hinzman, L.D., D.J. Goering, and D.L. Kane (1998). A distributed thermal model for calculating temperature profiles and depth of thaw in permafrost regions. J. Geophys. Res., (Atmospheres), 103(D22): 28,975–28,991.

Hinzman, L.D., D.L. Kane, and M.K. Woo (2005). Permafrost hydrology. In: Encyclopedia of Hydrological Sciences (M.G. Anderson, Ed.), John Wiley & Sons, Ltd., pp. 2679–2693.

Kane, D.L., L.D. Hinzman, M.K. Woo, and K.R. Everett (1992). Arctic hydrology and climate change. In: Arctic Ecosystems in a Changing Climate: An Ecophysical Perspective (F. Chapin, R. Jefferies, J. Reynolds, and J. Svoboda, Eds.), Academic Press, Inc., pp. 35–57.

Kane, D.L., K.M. Hinkel, D.J. Goering, L.D. Hinzman, and S.I. Outcalt (2001). Non-conductive heat transfer associated with frozen soils. Global and Planetary Change, 29: 275–292.

Kane, D.L., J.P. McNamara, D. Yang, P.Q. Olsson, and R.E. Gieck (2003). An extreme rainfall/runoff event in Arctic Alaska. J. Hydrometeorology, 4(6): 1220–1228.

Kane, D.L., R.E. Gieck, D.C. Kitover, L.D. Hinzman, J.P. McNamara, and D. Yang (2004). Hydrological cycle on the North Slope of Alaska. In: Kane, D.L. and D. Yang (Eds.) Northern Research Basins Water Balance. IAHS Publ. 2090, Wallingford, pp. 224–236.

Kane, D.L, L.D. Hinzman, R.E. Gieck, J.P. McNamara, E.K. Youcha, and J.A. Oatley (2008a). Contrasting extreme runoff events in areas of continuous permafrost. Arctic Alaska. Hydrology Research, 39(4): 287–289.

Kane, D.L., R.E. Gieck, and L.D. Hinzman (2008b). Water balance for a low-gradient watershed in Northern Alaska. In: Proceedings of the 9th International Conference on Permafrost, D.L. Kane and K.M. Hinkel (Eds.), University of Alaska, Institute of Northern Engineering, pp. 883–888.

Kane, D.L., White, D., Lilly, M., Toniolo, H., Berezovskaya, S., Schnabel, W., Youcha, E.K., Derry, J., Gieck, R., Paetzold, R., Trochim, E., Remillard, M., Busey, R., and K. Holland (2009). Meteorological and Hydrological Data and Analysis Report for Bullen Point and Foothills Projects, 2006-2008, University of Alaska Fairbanks, Water and Environmental

Research Center, Report INE/WERC 08.18, Fairbanks, Alaska, 180 pp.

Kilpatrick, F. A., and E.D. Cobb (1985). Measurement of Discharge Using Tracers, Techniques of Water-Resources Investigations, TWI 03-A16, 52 pp.

Lilly, E.K., D.L. Kane, L.D. Hinzman, and R.E. Gieck (1998). Annual water balance for three nested watersheds on the North Slope of Alaska. Proceedings of the 7th International Permafrost Conference, A.G. Lewkowicz and M. Allard (Eds.), pp. 669–674.

McNamara, J.P., D.L. Kane, J.E. Hobbie, and G.W. Kling (2008a). Hydrologic and biogeochemical controls on the spatial and temporal patterns of nitrogen and phosphorus in the Kuparuk River, Arctic Alaska. Hydrological Processes, 3294–3309 (doi:10.1002/hyp.6920).

McNamara, J.P., Oatley, J.A., Kane, D.L., and L.D. Hinzman (2008b). Case study of a large summer flood on the North Slope of Alaska: Bedload transport. Hydrology Research 39(4): 299–308.

Oatley, J. (2002) “Ice, bedload transport, and channel morphology on the upper Kuparuk River”. Master thesis. University of Alaska Fairbanks. 92 pp.

Olsson, P.Q., Hinzman, L.D., Sturm, M., Liston, G., and D.L Kane (2002). Surface climate and snow-weather relationships of the Kuparuk basin on Alaska’s Arctic Slope. ERDC/CRREL Technical Report TR-02-10. U.S. Army Corps of Engineers. 49 pp.

Osterkamp, T.E., and V.E. Romanovsky (1997). Freezing of the active layer on the Coastal Plain of the Alaskan Arctic. Permafrost and Periglacial Processes, 8: 23–44.

Parker, G., Wilcock, P.R., Paola, C., Dietrich, W.E., and J. Pitlick (2007). Physical basis for a quasi-universal relations describing bankfull hydraulic geometry of single-thread gravel bed rivers. Journal of Geophysical Research 112: F04005.

PND Engineers, Inc. (2006). 2005 Spring Breakup and Hydrologic Assessment, Bullen Point Road Project for for Alaska Department of Transportation and Public Facilities, 55 pp.

PND Engineers, Inc. (2009a). Kadleroshilik River crossings hydrologic and hydraulic report, Bullen Point Road Project for Alaska Department of Transportation and Public Facilities, 20 pp.

PND Engineers, Inc. (2009b). Shaviovik River crossings hydrologic and hydraulic report, Bullen Point Road Project for Alaska Department of Transportation and Public Facilities.

PND Engineers, Inc. (2009b). No Name (U1) River crossings hydrologic and hydraulic report, Bullen Point Road Project for Alaska Department of Transportation and Public Facilities.

Romanovsky, V.E., and T.E. Osterkamp (1997). Thawing of the active layer on the Coastal Plain of the Alaskan Arctic. Permafrost and Periglacial Processes, 8: 1–22.

Rovansek, R.J., Kane, D.L., and L.D. Hinzman (1993). Improving estimates of snowpack water equivalent using double sampling. Proceedings of the 61st Western Snow Conference, 157–163.

Seibert, J. (2005). HBV light user's manual: Version 2. Environmental Assessment, Uppsala University, Dept. of Earth Science, 32 pp.

Sloan, C.E., Zenone, C., and L.R. Mayo (1975). Icings along the trans-Alaska pipeline route. U.S. Geological Survey, Open file Report 75-87, Anchorage, AK, 39 pp.

SMHI (Swedish Meteorlogical and Hydrological Institute) (2005). Integrated Hydrological Modelling System (IHMS, Featuring HBV ©SMHI 2005), Manual, Version 5.8.

Stieglitz, M., S.J. Dery, V.E. Romanovsky, and T.E. Osterkamp (2003). The role of snow cover in the warming of Arctic permafrost. Geophys. Res. Lett., 30(13): 1721.

Stuefer, S.L., Youcha, E.K, Homan, J.W., Kane, D.L. and R.E. Gieck (2011). Snow Survey Data for the Central North Slope Watersheds: Spring 2011. University of Alaska Fairbanks, Water and Environmental Research Center, Report INE/WERC 11.02, Fairbanks, Alaska, 47 pp.

Stone, R.S., G.D. Ellsworth, J.M. Harris, and D. Longenecker (2002). Earlier spring snowmelt in northern Alaska as an indicator of climate change. J. Geophys. Res., 107 (D10): 4089, 10.1029/2000JD

Tape, K., Sturm, M., and C. Racine (2006). The evidence for shrub expansion in Northern Alaska and the Pan-Arctic. Global Change Biology, 12: 686–702.

Toniolo, H. (under review). Bed forms and sediment load on the Tanana river Nenana, Alaska, USA. (submitted to Journal of Hydraulic Engineering).

US Geological Survey (2011). Water-resources data for the United States, retrieved from http://waterdata.usgs.gov/nwis/ November, 2011.

Wagner, C.R., and D.S. Mueller (2011). Comparison of bottom-track to global positioning system referenced discharges measured using an acoustic Doppler current profiler. Journal of Hydrology, 401: 250-258.

Woo, M.K., Kane, D.L., Carey, S.K., and D. Yang (2008). Progress in permafrost hydrology in the new millennium. Permafrost and Periglacial Processes, 19(2): 237–254.

Yang, C. (2003). Sediment transport: Theory and practice. Krieger Publishing Company. 396 pp.

Yang, D., Kane, D.L., Hinzman, L.D., Goodison, B.E., Metcalfe, J.R. , Louie, P.Y.T., Leavesley, G.H., Emerson, D.G., and C.L. Hanson (2000). An evaluation of the Wyoming gauge system for snowfall measurement. Water Resources Research, 36(9): 2665–2677.

Yoshikawa, K., Hinzman, L.D., and D.L. Kane (2007). Spring and aufeis (icing) hydrology in Brooks Range. J. Geophys. Res. (Biosciences), 112, G04S43, doi:10.1029/2006JG000294.

Youcha, E. K., Toniolo, H. A., and D. L. Kane (2010). Spring and Summer Runoff Observations 2009-2010, Umiat Corridor Hydrology Project. University of Alaska Fairbanks, Water and Environmental Research Center, Report INE/WERC 11.01, Fairbanks, Alaska, 55 pp

8 APPENDIX LIST

Appendix A: Air Temperature and Relative Humidity

Appendix B: Wind Speed and Direction/ Wind Roses

Appendix C: Soil Data (Soil Surface Temperature, Soil Temperature Profile, Soil Moisture)

Appendix D: Discharge Measurements and Rating Curves/Tables

Appendix E: Umiat Corridor Bridge Crossing